CRANFIELD UNIVERSITY

CRANFIELD BIOTECHNOLOGY CENTRE

Ph.D. THESIS

Academic Year 1996-1997

SOTIRIA D. PSOMA

FLUORESCENCE-BASED OPTICAL BIOSENSORS FOR CLINICAL AND ENVIRONMENTAL APPLICATIONS

Supervisor: Professor A.P.F. Turner

DECEMBER 1996

Dedicated to

the cherished memory

of my father Dimitrios G. Psomas

ΔΗΜΗΤΡΙΟΣ Γ. ΨΩΜΑΣ

(1936-1992)

THERMOPYLAES

Honour to those who have defined their
lives around the guarding of Thermopylaes.
Never deviating from their duty,
fairness and honesty in all their deeds,
but also pity and compassion;
generous whenever they are rich, and when
they're poor, still generous in little things,
still helping where they can;
they always speak the truth,
yet with no hate for those who lie.

And still more honour's due to them
when they foresee (and many do foresee)
that Ephialtis will betray them in the end,
and that the Medes will finally break through.

Constantinos Kavafis (1903)

ΘΕΡΜΟΠΥΛΕΣ

Τιμή σ' εκείνους όπου στην ζωή των
όρισαν και φυλάγουν Θερμοπύλες.
Ποτέ από το χρέος μη κινούντες,
δίκαιοι κ' ίσιοι σ' όλες των τες πράξεις,
αλλά με λύπη κιόλας κ' ευσπλαχνία·
γενναίοι οσάκις είναι πλούσιοι, κι όταν
είναι πτωχοί, πάλ' εις μικρόν γενναίοι,
πάλι συντρέχοντες όσο μπορούνε·
πάντοτε την αλήθεια ομιλούντες,
πλην χωρίς μίσος για τους ψευδομένους.

Και περισσότερη τιμή τους πρέπει
όταν προβλέπουν (και πολλοί προβλέπουν)
πως ο Εφιάλτης θα φανεί στο τέλος,
κ' οι Μήδοι επι τέλους θα διαβούνε.

Κωνσταντίνος Π. Καβάφης (1903)

ACKNOWLEDGEMENTS

I would like to express my sincere thanks and gratitude to Professor A.P.F. Turner for his supervision, encouragement, support and advice over the duration of this work. My thanks also to Professor M.I. Karayannis of University of Ioannina, Greece, Dr G. Pilidis of European Environmental Research Institute, in Ioannina, Greece and Dr S.R. Ahmad of the School of Electrical Engineering and Science at the Royal Military College of Science for allowing me to undertake part of the work in their laboratories. I must also include all the friends and colleagues at Cranfield Biotechnology Centre for their help and support.

I am indebted to the Commission of the European Union for their financial support through out my second and my last year of my Ph.D. studies which enabled the completion of the present work.

My deepest thanks also to my family, especially to my mother Alexandra and my sisters Yanna and Eleni for their continuous encouragement, love and support throughout these tough years.

Last, and by no means the least, I am deeply grateful to my best friend and fiancé Antonios for his understanding, support, patience, and advice during the writing of this thesis. He has been my inspiration and the one who with willingness sacrificed the most to make this work possible.

ABSTRACT

The aim of this thesis was to investigate the feasibility of simultaneous utilisation of pH- and oxygen-dependent fluorescent indicators for the development of a novel fibre-optical fluorescence-based biosensor. This approach would be used to measure simultaneously changes in the two indicator species generated by a single enzyme-catalysed reaction in response to one analyte where both the indicators and the enzyme are immobilised in the same sol-gel matrix, and to offer more accurate and reliable results using this portable optical biosensor in the clinical and environmental fields.

HPTS (1-hydroxypyrene-3,6,8-trisulfonic acid) and tris(2,2'-bipyridyl)ruthenium(II) chloride hexahydrate, respectively, were used as the target fluorescent indicators; these two indicators had no cross sensitivity separate or in the same solution and well-separated emission bands at 510 nm and 610 nm, respectively. The catalytic oxidation of glucose by the enzyme glucose oxidase was initially investigated using the two indicators, and subsequently the same principle was applied in other biocatalysed oxidations such as of lactate, xanthine and phenol. Substrate concentration was assessed by simultaneously measuring two parameters: oxygen consumption, through the reduction of the fluorescence intensity of tris(2,2'-bipyridyl) ruthenium(II) chloride hexahydrate; and the production of acid, through pH changes affecting the fluorescence intensity of HPTS. A thorough spectroscopic study of the enzymatic oxidation of glucose was performed using glucose oxidase in solution in a cuvette, in the presence of both indicators. A number of combinations of wavelengths of the indicators for excitation and fluorescence were utilised in order to establish calibration curves with the optimum performance for glucose detection in the diabetic range.

Similarly results were taken from the kinetic studies of lactate oxidase, xanthine oxidase and polyphenol oxidase for the detection of lactate and xanthine in blood and phenol in water at ppb-levels, using the above principle. The application and characterisation of immobilisation techniques for the fluorescence-based blood-glucose biosenor were carried out. The advantages of the microcapsulation sol-gel method over conventional immobilisation techniques for application in an optical biosensor, were elucidated and this immobilisation technique was implemented for glucose and phenol detection. Finally, additional solution studies were conducted and used to evaluate the implementation and performance of the above method when used for the detection and measurement of glucose concentration in biological samples such as human serum.

CONTENTS

LIST OF FIGURES

CHAPTER 1

INTRODUCTION

1.1 BIOSENSORS

1.1.1 Introduction and Definitions

Biosensors can satisfy an important need in today's world which requires accurate analytical information in real time particularly in clinical diagnosis, environmental surveillance, food analysis, pharmaceutical, petrochemical and water industries, space technology or even in security and defence (Higgins & Lowe, 1987; Luong *et al.*, 1991).

A biosensor may be defined as "an analytical instrument containing a sensing element of biological origin, which is either integrated within or in intimate contact with a physicochemical transducer. The usual aim is to produce a continuous electronic signal which is directly proportional to the concentration of a chemical or set of chemicals present in a sample" (Turner, 1992). Sensing elements impart a high degree of selectivity and sensitivity on the biosensor and may be biocatalysts (e.g. enzymes, organelles, micro-organisms, tissues) or affinity reagents (e.g. lectins, antibodies, nucleic acids, cell receptors and other ligands).

Standards for biosensor performance are (Kisaalita, 1992; Janata *et al.*, 1994; Connolly, 1995) reproducibility, accuracy, precision, selectivity, stability, sensitivity, dynamic range, response time, detection limit, life time, miniaturisation, portability, low cost, simplicity of operation, speed and sanitary operation. In general, the most significant characteristics are reproducibility, selectivity, stability and sensitivity. Biosensors are typically classified by their physicochemical transducers into four main categories (Coughlan *et al.*, 1988; Janata, 1992; Sethi, 1994): electrochemical (amperometric, potentiometric and conductimetric) (Frew & Hill, 1987; Cullen *et al.*, 1990); optical (employing a linear optical phenomenon, such as absorption, fluorescence or a non-

linear optical phenomenon, such as second harmonic generation) (Wolfbeis, 1991b); mass (e.g. piezoelectric and surface acoustic wave devices) (Clark *et al.,* 1987); and thermal (e.g. thermistor, calorimetric and pyroelectric devices) (Mosbach, 1991). From the above classes, the most popular are the electrochemical and optical biosensors (Brooks *et al.,* 1991; Coulet, 1991). Optical biosensors in particular are a tremendously fast growing area because they possess several advantages, in combination with fibre optic waveguides, for measurements of chemical and clinical parameters offering an exciting range of novel analytical devices just beginning to emerge in the marketplace.

1.2 OPTICAL BIOSENSORS

1.2.1 Introduction

Optical methods have been used for many years in various fields of analytical sciences. They are among the oldest, best established and most versatile tools for sensing chemical and biochemical analytes (Wolfbeis, 1991b; Rajeshwar *et al.,* 1992). Some of the best known applications can be traced back to 1930s, and include the utilisation of pH indicator strips for sensing pH, and oxygen by quenching the phosphorescence of silica-gel-adsorbed trypaflavin and fluorescein (Kautsky & Hirsch, 1935).

A major development step occurred when conventional optical sensing techniques were coupled with optical fibres (Lubbers & Opitz 1983; Seitz, 1984; Narayanaswamy *et al.,* 1985; Thompson & Ligler, 1988; Webb, 1989; Kosa, 1991; Narayanaswamy, 1991). Optical fibres exploit the phenomenon of total internal reflection allowing the propagation of the light and its interaction within the optical fibre (Senior, 1985; Chaimowicz, 1989; Bhattacharya, 1994; Smith, 1995). Although optical fibres were

originally used in the communication industry, they have been adapted to optical chemical sensors. In parallel, the development of high performance and high quality optical components, including light sources (lasers, light emitting diodes (LED)), photodetectors, amplifiers, etc., that can be used in combination with optical chemical sensors has resulted in rapid progress and has attracted great interest. Optical fibre chemical sensors are based on an interdisciplinary approach to their development with expertise and contributions coming from several areas including indicator/reagent synthesis, polymer chemistry, biochemistry, analytical chemistry, physics (optics, optical spectroscopy), fibre optics, and opto-electronics (Milanovich *et al.*, 1984; Wolfbeis, 1991a; Narayanaswamy, 1993). Progress in this field of chemical analysis relies mainly on the ease and way in which the chemical transduction system can be developed and linked with fibre optics. Finally, new methods in chemometrics, along with powerful microprocessors, which allow storage and rapid data analysis, have considerably enhanced the state-of-the-art of optical biosensors.

Various names have been given to optical sensors, with the more popular being "optrode" from "optical electrode" (Borman, 1981); and, "optode" from the Greek "οπτικη οδος", meaning the optical way, that has been introduced by Lubbers and Opitz (Lubbers & Opitz, 1975 & 1983; Opitz & Lubbers, 1984 & 1988). Optrode has become popular in Anglosaxon countries, and optode in continental European countries, both expressions underline the fact that the signal is optical rather than electrical.

In an optical fibre based chemical transducer, light from an appropriate source is transmitted into the optical fibre and guided to region where it interacts with a

measurand system or with a chemical transducer (Seitz, 1988; Arnold, 1990; Narayanaswamy, 1993). This interaction causes a modulation of the optical signal, and the modulated light encoded with chemical information, is collected by the same or another optical fibre and directed to a light-detection system. The optical signal measured can be absorbance, reflectance, luminescence or scattering, depending on the particular measurement device and the optical principles employed. The chemical transducer usually consists of immobilised reagent(s) specific for each particular analyte and is often capable of measuring trace levels of the analyte.

1.2.2 Advantages and Disadvantages of Optical Biosensors

Optical biosensors offer several advantages over other types of biosensors in a wide range of practical applications including biomedical, environmental and process control fields (Wolfbeis, 1991a). Some of these advantages are listed as follows:

i) Optical biosensors do not require a reference signal, in contrast e.g. to potentiometric methods where the difference of two absolute potentials is measured.

ii) Ease of miniaturisation allows the development of very small, light and flexible fibre sensors. This is significant in the case of minute sample volumes and in designing small catheters for invasive sensing in clinical chemistry and medicine.

iii) Low-loss optical fibres allow transmittance of optical signals over long distances, typically 10 to 1,000 meters. Remote sensing renders it possible to perform analyses in ultraclean rooms, when samples are difficult to reach, dangerous, of very high or low temperature, in harsh environments, or radioactive.

iv) Since the primary signal is optical, it is not subject to electrical and electromagnetic interferences by static electricity of the body, strong magnetic fields, or surface potentials of the biosensor head.

v) Analyses can be performed in almost real-time since no sampling, with its inherent disadvantages, is necessary.

vi) Optical sensors can be developed for chemical and biochemical analytes for which other sensing devices are not suitable or available.

vii) Many sensors are simple in design and can easily be replaced by substitute parts.

viii) Optical sensors offer cost advantages over electrodes because of the low price of fibres; and, sensor layers can be fabricated so cheaply that they can be part of a disposable test kit.

ix) Fibre optics are manufactured from non-rusting materials, resulting in excellent stability when in permanent contact with electrolyte solutions, and also can transmit much more information than an electrical lead.

x) Biosensors with immobilised indicator or reagent layers are not subject to inner filter effects (i.e., the absorption of part of the exciting light as it enters the zone viewed by the detector) caused by interfering analytes having similar absorption. This is due to the usually high optical density of the indicator layer which (with certain limitations) may also serve as a filter to the underground emission from the sample.

xi) Most fibre sensors can be employed over a wider temperature range than electrodes and some have a smaller temperature dependence.

Despite their numerous advantages, optical biosensors present certain disadvantages:

i) Ambient light can interfere with the measurement of optical signals. Therefore, either the sensors must be used in dark environment or the optical signal must be modulated to resolve it from the ambient light in which the detector would also be modulated to receive only those modulated optical signals.

ii) Optical bioensors based on the use of indicator phases are likely to have limited long-term stability as a result of photodegradation or leaching effects. These can be compensated to some extent by the use of the ratio of optical signals of two measurement wavelengths.

iii) Sensors with immobilised pH indicators or chelating reagents have limited dynamic ranges as compared to electrodes since their association equilibria obey the mass action law rather than the Nernst equation. Plots of signal versus log analyte concentration are sigmoid rather than linear.

iv) More selective indicators are required for various important analytes and the immobilisation chemistry needs to be improved to achieve both better selectivity and sensitivity.

v) Commercial accessories of the optical system are not optimal yet. Stable and long-lived lights sources, better connectors, terminations, optical fibres, inexpensive lasers, and, in particular, blue LEDs and semiconductor lasers for the whole visible range are required.

vi) Many indicators suffer a reduction in sensitivity after immobilisation or when dissolved in a polymer resulting in smaller slopes of the response curves. In particular, dynamic quenching efficiency is frequently drastically diminished in which case the respective conventional method will be much more sensitive than the opto-sensor method.

vii) In indicator phase sensors for pH and electrolytes it is the concentration of the dye that is quantitatively determined, rather than the analyte itself. The relationship between indicator concentration and analyte concentration can vary with ionic strength, solvent composition, and matrix composition. This may cause considerable bias in precision. In addition, the sensor registers the concentration of a species rather than its activity, as in the case of electrodes.

In conclusion, optical biosensors offer a variety of new technological aspects. Despite their limitations, they have the potential of becoming an attractive alternative to other sensing methods and to perform diagnostic, environmental, or clinical functions better, faster, more accurately with less drift, or cheaper than existing approaches. The major advantages of using optical biosensors compared to conventional electrochemical methods include very small size and flexibility offering an attractive possibility as trend monitors or alarm-type systems (indicating an analyte concentration to be outside the normal range), in bedside monitoring and testing and in invasive analysis, and, they can be produced easily at low cost without sacrificing accuracy.

1.2.3 Classification of Optical Biosensors

Optical biosensors may be divided into two general categories, extrinsic and intrinsic devices, depending on the characteristics of the sensing element (Seitz, 1988; Moore & De Paula, 1989; Coulet, 1992). Extrinsic sensors involve a sensing element that is external to the optical fibre itself, where this sensing element is an immobilised reagent phase that changes optical properties upon interaction with an analyte. This type of biosensor may be subdivided into three groups: the first generation, where the optical

fibre acts as a light guide and also called bare-ended fibre sensors or passive optodes; the second generation, in which the analytical information is mediated by some sort of indicator chemistry, and also referred to as active optodes; and, the third generation sensors, in which a biocatalytic process is usually coupled to either plain fibre sensors or an indicator-mediated sensor, such as an oxygen optode (Wolfbeis, 1991c). Intrinsic biosensors utilise the optical fibre itself as the sensing element by relying on chemically-induced changes in the optical properties in the fibre core, cladding, or jacket materials. The main types of intrinsic optical biosensors are evanescent-field spectroscopic probes, core-based sensors, cladding-based sensors, and jacket-based sensors. Extrinsic optical fibre sensors are the most common of these two types utilised for chemical and biochemical analysis.

Another classification is based on the nature of optical techniques which can be used for biosensor development (Gopel *et al.*, 1992; Seitz, 1993). This may employ a linear optical phenomenon, including absorption, fluorescence, phosphorescence, rotation, polarisation, interference, etc., or a non-linear optical phenomenon, such as second harmonic generation (Takahashi *et al.*, 1993; Okazaki *et al.*, 1988). An alternative categorisation is according to the application field and to divide sensors into chemical, enzyme-based biosensors, and immunosensors (Wolfbeis, 1989).

As far as the technological approach to the construction of optical sensors is concerned, there are two different types. In the first, the chemical parts of the sensor are manufactured first and then attached to the fibre or fibre bundle. The sensor layers are usually produced on planar supports such as glass, cellulose, or plastic and then they are

stuck or mechanically fixed at the fibre tip. In the second type, the chemical parts are manufactured directly on the fibre, after coating and cladding have been removed from the end. It appears that planar sensors can be produced more reproducibly and in larger quantities and they are more easily subject to quality control. In most instances, the sensing material is composed of an indicator layer (and/or an enzyme layer) placed in, or on, a polymeric support using a suitable immobilisation method. The indicator acts as a transducer for the chemical species that cannot be detected directly by optical means.

According to the above categorisation, the experimental work presented in this thesis can be either classified among the third generation of extrinsic biosensors employing the indicators, tris(2,2'-bipyridyl)ruthenium(II) chloride hexahydrate, and 1-hydroxypurene-3,6,8-trisulfonic acid (HPTS), in the fluorescence-based biosensors category, or among the class of enzyme-based biosensors using the technique of sol-gel immobilisation.

1.2.4 Immobilisation Procedures for Biosensors

The biological nature of biosensors, imparts the disadvantage of thermal and chemical instability, and consequently among the greatest efforts to optimise biosensors have been focused on the development of methods for the stabilisation of the biological components (Gopel *et al.*, 1992). The selectivity, the long-term stability and reliability of a biosensor are dependent on the biochemical recognition elements fixed closely to the surface of the transducer. The immobilisation procedures used must be applicable to enzymes, cofactors, microorganisms, antibodies, lectins, organelles, tissue slices, or liposomes. The major advantages of protein immobilisation are close control of the reaction medium and conditions, prevention of bacterial and chemical degradation, cost-

effective reusability of the protein and enhanced biomolecular stability. The immobilisation of enzymes or other proteins appears as one of the general areas of biosensor research. Various methods for the immobilisation of these biochemical recognition systems have been reported (Schmidt *et al.*, 1992) :

i) physical adsorption at a solid interface;

ii) physical entrapment behind a semipermeable membrane;

iii) entrapment into a ramified network of a polymer;

iv) crosslinking with an inert protein by bifunctional reagents;

v) covalent binding to a solid support.

Extensive reviews on immobilisation procedures (e.g. Mosbach, 1976; Chibata, 1978; Carr & Bowers, 1980; Woodward, 1985; Scouten, 1987; Wilson & Thevenot, 1990; Scheller & Schubert, 1992; Eisenthal & Danson, 1993), the characterisation of immobilised biomolecules (Buchholz & Klein, 1987; Blum & Gautier, 1991; Kauffmann & Guilbault, 1991; Schaffar & Wolfbeis, 1991) and the fixation of microorganisms (Bennetto *et al.*, 1987; Karube & SangMok Chang, 1991) and plants cells (Hulst & Tramper, 1989) have appeared. A large number of different and in many cases very special immobilisation procedures have been published, and it becomes obvious that no immobilisation method is appropriate for solving all the problems that arise with the immobilisation of different enzymes onto different transducer surfaces (Coulet, 1992). However, any immobilisation method must guarantee, as far as possible, that the activity of the biomolecule is maintained, that the accessibility of the substrate to the active sites of the bound biomolecules is not sterically hindered, and that mass transport of substrates and products through the enzyme layer is possible. It should be

ensured that the biological compounds retain their native stabilities and reactivities or should even be stabilised by the immobilisation reaction. Finally, the choice of a particular immobilisation technique depends on a variety of issues:

i) nature and type of biocompound;

ii) transduction surface;

iii) stabilising and mediating chemicals and biochemicals;

iv) biosensor storage aspects;

v) manufacturing process;

vi) the environment in which the biosensor will be utilised.

It is remarkable that despite the large amount of previous effort, recent research has demostrated an alternative immobilisation method for biosensors, sol-gel encapsulation. Proteins can be trapped in a sol-gel prepared silicate glass matrix and can retain biological function. The method is ideal for use in optical biosensors (Dave *et al.*, 1994; Dunbar *et al.*, 1996).

1.2.5 The Sol-Gel Immobilisation Procedure

The sol-gel process is a chemical synthesis technique for preparing gels, glasses and ceramic powders at low temperature by hydrolysis and polymerisation of organic precursors (Hench & West, 1990; Brinker & Scherer, 1990). In general, it deals with the formation of inorganic oxides. The process typically involves a metal oxide, water, a solvent and frequently a catalyst, which are mixed thoroughly to achieve homogeneity on a molecular scale. Chemical reactions (hydrolysis and condensation polymerisation) between the molecules lead to the formation of microscopic clusters in three

dimensions, increased solution viscosity and eventually, formation of a gel (Scherer, 1988). This gel is essentially an amorphous, porous material with liquid solvents still contained within pores. Low temperature (typically lower than 100 °C) curing expels all liquids and leaves the porous oxide. Further curing at higher temperatures causes the pores to collapse and leads to densification of the material.

The method has received considerable attention because it possesses a number of desirable characteristics. For example, it enables the preparation of glasses at far lower temperatures than is possible by using conventional melting. In addition, it is a high purity process which leads to excellent homogeneity, and it is adaptable to producing bulk pieces as well as films. During the past 5 years it has been widely recognised that with the sol-gel process is possible to encapsulate a wide variety of organic and organometallic molecules in the inorganic medium (Dunn & Zink, 1991; Yamanaka *et al.,* 1992). Prior to the sol-gel work, the incorporation of organic molecules in solids generally was restricted to the use of frozen solvents or organic polymer matrices.

The present approach represents a totally new type of organic/inorganic composite material because the oxide matrix not only offers a significantly more ionic environment but also it is thermally, chemically and dimensionally more stable. Also, the chemistry of dopants in these sol-gel matrices remains the same as that in solution. Thus, studies of organic-doped sol-gels have begun to develop substantial breadth, from investigations of doped sol-gels for spectroscopic and matrix-isolation photochemistry, to the effect of solvent chemistry on luminescence properties, and the development of lasers and non-linear optical materials.

In comparison to conventional methods of enzyme immobilisation, the sol-gel encapsulation method offers important advantages (Dave *et al.,* 1994). For example, covalent attachment of proteins to a matrix requires that specific functionalities be present on the biomolecule. By contrast, entrapment in sol-gel matrices is independent of the functionalities on the protein. Another advantage of the sol-gel encapsulation method over covalent attachment is that physical entrapment is functionally non-invasive and preserves the integrity and directional homogeneity of the protein surface microstructure (Narang *et al.*, 1994). By contrast, covalent attachment of proteins via surface modification fixes the orientation of the exposed protein and in certain cases may block substrate access to the protein's active site. In addition, the sol-gel entrapment method is mostly independent of the size of the biomolecule because the matrix forms around it by contrast with physical absorption method. In addition, the absence of covalent interactions between the protein, enzyme and the surrounding medium is of utmost importance for maintaining stability and reactivity (Dill, 1990).

Sol-gel science offers new and interesting approaches in the field of biosensors (Zusman *et al.,* 1990; Audebert *et al.,* 1993). Optical-based biosensors are especially convenient and accurate because changes in the absorbance or luminescence of the medium containing the biosensor can be readily measured or even visually detected. Sol-gel prepared silicate glass matrices are almost ideal host matrices for optical biosensors (Dunn & Zink, 1991; MacCraith *et al.,* 1991; Dave *et al.,* 1994). They have the obvious advantages of chemical inertness, mechanical stability, optical transparency (permitting optical monitoring of the spectroscopic properties of the encapsulated biomolecules) and

ease of processing the glass materials. The silicate monoliths provide an efficient design that restricts movement of the recognition molecule but allows free flow of analytes.

More importantly, they are able to encapsulate the indicator molecule or/and enzymes physically in pores in the glass such that these molecules are immobilised and cannot be leached out, while at the same time they are porous enough to allow transport of metal ions, solvent and other small molecules into the interior of the glass (Braun *et al.*, 1990). Also, these biofuctional glasses make it possible to retain the specificity and reactivity of biological molecules in the aqueous microenvironment inside the pores of the silicate glass and provide morphological and structural control that is not available when the biological molecules are simply dissolved in aqueous media. The glasses can be fabricated into desired shapes and sizes such as monolithic blocks or thin films for specific applications.

The two leading research groups in this new biosensor field of encapsulation of enzymes in sol-gel matrices are these of Avnir and Braun, and Zink and Dunn (Zusman *et al.*, 1990; Dunn & Zink, 1991). In 1990, Avnir *et al.* reported the first attempts at protein encapsulation inside silica glasses (Braun *et al.*, 1990). They described the preparation and properties of a biochemically active sol-gel glass, obtained by trapping the enzyme alkaline phosphate in a polymerising tetramethoxysilane. The resulting glasses showed 30% retention of enzymatic activity. Two years later, Zink and his colleagues presented an improved sol-gel method for the detection of glucose oxidase activity and the development of an optical glucose biosensor (Yamanaka *et al.*, 1992; Ellerby *et al.*, 1992). Optically transparent silica glass containing the active enzymes,

glucose oxidase and peroxidase, was synthesised by the sol-gel method. The enzymes were immobilised, but small molecules, like glucose, diffused readily through the porous glass. The enzymatic reactions that occur normally in solution were readily carried out in the pores of the glass matrix. When all of the enzymes and colorimetric precursors were encapsulated and the glass was exposed to glucose solutions, the coloured products which were formed in the glass produced a coloured glass which was suitable for use as the active element in a solid-state optically-based detector. The turnover number for encapsulated glucose oxidase with β-D-glucose was the same in the glass and in solution. The results showed not only that the enzymes retain similar activities when immobilised in an inorganic matrix but also that optically transparent biochemically active glasses can be synthesised and can be used as the active medium in optically based glucose biosensors.

A similar approach to the above mentioned immobilisation method, has been implemented in the present study for the encapsulation of the fluorescence indicators, tris(2,2'-bipyridyl)ruthenium(II) chloride hexahydrate and 1-hydroxypurene-3,6,8-trisulfonic acid (HPTS), and the enzyme glucose oxidase; and also for the immobilisation of the fluorescence indicator, tris(2,2'-bipyridyl)ruthenium(II) chloride hexahydrate, and the enzyme tyrosinase, as will be described in more detail in Chapters 7 and 6 of this thesis, respectively.

Several recent reports have revealed the feasibility of the sol-gel encapsulation method. Audebert and his co-workers described the electrochemical probing of glucose oxidase activity embedded sol-gel matrices for the development of electrochemical biosensors

(Audebert *et al.*, 1993). The enzymatic activity of glucose oxidase, determined using electrochemistry of a mediator, was retained in two types of silica gels. Quantitative results showed that a satisfactory agreement with theoretical predictions was obtained, especially in colloidal silica gels where organic solvents were avoided and only water came into contact with the enzyme.

A new moulding procedure was demonstrated in order to entrap glucose oxidase in the vanadium oxide sol-gel matrix (Glezer & Lev, 1993). This prototype class of enzyme electrodes made of conductive, porous vanadium pentaoxide was prepared by the sol-gel doping method in order to be used in electrochemical biosensors. Also, Wang and his colleagues reported the first attempt to encapsulate intact antibodies in a sol-gel glass (Wang *et al.*, 1993). Specifically, they have investigated the affinity of sol-gel encapsulated antifluorescein using steady-state and time-resolved fluorescence spectroscopy. The results demonstrated that the form of the antifluorescein-fluorescein equilibrium remained unchanged upon encapsulation in a sol-gel matrix; the storage time and conditions affected the affinity of the encapsulated antibody significantly. Finally the authors claimed that the ability to easily encapsulate and retain the affinity of antibodies within a sol-gel matrix will find many applications in biosensor technology.

A different application of the sol-gel method was the encapsulation of the photosynthetic membrane protein of bacteriorhodopsin in an optically transparent and porous silica matrix using a modified sol-gel procedure (Wu *et al.*, 1993). The optical and photocycle properties have been measured and found to be retained throughout the gel formation processes. This system has been presented as an attractive material for

potential use in optical imaging processing and optically based solid-solid ion sensing. Also, another glucose biosensor based on a sol-gel-derived platform was reported (Narang *et al.,* 1994). The immobilisation of glucose oxidase was carried out in three ways, namely, physisorption, microcapsulation and a novel sandwich configuration. Due to high loading of the enzyme and a relatively fast response time, the sandwich configuration showed the most promise for future biosensor development. This particular scheme offered stability for at least 2 months under ambient storage conditions. Amperometric and photometric detection modes were used to study the response profiles and in turn quantify glucose.

A different study has demonstrated the feasibility of measuring and detecting light emission from micrometer-sized channels etched in silicon using a range of luminometers (Kricka *et al.,* 1994). Light emission from branching silicon channel structures was readily detected and resolved using two different imaging systems. These simple silicon-glass chips have served as models of analytical devices that could be developed for multianalyte assays based on spatially resolved microchannel test areas.

In 1995, the results of a feaseability study on the measurement of dissolved oxygen in water using visible absorption spectral changes of sol-gel glass-encapsulated myoglobin gels were published (Chung *et al.*, 1995). Also, a new optical sensing platform based on a combination of planar waveguiding and sol-gel processing technologies was reported (Yang & Saavedra, 1995). Planar integrated optical waveguide (IOW)-attenuated total reflection (ATR) biosensors for dissolved Pb^{2+} and pH were both sensitive and rapid, features that are difficult to achieve simultaneously in monolithic sol-gel glass

biosensors. Recently, Bright and his colleagues have presented a detailed investigation on the evolution and performance of sol-gel-derived thin films as used for chemical sensing platforms (Dunbar *et al.*, 1996). In conclusion, sol-gel based biosensors appear to be promising, in comparison to conventional biosensors, and should allow greater selectivity and sensitivity, miniaturisation potential, and also, the development of multienzymatic, multilayer sensing systems for the simultaneous detection of multiple analytes.

1.2.6 Optical Techniques

The optical sensing of chemical species is based on their interaction with light. In optical chemical sensors, three of the optical techniques commonly employed for measurements are the absorption, luminescence (fluorescence and phosphorescence) and reflection or scattering of light. The present research deals with the largest of these groups, fluorescence-based biosensors.

1.2.7 Fluorescence-based Optical Biosensors

Fluorescence spectroscopy along or in combination with fibre optic technology has become an established spectroscopic method for chemical analysis because of its high sensitivity, selectivity and versatility (Leiner, 1991; Lippitsch and Draxler, 1993). Because fluorescence is emitted in all directions, there is no need to design a reagent phase to redirect incident light, and also, because of its sensitivity, very low fluorophore levels can be detected (Wolfbeis *et al.*, 1992). In addition, the coupling of fluorescence to fibre-optic technology offers the possibility of remote analysis. Also, fluorescence spectroscopy, due to certain advantages over absorption spectroscopy (i.e. more

sensitive than absorbance due to the Stoke's shift and because it is more flexible in that a great variety of analytes and influences are known to change the emission of particular fluorophores) has established itself as one of the techniques that meets the requirements of high sensitivity without loss of specificity or precision (Thompson, 1991). The time required for analysis can be short and automatic processing is possible. In addition, fluorescence is particularly well suited for optical sensing because emitted light returning from the sensor can easily be distinguished from the exciting light (Angel, 1987; Opitz & Lubbers, 1987; Leiner & Wolfbeis, 1991; Komives & Schultz, 1992; Coulet *et al.*, 1993).

Among various techniques used, fluorescence quenching, because of its simplicity and ease of automation, is of particular interest. There exists a large and growing literature describing analytical methods employing fluorescence quenching, in particular on optical fibre-based sensors (Guilbault, 1992; Peterson *et al.*, 1984; Seitz, 1988; Wolfbeis, 1991b). The essence of fluorescence analysis is to understand and exploit changes in fluorescence. These changes may be in the intensity, lifetime, colour, and/or polarisation of the emission (Szmacinski & Lakowicz, 1993). Indeed, any interpretable observation of fluorescence might form the basis of a biosensor. Intensity measurements suffer from some disadvantages (Draxler & Lippitsch, 1996). Photoemissive devices such as tungsten lamps, LEDs and semiconductor lasers are not stable as conventional electron sources. As the device ages, the output of the light source changes, and the sensor's initial calibration begins to drift. Further, the sensitivity of the photodetector is highly dependent on temperature. In order to avoid signal fluctuations originating from optoelectronic equipment, proper regulation of the intensity of the light source and

temperature control of the photodetector and amplifiers are essential. As a result, signal-to-noise ratios ranging from 2000 to 4000 can be achieved.

Another source of error is responsible for a constant, analyte-independent signal level. This can be caused by light from the light source passing the blocking region of the interference filter, "cross-talk" between the fibres of the input and output bundles, mirror-type reflection at the interface between the light guide and the sensor support, diffuse reflection, Rayleigh scattering by molecules or aggregates of molecules, Mie scattering by particles of colloidal size in the sensing layers and the intrinsic background fluorescence of the sensor material and the fibres. This type of light is referred to as "false light" (Leiner & Hartmann, 1993).

Apart from measuring the fluorescence intensity, measurements of fluorescence lifetime, energy transfer or polarisation can also be used. The measurement of fluorescence lifetime shows some decisive advantages over the measurement of light intensity; it is intrinsically self-referenced, has negligible signal drift because the decay time is fairly independent of the fluorophore concentration and fluctuations in light source intensities and photodetector sensitivity play almost no role (Lippitsch & Draxler, 1993). In general, fluorescence lifetimes are largely intensity-independent and therefore are increasingly utilised.

1.2.8 Instrumentation

An optical fibre fluorosensor essentially consists of a light source, optical fibres (if required), a fibre light guide including light couplers and decouplers, a sensing zone or

layer (if the analyte is non fluorescent), and a light detector which transforms the optical signal into voltage, and finally, this signal is then amplified, processed, and displayed or printed out (Wolfbeis, 1988; Blum *et al.*, 1989). The instrumental design is different for the various requirements imposed on sensors, but the principle is generally the same.

The concept of the application of the optodes is shown in Figure 1.1 (Leiner, 1991). Light from the light source is focused at a set of optical filters at which the appropriate excitation wavelength for the indicator is selected. A bundle of optical fibres guides the excitation light to the analyte-sensitive layer. The emitted fluorescence is guided through a second bundle of fibres and an optical filter to the photodetector (Coulet & Bardeletti, 1991).

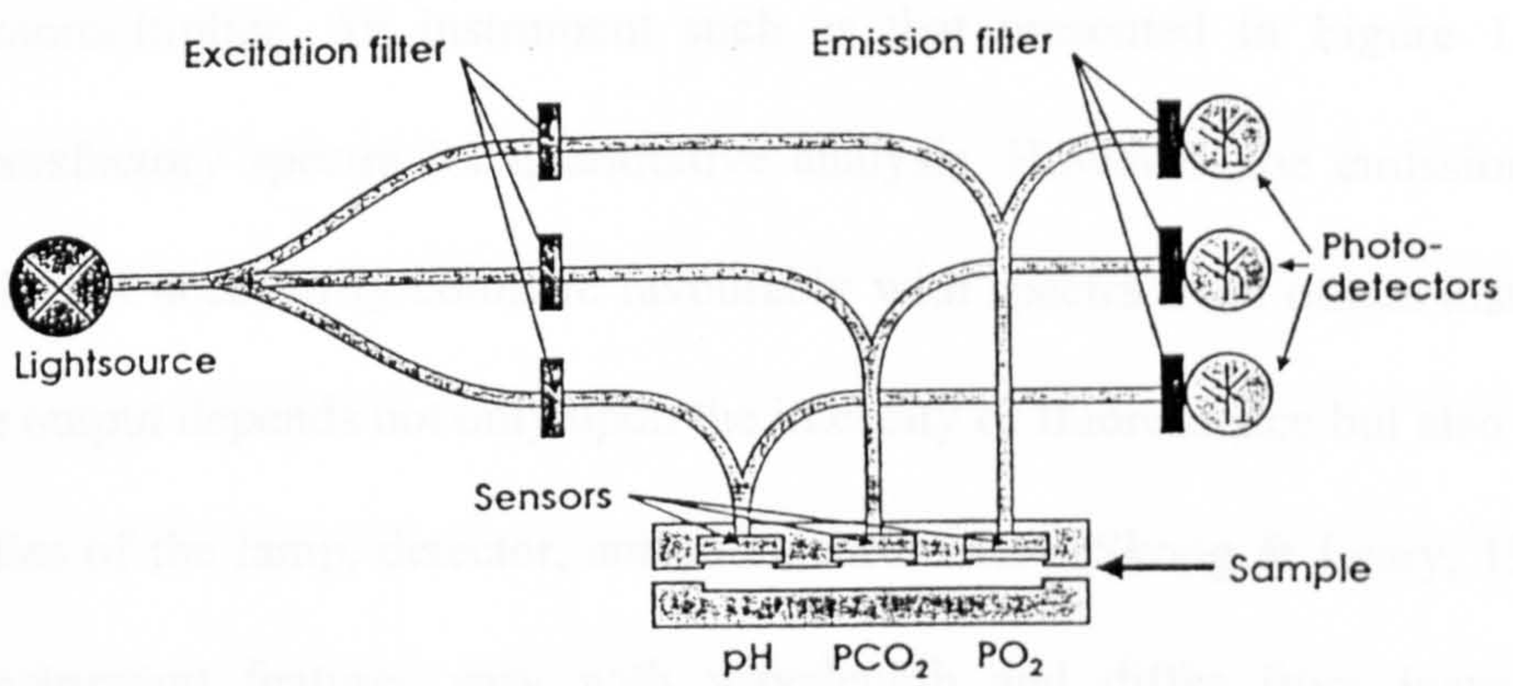

FIGURE 1.1 Application of the optodes for the measurement of blood gases (Leiner, 1991).

Alternatively, a single fibre can be utilised to separate the exciting and emitted light through more sophisticated optical arrangements. The optode is placed in a chamber which allows the introduction of calibrants and the sample. Single fibre optodes are used for measurements *in vivo* or in small sample volumes. In most other cases, however, the use of a fibre bundle is preferred because more light can be transported, and background from intrinsic fluorescence of the fibre is strongly reduced, resulting in higher signal intensities.

Several instrument manufacturers offer spectrofluorometers capable of providing both excitation and emission spectra. As an example, the optical design of one of these, which employs two grating monochromators, is shown in Figure 1.2 (Skoog & Leary, 1992). Radiation from the first monochromator is split into two parts; the first part passes to a reference photomultiplier and the second part to the sample. The resulting fluorescence radiation, after dispersion by the second monochromator, is detected by the second photomultiplier. An instrument such as that presented in Figure 1.2 offers perfectly satisfactory spectra for quantitative analysis. However, the emission spectra obtained will not necessarily compare favourably with spectra from others instruments, because the output depends not only upon the intensity of fluorescence but also upon the characteristics of the lamp, detector, and monochromators (Skoog & Leary, 1992). All of these instrument features vary with wavelength and differ from instrument to instrument. A number of methods have been developed for obtaining a corrected spectrum, which is the true fluorescence spectrum which is free from instrumental effects; many of the newer and more sophisticated commercial instruments provide a means for obtaining corrected spectra directly.

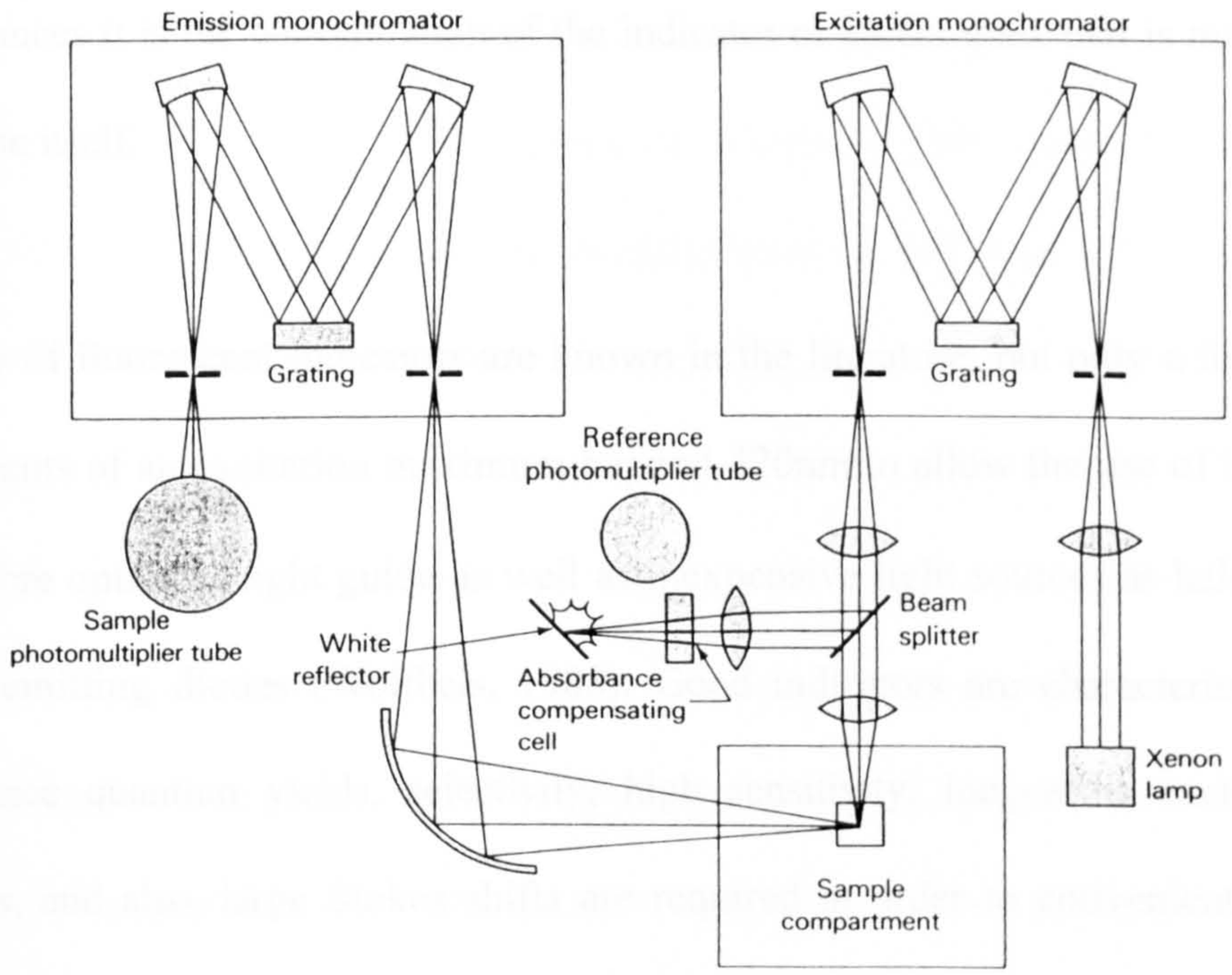

FIGURE 1.2 A schematic diagram of a commercial spectrofluorometer (Skoog & Leary, 1992).

1.2.9 Fluorescent Indicators

Fluorescent indicators provide distinctly improved sensitivity (which is important with minute sensor size) high specificity for the analyte of interest and selectivity because it is unlikely that an interfering species will have the same absorption and emission as the indicator. In the development of optode biosensors, the preparation of suitable sensing layers, fluorescent indicators, is one of the critical steps in order to produce a sensing layer as sensitive as possible (Wolfbeis, 1988). In conventional fluorimetry, a definite amount of indicator is added to the sample of interest, and the change in intensity is then measured and, eventually, compared with data from a calibration curve. In an optode biosensor, the indicator is immobilised on a solid support, and its fluorescence as a function of the

analyte concentration is followed. It should be kept in mind that in these experimental circumstances it is the concentration of the indicator or its complex that is measured, not the analyte itself.

A variety of fluorescent indicators are known in the literature, but only a few meet the requirements of an excitation maximum beyond 420nm to allow the use of inexpensive plastic fibre optics as light guide as well as inexpensive light sources as halogen lamps or light emitting diodes (Wolfbeis, 1988). Good indicators are characterised by high fluorescence quantum yields, selectivity, high sensitivity, long-wave excitations and emissions, and also, large Stokes shifts are required in order to conveniently separate scattered exciting light from fluorescence light with inexpensive light filters (Leiner & Wolfbeis, 1991). Further requirements are the lack of toxicity, photochemical stability, and the presence of functional chemical groups suitable for immobilisation on a rigid support without change the physicochemical constants of the indicator. More popular for the design of fluorescence-based optical biosensors are fluorescent indicators sensitive to ionic and oxygen concentrations (Owen, 1996).

1.2.9.1 Fluorescent pH Indicators

Rapid and continuous monitoring of pH is required practically in all kinds of sciences, including chemical, biochemical and environmental (Leiner & Wolfbeis, 1991). Fluorescent pH-dependent indicators are based on changes of the quantum yield of fluorescence or the spectrum of fluorescence when changes in the pH are produced. At present, over two hundred fluorescence pH indicators are known (Berlman, 1971). Fluorescent pH indicators can be categorised, according to their structures, as follows:

coumarins (i.e. 7-hydroxycoumarin-3-carboxylic acid), *fluoresceins* (i.e. isothiocyanate), *naphthyl and pyrene derivatives* (i.e. HPTS), and *lipophilic pH indicators* (Skoog & Leary, 1992; Leiner & Wolfbeis, 1991; Stadelmann, 1970). A suitable pH indicator for optical sensing should possess the following properties (Wolfbeis *et al.*, 1983; Leiner & Hartmann, 1993):

i) A pK_a-value in the 6 to 8 range, perfectly 7.4.

ii) High fluorescence quantum yield.

iii) High molar absorptivity in order to make optimal use of incident light.

iv) The excitation maximum should lie in the visible part of the spectrum to allow use of lamps rather than the more expensive uv-light sources. Also, fibre optics for visible light are cheaper than those for uv-light. Specifically, the excitation wavelength of the indicator should favourably be beyond 420 nm to allow the use of inexpensive fibres, ideally, it should be at 480 nm or higher to make it LED excitable.

v) A fluorescence maximum beyond 450 nm to minimise interference due to background emissions from biological fluids. This background is usually high at around 340 and 450 nm. In the case of blood, bilirubin fluorescence at 520 nm may also interfere.

vi) Sufficient water solubility.

vii) Fluorescence should not be influenced (e.g. quenched) by other molecules in solution.

viii) Photostability.

ix) A large Stokes'shift between excitation and emission maximum that alows the use of commercially available glass filters without filtering off parts of the incident or emitted light.

x) Large differences in the absorption spectra of dissociated and associated species, thus allowing selective excitation of one species only.

xi) Easy accessibility and reasonable price.

xii) An additional functional group which allows the immobilisation of the indicator in a polymeric support.

Optical pH sensing techniques are capable of measuring extreme values of pH with great precision and sensitivity (Gabor & Walt, 1991). pH optodes are based on pH-dependent changes in the optical properties of a thin reagent (indicator) layer, which reacts reversibly with photons of the sample (Offenbacher *et al.*, 1986; Leiner, 1991). In the most popular design, the pH optodes rely on indicator dyes which are weak electrolytes and that exist in both acidic and basic form in the pH range of interest (e.g. Schulman *et al.*, 1980; Boisde & Perez, 1987; Posch *et al.*, 1989; Schulman *et al.*, 1991). Acids and conjugate bases have different excitation and/or fluorescence properties (Wolfbeis *et al.*, 1983). In 1980, the first fibre optic probe for pH monitoring has been developed based on the use of a dye indicator (Peterson *et al.*, 1980). Microspheres of polyacrylamide containing bound phenol red and smaller polystyrene microspheres for light scattering were packed in an envelope of cellulosic dialysis tubing at the end of a pair of plastic optical fibres. The probe measured pH over the physiological pH range of 7.0 to 7.4 to the nearest 0.01 pH unit, and its diameter was about 0.4 mm.

The fundamental difference between optical techniques and potentiometric measurements of pH is that potentiometric pH determinations depend linearity on the activity of hydrogen ions (Leiner & Hartmann, 1993). Optical measurements are a function of the concentration of the acid and bases forms of the indicator, but not of the

activity of the hydrogen ion. Since the degree of dissociation of the indicator dye is a function of pH, the latter can be determined by measuring the relative concentrations of both forms of the dye, e.g. by absorption or fluorescence intensity. Also, ionic strength, nature of the solution and temperature are known to affect the dissociation constant of weak electrolytes such as pH indicators (Wolfbeis & Offenbacher, 1986; Opitz *et al.*, 1994). The pH error, in pH optodes, caused by ionic strength depends on the type of indicator and matrix used. The resulting errors are particularly significant when the salt composition of the sample solution differs significantly from the calibration solutions or when it changes during measurements. Because of the effects of salt composition of the sample, pH optodes perform best under well-defined sample conditions (Seitz, 1984; Janata, 1987; Edmonds *et al.*, 1988).

As mentioned above, fluorometry offers a broad variety of additional techniques other than intensity measurements, such as measurement of fluorescence lifetime (Aussenegg *et al.*, 1986; Lakowicz & Szmacinski, 1993), energy transfer (Jordan *et al.*, 1987) or combinations thereof. Lifetime-based pH optodes can have particular advantages over other types because of negligible signal drift arising from leaching and bleaching, or fluctuations arising from light-source intensity and photodetector sensitivity (Draxler *et al.*, 1993; Draxler & Lippitsch, 1996; Thompson & Lakowicz, 1993; Moreno-Bondi *et al.*, 1990a).

1.2.9.2 Fluorescent Oxygen Indicators

Fluorescent oxygen optodes based on the quenching of fluorescence are attracting much attention because there are great demands to measure oxygen in various fields of clinical

analysis, environmental monitoring or process control. In particular, monitoring of oxygen partial pressure is of most importance in medical diagnosis and treatment of critically ill patients in operating rooms and intensive care units, in artificial respiration, in breath by breath analysis and the determination of respiratorial coefficients, and in pulmonary examinations. The phenomenon of quenching of the fluorescence of dyes by oxygen was known since the turn of this century, and had been studied as a means of oxygen measurement in gases by Kautsky and Hirsch in the 1930s (Kautsky & Hirsch, 1935; Kautsky, 1939; Pollack *et al.*, 1944).

Most optical oxygen biosensors described so far are based on dynamic fluorescence quenching of a suitable indicator resulting in a decrease in luminescence intensity of the biosensor material as a function of the oxygen tension (Cox & Dunn, 1985; Bacon & Demas; 1987; Wolfbeis, 1991c). Dynamic quenching of fluorescence of polycyclic aromatic hydrocarbons has been known for a long time, but the effect was not utilised for optical sensors until 1968 when Bergman described the first oxygen fluorosensor (Bergman, 1968). It was based on the measurement of atmospheric oxygen using the fluorescence of fluoranthene adsorbed on Vycor glass or included in a polyethylene matrix, and by adsorption or inclusion the quenching effect was reduced considerably. Recently, the application of such fluorescent probes is being advanced by the development of optical fibres (Li & Narayanaswamy, 1989; Wolfbeis, 1992). Electrochemical oxygen biosensors using amperometry to measure the reduction current of oxygen have been utilised widely, since they are simple and inexpensive (Lee & Tsao, 1979). The advantages of fluorescent oxygen biosensors over electrochemical devices are their applicability in the presence of electromagnetic disturbances and the

possibility for micro-type sensors (Ishiji *et al.*, 1994). Since, fluorescent sensors are usually fabricated by coating a polymer film containing a fluorescent probe on the top of an optical fibre, rapid response would be expected in the future because the film can be very thin.

A variety of chemically different indicators have been applied for sensing oxygen (Berlman, 1971). The first type of useful oxygen optodes were based on the use of fluorophores out of the group of polycyclic aromatic hydrocarbons (PAHs) such as pyrene, pyrenebutyric acid, fluoranthene, decacyclene, diphenylanthracene and benzo(ghi)perylene (Liu & Ware, 1993; Schaffar & Wolfbeis, 1990; Trettnak *et al.*, 1988b; Peterson *et al.*, 1984; Wolfbeis *et al.*, 1984). They are suitable indicators because they are efficiently quenched and fairly soluble in silicone (the most frequently used polymer) (Cox & Dunn, 1985; Lee *et al.*, 1987a; Opitz *et al.*, 1988; Leiner, 1991; Peterson & Stefansson, 1991). Also, they are all strongly luminescent and have natural lifetimes to 200 nm, which makes them very amenable to quenching by oxygen.

In addition, they display excellent photostability and this is probably the reason that long-wave absorbing PAHs are still being used in commercial instrumentation. Unfortunately, such fluorophores only absorb light in UV and near-visible range, hence rather expensive light (and heat) sources such as xenon of halogen tungsten lamps are required for fluorescence excitation. Alternatively, a variety of long-wave absorbing dyes such as perylene dibutyrate and heterocyclics including fluorescent yellow, trypaflavin and porphyrins (e.g., chlorophyll) are known to be quenched by oxygen when absorbed on polar materials (e.g. silica gel) (Papkovsky, 1993). They have

favourable absorptions and emissions, but their photostability is generally poor. In addition, fluorescence decay is very fast and quenching graphs are distinctly non-linear.

A third group of indicators are transition-metal complexes of ruthenium, osmium, iridium, and platinum (Bock *et al.*, 1975; Carraway *et al.*, 1991). They have strong metal-to ligand energy transitions and long-lived excited states (up to 5 μs), which makes them useful for lifetime-based oxygen sensors. Specifically, platinum and palladium porphyrins display strong room temperature phosphorescence with high quantum yields and long natural lifetimes, which makes them also useful in optical oxygen sensing (Lee *et al.*, 1993). In contrast to PAHs, they have absorption maxima ranging from 530 to 550 nm. Because their absorption bands are rather small, only a few can be excited with green LEDs. In addition, they are photolabile in suffering from oxidation when illuminated in the presence of singlet oxygen. So far, this has prevented their use in oxygen optodes.

More recently, a frequently used group of oxygen indicators comprising certain luminescent ruthenium(II) complexes having diimin ligands such as 2,2'-bipyridyl, 1,10-phenanthroline and 4,7-diphenyl-1,10-phenanthroline, have been applied for the monitoring of oxygen levels using fibre-optic devices (Klimant *et al.*, 1994; Hartmann *et al.*, 1995; Draxler *et al.*, 1995; DeGraff & Demas, 1994; Xu *et al.*, 1994; Anders *et al.*, 1993; Carraway *et al.*, 1991; Moreno-Bondi *et al.*, 1990b). Their absorption maxima range from 440 to 480 nm and, hence, they can be excited by halogen lamps or blue LEDs only. These complexes are characterised by a relatively high fluorescence quantum yield (0.3-0.6), and more photostability compared to platinum and palladium

porphyrins and, when immobilised in polymer matrices, they are efficiently quenched by oxygen. Also, they are viable probes for measuring oxygen via fluorescence lifetime with a long excited state lifetime (1-5 μs) and a high Stern-Volmer quenching rate constant in the presence of oxygen (Draxler & Lippitsch, 1996; Draxler *et al.*, 1995; Bambot *et al.*, 1994; Orellana *et al.*, 1992; Bacon & Demas, 1987).

1.3 APPLICATIONS OF OPTICAL BIOSENSORS

Optodes offer a wide field of application and are of potential utility in all kinds of analytical sciences including those covered by electrodes at present. Typical areas are pollution and process control (Klainer *et al.*, 1993; Boisde *et al.*, 1988), biotechnology (Andres *et al.*, 1993; Scheper *et al.*, 1994), defence, relative air humidity (Papkovsky *et al.*, 1994), seawater analysis and environmental monitoring (Klainer *et al.*, 1993), clinical chemistry and medicine (Claremont, 1987; Leiner,1991; Narayanaswamy, 1991; Lubbers, 1993) and invasive biomedical techniques (Seitz, 1988; Wolfbeis, 1991a).

A variety of optical sensors for primary pollutants are known to work in principle (Wolfbeis, 1991b; Klainer *et al.*, 1993). Thus, air pollution sensing for industrial applications and environmental research may be carried out with a network of specific optodes connected to a central measurement station by optical fibres. The sensors may be instantaneously concentration-sensitive or be designed for cumulative measurements of the total integrated exposure (fibre dosimeters). Biosensors have been developed for formaldehyde, ammonia (Werner *et al.*, 1995), nitrogen oxides, hydrogen sulphide, sulphur dioxide (Wolfbeis & Sharma, 1988), glucose (Liu *et al.*, 1992; Papkovsky *et al.*, 1993b; Furbee *et al.*, 1994), biological oxygen demand (BOD) (Preininger *et al.*, 1994),

relative humidity of air (Papkovsky *et al.*, 1994) and reactive hydrocarbons. Finally seawater quality and pollution control can be expected to become a major future field of application that is readily compatible with fibre sensing methods.

Possibly the greatest field of application is sensing clinically and biochemically important analytes such as blood gases and electrolytes, metabolites, enzymes, coenzymes, immunoproteins, bacteria and inhibitors (Peterson & Vurek, 1984; Collison & Meyerhoff, 1990; Leiner, 1991, Narayanaswamy, 1991; Mascini, 1992). Optodes for blood analytes are being used and will be used *in vivo* as sensors for the continuous monitoring of the critically ill and as devices for testing blood samples *in vitro* (Lubbers, 1993). Optodes may be used for continuous measurements of critical parameters which give warning of life-threatening trends (Seitz, 1988; Leiner, 1991) such as pH, oxygen, carbon dioxide (Wolfbeis *et al.*, 1988; Moreno-Bondi *et al.*, 1990a; Parker *et al.*, 1993; Weigl *et al.*, 1994), blood-glucose and lactate (Volkl *et al.*, 1981), urea in serum (Xie *et al.*, 1991), Zn(II) ions (Cordier *et al.*, 1995), calcium (Schaffar & Wolfbeis, 1989a; Blair *et al.*, 1994), chloride, potassium and sodium ions (Schaffar & Wolfbeis, 1989b), ionic strength (Lubbers & Opitz, 1983), blood pressure, and using competitive inhibition of an enzyme to quantify substrate concentration like the enzyme alkaline phosphatase (Freeman & Bachas, 1992). Many of these are well established in principle and practice (Gopel *et al.*, 1992; Wolfbeis, 1991b).

1.4 AIM OF THESIS

The aim of this thesis was to facilitate the development of a simple and accurate optical biosensor based on fluorescence quenching for monitoring blood-glucose and lactate,

xanthine and phenols, in clinical and environmental samples, respectively. The technique is based on the enzymatic oxidation of the specific analyte and the use of fluorescent indicators simultaneously, sensitive to pH and oxygen, for the detection of two parameters concurrently, which may enable more accurate detection of the analyte concentration in a single biosensor.

The main areas covered are listed below:

- Spectroscopic studies and characterisation of particular fluorescent pH and oxygen indicators in order to investigate their suitability for the proposed optical biosenor.
- Study of the enzymatic oxidation of glucose using the fluorescent indicators in solutions.
- Study of the enzymatic oxidation of lactate utilising the fluorescent indicators in solutions.
- Study of the enzymatic oxidation of xanthine using the fluorescent indicators in solutions.
- Study of the enzymatic oxidation of phenol using the fluorescent indicators in solutions, and in sol-gel immobilisation.
- Study of immobilisation techniques, with emphasis on sol-gel immobilisation, and implementation of the current optical glucose biosensor using real samples, human serum, during solution experiments.
- The proposal of concepts for hardware design for the realisation of the proposed miniaturised optical biosensor.

CHAPTER 2

INVESTIGATION OF FLUORESCENT INDICATORS

2.1 INTRODUCTION

Spectroscopic investigations were carried out to illustrate the suitability of simultaneous utilisation of a pH-dependent and an oxygen-dependent fluorescent indicators for the development of future fibre optic biosensors based on the phenomenon of fluorescence quenching; HPTS (1-hydroxypyrene-3,6,8-trisulfonic acid) and tris(2,2'-bipyridyl) ruthenium(II) chloride hexahydrate, respectively, were used as the target fluorescent indicators, to investigate extensively the catalytic oxidation of glucose by the enzyme glucose oxidase, and also to apply the same principle in some other biocatalysed oxidations.

The spectral properties (absorption and fluorescence spectra) of each indicator were studied separately, as well as together. The optimum operating conditions of the above systems with respect to concentrations of oxygen, hydrogen peroxide and the pH of the system, as the three parameters varying during an enzymatic oxidation, were established. Experiments were carried out to determine that both of these indicators can be used together in the same solution without altering their individual spectroscopic characteristics, and also to characterise their behaviour with pH changes, and under different concentrations of oxygen and hydrogen peroxide.

2.2 HPTS Indicator

As discussed in Chapter 1, fluorescent pH-dependent indicators are based on changes of the quantum yield of fluorescence or the spectrum of fluorescence when changes in the pH occur. HPTS was chosen among other fluorescent pH indicators because of its major advantages including:

i) high fluorescence quantum yield,

ii) high water solubility,

iii) visible excitation and emission,

iv) large Stokes' shift,

v) its ground-state pK_a in solution is 7.3,

vi) possibility for two wavelength excitation,

vii) very low toxicity, and

viii) the presence of sulphonato groups suitable for easy covalent (Furlinger, 1982; Schulman *et al.*, 1995) and electrostatic (Zhujun & Seitz, 1984) immobilisation (Leiner & Wolfbeis, 1991; Leiner & Hartmann, 1993).

In addition, several fluorescent indicators have been used to sense pH in the physiological range, of these, HPTS seems to offer the best combination of characteristics for physiological pH sensing (Wolfbeis *et al.*, 1983; Offenbacher *et al.*, 1986).

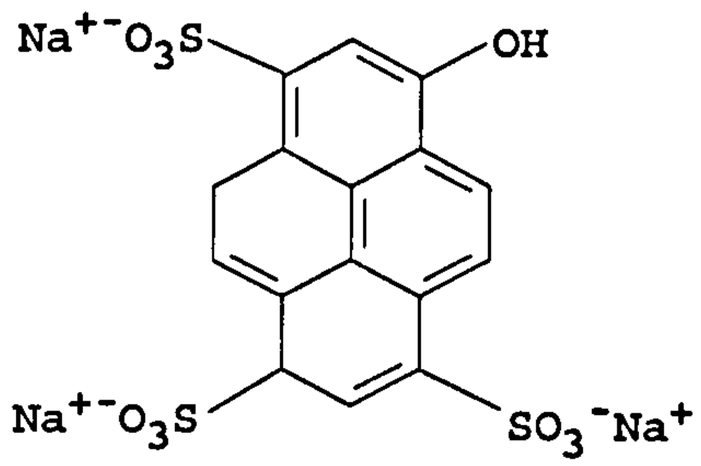

FIGURE 2.1 Structure of HPTS in ground state.

HPTS is a pyrene derivative with the molecular structure shown in Figure 2.1, and can be synthesised according to Tietze and Baeyer (1939). Its molecular weight is 524.4 and this indicator appears as a yellow-green powder. It is a compound with very low toxicity, with 1050 mg/kg LD50 and excretion in urine 89%. In addition, the procedure for determining the binding properties of this dye in blood showed that HPTS was not bound with any protein contained in the blood (Lutty, 1978). Its fluorescence properties were first studied by Forster and later by Weller (Forster, 1950a & 1950b; Weller, 1958).

Most investigations for the development of a fluorescence pH optode were performed using the fluorescent pH indicators, phenol red or HPTS (Seitz, 1988). The first pH fluorosensor presented used HPTS and was obtained by covalent immobilisation of the indicator (as its trisulfochloride) onto amino groups of chemically modified cellulose dialysis membrane (cuprophane) of 8 to 19 μm thickness, and silica beads (μ-BBondapak -NH_2) fixed on solid supports (Furlinger, 1982). In 1984, Seitz and Zhujun obtained a fluorescence optical sensor for quantifying pH values in the physiological range by electrostatic immobilisation of HOPSA (8-hydroxyl-1,3,6-pyrene trisulfonic acid) on an anion-exchange membrane (Zhujun & Seitz, 1984). It allowed the measurement of pH in the range 6 to 8 by relating the ratio of fluorescence intensities emitted at 510 nm and excited at 405 nm (selective for acid form) and 470 nm (specific for base form). The sensor showed an approximately 10% loss in intensity after 4 hours of continuous illumination.

The preparation and performance of two optical sensing materials for continuous measurement of near-neutral pH values were also described (Offenbacher *et al.*, 1986).

HPTS and 7-hydroxycoumarin-3-carboxylic acid (HCC), respectively, were covalently immobilised on surface-modified porous glass (CPG) platelets. Analytical excitation and emission wavelengths were, respectively, 410 and 455 nm for the HCC-based sensor, and 465 and 520 nm for the HPTS-based sensor. On CPG, the pK values (6.8 for HPTS and 6.9 for HCC) were lower than those determined in solution (7.30 for HPTS and 7.01 for HCC). The fluorescence spectra of immobilised HPTS and HCC were similar to those in solution, except for a slight shift to longer wavelengths for HPTS.

Gehrich and colleagues have described a miniaturised fluorescence-based pH sensor designed for *in vivo* applications (along with an O_2 and CO_2) (Gehrich *et al.*, 1986). HPTS was covalently bound to a hydrophilic cellulose matrix attached to the distal end of a single optical fibre. Fluorescence intensity was measured at 520 nm with 460 and 410 nm excitation. These intensities were dependent upon the concentrations of the basic and acid form of the dye. The ratio of the two signals could be related to pH and it was relatively insensitive to optical throughput.

Later, Wolfbeis and colleagues presented a fibre-optic glucose sensor with a pH optrode as the transducer for continuously monitoring glucose concentrations (Trettnak *et al.*, 1988a). They used HPTS as a pH-sensitive dye. They reported that immobilisation of HPTS on the anion exchange material used by Zhujun and Seitz (1984) gave membranes of limited stability; they turned brown after periods of typically one week, particularly when exposed to light. Thus, they used a different anion exchange material which was found in QA 52 cellulose. HPTS, when immobilised on this support, was

stable for prolonged times and firmly retained by the cellulose. Its phenolate form on anion exchange cellulose was maximally excited at 450-470 nm and had a fluorescence peak at about 515 nm. The absorption and emission bands were rather broad and the quantum yield of the dye was close to unity in both the phenol and phenolate form.

A new fibre optic biosensor for urea has been developed, based on immobilised urease coupled to a fluorescence ammonia sensor (Xie *et al.*, 1991). The enzymatically generated ammonia diffused through the membrane into a solution of the fluorescent pH indicator HPTS. This sensor has been used for the determination of urea in serum samples with the suggestion that it could be utilised in clinical applications.

HPTS, covalently immobilised on cellulose attached to a plastic strip, has been used as fluorescent optical pH sensor for the neutral pH region (Schulman *et al.*, 1995). At near neutral pH, HPTS fluoresces green, i.e., from its conjugate base form, exclusively and independent of whether it was excited in its conjugate base form or acidic (phenol) form, or both. However, the fluorescence of immobilised HPTS also varied in the low pH region from about pH 3 to below pH 1, where not only did the green emission almost completely disappear, but also a second (blue) band appeared which could be attributed to the fluorescence of the conjugate acid (phenol). The proton transfer in the lowest excited singlet state which accounts for the variation of the fluorescence in the low pH region was evaluated kinetically. The application of this sensor to measure pH over a wide range of pH values was suggested.

2.2.1 MATERIALS & METHODS

2.2.1.1 Chemicals

The indicator, 1-hydroxypyrene-3,6,8-trisulfonic acid, trisodium salt "high purity" (HPTS) ($C_{16}H_7O_{10}S_3Na_3$), was obtained from Lambda Fluoreszenztechnologie GmbH (A-8053 Graz, Austria). Hydrogen peroxide was purchased from Sigma Chemical Company (Fancy Road, Poole-Dorset) in 30% solution. All other inorganic reagents were of analytical reagent quality and used as obtained from BDH Ltd. (Poole, Dorset). All solutions were prepared with doubly-distilled demineralised water, and solutions of varying oxygen tension were prepared by bubbling the appropriate gas (see Section 2.2.1.3.c) through 20 mM phosphate buffers for at least 15 min.

2.2.1.2 Buffer Solutions

The standard buffer solution was sodium phosphate buffer pH 7.2 at 22 °C with constant the ionic strength (20 mM) (Gomori, 1955), containing 20 mM $Na_2HPO_4 \cdot 12H_2O$ and 20 mM $NaH_2PO_4 \cdot 2H_2O$. The following buffer solutions were used to determine the pH profile of the indicator:

A) Citric acid - Na_2HPO_4 buffer solutions, pH 2.6 - 7.0 (McIlvaine, 1921)

pH 2.6 0.1 M citric acid - 0.2 M Na_2HPO_4

pH 3.0 0.1 M citric acid - 0.2 M Na_2HPO_4

pH 4.0 0.1 M citric acid - 0.2 M Na_2HPO_4

pH 5.0 0.1 M citric acid - 0.2 M Na_2HPO_4

pH 6.0 0.1 M citric acid - 0.2 M Na_2HPO_4

pH 7.0 0.1 M citric acid - 0.2 M Na_2HPO_4

B) <u>Na_2HPO_4 - NaH_2PO_4 buffer solutions, pH 6.0 - 8.0 (Gomori, 1955)</u>

pH 6.0 0.2 M Na_2HPO_4 - 0.2 M NaH_2PO_4; diluted with H_2O

pH 7.0 0.2 M Na_2HPO_4 - 0.2 M NaH_2PO_4; diluted with H_2O

pH 8.0 0.2 M Na_2HPO_4 - 0.2 M NaH_2PO_4; diluted with H_2O

C) <u>Clark and Lubs solutions, pH 8.3 - 9.6 (Bower & Bates, 1955)</u>

pH 8.3 0.1 M KCl and H_3BO_3 - 0.1 M NaOH; diluted with H_2O

pH 9.6 0.1 M KCl and H_3BO_3 - 0.1 M NaOH; diluted with H_2O

D) <u>Borate buffer solutions, pH 9.5 - 10.7 (Bates & Bower, 1956)</u>

pH 9.5 0.025 M $Na_2B_4O_7$ $10H_2O$ - 0.1 M NaOH; diluted with H_2O

pH 10.0 0.025 M $Na_2B_4O_7$ $10H_2O$ - 0.1 M NaOH; diluted with H_2O

pH 10.7 0.025 M $Na_2B_4O_7$ $10H_2O$ - 0.1 M NaOH; diluted with H_2O

E) <u>Phosphate buffer solutions, pH 11.0 - 11.9 (Bates & Bower, 1956)</u>

pH 11.0 0.05 M Na_2HPO_4 - 0.1 M NaOH; diluted with H_2O

pH 11.9 0.05 M Na_2HPO_4 - 0.1 M NaOH; diluted with H_2O

F) <u>Hydroxide - chloride buffer solutions, pH 12.0 - 13.0 (Bates & Bower, 1956)</u>

pH 12.0 0.2 M KCl - 0.2 M NaOH; diluted with H_2O

pH 13.0 0.2 M KCl - 0.2 M NaOH; diluted with H_2O

All experiments were performed at room temperature (22 ± 2 ^{0}C), using 0.03 μM HPTS.

pH measurements were recorded with a research digital pH-METER CG 804, CAMLAB (Schott-Gerate GmbH, Postfach 1130, Germany).

2.2.1.3 Instrumentation

2.2.1.3.a Fluorescence Spectrometer

Fluorescence measurements (excitation and emission spectra) were performed with an LS50 Luminescence Spectrometer, PERKIN ELMER (Perkin - Elmer Ltd., Buckingham). This is a computer controlled ratioing luminescence spectrometer capable of measuring fluorescence, phosphorescence or chemiluminescence and bioluminescence. Instrumental parameters are controlled by the Fluorescence Data Manager software. The light source is a Xenon discharge lamp, equivalent to 20 KW for 8 μs duration with pulse width at half peak height <10 μs.

There are two kinds of detectors, the sample detector and the reference detector. The sample detector gated photomultiplier with modified S5 response for operation to about 650 nm, and interchangeable red-sensitive photomultiplier available for use to 900 nm. The reference detector is a standard sample detector with fixed wavelength. The light passes through Monk - Gillieson type monochromators which cover the following wavelengths:

- Excitation 200 - 800 nm.
- Emission 200 - 900 nm. Standard emission ranges are 200 - 650 nm an 200 - 900 nm with an optional R928 photomultiplier.

The wavelength accuracy is ± 1.0 nm and the wavelength reproducibility ± 0.5 nm. The excitation slits are 2.5 - 15 nm and the emission slits 2.5 - 20 nm can be varied and selected in 0.1 nm increments. The scanning speed can be selected in increments of 1 nm from 10 - 1500 nm/min. The computer can select the following emission filters: 290, 350,

390, 430 and 530 nm; a blank (to act as a shutter), a 1% attenuator and clear beam position. Regarding the sensitivity of the instrument, the signal to noise ratio is 500:1 r.m.s. using the Raman band of water with the excitation at 350 nm and 10 nm excitation and emission bandpass slits.

All experiments were performed at a standard scanning speed value of 1000 nm/min with a standard excitation and emission slit width of 10 nm (Harris & Bashford, 1987). Samples were measured in a standard sample holder with a single position water thermostat holder for 10 mm quartz cuvettes (Hellma Ltd, Essex, SS0 7RA, England). The solutions were prepared immediately before the spectra were taken.

2.2.1.3.b Absorption Spectrometer

Absorption spectra were measured with a BECKMAN DU-8 UV/Visible spectrophotometer (Beckman Instruments, Inc., Fullerton, CA 92634, U.S.A.). This is a single-beam, digital reading spectrophotometer for measuring light levels at specified wavelengths. Light from either of the two sources, tungsten or deuterium, is directed to a single - grating monochromator. The tungsten lamp is used from 315 to 900 nm; the deuterium lamp is used from 190 to 315 nm. Neither lamp emits a constant light output with wavelength; indeed, the radiant energy varies considerably with wavelength. The monochromator consists of: an entrance slit, collimating mirror, grating and exit slit. On the DU-8 Spectrophotometer, optical energy is adjusted by selecting slit width. Different fixed mechanical slit widths can be selected to produce bandpasses of 0.1, 0.2, 0.5, 1.0, 2.0 and 5.0 nm.

All experiments used the standard slit width of 0.5 nm (Denney & Sinclair, 1987). The wavelength accuracy is ± 0.5 nm, the wavelength repeatability better than 0.1 nm throughout operating range with a wavelength resolution better than 0.2nm. The DU - 8 Spectrometer enables the operator to control the level of noise produced by the signal. Therefore as the slit width is increased the instrument reduces gain in order to maintain proper system energy. For example a slit width of 0.5 nm slit width, displays an average of 4 readings at 340 and 280 nm with a precision of ± 0.00005 A at 0.0 A; ± 0.0005 A at 2.0 A; and ± 0.001 A at 3.0A.

2.2.1.3.c Oxygen Analyser

Oxygen and nitrogen of +99.99% purity were supplied under pressure in cylinders from BOC Ltd. (Guildford, Surrey, GU2 3XY, England). Both gases were mixed in a mass flow controller (540A INDUSTRIAL OXYGEN ANALYSER, Servomex Model G, Sybron, Servomex Ltd., Sussex, England TN6 3DU), to yield mixtures of defined oxygen percentage. The gaseous mixtures were dried before entering to the Oxygen Analyser by passing through a flask containing silica gel (BDH). The precision of the mixing device was specified to within ± 1% of the actual value and the repeatability ± 0.005 % O_2. The gases were guided to the sensing membrane via 3 mm-i.d. PVC tubing. All experiments were performed at barometric pressure of about 736 Torr and room temperature of 22 ± 2 °C.

2.2.2 RESULTS

2.2.2.1 Spectroscopic Investigations of HPTS

HPTS dissolved in phosphate buffer to give a fluorescent green coloured solution. The absorption spectrum of a 50 μM solution of this compound is shown in Figure 2.2. The spectrum extended from 200 nm to 700 nm and the maximum absorption occured at 245 nm (a = 1.31) with two shoulders at 203 nm (a = 0.97) and another at 288 nm (a = 1.01). The absorbance then decreased to minimum values at 367 nm (a = 0.71) and 380 nm (a = 0.68), before HPTS absorption peaks again in the visible region at 402 nm (a = 0.95). The variation of absorbance against concentration (0 - 100 μM) is shown in Figure 2.3, and was linear. The excitation and emission fluorescence spectra of HPTS can be seen in Figure 2.4, which indicated that the maximum peak excitation is located at 401 nm and the maximum peak fluorescence was monitored at 510 nm.

Experiments were carried out to establish the dependence of fluorescence intensity of HPTS on the different ionic strengths of the buffer solution. It was found that the change in fluorescence intensity depended on the ionic strength of the buffer solution. When the ionic strength of the buffer solution increased (e.g. 1 M sodium phosphate buffer) then its corresponding fluorescence intensity increased as well, and the opposite took place also. Low capacity buffer solution was used in the following experiments (20 mM sodium phosphate buffer). The spectra showing the decrease in the fluorescence intensity with the corresponding concentrations of HPTS (0.01 - 0.1 μM) are presented in Figure 2.5. The corresponding plot of fluorescence intensity versus indicator concentration is shown in Figure 2.6, which follows a linear regression fit in the analytical range of 0.01 to 0.1 μM HPTS.

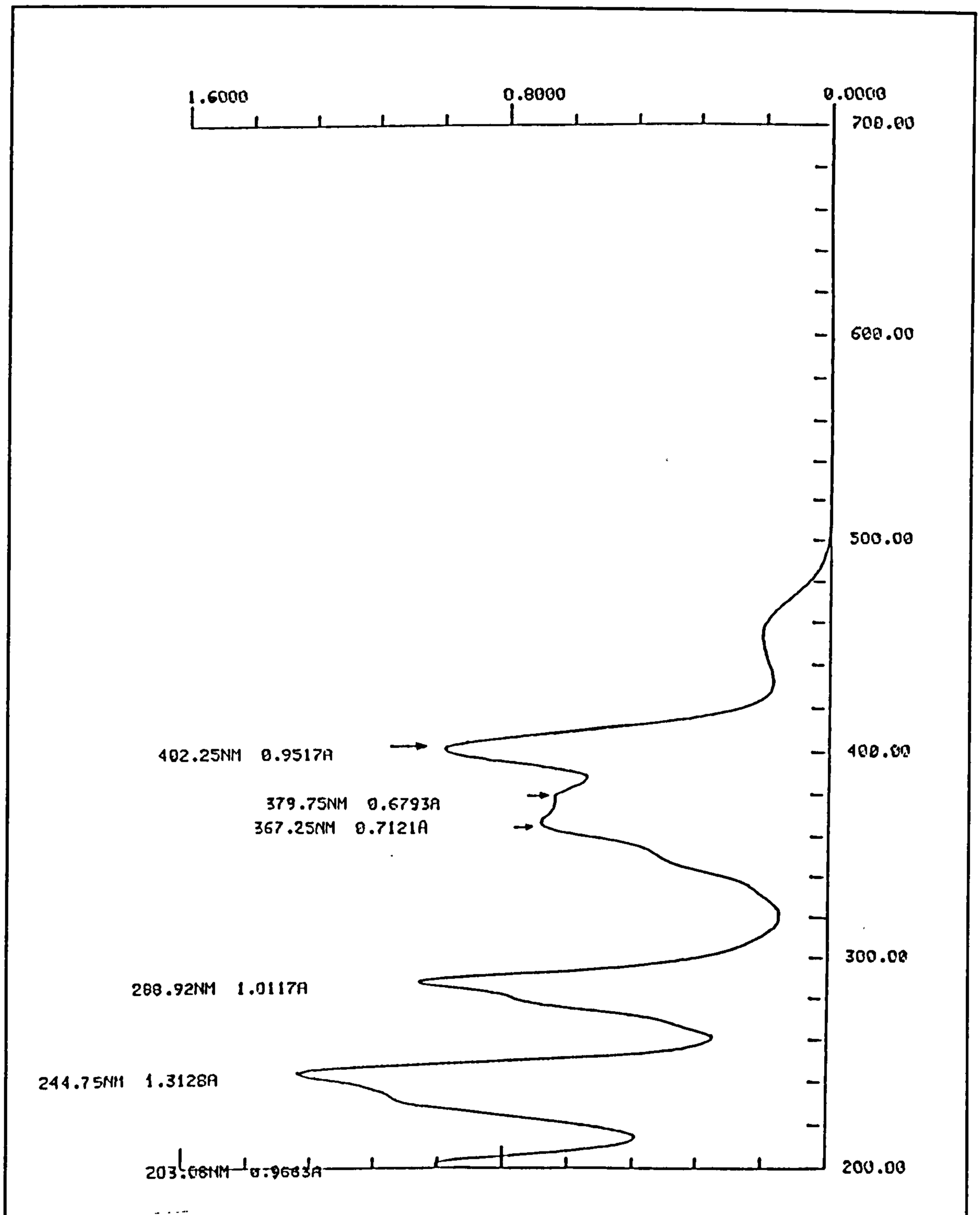

FIGURE 2.2 UV and Visible absorption spectrum of 50 μM HPTS in phosphate buffer pH 7.2 at 22 ^{0}C.

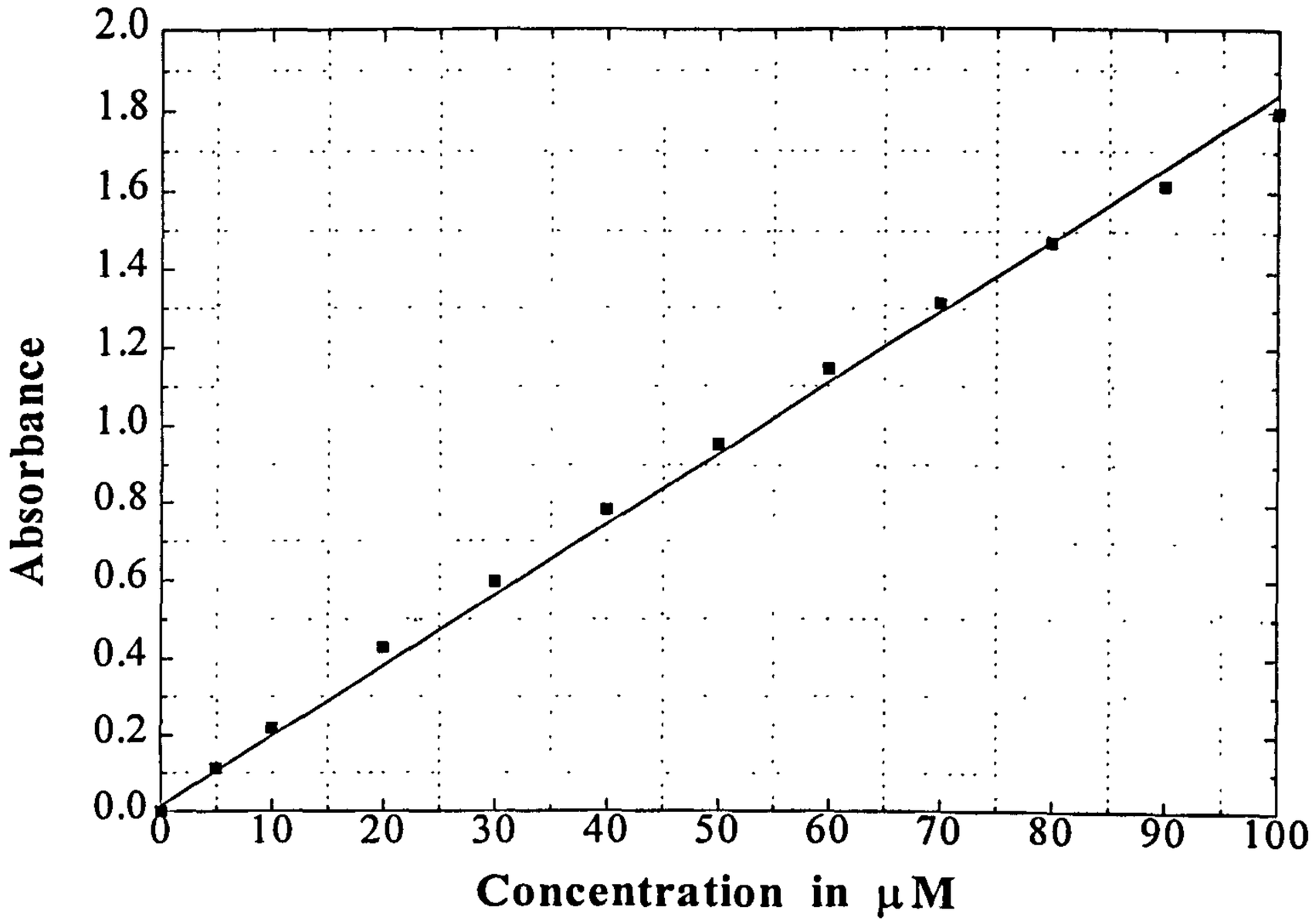

FIGURE 2.3 Absorbance versus concentration of HPTS (0-100 μM), at wavelength of 402 nm in phosphate buffer pH 7.2 at 22 ^{0}C.

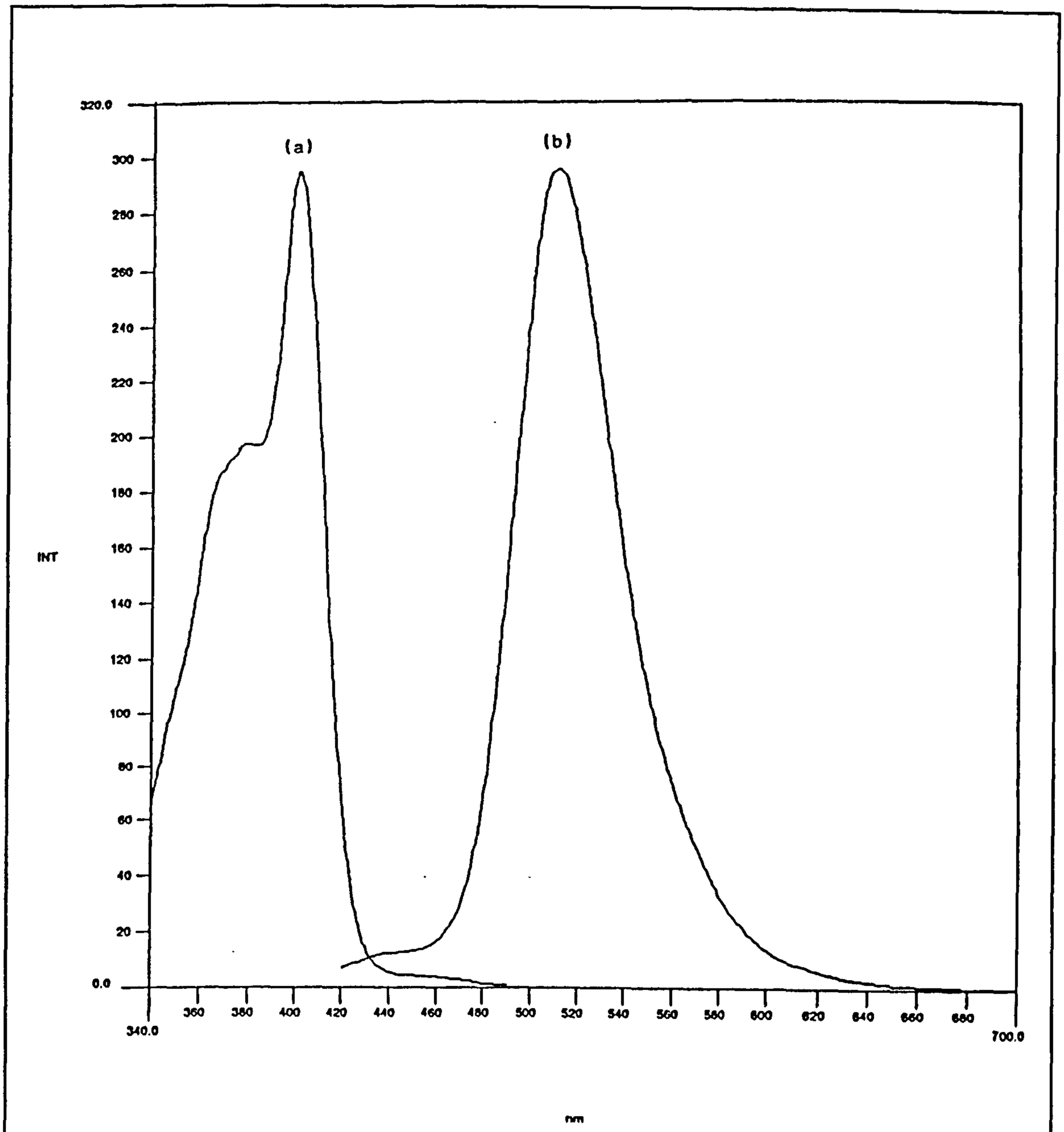

FIGURE 2.4 Excitation (a) and fluorescence (b) spectra of 0.03 μM HPTS with excitation wavelength at 401 nm and fluorescence monitored at 510nm, in phosphate buffer pH 7.2 at 22 ^{0}C.

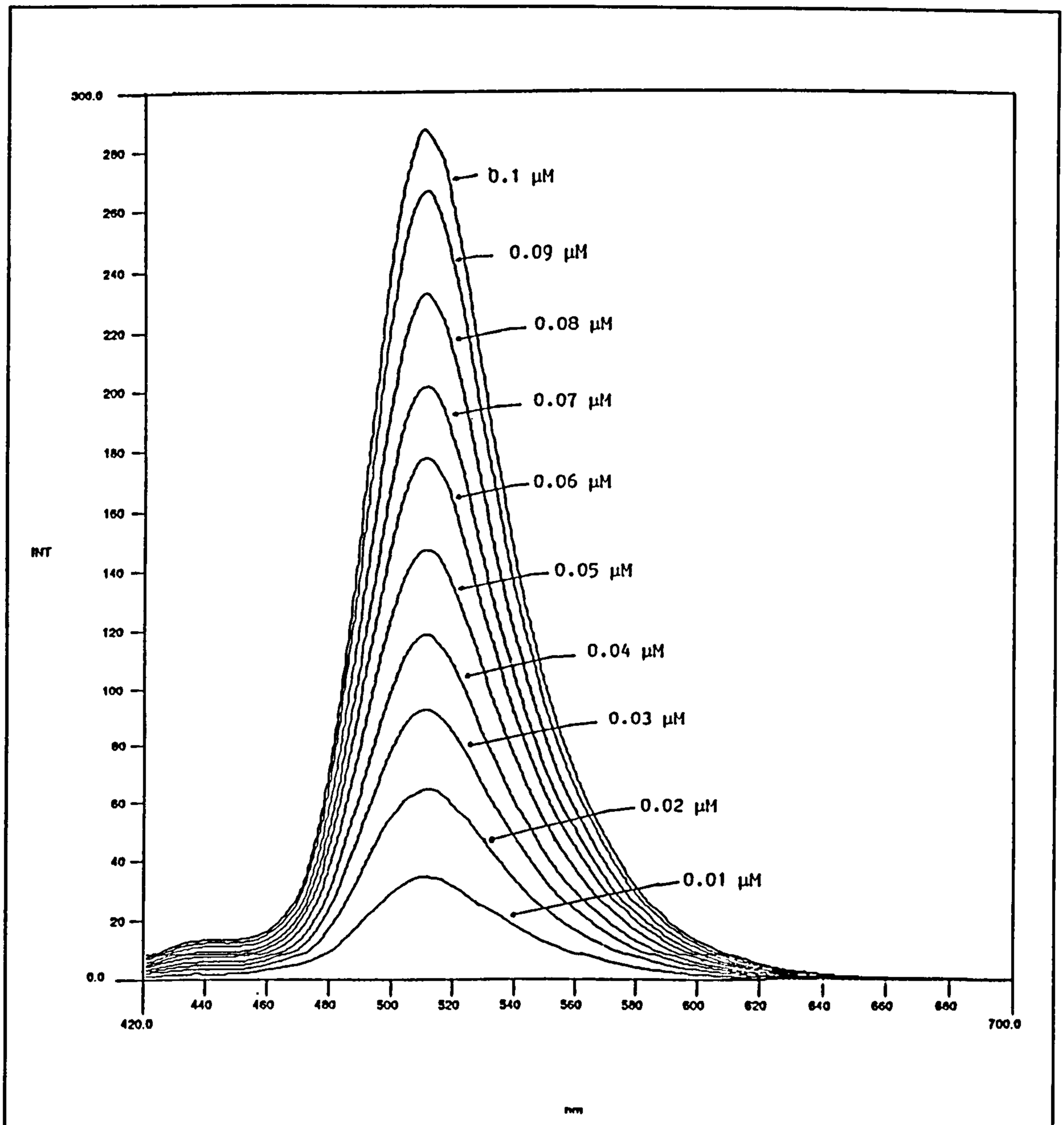

FIGURE 2.5 Fluorescence spectra of HPTS at various concentrations-values (0.01-0.1 µM) in phosphate buffer pH 7.2 at 22 ^{0}C. Solutions were excited with an excitation wavelength of 401 nm.

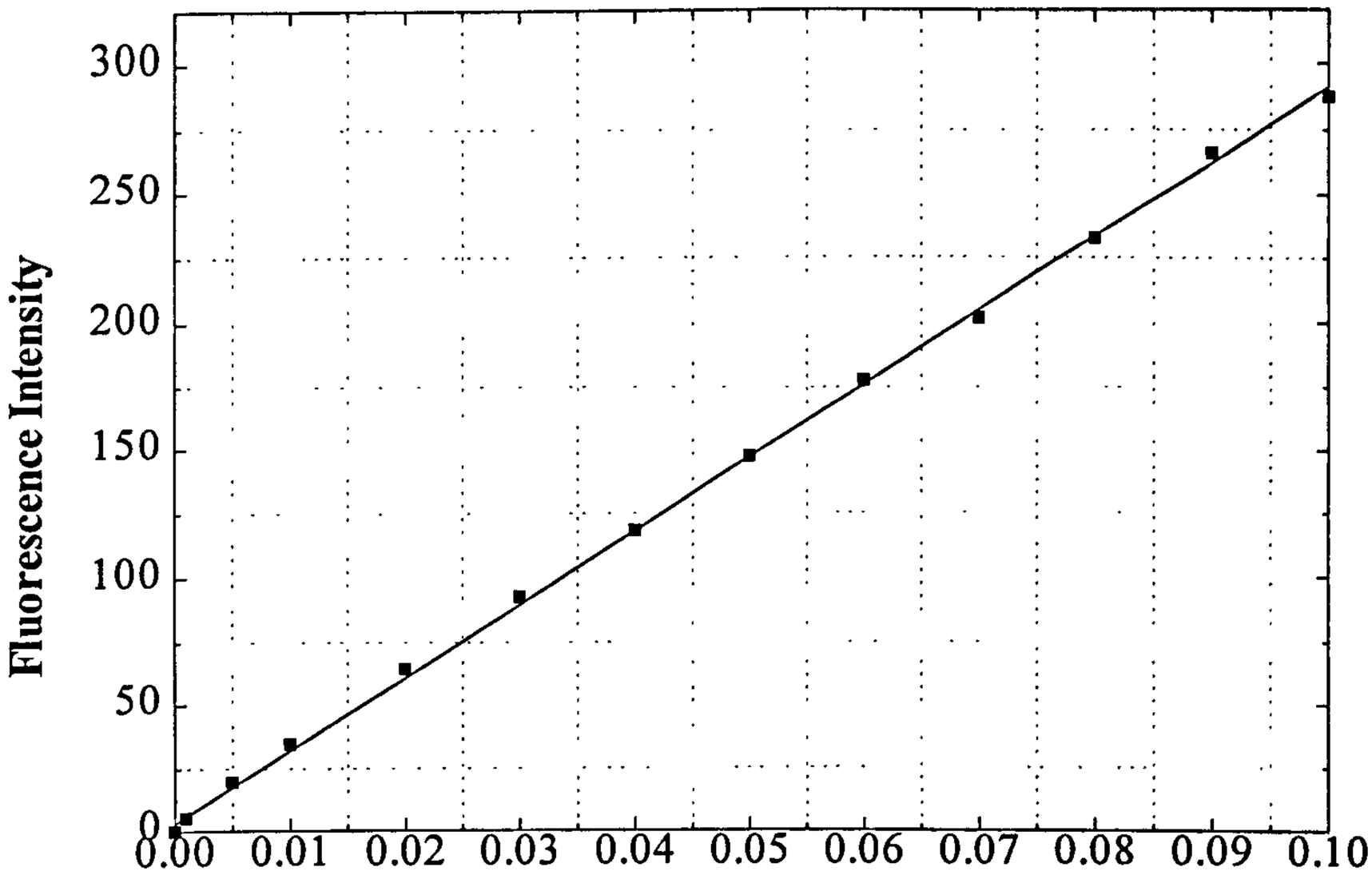

FIGURE 2.6 Concentration versus fluorescence intensity plot of HPTS (0-0.1 μM) in phosphate buffer pH 7.2 at 22 ^{0}C, excitation wavelength 401 nm.

2.2.2.2 Effect of pH changes, Oxygen and Hydrogen Peroxide on HPTS

After the determination of the spectroscopic characteristics of HPTS, the next step was to investigate the behaviour of the indicator in response to changes in pH of the buffer solution, and to different oxygen and hydrogen peroxide concentrations. These are the three parameters which change in oxidations catalysed by oxidases, i.e. acid production, oxygen consumption and hydrogen peroxide production.

The fluorescence quenching of HPTS (0.03 μM) is affected by pH when the indicator is in the acid form, and where the solutions are excited with an excitation wavelength of 401 nm. The corresponding variation of fluorescence intensity versus pH, as shown in Figure 2.7, indicates that the maximum fluorescence intensity of HPTS was measured when the indicator was in solution at pH 6. The influence of pH changes on the quenching of HPTS (0.03 μM), when the indicator was in base form, with an excitation wavelength of 455 nm can be seen in Figure 2.8, in this case the corresponding pH profile, shows that the maximum fluorescence intensity occured at pH 10.

The effect of different percentage oxygen concentrations (0 - 100 %) on the fluorescence quenching of HPTS (0.03 μM) is described below. A slight decrease in fluorescence intensity, corresponding to increased oxygen concentration (from 0% - 100%), was observed for 0.03 μM HPTS. On changing from nitrogen to oxygen saturated buffer the fluorescence intensity was diminished only by less than 3%, which is not a significant effect. Therefore, HPTS was practically unaffected by the changes in percentage saturation of the oxygen enviroment.

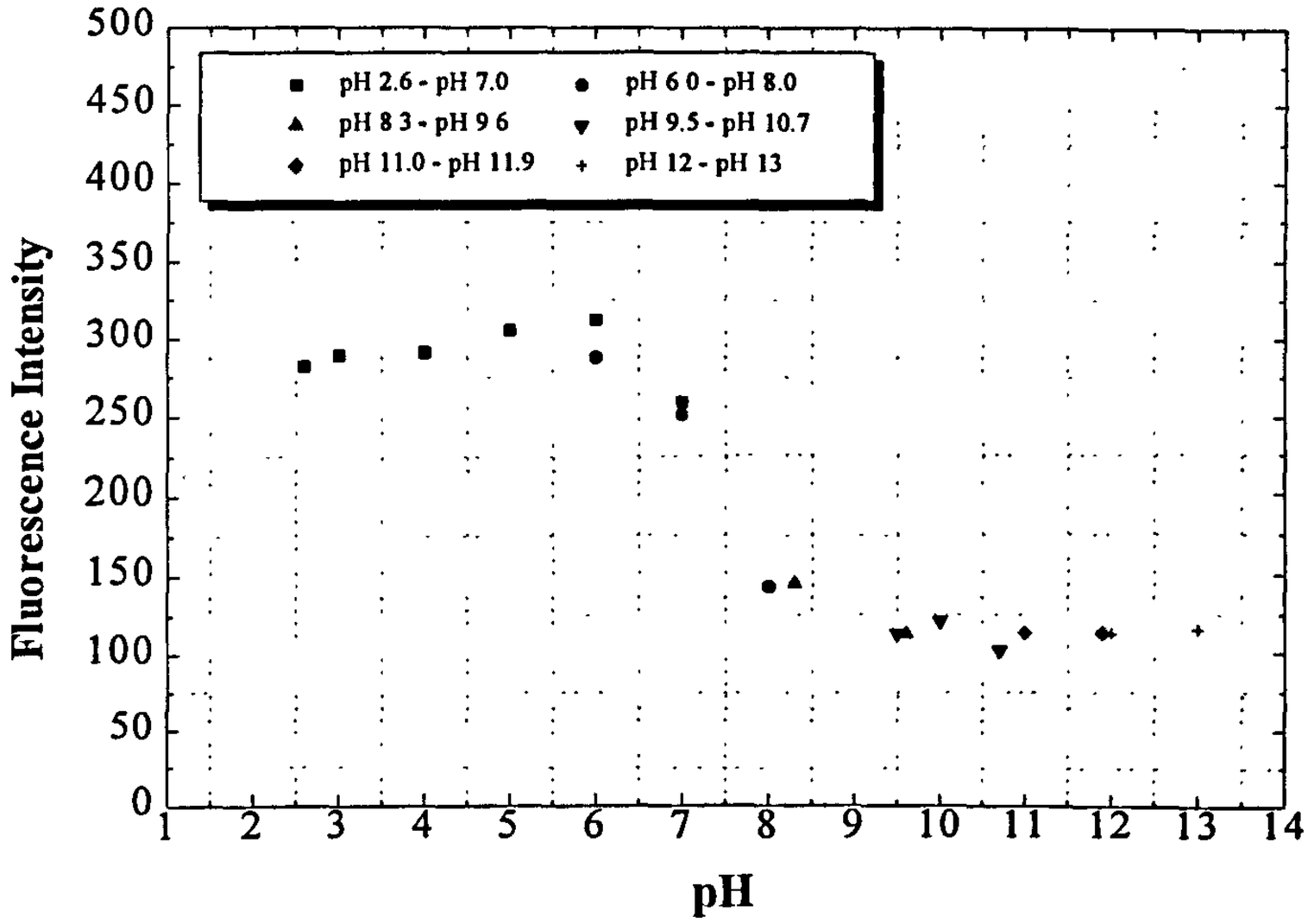

FIGURE 2.7 Plot of HPTS (0.03 μM) fluorescence intensity at 510 nm as a function of the pH-value at excitation wavelength of 401 nm (acid form).

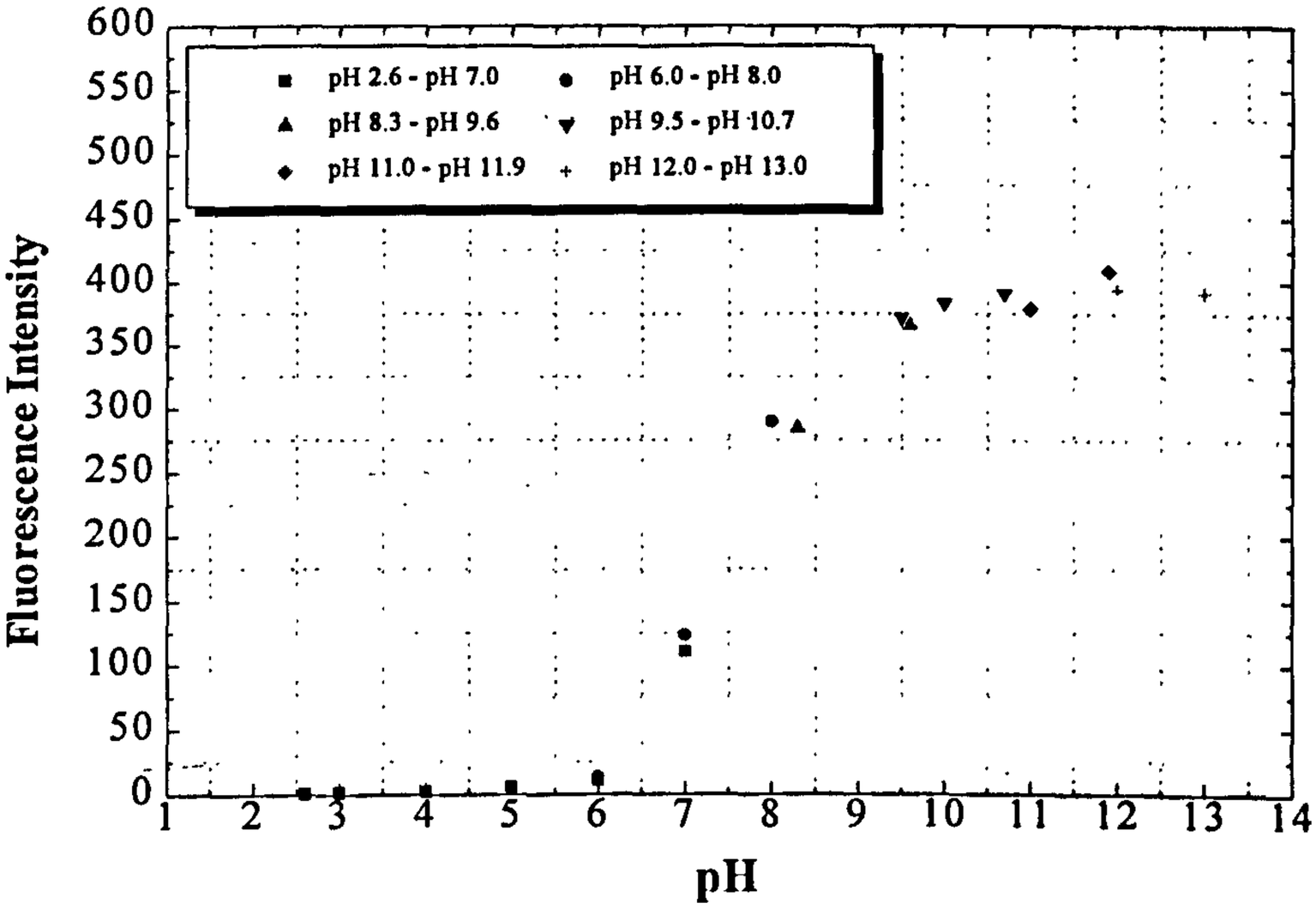

FIGURE 2.8 Plot of HPTS (0.03 μM) fluorescence intensity at 510 nm as a function of the pH-value at excitation wavelength of 455 nm (base form).

Initial experiments were devised to establish the effect of low concentrations of hydrogen peroxide (10 - 100 mM) on the quenching of the indicator, since hydrogen peroxide is produced in low concentration in oxidase-based sensors. The fluorescence intensity of 0.03 μM HPTS decreased very slowly, after taking into account the experimental error due to the use of very small amounts of indicator. Subsequent experiments were performed at higher concentrations of hydrogen peroxide (0.1 - 4.4 M). As previously, there was no significant effect of different concentrations of hydrogen peroxide on the quenching of 0.03 μM HPTS (allowing for experimental errors during the preparation of the indicator solutions). For example, for 0.1 M to 4.4 M concentrations of hydrogen peroxide the quenching of HPTS was only 2.1%.

2.2.3 DISCUSSION

HPTS was found to have a strong absorption in the visible region (λ_{max} = 402 nm) and a strong fluorescence intensity (λ_{em} = 510 nm) when it was excited at a wavelength of 401 nm (acid form) or at wavelength of 455 nm (base form), and also, a large Stokes'shift around 110 nm. These values are close to the published data in the literature. Wolfbeis and colleagues reported an excitation wavelength of 403 nm in acidic solution and 454 nm in alkaline solution for the HPTS indicator; fluorescence was monitored at 512 nm in both cases (Wolfbeis *et al.*, 1983). The published data for HOPSA (8-hydroxyl-1,3,6-pyrene trisulfonic acid) are also similar; excitation wavelengths at 405 and 470 nm for acid and base forms respectively, and emission wavelength at 520 nm (Zhujun & Seitz, 1984). Another study for the construction of a fibre-optic biosensor for urea reported that the basic form of HOPSA could be excited at 470 nm and emitted fluorescence at 518 nm (Xie *et al.*, 1991). Recently, Leiner and Hartmann (1993) published that the deprotonated

form of HPTS bound to cellulose could be excited at 475 nm to give a fluorescence emission at 530 nm; and, this emission increased with increasing pH. The acid form of HPTS could be excited at 410 nm to give fluorescence from the same band as the base form.

The visible excitation and emission wavelengths allow the utilisation of inexpensive light sources, photodetectors and plastic optical fibres for the construction of a biosensor. Also, the large Stokes' shift offers the advantage that scattered excitation light could easily be separated from luminescence. HPTS has a pK_a of 7.30 at 22 °C and of 7.15 at 37 °C, both determined in the same buffer of ionic strength 20 mM, which is close to the pH of blood (7.38) and consequently it can be used for optical measurement of pH in blood or serum. The above values are in agreement with data published by Schulman *et al.* (1995) with the difference that the buffer used had an ionic strength of 160 mM. In addition, the high fluorescence quantum yield of the indicator facilitates the use of very small amounts of HPTS in the order of 10^{-2} μM. According to Figures 2.5 and 2.6, the calibration curve is shown to be linear in the range of the above indicator concentrations. Wolfbeis *et al.* (1983) reported concentrations for fluorescence measurements of HPTS in the analytical range of 0.1 to 10 μM.

HPTS was practically unaffected by different concentrations of hydrogen peroxide, and also, by changes in percentage saturation of the oxygen environment. On changing from nitrogen to oxygen saturated buffer the fluorescence intensity was reduced only by less than 3%. This occurs because of the low fluorescence decay times of HPTS, which are, according to Weller, invariably 5.7 ns in the pH 2-13 range, as opposed for example to

pyrene, which due to its long decay time of 200 ns is strongly quenched by oxygen (Weller, 1958). Similar results have been published which indicated that the fluorescence of HPTS was quenched by only 3.5% on moving from pure nitrogen to pure oxygen, which was considered to be negligible (Wolfbeis *et al.*, 1988). Also, in another previous study, Wolfbeis and colleagues presented that fluorescence intensity of HPTS was diminished by approximately 5% during changes from nitrogen to pure oxygen saturated buffer solution, and therefore, HPTS remained almost unaffected from oxygen changes (Wolfbeis *et al.*, 1983). Similarly, Schulman *et al.* (1995) reported that the fluorescence of HPTS was quenched by approximately 5% in going from pure nitrogen to pure oxygen.

Fluorescence intensity of HPTS was subject to dependence on the ionic strength of the buffer solution. For this reason a buffer solution with low ionic strength of 20 mM was chosen for low concentration of HPTS (e.g. 0.03 μM). This dependence has been subject of a study by Wolfbeis and his colleagues (Wolfbeis & Offenbacher, 1986; Offenbacher *et al.*, 1986). They reported that, in principle, all pH determinations by either photometry or fluorometry are subject to interferences from ionic strength. This is in contrast to pH determinations with the glass electrode, where hydrogen ion activities are measured via a diffusion potential which is independant of ionic strength. In the sensor proposed in the above study, adverse effects of ionic strength were almost completely eliminated by appropriate treatment of the glass surface on which the indicator was immobilised, thereby creating a well-defined and highly charged environment for the indicator.

An interesting feature of the indicator is the possibility of choosing between two excitation wavelengths, each of which results in a different pH response curve (Figures 2.7 and 2.8).

Hence, HPTS may be excited at either 401 nm (acid form) or 455 nm (base form), where fluorescence decreased or increased with pH changes, respectively. The signal differences were much larger under excitation at 455 nm than at 401 nm. Consequently, the existence of two distinct pH-sensitive inflection regions simplifies the translation of measured spectral information into pH and makes HPTS a suitable pH indicator for the construction of an optical fluorescence-based biosensor. This is in agreement with the use of this indicator for the measurement of near neutral "physiological" pH values reported by Wolfbeis *et al.* (1983), Zhujun and Seitz (1984), Offenbacher *et al.* (1986) and Leiner & Hartmann (1993).

2.3 Tris(2,2'-bipyridyl)ruthenium(II) chloride hexahydrate Indicator

The most common type of oxygen optodes are those based on the quenching of the fluorescence of suitable fluorescent probes by molecular (triplet) oxygen. A number of fluorescent indicators for oxygen analysis have been reported, almost all of them were aromatic compounds, which were excited only by ultraviolet light (see Chapter 1). Use of these materials, is limited due to the hazardous effect of the ultraviolet light on the measurement system.

Tris(2,2'-bipyridyl)ruthenium(II) chloride hexahydrate was regarded as an excellent candidate for a fluorescence oxygen biosensor because this dye possesses critical properties for biosensing, including suitable excited state lifetimes, quenching by molecular oxygen and resistance to photodegradation, and also, can absorb and emit in the visible light region. This visible light region indicator can be used for the measurement of

dissolved oxygen in biological systems, and in addition, inexpensive plastic optical fibre can be used as a waveguide (Wolfbeis *et al.*, 1986; Ishiji & Kaneko, 1990; Kaneko *et al.*, 1992; Ishiji *et al.*, 1994; Klimant *et al.*, 1994).

Tris(2,2'-bipyridyl)ruthenium(II) chloride hexahydrate has been proposed as fluorescent redox indicator (Gratzel, 1982). This compound changes its fluorescent emission according to the state of oxidation of the indicator. Typical examples of these indicators are the rhodamine B and 6G, the derivatives of hydroxyphthalic acid, and some other complexes of Ru(II) with tris(1,10-phenanthroline), tris(4,4'-dimethyl-2,2'-bipyridine), 5-methyl-1,10-phenanthroline and 5,6-dimethyl-1,10-phenanthroline. Tris(2,2'-bipyridyl) ruthenium(II) chloride hexahydrate is an azo dye, and its molecular structure is shown in Figure 2.9. It has a molecular weight of 748.63, appears as a red-orange powder in the form of fine crystals and it is easily soluble in water and alcohol, but insoluble in acetone, chloroform, benzene and petroleum (Burstall, 1936).

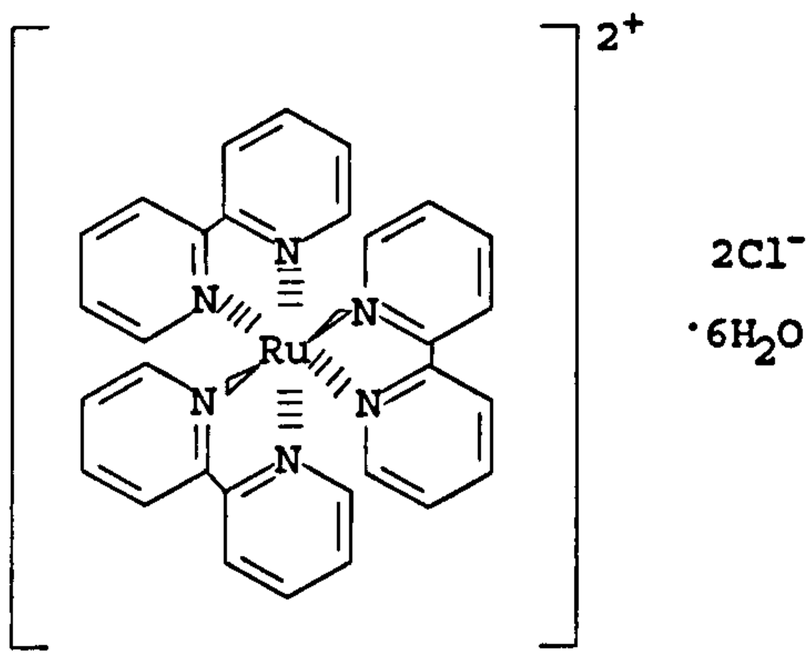

FIGURE 2.9 Structure of tris (2,2'-bipyridyl)ruthenium(II) chloride hexahydrate in ground state.

In 1988, Lippitsch and his colleagues presented a fibre-optic oxygen sensor with fluorescence decay time as the information carrier using as fluorescent oxygen-sensitive indicator tris(2,2'-bipyridyl)ruthenium(II) dichloride hydrate (Lippitsch *et al.*, 1988). The ruthenium complex used had long-term stability with an excitation and emission maxima at 460 nm and 610 nm, respectively, that made it particularly suitable for excitation by the blue LED used. A simple opto-electronic device was described for measuring lifetimes of the long-lived fluorophore with a frequency-modulated LED as light source, and the detection limit was approximately 2 Torr of oxygen.

Another way of utilising the above oxygen indicator has been demonstrated. It is the development of a detection method based on the electrogenerated chemiluminescence of tris(2,2'-bipyridine)ruthenium(II) immobilised in a Nafion film coated on an electrode (Downey & Nieman, 1992). This sensor has been used in flow injection analysis to determine oxalate, alkylamines and NADH, with detection limits 1μM, 10 nM and 1μM, respectively. Emission intensities of the indicator were shown to increase with temperature, and significant amounts were also shown to be capable of storage within the film. The sensor remained stable for several days with suitable storage conditions. Also, the evaluation of use of tris(2,2'-bipyridyl) ruthenium(III) as a chemiluminescent reagent for quantitation in flowing streams has been demonstrated (Lee & Nieman, 1995).

In 1994, a study was presented of the quenching, by oxygen, of the luminescence of tris(2,2'-bipyridine)ruthenium(II) complexes immobilised in thin, transparent, polymer-based films (McMurray *et al.*, 1994). Luminescence lifetimes were studied in relation to oxygen concentration in a gas stream contiguous with the film medium, film thickness and

concentration of the metal complex within the film medium. It was found that the micro-heterogeneous environment of the luminescent complex, which has been implicated in the non-linear quenching responses of polymer-immobilised, transition metal complex oxygen sensors, may have arisen simply as a consequence of the limited solubility of the resulting complex in the film medium. When solubility was limited, the partial precipitation of the complex resulted in a colloidal dispersion of luminescent particles which exhibited non-uniform susceptibilities to quenching by oxygen. Solubility and therefore linear quenching characteristics were promoted by methyl substitution of the bipyridyl ligand and by use of a plasticiser (tributylphosphate) with marked cation solvating powers.

The photoluminecent characteristics of tris(2,2'-bipyridine)ruthenium(II) incorporated into a Nafion film and its quenching by oxygen have been studied (Ishiji *et al.*, 1994). Linear relationships of Stern-Volmer plots were obtained when the indicator/Nafion film was dipped in water and methanol, showing that it could be used as photoluminescent oxygen sensor in these media. The results of emission decay and efficiency of quenching by oxygen indicated that the complex was present at the boundary between the hydrophilic and hydrophobic regions of the Nafion. The lower quenching efficiency in the film than in a solution was explained mainly by the lower oxygen diffusion coefficient in the film.

2.3.1 MATERIALS & METHODS

2.3.1.1 Chemicals

Tris(2,2'-bipyridyl)ruthenium(II) chloride hexahydrate ($C_{30}H_{24}ClN_6Ru{\cdot}6H_2O$) was purchased from Fluka Chemie AG (CH-9470 Buchs - Switzerland). All other inorganic reagents were of analytical reagent quality and used as obtained from BDH Ltd. (Poole,

Dorset). The standard buffer solution was sodium phosphate buffer pH 7.2 at 22 ^{0}C with constant ionic strength (20 mM), containing 20 mM $Na_2HPO_4 \cdot 12H_2O$ and 20 mM $NaH_2PO_4 \cdot 2H_2O$. The same buffer solutions have been used for determination of the pH profile of the indicator, as in HPTS (Section 2.2.1.2). All experiments were performed at room temperature (22 ± 2 ^{0}C) and were prepared with doubly distilled, deionized water. Solutions of varying oxygen tension were prepared by bubbling 20 mM phosphate buffers with appropriate gas for at least 15 min.

2.3.1.3 Instrumentation

The instrumentation used was as described previously for HPTS (see Section 2.2.1.3)

2.3.2 RESULTS

2.3.2.1 Spectroscopic Investigations of Tris(2,2'-bipyridyl)ruthenium(II) Chloride Hexahydrate

Tris(2,2'-bipyridyl)ruthenium(II) chloride hexahydrate was dissolved in phosphate buffer to give an orange coloured solution. The absorption spectrum of a 50 μM concentration solution of this compound is presented in Figure 2.10. The spectrum extended from 200 nm to 700 nm; and the maximum absorption for 50 μM indicator occurred at 275 nm (a = 0.91) in the UV region with another peak in the visible region at 452 nm (a = 0.74). The graphs of absorbance versus tris(2,2'-bipyridyl)ruthenium(II) chloride hexahydrate concentration (0 - 1 mM) at wavelengths of 275 nm and 452 nm are shown in Figures 2.11 and 2.12, respectively. These figures show that the absorbance of this indicator was about 200% greater at a wavelength of 452 nm, than at a wavelength of 275 nm.

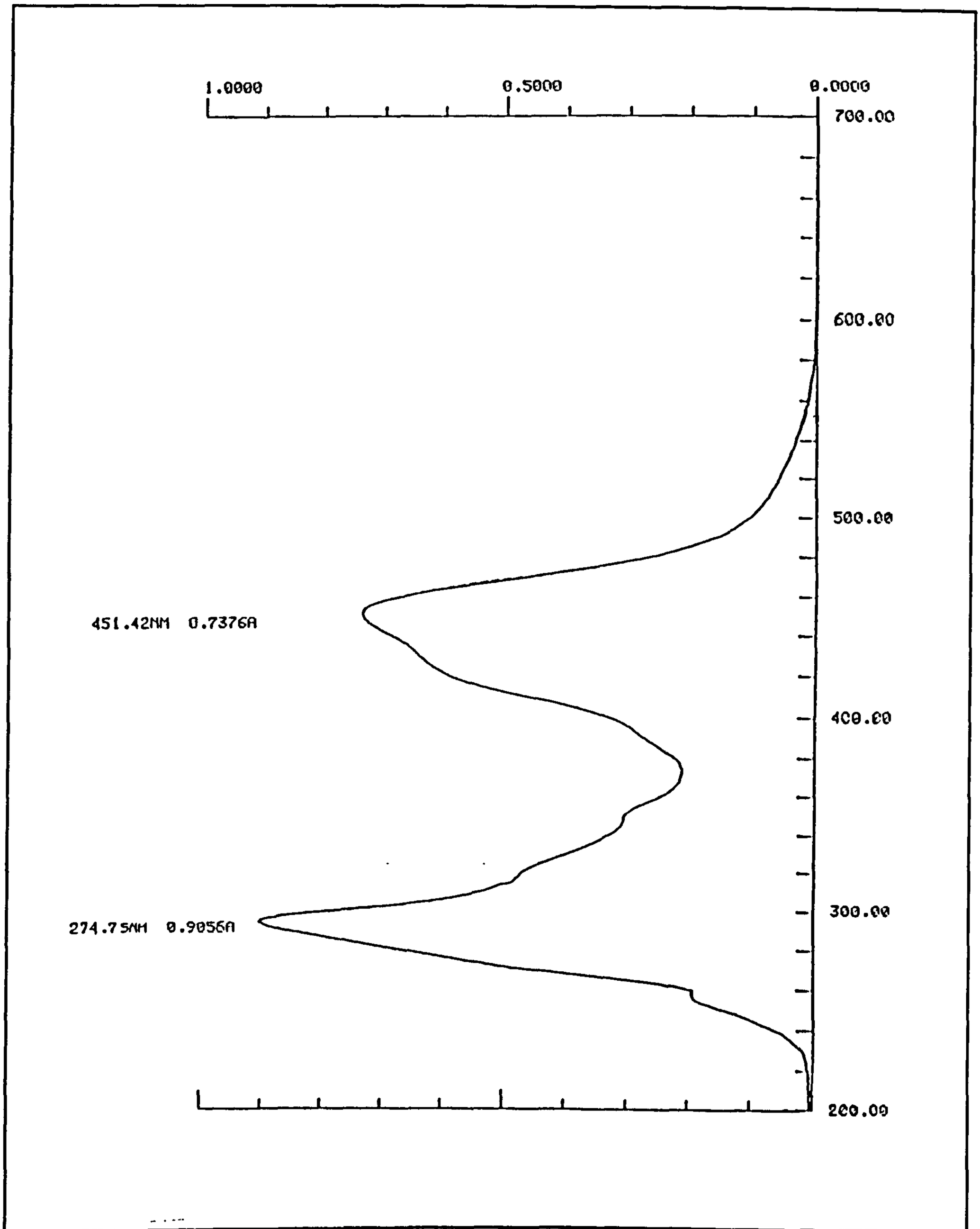

FIGURE 2.10 UV and Visible absorption spectrum of 50 μM tris(2,2'-bipyridyl) ruthenium(II) chloride hexahydrate in phosphate buffer pH 7.2 at 22 ^{0}C.

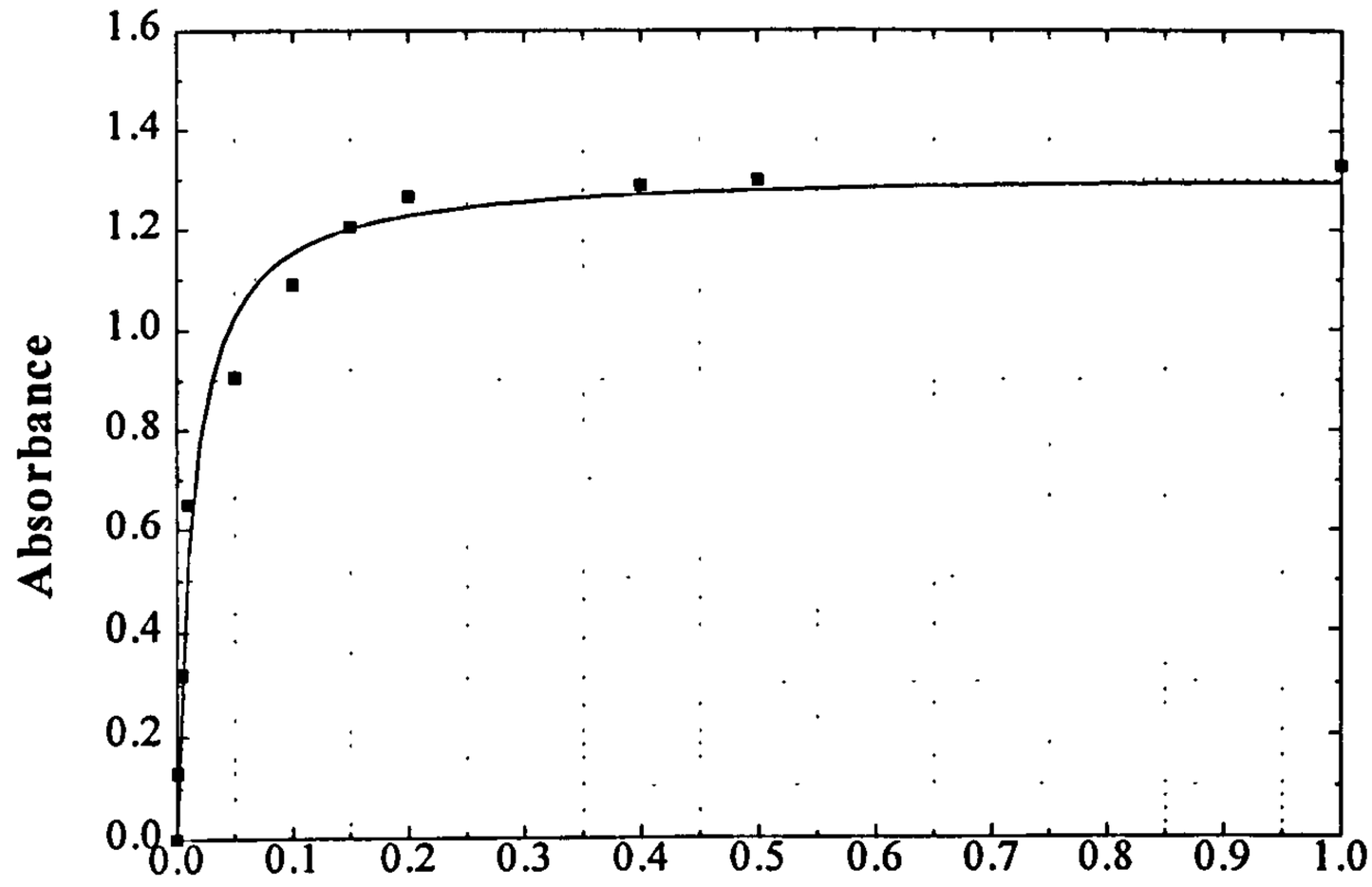

FIGURE 2.11 Absorbance versus concentration of tris(2,2'-bipyridyl)ruthenium(II) chloride hexahydrate (0-1 mM), at wavelength of 275 nm, in phosphate buffer pH 7.2 at 22 ^{0}C.

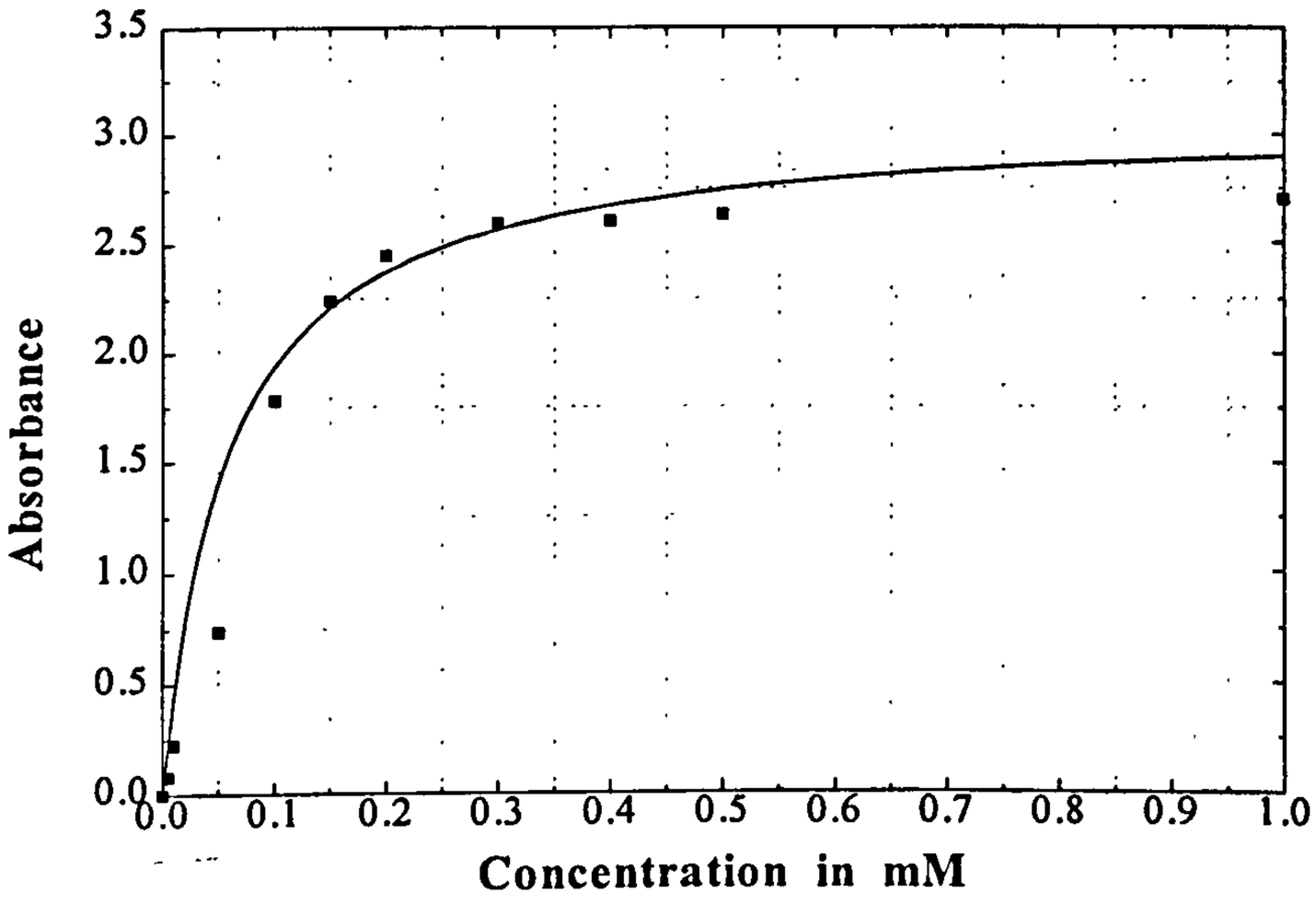

FIGURE 2.12 Absorbance versus concentration of tris(2,2'-bipyridyl)ruthenium(II) chloride hexahydrate (0-1 mM), at wavelength of 452 nm, in phosphate buffer pH 7.2 at 22 ^{0}C.

Futhermore, Figure 2.13, which compares the absorbance at these wavelengths for 0 - 0.1 mM indicator concentration, illustrates that the variation of absorbance against concentration of tris(2,2'-bipyridyl)ruthenium(II) chloride hexahydrate, was only linear at 452 nm. This characteristic was confirmed in Figure 2.14, which shows typical data from an experiment which was repeated five times.

The excitation and emission fluorescence spectra of the above molecule are given in Figure 2.15, from which it can be observed that the peak excitation was located at 456 nm. Excitation radiation of 456 nm was used in the quenching experiments and the emission was monitored at 610 nm. The fluorescence quenching of this indicator for (1 - 100) μM concentrations is presented in Figure 2.16, which shows that the fluorescence intensity was not linear for the above concentrations. However, in comparison with the corresponding absorption spectra, Figures 2.17 and 2.18 indicate that fluorescence intensity followed a linear regression fit in the analytical range of 1 to 10 μM of tris(2,2'-bipyridyl)ruthenium(II) chloride hexahydrate.

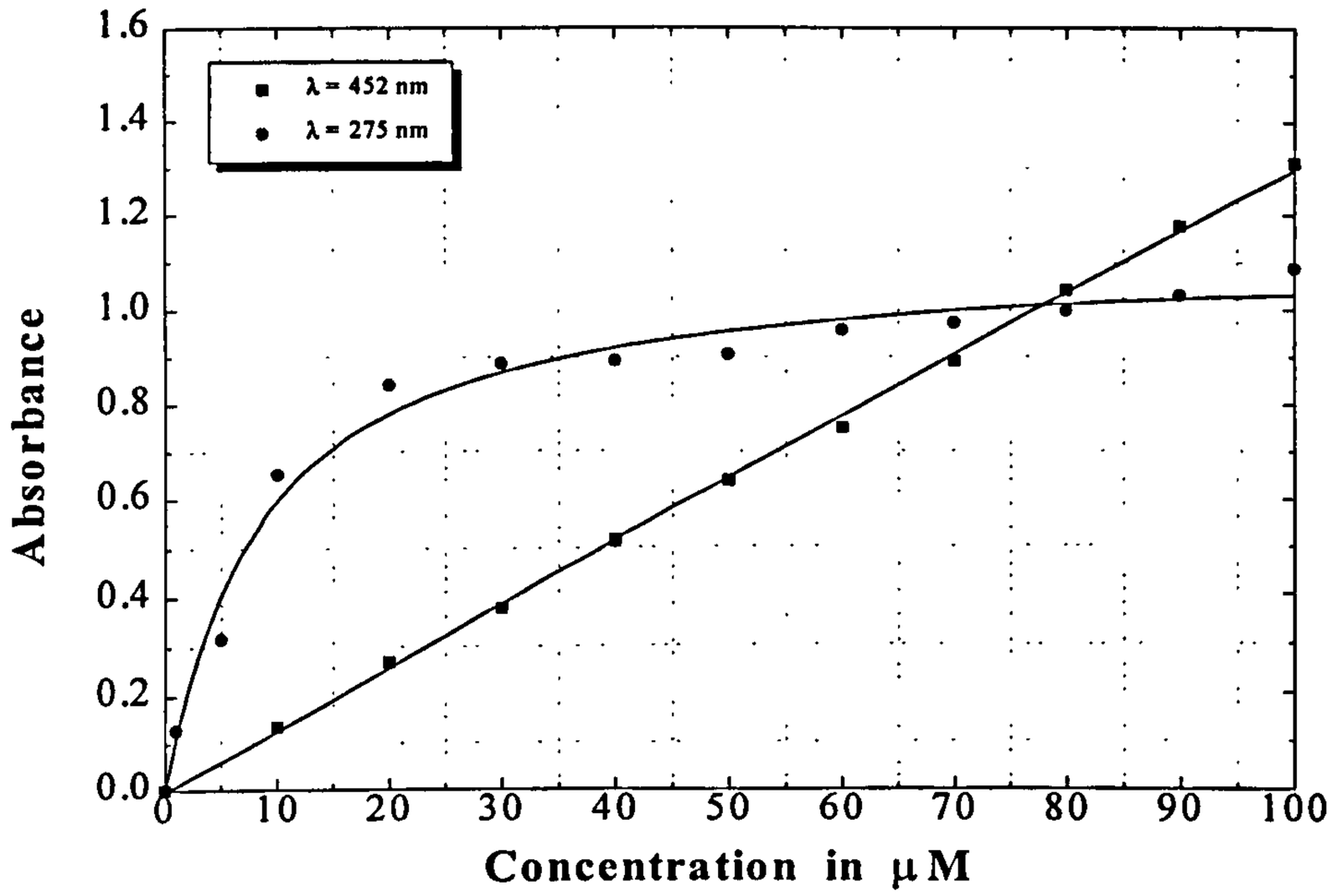

FIGURE 2.13 Absorbance versus concentration of tris(2,2'-bipyridyl)ruthenium(II) chloride hexahydrate (0-0.1 mM), at wavelengths of 275 nm and 452 nm, in phosphate buffer pH 7.2 at 22 ^{0}C.

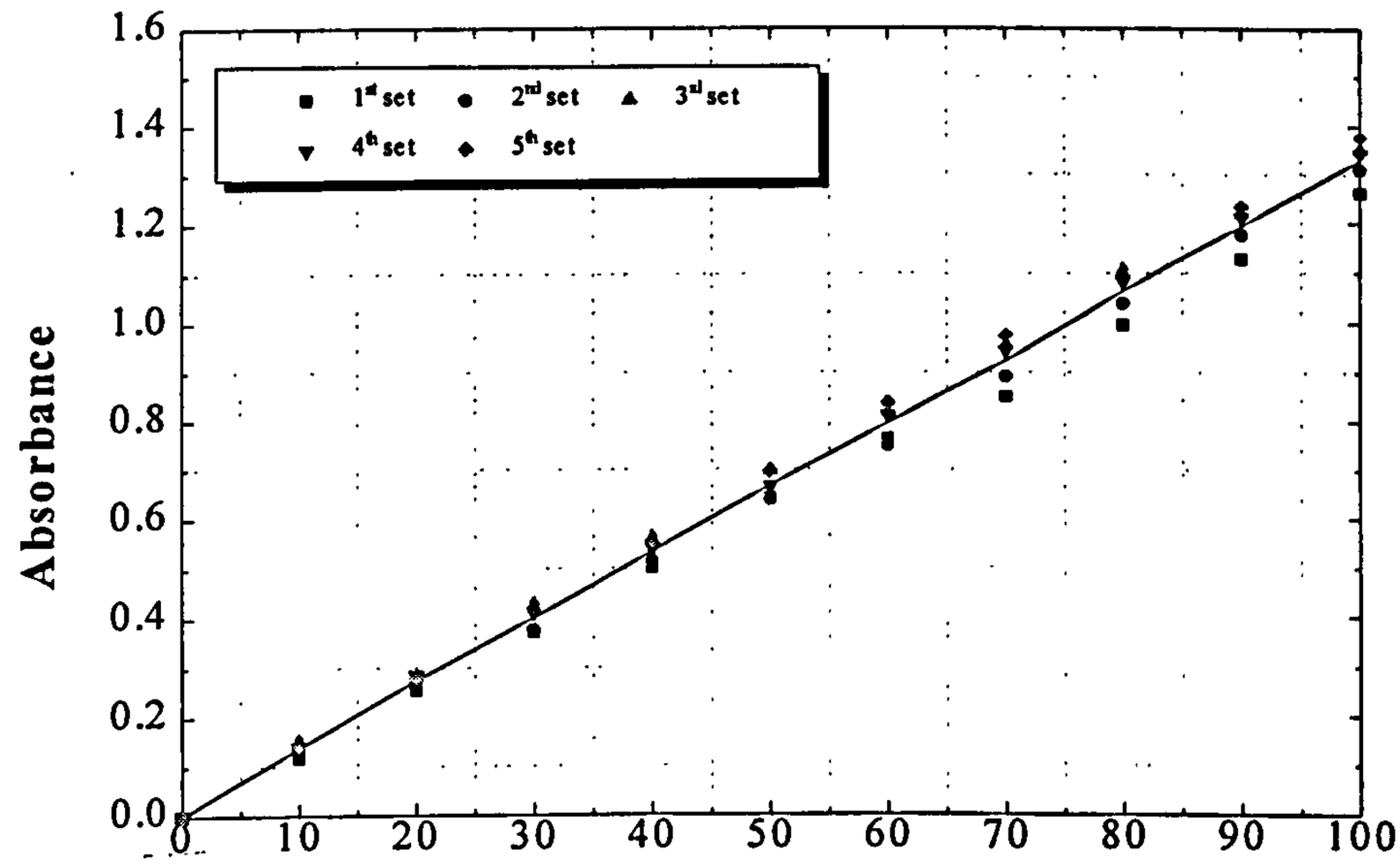

FIGURE 2.14 Absorbance versus concentration of tris(2,2'-bipyridyl)ruthenium(II) chloride hexahydrate (0-0.1 mM), at wavelength of 452 nm, in phosphate buffer pH 7.2 at 22 ^{0}C (results determined 5 times).

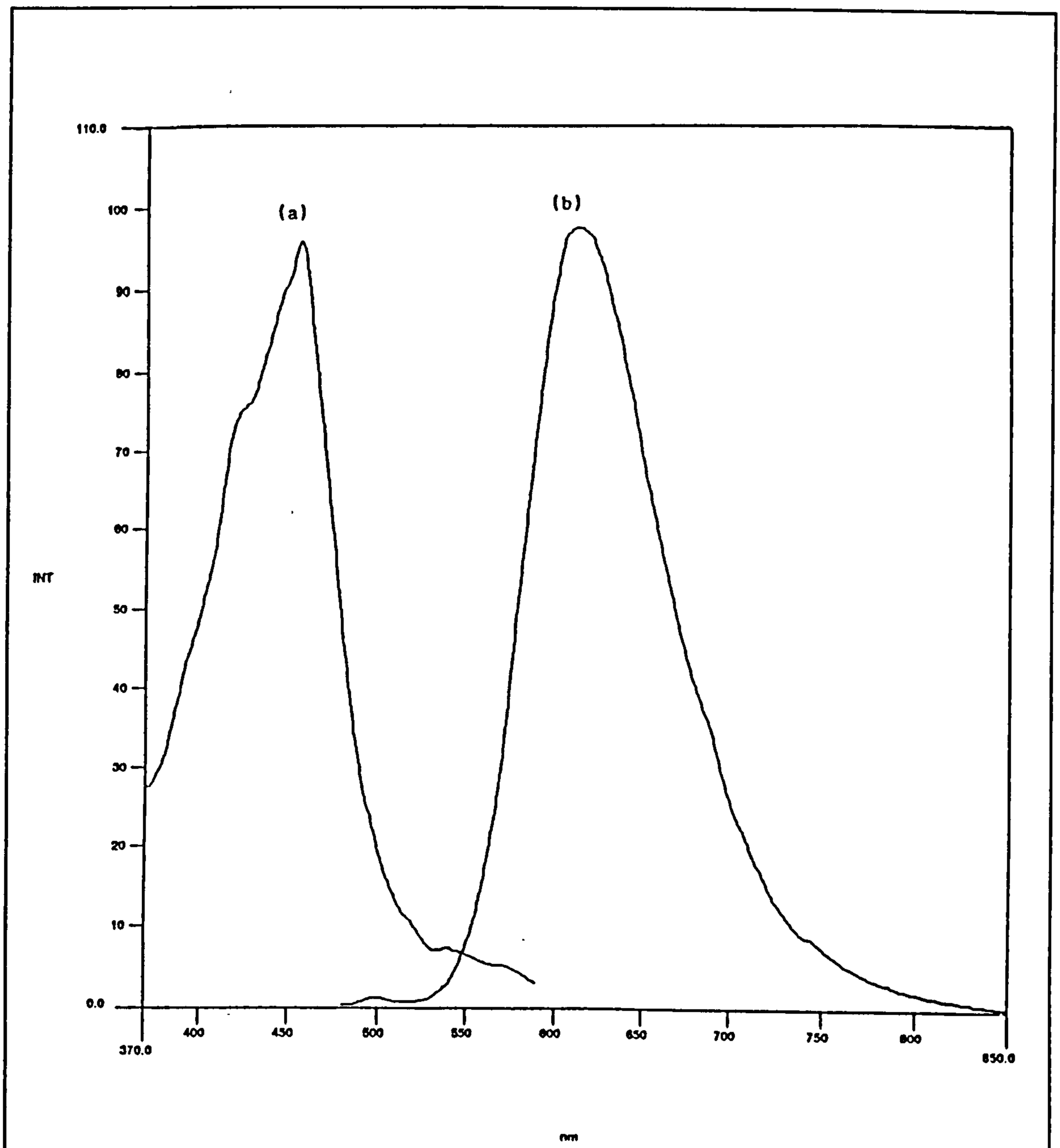

FIGURE 2.15. Excitation (a) and fluorescence (b) spectra of 7 μM tris(2,2'-bipyridyl) ruthenium(II) chloride hexahydrate with excitation wavelength at 456 nm, and fluorescence monitored at 610 nm, in phosphate buffer pH 7.2 at 22 ^{0}C.

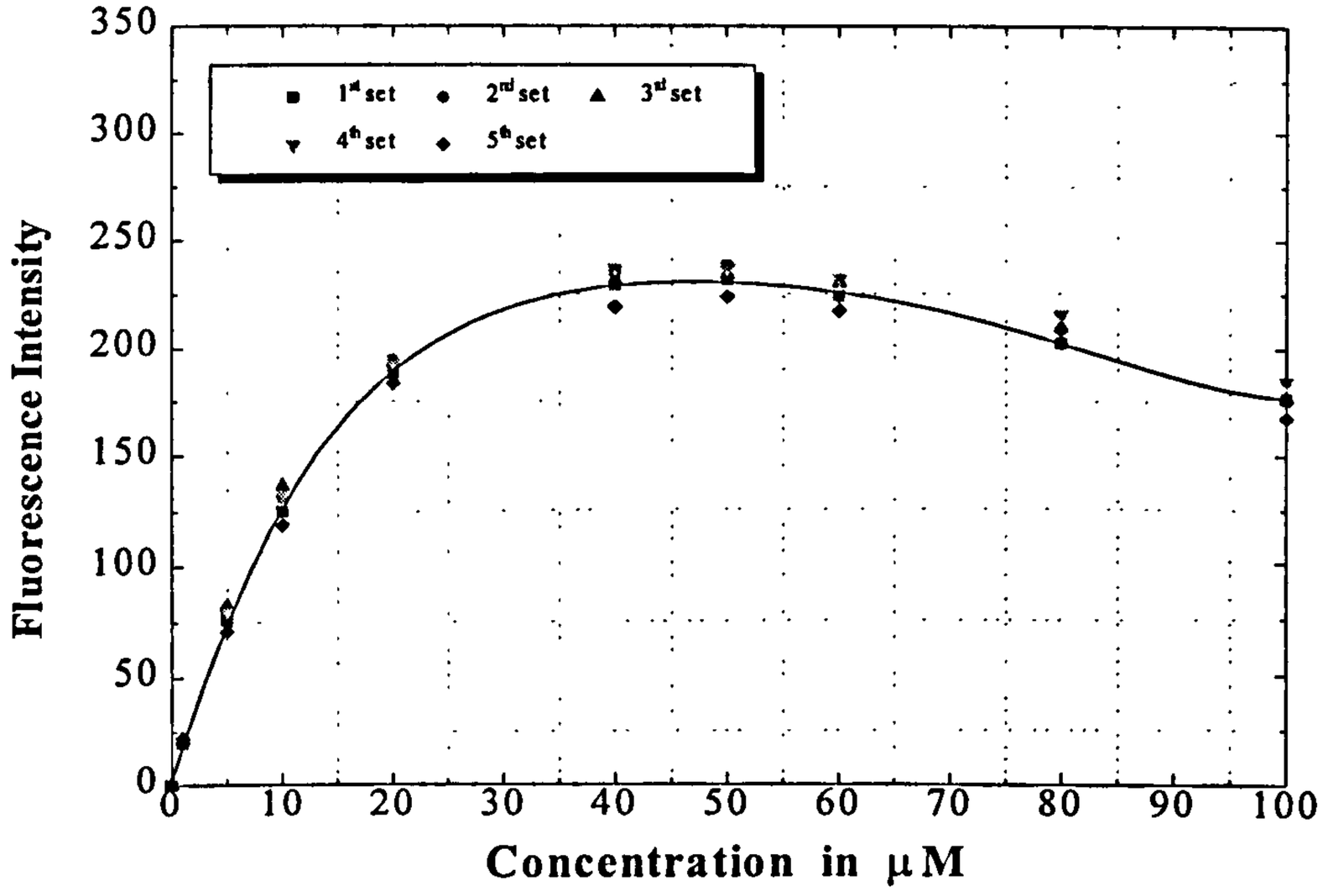

FIGURE 2.16 Fluorescence intensity versus concentration of tris(2,2'-bipyridyl) ruthenium(II) chloride hexahydrate (0-100 μM) in phosphate buffer pH 7.2 at 22 ^{0}C, excitation wavelength 456 nm (results determined 5 times).

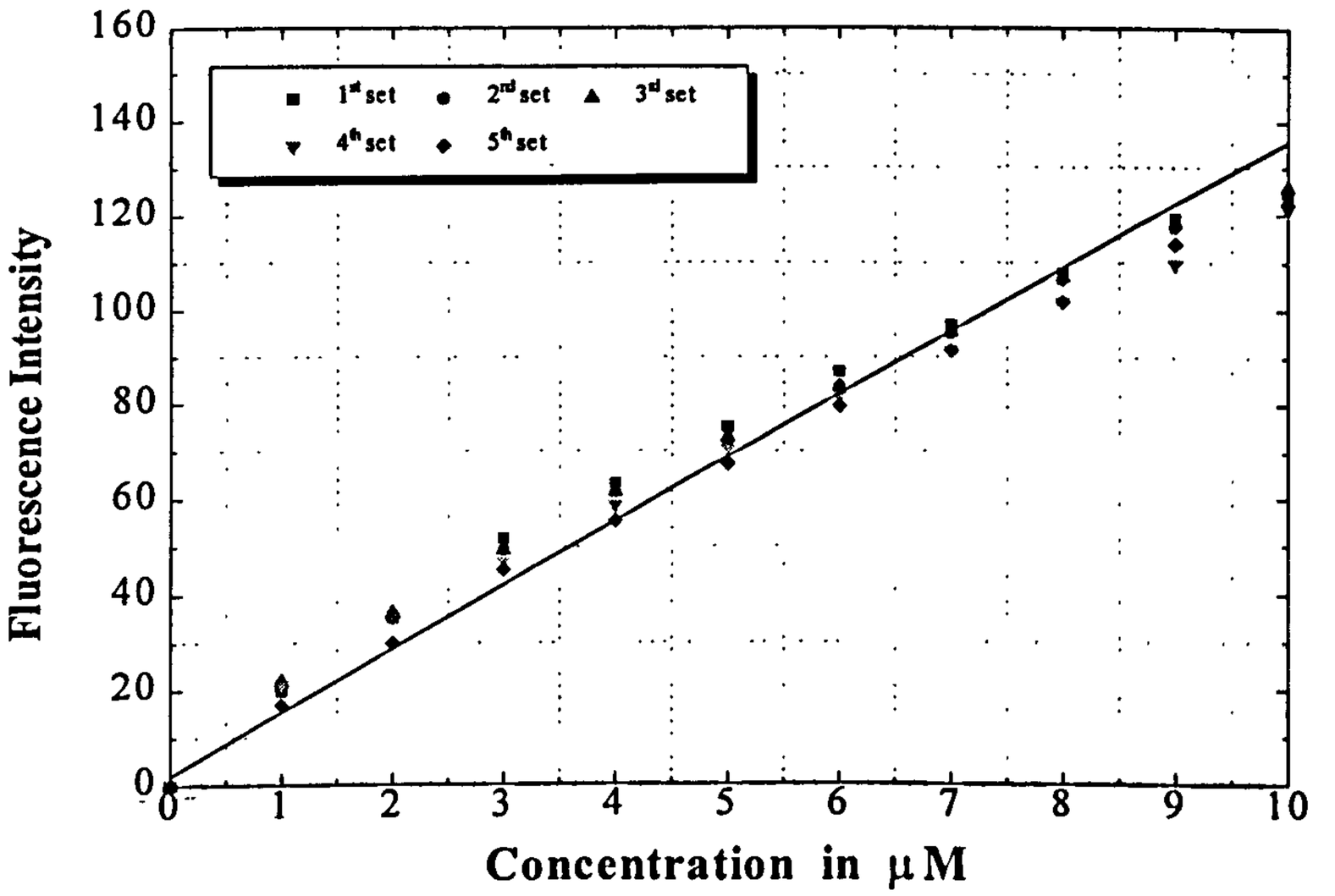

FIGURE 2.17 Fluorescence intensity versus concentration of tris(2,2'-bipyridyl) ruthenium(II) chloride hexahydrate (0-10 μM) in phosphate buffer pH 7.2 at 22 ^{0}C, excitation wavelength 456 nm (results determined 5 times).

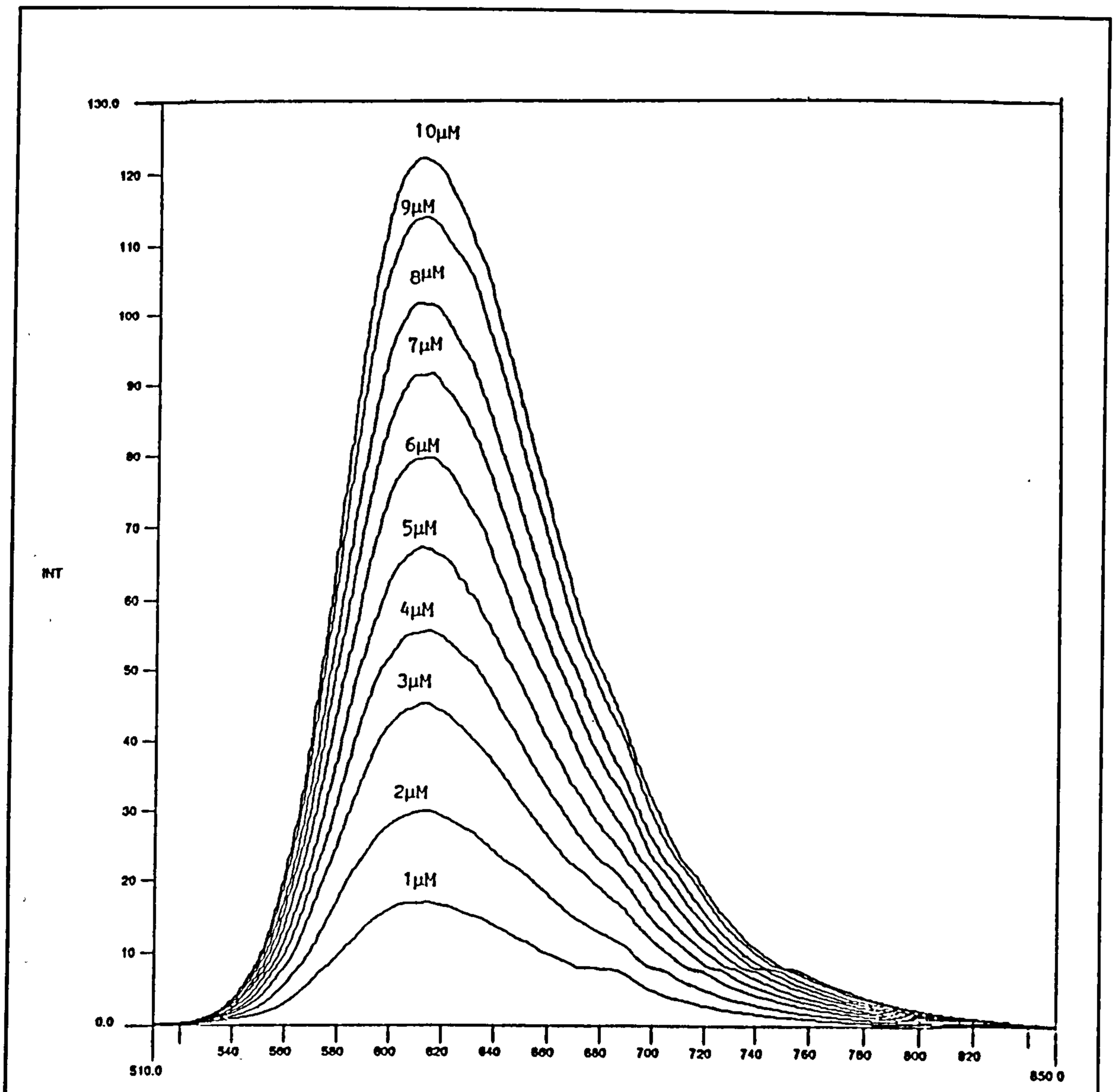

FIGURE 2.18 Fluorescence spectra of tris(2,2'-bipyridyl)ruthenium(II) chloride hexahydrate at various concentrations (0-10 μM) in phosphate buffer pH 7.2 at 22 ^{0}C. Solutions were excited with an excitation wavelength of 456 nm.

2.3.2.2 Effect of pH changes, Oxygen and Hydrogen Peroxide on Tris(2,2'-bipyridyl) Ruthenium(II) Chloride Hexahydrate

The influence of pH changes (pH 2.6 - pH 13) on the fluorescence quenching of the above indicator was extensively investigated using the buffer solutions described in Section 2.2.1.2 and it was found out that the fluorescence of tris(2,2'-bipyridyl) ruthenium(II) chloride hexahydrate was unaffected by pH changes of the buffer solution.

The influence of oxygen, on the quenching of the indicator at a fixed temperature is described below. Initially, the effect of different percentage oxygen concentrations (0-100%) on the fluorescence quenching of tris(2,2'-bipyridyl)ruthenium(II) chloride hexahydrate (7 μM) is presented in Figure 2.19. The most useful range of oxygen between 0% - 30% (i.e., the clinically most interesting range is 7% to 20% oxygen) indicates that the fluorescence quenching of the above indicator decreased substantially, when the added percentage oxygen concentration was increased, (fluorescence intensity decreased from 145 to 90 as oxygen increased from 0% to 30 %). The same phenomenon is illustrated in Figure 2.20, for the complete range of oxygen concentrations from 0% to 100% percentage oxygen concentrations.

As can be observed in Figure 2.20, the rate of quenching of the indicator has been dramatically decreased in the range from 30% to 100% oxygen to about half the value in comparison with the changes which occurred from 0% to 30% pure oxygen. Figure 2.21 shows the corresponding Stern-Volmer plot of the quenching by oxygen of the tris(2,2'-bipyridyl) ruthenium(II) chloride hexahydrate (7 μM), which appears to be linear for all the changes between pure nitrogen to pure oxygen.

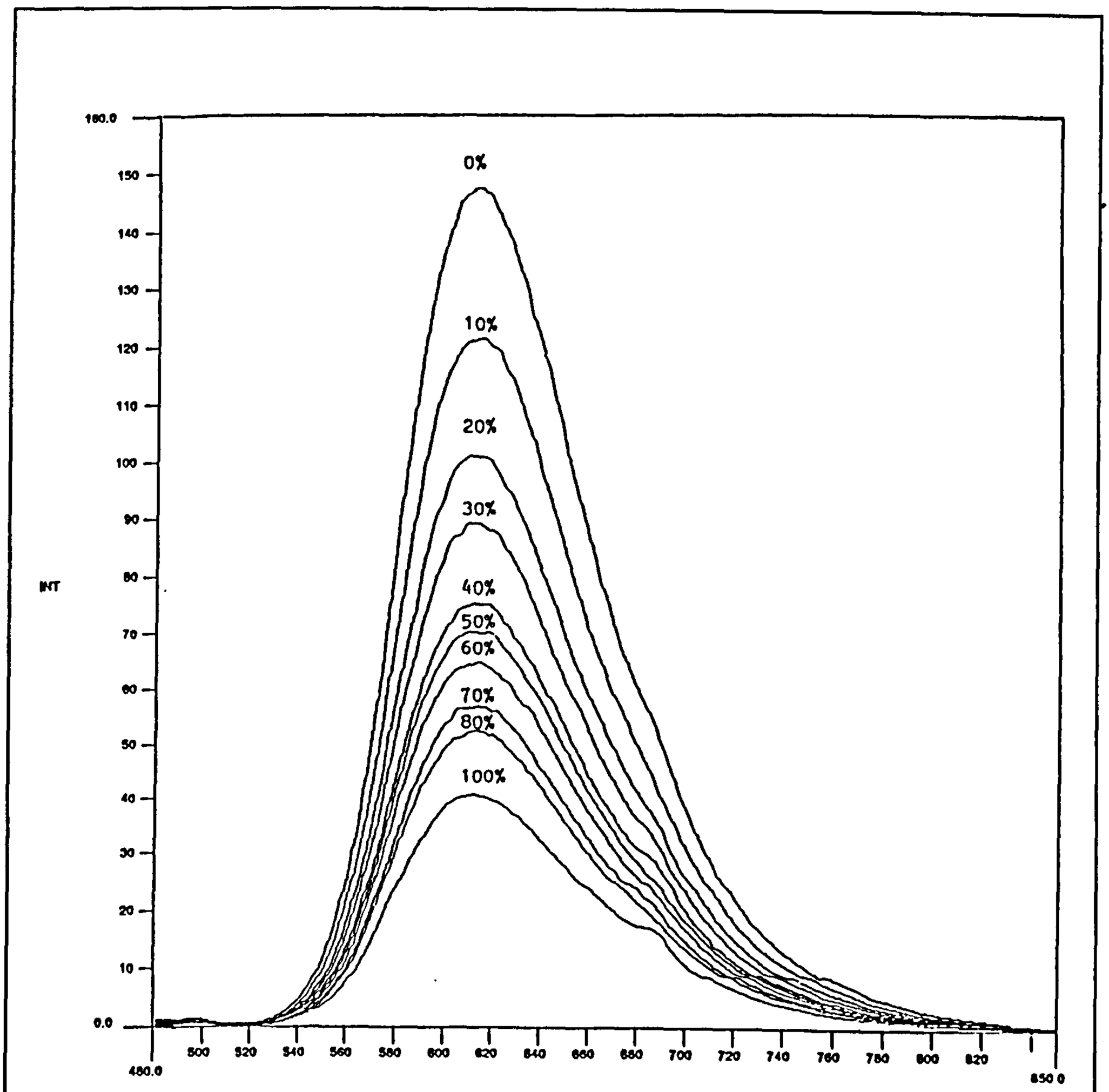

FIGURE 2.19 Effect of different percentage oxygen concentrations on the quenching of tris(2,2'-bipyridyl)ruthenium(II) chloride hexahydrate (7 μM) in phosphate buffer pH 7.2 at 22 ^{0}C. Solutions were excited with an excitation wavelength of 456 nm.

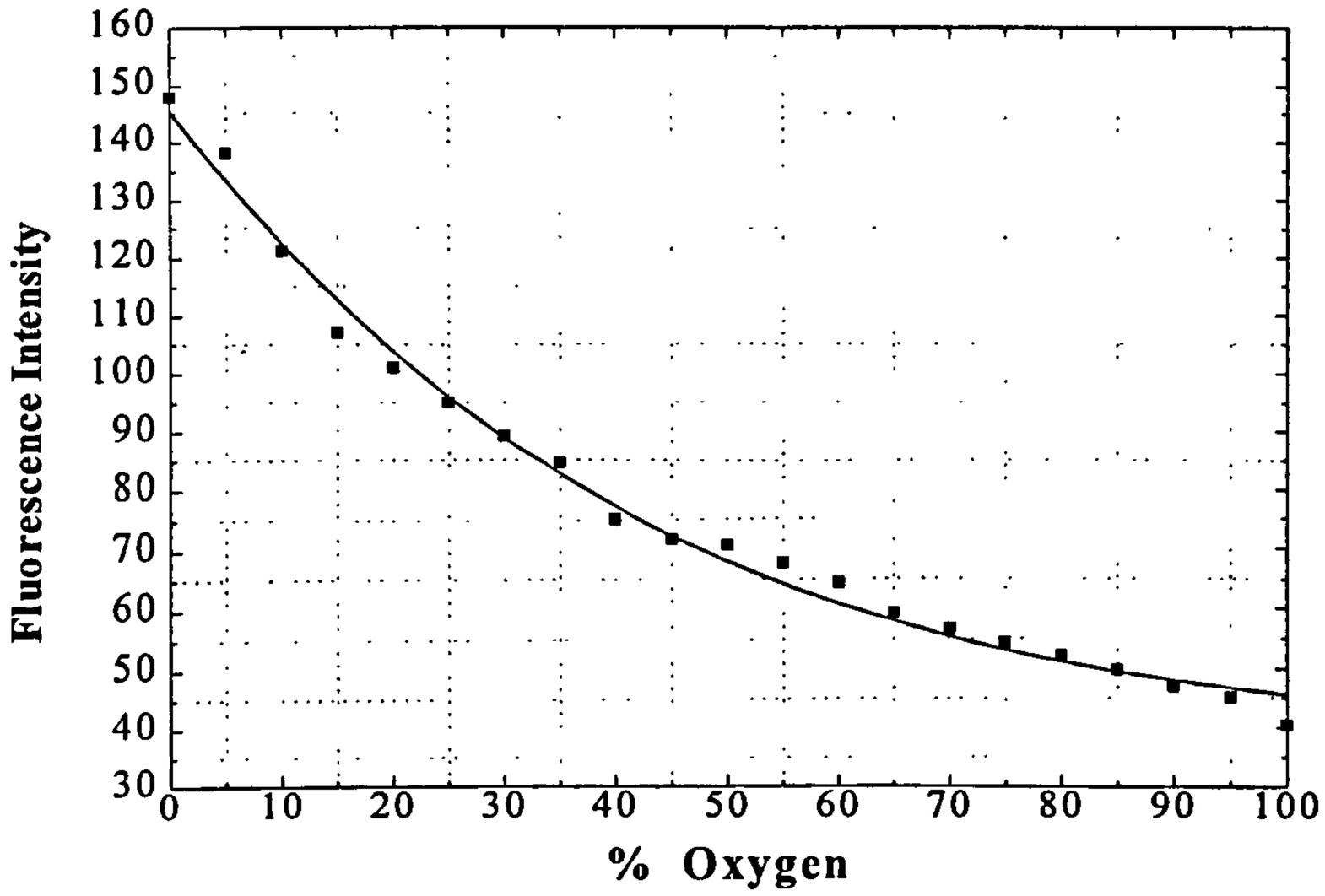

FIGURE 2.20 Fluorescence intensity versus oxygen concentration (0-100%) of tris(2,2'-bipyridyl)ruthenium(II) chloride hexahydrate (7 μM) in phosphate buffer pH 7.2 at 22 ^{0}C. Solutions were excited with a wavelength of 456 nm.

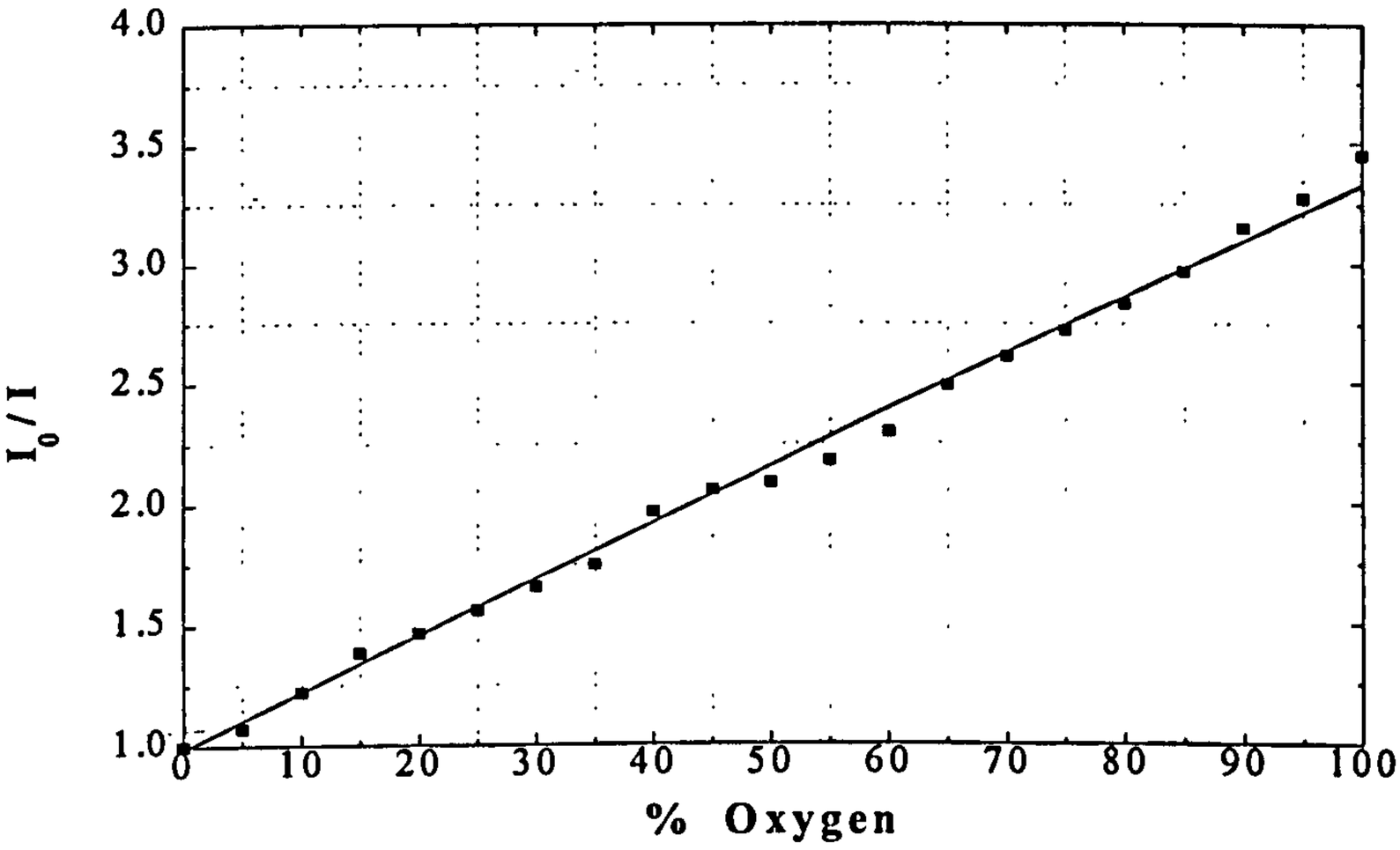

FIGURE 2.21 Stern-Volmer plot of the quenching by oxygen of tris(2,2'-bipyridyl) ruthenium(II) chloride hexahydrate (7 μM) in phosphate buffer pH 7.2 at 22^{0}C.

Initial experiments were devised to establish the influence of low concentrations of hydrogen peroxide (10-100 mM) on the quenching of the indicator, since hydrogen peroxide is produced in low concentration in biocatalysed oxidations, depending upon the amount of the enzyme, its activity and the concentration of the analyte. The fluorescence intensity of 7 μM tris(2,2'-bipyridyl)ruthenium(II) chloride hexahydrate decreased slightly with hydrogen peroxide (H_2O_2) concentration of 100 mM (the fluorescence intensity of the indicator was 104.5, and with 10 mM H_2O_2 the fluorescence intensity was 101.1).

Subsequent experiments were performed at higher concentrations of hydrogen peroxide (0.1 - 4.4 M). The effect of these higher concentrations of hydrogen peroxide on the quenching of tris(2,2'-bipyridyl) ruthenium(II) chloride hexahydrate (7 μM) are depicted in Figure 2.22. This shows that the fluorescence quenching of the indicator decreased when the added concentration of hydrogen peroxide increased (i.e. fluorescence intensity decreased from 104 to 62, between 0.2 and 4.4 M H_2O_2).

In addition, the above phenomenon of fluorescence quenching of tris(2,2'-bipyridyl) ruthenium(II) chloride hexahydrate by hydrogen peroxide was significant for concentrations above of 0.5 M hydrogen peroxide; it appeared to be negligible for concentrations of less than 200 mM hydrogen peroxide.

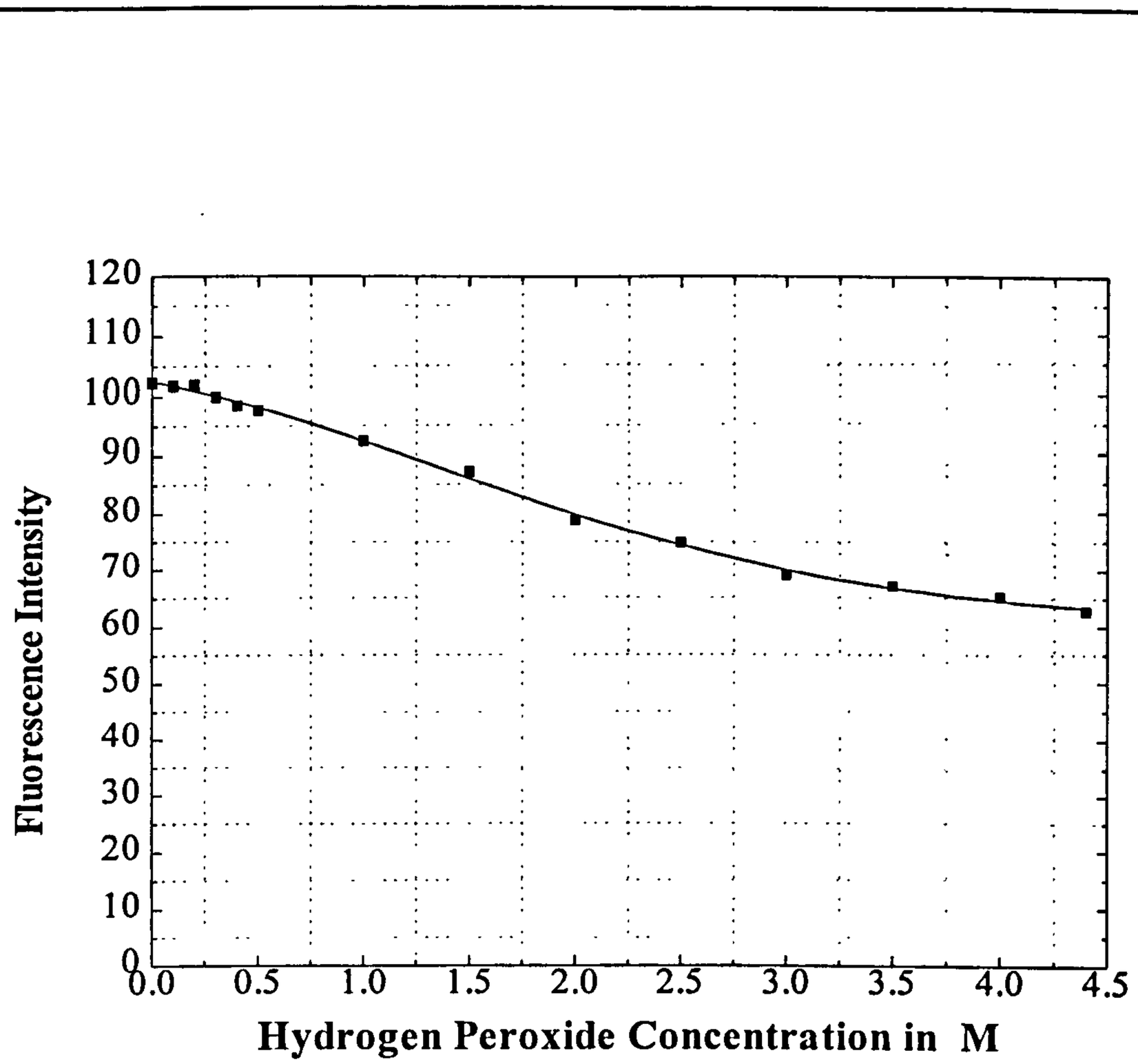

FIGURE 2.22 Fluorescence intensity versus H_2O_2concentration of tris(2,2'-bipyridyl) ruthenium(II) chloride hexahydrate (7 μM) in phosphate buffer pH7.2 at 22 ^{0}C. Solutions were excited with a wavelength of 456 nm.

2.3.3 DISCUSSION

Tris(2,2'-bipyridyl)ruthenium(II) chloride hexahydrate showed favourable analytical wavelengths in the visible range, excitation maximum 456 nm and emission maximum 610 nm. These results are close to the published data in the literature. Lippitsch *et al.* (1988) described a fibre-optic oxygen sensor using the same indicator as in the present study and they reported as excitation wavelength 460 nm and emission 610 nm. Similarly, for the above indicator, Wolfbeis and colleagues reported an excitation wavelength of 460 nm and an emission wavelength of 630 nm (Wolfbeis *et al.*, 1988). An oxygen sensor has been presented, based on the photoluminescent characteristics of tris(2,2'-bipyridine) ruthenium(II) incorporated into a Nafion film, and for this an excitation wavelength of 452 nm and emission of 605 nm were reported (Ishiji *et al.*, 1994).

In addition, the analytical wavelengths of compounds related to the indicator used in the present study, have been discussed and they presented values close to tris(2,2'-bipyridyl)ruthenium(II) chloride hexahydrate. For example, tris(1,10-phenanthroline) ruthenium(II) dichloride showed excitation wavelength at 452 nm and emission at 603 nm (Moreno-Bondi *et al.*, 1990b). This indicator was used for the design of an oxygen optrode in a fibre-optic glucose biosensor. Recently, Hartmann *et al.* (1995) reported a related compound, tris(4,7'-diphenyl-1,10'-phenanthroline)Ru(II) perchlorate, with excitation wavelength 470 nm and emission 610 nm, which has been utilised for the construction of an optical oxygen sensor. These wavelengths in the visible range render the indicator, tris(2,2'-bipyridyl)ruthenium(II) chloride hexahydrate, suitable for excitation by a blue LED. More specifically, a LED could be used as a light source, despite its poor light intensity for two reasons: it can operate with very low power requirements (typically 3.5 V

at 200 nA), and its modulation frequency can easily be tuned over a wide range. Various lasers, would be better excitation sources, but their cost and power requirements are prohibitive for the design of an instrument for practical use. Also, the extremely large Stokes's shift of 150 nm permits an easy separation of scattered light from fluorescence (Lippitsch *et al.*, 1988; Klimant *et al.*, 1994).

Diluting the stock solution of tris(2,2'-bipyridyl)ruthenium(II) chloride hexahydrate (10 mM) with known volumes of sodium phosphate buffer allowed the determination of the relative fluorescence intensity as a function of fluorophor concentration. Since fluorescence quenching by molecular oxygen reduces the fluorescence intensity, a large initial fluorescence intensity was desirable; however, too much fluorescent compound can result in a reduced fluorescence intensity because of concentration quenching and/or inner cell effects (i.e. Figure 2.16). Therefore, the range of fluorophor concentration where fluorescence intensity remained linear was established as the optimum concentration of tris(2,2'-bipyridyl) ruthenium(II) chloride hexahydrate and lay in the range of 1-10 μM, which will be used in the following experiments. A similar range of concentrations of the indicator used in solutions has been reported. Ishiji *et al.* (1994) reported that the quenching of the above indicator solution by oxygen was measured using 50 μM concentration of the indicator (7 μM concentration was used in the present study during the experiments on quenching of the indicator by oxygen).

The changes in the fluorescence intensity, and spectral properties, of tris(2,2'-bipyridyl) ruthenium(II) chloride hexahydrate observed in the presence of different hydrogen peroxide concentrations, indicate that this compound may also be used for the detection of

concentrations at the mM and M level of hydrogen peroxide, but not in the range of μM, and consequently it is not suitable for the detection of hydrogen peroxide production from enzymatic oxidations. In the literature, a study presented tris(2,2'-bipyridine)ruthenium(II) dichloride as a peroxide-producing replacement for enzymes as chemical labels using flow injection analysis and direct photolysis techniques (Ismail & Weber, 1991). The concentration of the ruthenium-based label was determined from the rate of hydrogen peroxide production elicited by photolysis. Also, tris (2,2'-bipyridyl)ruthenium(II) chloride hexahydrate does not respond to changes in pH, as opposed to HPTS. Wolfbeis *et al.* (1988) reported that the above indicator had a pH-independent fluorescence especially in the pH range from 6 to 8.

Figures 2.19 and 2.20 show the response of the indicator on changing from pure nitrogen to pure oxygen. The signal was reduced with increasing oxygen partial pressure and approached a minimum value, which was not zero under pure oxygen. The curve in Figure 2.20 is vital for any application of the fluorescence quenching method to oxygen measuring devices, and it serves as the calibration curve for calculating oxygen concentrations from fluorescence intensity together with the corresponding almost linear Stern-Volmer plot of Figure 2.21. According to Lippitsch *et al.* (1988), Stern-Volmer plots of practically all sensors based on quenching and intensity measurement are not linear, mainly because both static and dynamic quenching occur simultaneously, and also, because the indicator is usually embedded (immobilised) in an inhomogeneous environment. Also, it was found that the quenching of certain amount of the indicator by oxygen was slightly dependent on the changes of temperature, and for this reason all the experiments were performed at almost constant room temperature of $22 \pm 2\ ^{0}C$.

In conclusion from the above results, tris(2,2'-bipyridyl)ruthenium(II) chloride hexahydrate can be used as an oxygen-sensitive indicator for the design of an optical biosensor based on dynamic fluorescence quenching. This is in agreement with related studies on the above indicator or related complexes which have been published during the last decade; for example, Peterson *et al.* (1984), Lippitsch *et al.* (1988), Wolfbeis *et al.* (1988), Ishiji *et al.* (1994), Bambot *et al.* (1994) and Li and Walt (1995).

2.4 The Mixed Solution containing HPTS and Tris(2,2'-bipyridyl)Ruthenium(II) Chloride Hexahydrate

An example of simultaneous detection of two parameters for the development of a fibre optic biosensor was demonstrated in 1988 by Wolfbeis and his colleagues; they reported a fibre-optic fluorosensor for oxygen and carbon dioxide measurements (Wolfbeis *et al.*, 1988). The oxygen-sensitive material (which essentially was a suspension of Kieselgel particles, dyed with tris(2,2'-bipyridyl)ruthenium(II) dichloride, in E43 silicone rubber) and CO_2-sensitive material (an immobilised pH indicator, HPTS, in a buffer solution) were entrapped in a gas-permeable polymer matrix that was attached to the distal end of the fibre. Both indicators had the same excitation wavelength (around 460 nm), but quite different emission maxima (630 nm and 520 nm, respectively). Oxygen could continuously be determined in the 0-200 Torr range and CO_2 in the 0-150 Torr range, with ± 1 Torr accuracy in both cases and about 0.5 Torr at low partial pressure. In the current work, the simultaneous detection of multiple parameters resulting from a single enzymatic reaction were explored.

2.4.1 MATERIALS & METHODS

Materials and Methods were as described in Sections 2.2.1 and 2.3.1

2.4.2 RESULTS

2.4.2.1 Spectroscopic investigation of a mixed solution containing HPTS and Tris(2,2'-bipyridyl)Ruthenium(II) Chloride Hexahydrate

According to Sections 2.3.3 and 2.2.3, the optimum concentration of tris(2,2'-bipyridyl) ruthenium(II) chloride hexahydrate of 7 μM was chosen corresponding to maximum value of fluorescence intensity. For HPTS a concentration of 0.03 μM was chosen, because of the similar fluorescence intensity to that of 7 μM tris(2,2'-bipyridyl)ruthenium(II) chloride hexahydrate, in order to have a balance in the measurements of the fluorescence intensities of both indicators in the following experiments. The excitation spectra of HPTS and tris(2,2'-bipyridyl)ruthenium(II) chloride hexahydrate with emission wavelength at 510 nm and 610 nm, respectively, are shown in Figure 2.23; where it can be seen that the common emission wavelength is equal to 412 nm.

Similarly, a common excitation wavelength from Figure 2.24, was found at 565 nm. The term "common" is used to describe the wavelength at which both indicators present the same fluorescence intensity. Using the common excitation wavelength for a mixed solution of 0.03 μM HPTS and 7 μM tris(2,2'-bipyridyl)ruthenium(II) chloride hexahydrate, the fluorescence spectrum obtained is presented in Figure 2.25. The corresponding absorption spectrum of this solution (Figure 2.26) demonstrates two distinct absorption peaks. The first peak at 403 nm originates from HPTS, whilst the second peak at 453 nm is from tris(2,2'-bipyridyl)ruthenium(II) chloride hexahydrate.

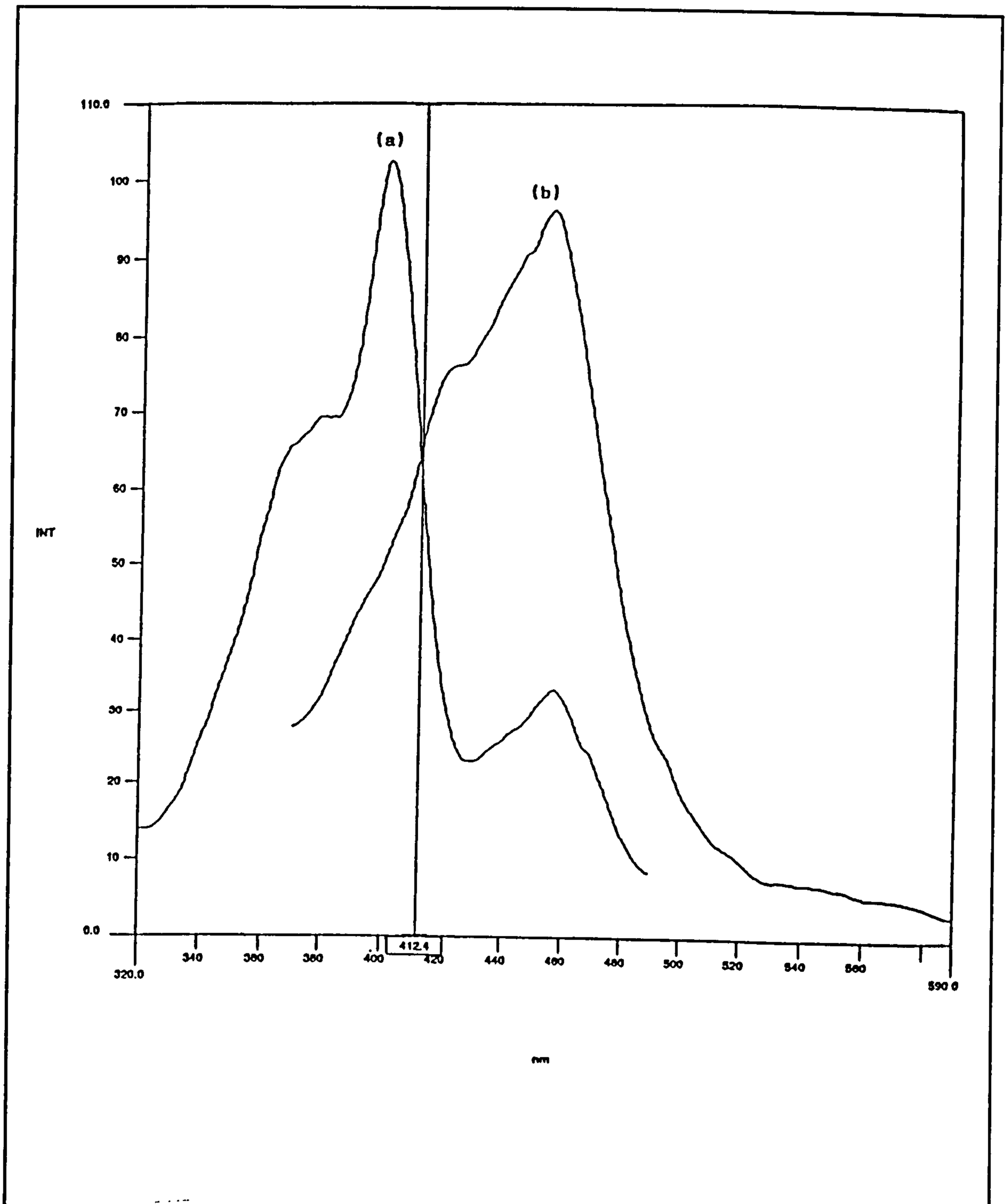

FIGURE 2.23 Excitation spectra of (a) 0.03 μM HPTS and (b) 7 μM tris(2,2'-bipyridyl) ruthenium(II) chloride hexahydrate in phosphate buffer pH 7.2 at 22 ^{0}C (for curve (a) the fluorescence taken at 510 nm and for curve (b) at 610 nm).

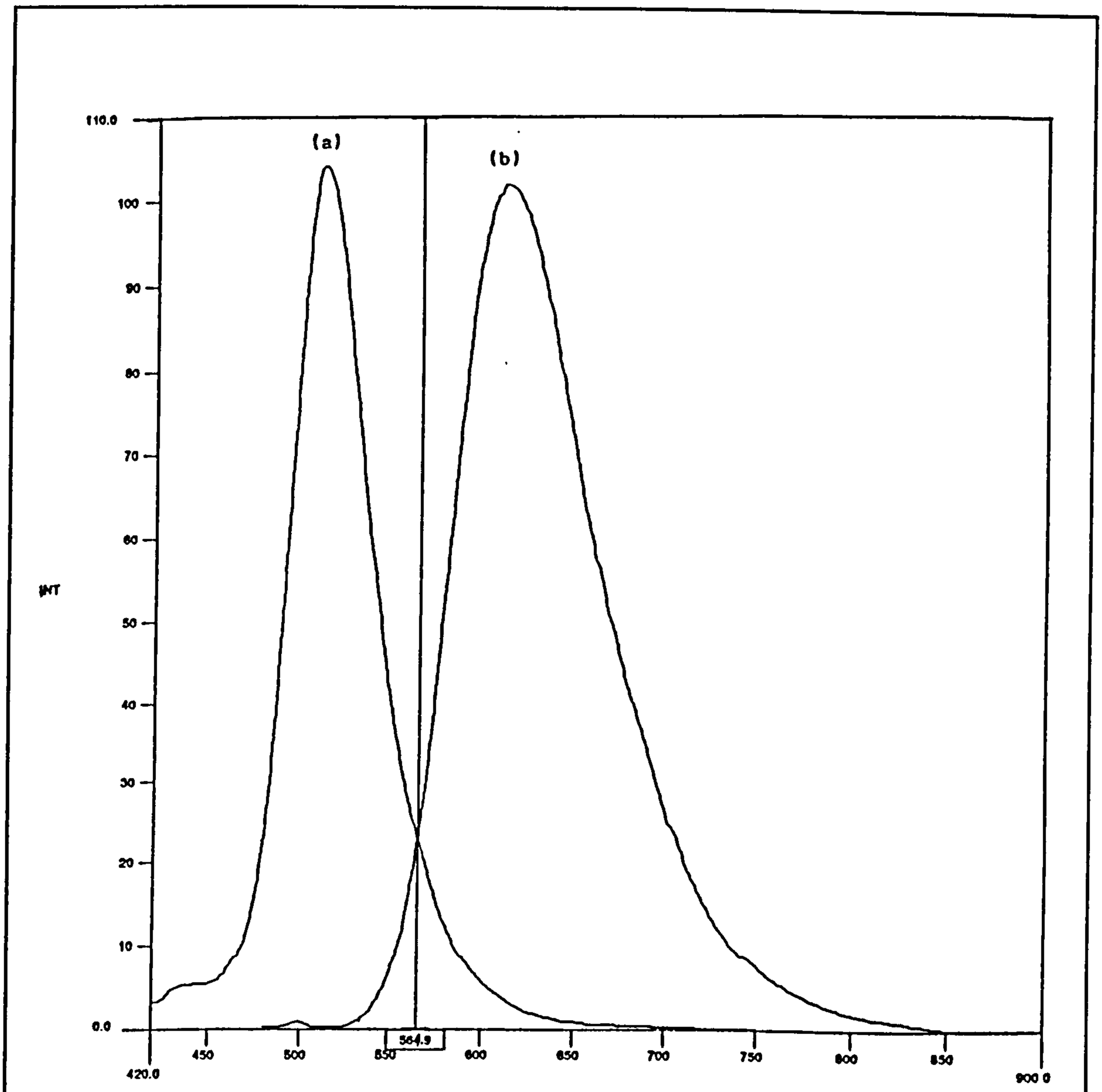

FIGURE 2.24 Fluorescence spectra of (a) 0.03 μM HPTS and (b) 7 μM tris(2,2'-bipyridyl)ruthenium(II) chloride hexahydrate in phosphate buffer pH 7.2 at 22 ^{0}C (excitation wavelength for (a) at 510 nm and for (b) at 610 nm).

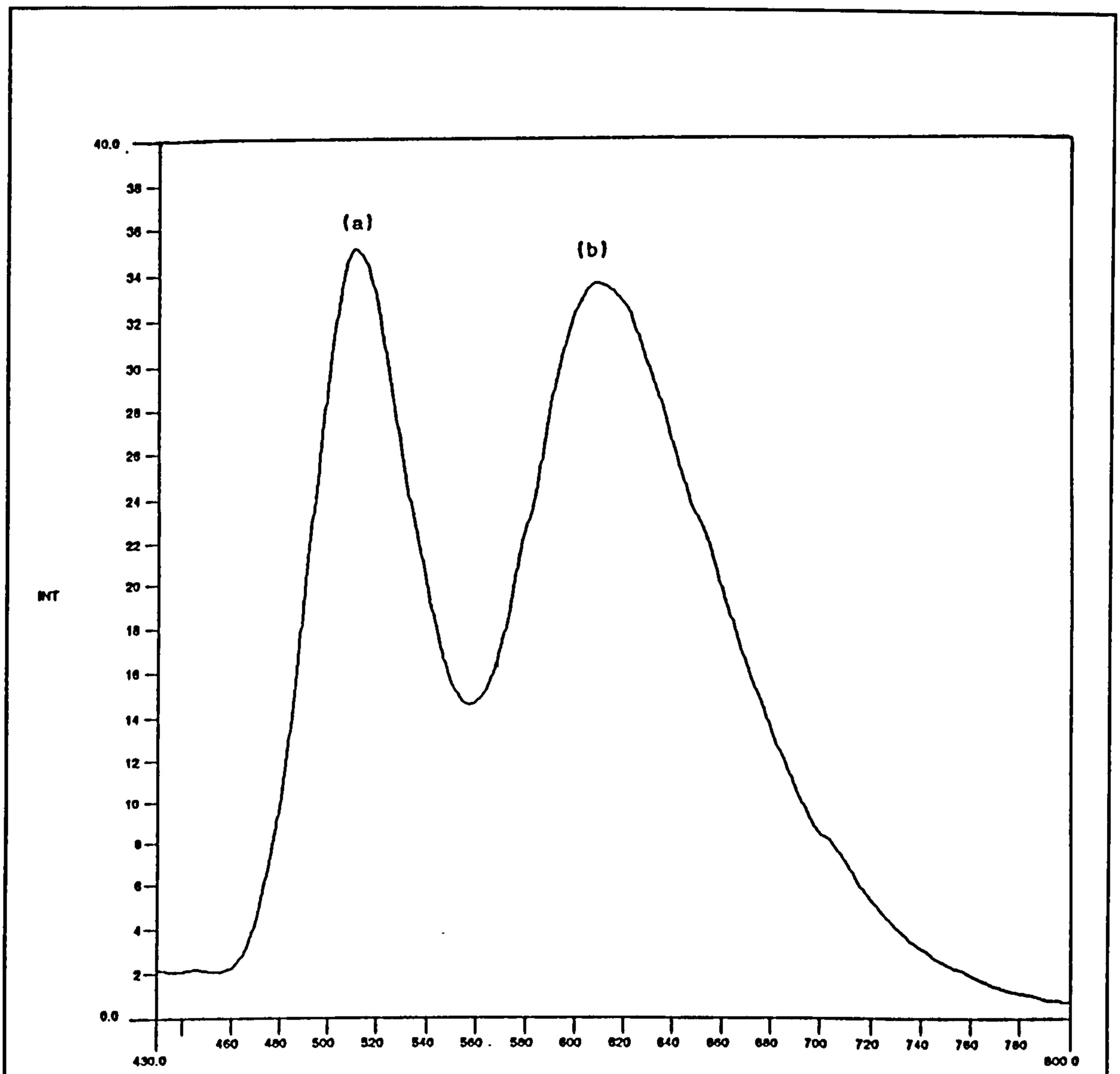

FIGURE 2.25 Fluorescence spectrum of a mixed solution containing HPTS (0.03 μM, (a)) and tris(2,2'-bipyridyl)ruthenium(II) chloride hexahydrate (7 μM, (b)) in phosphate buffer pH 7.2 at 22 ^{0}C (excitation wavelength at 412nm).

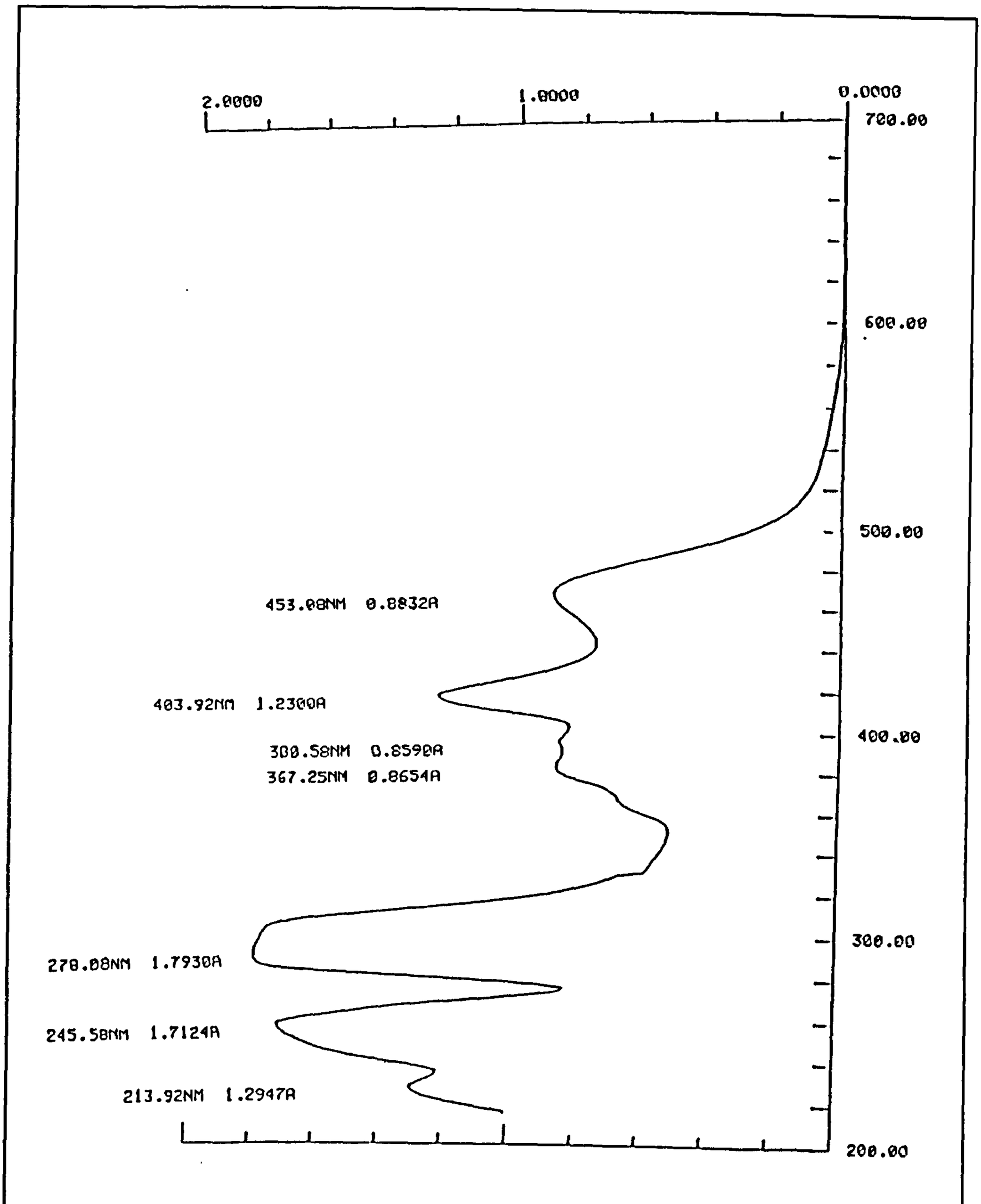

FIGURE 2.26 UV and Visible absorption spectrum of a mixed solution containing HPTS (50 μM) and tris(2,2'-bipyridyl)ruthenium(II) chloride hexahydrate (50 μM) in phosphate buffer pH 7.2 at 22 ^{0}C.

2.4.2.2 Effect of pH changes, Oxygen and Hydrogen Peroxide on the Mixed Solution containing HPTS and Tris(2,2'-bipyridyl)Ruthenium(II) Chloride Hexahydrate

The last experiment relative to the effects of oxygen, was performed in order to determine how the quenching of a mixed solution containing HPTS (0.03 μM) and tris(2,2'-bipyridyl) ruthenium(II) chloride hexahydrate (7 μM) were affected by different percentage oxygen concentrations; the corresponding fluorescence spectra are presented in Figure 2.27. These spectra and the corresponding graphs in Figures 2.28 show that when the indicators are both present in the same solution, under the influence of different percentage oxygen concentrations, their separate spectroscopic characteristics do not change. Thus, tris(2,2'-bipyridyl)ruthenium(II) chloride hexahydrate may be used as a sensitive indicator for oxygen, whilst HPTS is unaffected by the changes in percentage saturation of the oxygen environment.

Finally, Figure 2.29 demonstrates the influence of different concentrations of hydrogen peroxide (0.1 - 2.5 M) on the quenching of a mixed solution containing 0.03 μM HPTS and 7 μM tris(2,2'-bipyridyl)ruthenium(II) chloride hexahydrate. The spectra and the corresponding graphs in Figures 2.29 and 2.30, show that the distinctive spectroscopic characteristics of each indicator in the presence of different concentrations of hydrogen peroxide, did not change when they were together in the same solution. The changes in the fluorescence intensity, and spectral properties, of tris(2,2'-bipyridyl)ruthenium(II) chloride hexahydrate observed in the presence of different hydrogen peroxide concentrations, indicate that this compound may be used for the detection of concentrations of hydrogen peroxide at mM and M level.

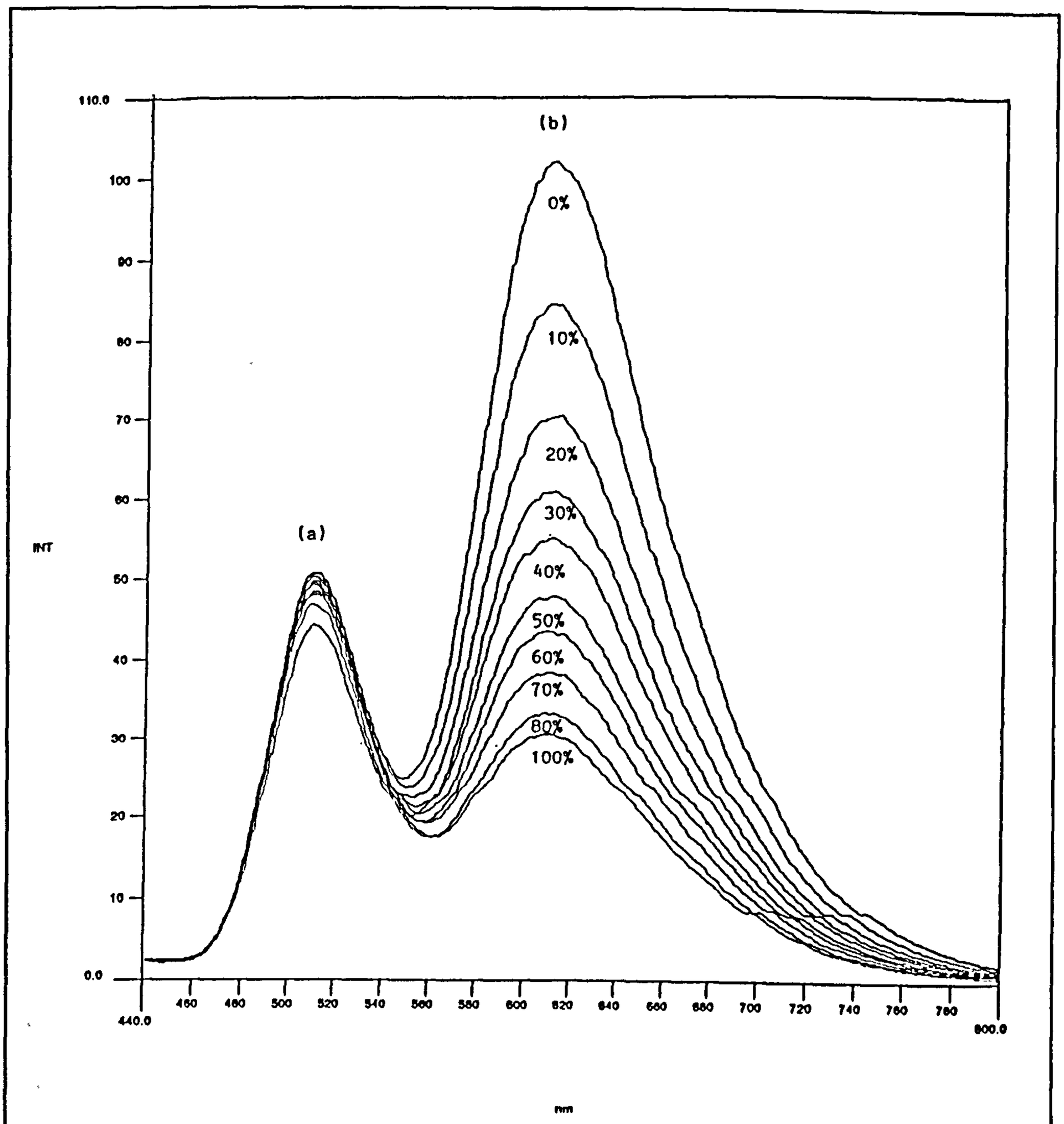

FIGURE 2.27 Effect of different percentage oxygen concentrations on the quenching of a mixed solution containing HPTS (0.03 μM) and tris(2,2'-bipyridyl)ruthenium(II) chloride hexahydrate (7 μM) in phosphate buffer pH 7.2 at 22 ^{0}C. Solutions were excited with a wavelength of 412 nm.

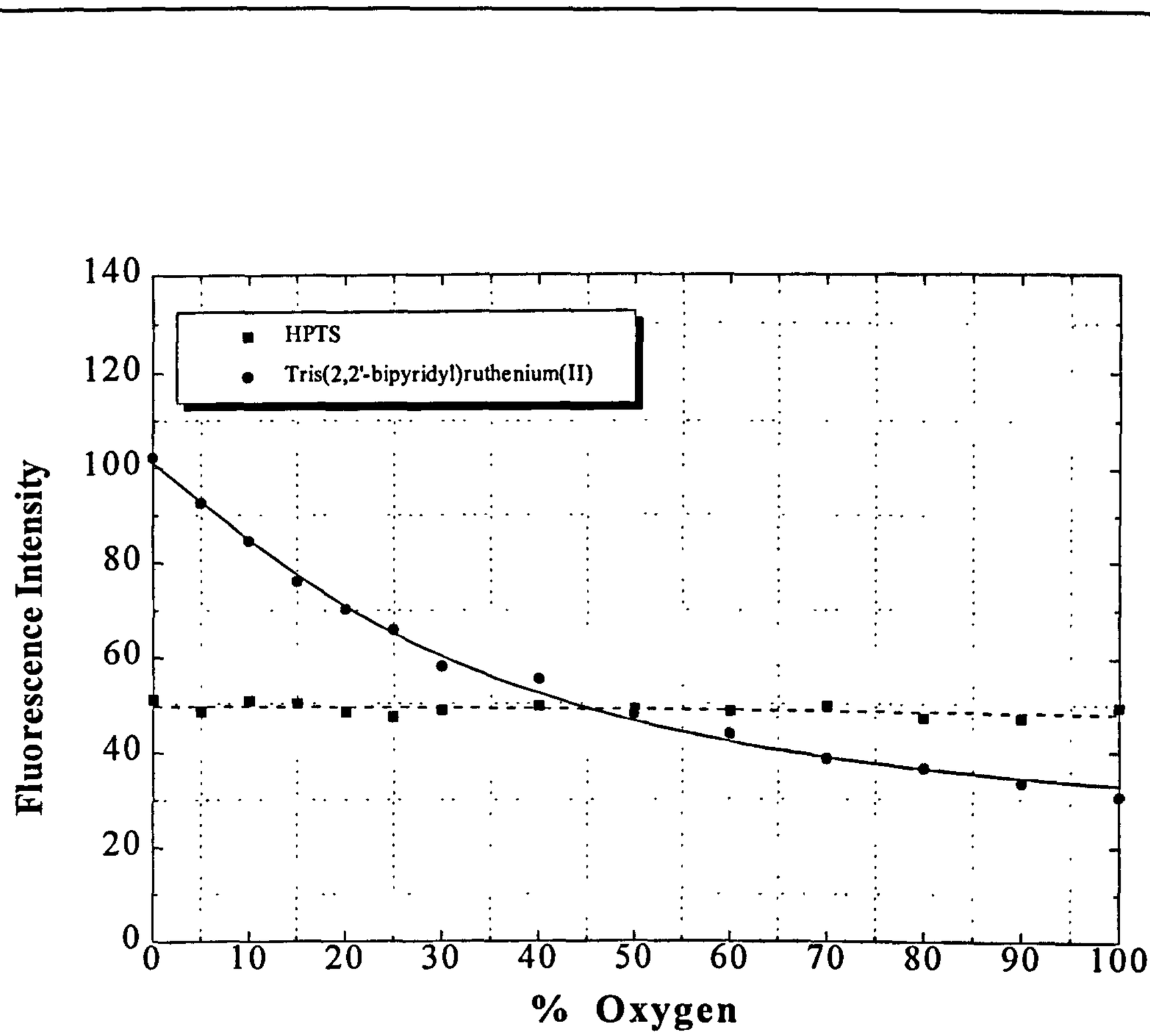

FIGURE 2.28 Fluorescence intensity versus oxygen concentrations of a mixed solution containing HPTS (0.03 μM) and tris(2,2'-bipyridyl)ruthenium(II) chloride hexahydrate (7 μM) in phosphate buffer pH 7.2 at 22 ^{0}C. Solutions were excited with a wavelength of 412 nm.

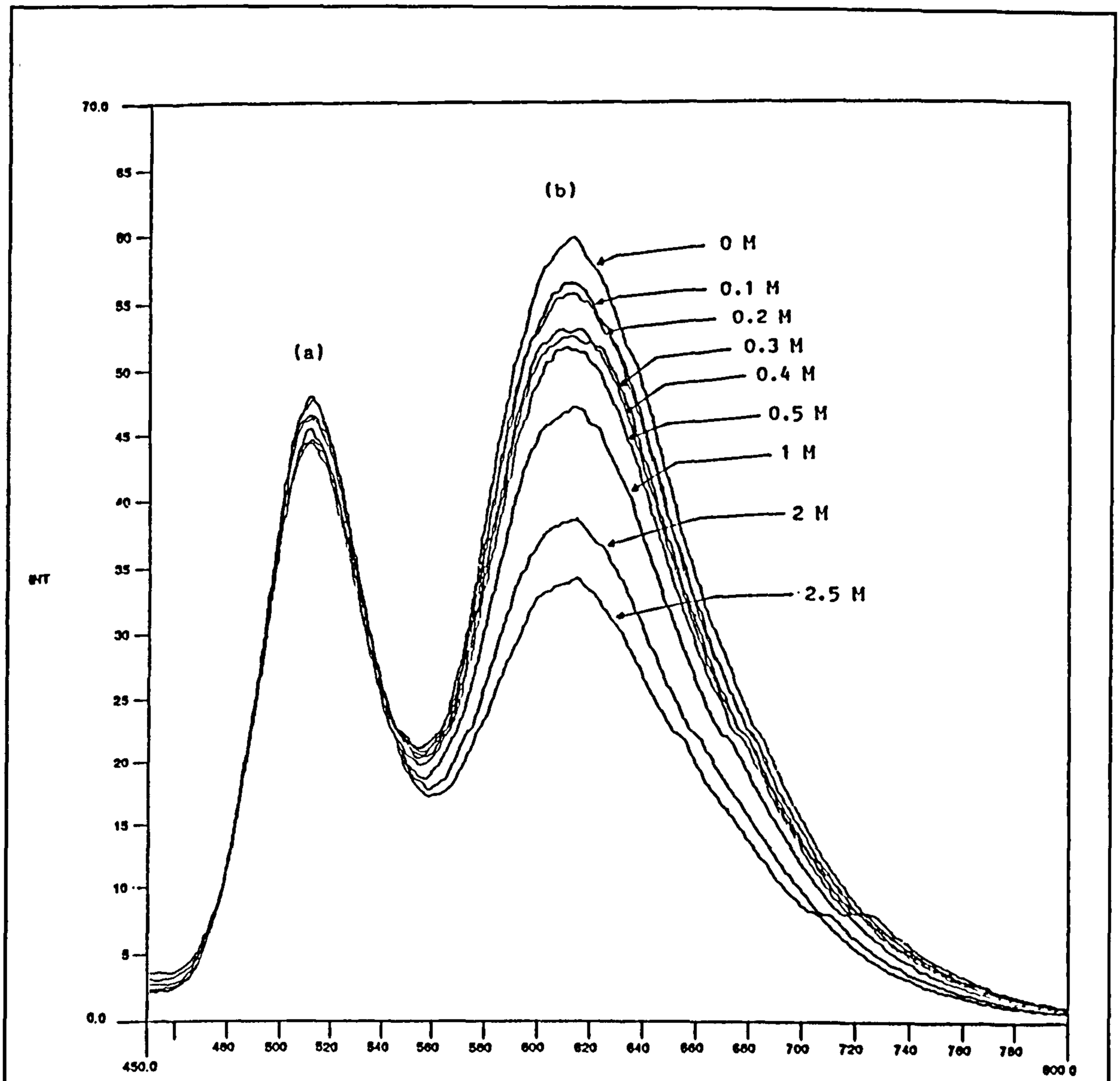

FIGURE 2.29 Effect of different concentrations of H_2O_2 on the quenching of a mixed solution containing HPTS (0.03 μM) and tris(2,2'-bipyridyl)ruthenium(II) chloride hexahydrate (7 μM) in phosphate buffer pH 7.2 at 22 ^{0}C. Solutions were excited with a wavelength of 412 nm.

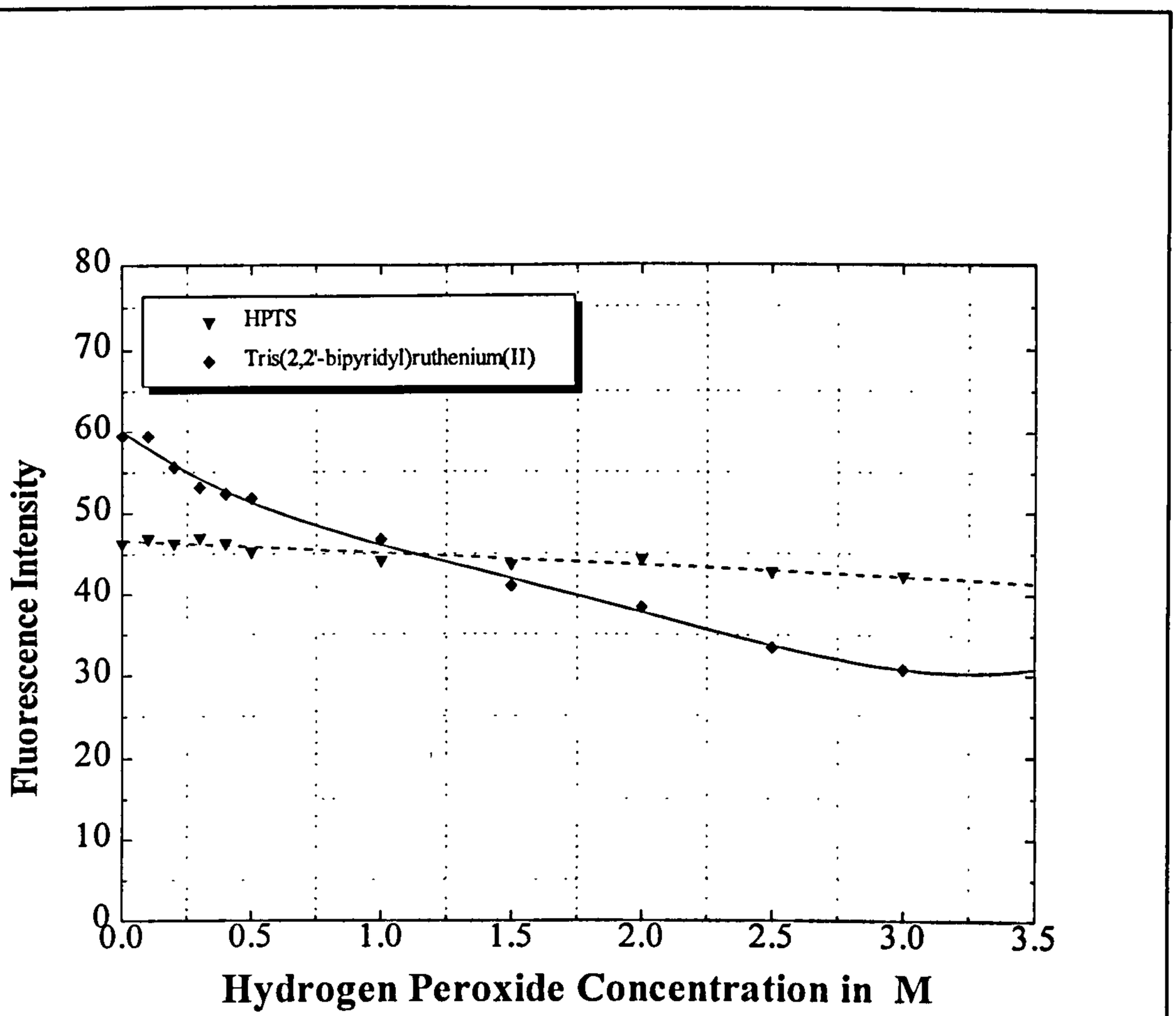

FIGURE 2.30 Fluorescence intensity versus concentrations of H_2O_2 of a mixed solution containing HPTS (0.03 μM) and tris(2,2'-bipyridyl)ruthenium(II) chloride hexahydrate (7 μM) in phosphate buffer pH 7.2 at 22 ^{0}C. Solutions were excited with a wavelength of 412 nm.

2.4.3 DISCUSSION

The optimum concentrations chosen for tris(2,2'-bipyridyl)ruthenium(II) chloride hexahydrate and HPTS were 7 μM and 0.03 μM, respectively, because as already mentioned both indicators exhibited a linear fluorescence intensity response against concentration, and also similar levels of intensity at the optimum values. The large difference between the levels of optimum concentration of each indicator occurs because HPTS has a fairly high absorbance and very high quantum yield (close to 1.0), whereas tris(2,2'-bipyridyl)ruthenium(II) chloride hexahydrate has low absorbance and low quantum yield (ca. 0.1) (Wolfbeis *et al.*, 1988).

In the present study, the above two fluorescent indicators have been extensively investigated in order to establish their suitability for the construction of an optical biosensor based on the principle of monitoring two parameters simultaneously, oxygen consumption and pH changes during a biocatalytic oxidation. This idea of measuring two or more parameters simultaneously has been explored by a few researchers in the past. Miller *et al.* (1987), for example, developed a triple sensor for blood pH, oxygen and carbon dioxide. This sensor consisted of three 100-μm fibers with appropriate chemistries at their ends. In the current work, however, the use of only one fibre optic with both indicators immobilised at its end is explored. Futhermore, this would be used to measure changes in two indicator species generated by a single enzyme-catalysed reaction in response to one analyte.

The closest sensor to the one proposed in the current study, is that reported by Wolfbeis *et al.* (1988). This was based on an oxygen-sensitive material and carbon dioxide-sensitive

material which were entrapped in a gas-permeable polymer matrix attachable to the distal end of a fibre optic. In this sensor, the same fluorescent indicators were used, tris(2,2'-bipyridyl) ruthenium(II) dichloride for oxygen monitoring, and HPTS for carbon dioxide detection via pH changes in the sensor. HPTS was used in its base form, and thus, the same excitation wavelength (460 nm) for both indicators was employed and the individual emission maxima for each separate indicator at 520 nm and 630 nm were monitored. In the present study, a common excitation wavelength (412 nm) and the common emission (555 nm) were used

2.5 CONCLUSIONS

The indicators, HPTS and tris(2,2'-bipyridyl)ruthenium(II) chloride hexahydrate, have shown entirely different emission maxima (510 nm and 610 nm, respectively), where the spectral overlap and the efficiency of energy transfer of the two indicators appear negligible. Otherwise, there would be some interference to be observed, which could be created by a strong overlap of the fluorescence emission bands of the indicators, so that an analyte-specific wavelength with sufficient signal intensity could not be found. Also, the emission band of each indicator did not overlap with the absorption band (and therefore, excitation spectrum), because otherwise, it would give rise to energy transfer between analyte-sensitive and analyte-insensitive indicators (Wolfbeis *et al.*, 1988).

The utilisation of a common excitation wavelength offers the possibility to excite at one particular wavelength and to have information for the fluorescence intensity of both indicators. As can be observed in Figure 2.25, there were two clear peaks in the emission spectrum from each indicator, which means that there was no spectral interference

between the separate indicators (i.e. HPTS and tris(2,2'-bipyridyl) ruthenium(II) chloride hexahydrate), present in the same solution. Also, the visible excitation wavelength offers the advantage of using conventional light sources, as opposed to expensive UV light sources, lasers and fused silica fibres. In addition, the signal from the sensors is intense enough to be detected with a photodiode rather than with a more expensive photomultiplier tube. All these facts contribute to keep the costs for the construction of the proposed optical biosensor to a minimum.

Another important feature of the mixed solution containing both indicators, is that each indicator is specific for a given analyte (HPTS for pH changes and tris(2,2'-bipyridyl) ruthenium(II) chloride hexahydrate for oxygen) and they retained the same behaviour as when they were separate. This means that, in the mixed solution, HPTS had the same sensitivity to pH changes as in a separate solution, was not affected by hydrogen peroxide and its fluoresence was quenched by less than 3% in going from pure nitrogen to pure oxygen, which is negligible. On the other hand, the fluorescence of tris(2,2'-bipyridyl)ruthenium(II) chloride hexahydrate, in the mixture of both indicators, was not affected by pH changes (specially in the pH 6-8 range), but it was distinctly sensitive to oxygen. It also responded to hydrogen peroxide, but only in the range of mM and M, which is not relevant to the hydrogen peroxide concentrations usually produced in enzymatic oxidations.

Consequently, the two indicators have no cross sensitivity separate or in the same solution, and can be used for the construction of an accurate and inexpensive optical fluorescence biosensor based on an enzymatic oxidation. Substrate concentration may be assessed by

simultaneously measuring two parameters: oxygen consumption, through the reduction of the fluorescence intensity of tris(2,2'-bipyridyl)ruthenium(II) chloride hexahydrate; and the production of acid, through pH changes affecting the fluorescence intensity of HPTS. The sensing method is based on the simultaneous excitation of the two fluorescent indicators with well-separated emission bands. This application will be discussed, in detail, in the next chapter where the enzymatic oxidation of glucose is studied.

CHAPTER 3

FLUORESCENCE-BASED OPTICAL BIOSENSORS FOR BLOOD-GLUCOSE MONITORING: SOLUTION STUDIES

3.1 INTRODUCTION

This chapter describes the simultaneous utilisation of the two well-known fluorescent indicators, HPTS and tris(2,2'-bipyridyl)ruthenium(II) chloride hexahydrate, in solution studies, in order to develop a novel optical fluorescence biosenor for the measurement of blood-glucose. This biosensor was based on the enzymatic oxidation of glucose using the enzyme glucose oxidase (GOD). The determination of glucose was performed through the simultaneous measurement of the changes in the fluorescence intensity of both indicators. HPTS indicated pH changes during gluconic acid production and tris(2,2'-bipyridyl) ruthenium(II) chloride hexahydrate measured oxygen consumption due to the catalytic oxidation of glucose.

Initial experiments were carried out in order to determine the fluorescence quenching of glucose oxidase itself due to the FAD (flavin adenine dinucleotide) coenzyme, and define the optimum concentration of this enzyme used in the kinetic measurements experiments. A thorough spectroscopic study of the enzymatic oxidation of glucose was performed using glucose oxidase in solution in a cuvette, in the presence of both indicators. A number of combinations of wavelengths of the indicators for excitation and fluorescence were utilised in order to establish calibration curves with the optimum performance for glucose detection using kinetic measurements of the glucose oxidase reaction. All the experiments were carried out in conditions close to blood-glucose parameters in order to establish the principles of the development and characterisation of an optical fluorescence glucose biosensor for clinical applications, and especially, for the world-wide scourge, diabetes mellitus.

3.1.1 Diabetes Mellitus

Diabetes mellitus may be defined as "a condition in which there is a chronically raised blood glucose concentration. It is not a single disease but a collection of disorders related by the presence of hyperglycaemia and due to a relative or absolute lack of insulin" (Turner and Pickup, 1985). **Insulin** is the most important hormone for the regulation of blood glucose concentration and is produced by the beta cells of the islets of Langerhans in the pancreas. It promotes glycogenesis and lipogenesis, with a resultant decrease in blood glucose levels and another important action is to increase the permeability of cells to glucose (Caraway, 1976; Zubay, 1993). Another endocrine function of the pancreas is from the alpha cells which secrete glucagon and increase blood glucose levels. These hormones are mutually antagonistic in their actions on carbohydrate, fat and protein metabolism and the effects of either on the blood glucose level promotes the compensatory secretion of the other.

The maintenance of blood glucose levels within a very narrow range is extremely important because glucose is the major source of energy and heat for the human body, and glucose is essentially the sole fuel for the brain. The blood glucose level in a well-fed person typically ranges from 4.4 mM (80 mg/dl) to 6.7 mM (120 mg/dl) (Stryer, 1995). After a meal, the rise in the blood glucose level leads to increased secretion of insulin and decreased secretion of glucagon. Loss of control of the circulating blood glucose level is the earliest manifestation of the disease diabetes mellitus (Albisser, 1982). Specifically, blood glucose concentrations in the range of 1-30 mM are commonly observed in diabetic patients. With deficiency in effective insulin (diabetes), the fasting blood glucose level tends to increase (**hyperglycaemia**) and the body shows

less ability to metabolise carbohydrates. At the other extreme, an islet cell tumor can produce an excess of insulin, resulting in very low levels of blood glucose (**hypoglycaemia**). This causes mental confusion and if sustained, coma and death. On the other hand, hyperglycaemia causes unpleasant short-term symptoms such as thirst, frequent urination, nausea and vomiting. If insulin injections are not available for treatment this ends in coma and death. Hyperglycaemia is also a major influence in the long term development of tissue damage in blood vessels, eyes, nerves and kidneys (Albisser *et al.*, 1978; Santiago, 1993a; Reach, 1994b; DCCT Research Group, 1993).

Scientists still do not have a clear picture of the basic biochemical defect(s) which cause diabetes and it is a serious health problem, involving at least 2% of the population in Europe and North America or otherwise more than 30 million people world-wide (Foster & McGarry, 1983; Foster, 1989; Atkinson & Maclaren, 1990; Steiner *et al.*, 1990; Reach & Wilson, 1992). Two major types of diabetes are recognised: **type I** or insulin-dependent diabetes mellitus (IDMM), juvenile onset, which usually begins before age 20, and **type II** or non-insulin-dependent diabetes mellitus (NIDDM), maturity onset, which typically arises later in life than does the insulin-dependent form (Kruise, 1993).

Type I diabetics have an absolute insulin deficiency and therefore, must receive insulin replacement to live (Santiago, 1992 and 1993a). Without insulin injection at the right moments these patients become severely ill as the blood glucose levels rise. About 20% of the diabetic patients in the UK belong to type I. The other 80% of the diabetic population suffers from type II diabetes and they are often managed by a diet or special

drugs which release insulin from pancreas. Insulin, diet and oral hypoglycaemic drugs are able to control the acute symptoms of hyperglycaemia, but serious complications often appear after many years (Granner & O'Brien, 1992). The need for regular monitoring of glucose was highlighted in a recent study by the Diabetes Control and Complications Trial Group, known as DCCT, in June 1993 during the annual meeting of the American Diabetes Association in Las Vegas, Nevada of USA (DCCT Research Group, 1993). The results of this extensive study, more than a decade of careful planning and research, proved that intensive therapy with the goal of maintaining blood glucose concentrations close to the normal range reduce the risk of severe complications associated with IDDM patients by up to 60 % and delay the progression of the incidence of these microvascular complications (Scharp *et al.*, 1991; Santiago, 1993b; Reach, 1994b; Betts *et al.*, 1996).

For the above reasons, it is very important to improve metabolic control in diabetic patients by developing more physiological strategies of insulin administration (Pickup & Rothwell, 1984). Approaches to the treatment of diabetes mellitus have been classified into the following categories (Turner & Pickup, 1985) :

a) Electromechanical devices for infusion of insulin, preferentially combined with a glucose sensor for feedback control;

b) transplantation of the pancreas or isolated islets of Langerhans, in order to restore the insulin regulation;

c) self-monitoring of blood glucose samples and adjustment of the amount of injected insulin, based on the results.

Electromechanical infusion devices may be divided into two categories: open- or closed-loop, dependent on whether or not there is automatic glucose sensing and feedback (Santiago *et al.*, 1979; Schultz *et al.*, 1982; Miller *et al.*, 1987; Rabenstein *et al.*, 1988; Rebrin *et al.*, 1992; Reach, 1994a; Nicholson *et al.*, 1995). However, these devices are usually large, expensive and complex, with associated risks to patients of thrombosis, embolism and septicaemia. Transplantation of the pancreas is a difficult operation and often unsuccessful, due to the destruction of the new cells of the islets of Langerhans from host antibodies developed to protect the patient from the foreign transplant (Scharp *et al.*, 1991; Pueyo *et al.*, 1995).

Self-monitoring techniques involve placing a finger-prick blood sample onto a disposable strip impregnated with glucose oxidase. This technique enables improved control since patients can monitor blood glucose levels and then alter the insulin injected or food ingested according to the strip result (Tattersall, 1985; Pickup *et al.*, 1987; Fischer, 1991; Poitout *et el.*, 1993). Home blood glucose meters are based on either electrochemical methods (amperometric) (Tieszen *et al.*, 1993; Greenough *et al.*, 1994) or optical (reflectance photometry or absorbance) techniques.

3.1.2 Optical Fluorescence-Based Glucose Biosensors

A variety of analytical optical techniques have been researched to provide reversible fibre-optic glucose biosensor measurements, including: polarisation modulation (Smith *et al.*, 1992), chemiluminescence (Abdel-Latif & Guilbault, 1988; Zhou & Arnold, 1995), flow-injection analysis (Dremel *et al.*, 1989a and 1992; Gunasingham & Tan, 1992) and scanning electron microscopy (Kim & Lee, 1988). Most popular, however, are absorbance

(Abdel-Latif *et al.*, 1988; Mansouri *et al.*, 1988; Arnold & Small, 1990), and fluorescence (Meadows & Schultz, 1988) techniques, the latter of which is utilised in the present study.

In 1984, Uwira and colleagues reported the first optical determination of glucose levels by measurement of the oxygen partial pressure in the analyte sample (Uwira *et al.*, 1984). In their device, changes in the oxygen level were measured via quenching of the fluorescence of an oxygen-sensitive indicator during the enzymatic oxidation of glucose with glucose oxidase (GOD). This was followed by the development of a theoretical model of a glucose/oxygen sensor that described the coupling of glucose concentration to relative fluorescence intensity, the experimental measurement of the key parameters in this model (the local oxygen concentration through the oxidation of glucose by a fluorescent oxygen indicator), and the evaluation of the sensitivity of the fluorescence intensity of the composite material to ambient glucose concentration (Parker & Cox, 1986). The solid phase material consisted of a fluorophor (for optical response via fluorescence quenching) and an enzyme, GOD (for chemical specificity to glucose), physically entrapped within a hydrophilic polymer or PHEMA. They claimed that chemical reactions could be coupled to photophysical reactions, in particular, oxygen quenching.

Later, Wolfbeis and his colleagues described a fibre-optic fluorosensor for continuous monitoring of glucose that used a pH-sensing fluorescent dye (HPTS) as a transducer (Trettnak *et al.*, 1988a). GOD was physically immobilised in a sensing layer at the end of a fibre optic light guide. The enzyme catalysed the oxidation of glucose to give gluconic acid, which, in turn lowered the pH in the microenvironment of the sensor and was monitored by following changes in the fluorescence of the pH-sensitive dye. The response

time to 90% of the total signal was 8-12 min and the detection limit was 0.1-2 mM glucose concentrations. A generic hydrogen peroxide sensor with application to the detection of glucose levels in serum was developed (Genovesi *et al.*, 1988). It was based on the fluorometric determination of hydrogen peroxide concentration as a product of the oxidation of glucose using a fluorescent phenolic-based indicator.

In 1989, a different fibre-optic glucose biosensor was presented, which was based on the intrinsic fluorescence of glucose oxidase (Trettnak & Wolfbeis, 1989b). It was observed that the fluorescence of GOD changes during interaction with glucose. However, overall sensor performance was suboptimal, with poor response time and detection limit of glucose concentrations. Wolfbeis and his colleagues also presented a fibre-optic glucose biosensor based on a sensitive oxygen transducer (Moreno-Bondi *et al.*, 1990b). The sensor related oxygen consumption (as a result of enzymatic oxidation) to glucose concentration via the dynamic quenching of the fluorescent indicator, tris(1,10-phenanthroline)-ruthenium(II) cation by molecular oxygen. The response time was around 6 min and the detection limit 0.06-1 mM glucose.

A fluorescence lifetime-based sensing of glucose has been described (Lakowicz & Szmacinski, 1993). This lifetime-affinity assay was based on fluorescence energy transfer between a donor covalently linked to Con A and an acceptor linked to a sugar that bound to Con A. Binding of the acceptor-labeled sugar to Con A was expected to decrease the decay time. Glucose in the sample displaced some of the labeled sugar, resulting in an increase in lifetime that could be measured by phase and/or modulation of the donor emission. Also, a new fibre optic sensing technique based on coupling the swelling of a

polymer gel to a change in fluorescence intensity for monitoring glucose concentrations was discussed (McCurley, 1994). A fluorophore, an amino functional group and the enzyme GOD were each incorporated into a crosslinked polymer gel, which was formed on the end of a fibre optic rod. While the amount of fluorophore remained constant, the gel volume changed in response to a change in the ionisation state of the amino moiety and this change was related to glucose concentration.

Li and Walt (1995) presented a fibre-optic sensor for the continuous and simultaneous determination of glucose and oxygen. The sensor comprised dual-analyte sensing sites in defined positions using localised photopolymerization of appropriate fluorescent indicators or enzymes on the distal end of an imaging fibre. The changes in the optical properties at each site were transmitted through an imaging fibre through distinct optical pathways and simultaneously monitored with a charged-coupled device (CCD) camera. The oxygen sensing site consisted of an oxygen-sensitive ruthenium complex in a hydrophobic gas-permeable copolymer on the distal end of an imaging fibre. The glucose sensing site was composed of a second oxygen sensing polymer cone coated with poly(hydroxyethyl-methacrylate) containing immobilised GOD. The concentrations of glucose and oxygen were proportional to the changes in the fluorescence intensities of the ruthenium complex at each sensing site. The response time varied from 9 to 28 sec, depending on the different thickness of the enzyme layer, and the detection limit was 0.6 mM glucose.

In 1996, a micrometer-sized fibre-optic fluorescence biosensor for glucose was fabricated incorporating glucose oxidase (Rosenzweig & Kopelman, 1996). Tris(1,10-

phenanthroline)ruthenium chloride, an oxygen indicator, was used as a transducer. The ruthenium complex and GOD were incorporated into acrylamide polymer that was attached covalently to a silanised optical-fibre tip surface by photocontrolled polymerisation. The response time was around 2 sec and the detection limit was around 1×10^{-15} M glucose.

3.1.3 Glucose Oxidase (GOD)

Glucose oxidase (β-D-glucose: O_2 oxidoreductase, EC 1.1.3.4) has been highly purified mainly from the extracts of three fungi, *Penicillium notatum*, *Penicillium amagasakiense* and *Aspergillus niger* (Coulthard *et al.*, 1945; Kusai *et al.*, 1960; Pazur *et al.*, 1964; Schepartz & Subers, 1964). The present study used GOD from *Aspergillus niger*, which is the most widely used enzyme in the development of biosensors due to its high specificity, stability and turnover number (Swoboda & Massey; 1965; Wilson & Turner, 1991; Janata, 1992; Saudan *et al.*, 1994).

The *A. niger* enzyme is a dimer, containing two molecules of bound flavin adenine dinucleotide per molecule of protein. Various values have been given for its molecular mass in the range 151×10^3 to 186×10^3 Da, but most values lie in the range $155 \times 10^3 \pm 5 \times 10^3$ Da (Wilson & Turner, 1991). Lyophilised glucose oxidase is extremely stable up to 2 years at 0 ^{0}C and up to 8 years at -15 ^{0}C. It has very high solubility in water, and its stability, in solution, is dependent on pH. The enzyme shows a broad activity plateau between pH 4.0 and pH 7.0, with optimum pH 5.5-6.5. The isoelectric point is pH 4.2. Below pH 2 and above pH 8 its catalytic activity is rapidly lost (Coulthard *et al.*, 1945). GOD is highly specific for β-D-glucose, but also oxidises other monosaccharides at much

lower rates (Adams *et al.*, 1960; Leary *et al.*, 1992). It is inhibited by micromolar amounts of heavy metals such as mercury, silver and lead (Nakamura & Ogura, 1962). The preclinical safety studies regarding the toxicological and pharmacokinetic properties of glucose oxidase have been reported by Samoszuk *et al.* (1993), and they concluded that GOD has reasonably predictable toxicities and is, therefore, safe for human trials.

The fundamental aspects of the kinetic mechanism were incisively established for the first time by Nakamura and Ogura (1962) and Gibson *et al.* (1964). GOD catalyses the oxidation of β-D-glucose by molecular oxygen producing gluconolactone (hydrolysed further to gluconic acid) and hydrogen peroxide (Nakamura & Ogura, 1962; Duke *et al.*, 1969; Weibel & Bright, 1971; Atanasov & Wilkins, 1994):

$$\beta\text{-D-glucose} + O_2 + H_2O \xrightarrow{\text{GLUCOSE OXIDASE}} \beta\text{-D-gluconic acid} + H_2O_2 + \text{Energy} \qquad (3.a)$$

The increase in gluconic acid and hydrogen peroxide concentrations and the decrease in oxygen concentration due to this reaction may be detected electrochemically or optically and are proportional to the glucose concentration. Literature values for the Michaelis constant (K_m) of glucose oxidase with glucose lie around 20-33 mM, and with dioxygen around 0.25 mM (Kresse, 1990; Wilson & Turner, 1991). Since temperature increase causes the oxygen concentration to decrease, the normal increase of activity caused by higher temperatures is counteracted. Little change in activity occurs between 15 ^{0}C and 60 ^{0}C (Wilson & Turner, 1991).

3.2 MATERIALS & METHODS

3.2.1 Chemicals

The enzyme, glucose oxidase (β-D-Glucose, oxygen 1-oxidoreductase; EC 1.1.3.4) (176 units/mg type VII, from *Aspergillus niger*) and β-D(+)Glucose (97+%, containing up to 3% α-anomer) were purchased from Sigma Chemical Co. (Poole, Dorset). One unit of the enzyme will oxidise 1.0 μM of β-D-glucose to D-gluconic acid and H_2O_2 per min at pH 5.1 at 35 ^{0}C, equivalent to an O_2 uptake of 22.4 μl per min; if the reaction mixture is saturated with oxygen, the activity may increase by up to 100%. The purchase of the indicators, HPTS and tris(2,2'-bipyridyl)ruthenium(II) chloride hexahydrate, was mentioned in the previous chapter (Section 2.2.1.1). All other chemical reagents were of analytical reagent quality and used as obtained from BDH Ltd. (Poole, Dorset).

All experiments were performed at room temperature (22±2 ^{0}C) and buffers were prepared with doubly-distilled, deionized water. For the kinetic measurements the standard buffer solution was 0.1 mM sodium phosphate buffer containing 0.1 M NaCl, pH at 7.4. Stock solutions of indicators were prepared by bubbling 1 mM phosphate buffer with pure oxygen for at least 15 min. All components of the assay mixtures were freshly prepared except for stock solutions of glucose for kinetic measurements, which were freshly prepared daily and stored in the refrigerator for at least 12 hours before use to allow equilibration of mutarotation between α-D-glucose and β-D-glucose.

In the kinetic experiments (Experimental Modes), a small stirrer bar was placed in the bottom of the cuvette in order to keep the solution homogeneous during the reaction and it

was rotated at constant speed for all the experiments by maintaining the applied voltage and current of its motor at a fixed value. The motor was placed under the cuvette holder inside the spectrofluorometer. All additions of stock solutions (in the range of μl) were made outside the instrument and only the specific amount of glucose oxidase was added after the cuvette had been placed inside the instrument and the software was ready to run the definite timedrive program, in order to monitor the reaction from the beginning.

3.2.2 Instrumentation

Fluorescence Spectrometer. All the fluorescence data for the experiments of the present and the following chapters were obtained using a commercial instrument, FluoroMax™ Spectrofluorometer DM3000F, SPEX (SPEX Industries, Inc., Edison, New Jersey, USA). This is a computer controlled ratioing luminescence spectrometer capable of measuring fluorescence, phosphorescence or chemiluminescence and bioluminescence. In this instrument both the excitation and emission monochromators are each equipped with a single grating, mounted in the Czerny Turner configuration and are tunable between 200 nm and 600 nm. A reference photodetector at the excitation monochromator stage compensates for source (150 W continuous ozone free Xenon discharge lamp) intensity fluctuation. Instrument and data acquisition parameters are controlled by dedicated computer software (DataMax Data Manager software, Version 1.03) which is also used for data logging and retrospective analysis.

Before any routine analysis of samples was undertaken, the FluoroMax™ instrument was calibrated and its performance was optimized. In order to calibrate both the monochromators, two experiments were performed. Firstly the excitation spectrometer

was calibrated by using a known spectral peak (at 467.1 nm) using the xenon lamp spectrum as a reference, and the integrated software of the fluorometer. Once the excitation spectrum calibration had been verified then the emission monochromator was calibrated by acquiring a water Raman scan using a bandpass of 5 nm and an excitation wavelength of 350 nm. The increment was set at 0.5 nm and an exposure time of 0.5 seconds was used. At this excitation wavelength the water Raman peak should occur at 397 nm and this peak position was used to verify the calibration of the emission monochromator. The intensity specifications of the water Raman peak using these parameters was 160,000 counts. The bandpass or resolusion of the scan was calculated by multiplying the dispersion of the emission gratings with emission spectrometer slit width (in mm) and is shown in the following equation:

$$\text{Bandpass} = \text{Slit Width (mm)} \times \text{System Dispersion (nm/mm)} \qquad (3.b)$$

The dispersion of the monochromator with gratings of 1200 gr/mm was 4.25 nm/mm.

All experiments used excitation and emission slit width, wavelength resolution and scan rate at 1 mm, 1 nm and 0.5 nm/sec respectively. The samples were placed in a quartz cuvette (10 mm^3) (Hellma Ltd, Essex) irradiated at 90^0 (from the plane of the surface) and the fluorescence was recorded at 90^0 to the direction of the incident beam. The mixed solutions in the cuvette were prepared immediately before the spectra were taken.

As described in the preceding chapter, the LS50 Luminescence Spectrometer from Perkin-Elmer was used for the spectroscopic investigation of the fluorescent indicators. However, in the present and following chapters another fluorometer was used, the Fluoromax from

SPEX, and as a result a small shift in the peak wavelengths of the indicators appears. In particular, the maxima excitation and emission wavelengths of HPTS were obtained with the Perkin-Elmer spectrometer at 510 nm and 401 nm, and with the SPEX spectrometer, at 507 nm (3 nm shift) and 401 nm (no shift), respectively. Also, the maxima excitation and emission wavelengths of tris(2,2'-bipyridyl)ruthenium(II) chloride hexahydrate were found with the Perkin-Elmer spectrometer at 610 nm and 456 nm, and with the SPEX spectrometer at 597 nm (13 nm shift) and 452 nm (4 nm shift), respectively. Finally, the common excitation and emission wavelengths were found at 565 nm and 410 nm using the Perkin-Elmer spectrofluorometer and at 555 nm (10 nm shift) and 410 nm (no shift), respectively, using the SPEX spectrofluorometer. The wavelengths obtained from SPEX spectrometer, were used in the following experiments instead of the corresponding wavelengths obtained during the experimental investigations described in Chaper 2.

The two instruments were calibrated using a standardised procedure. The above mentioned differences in the peak wavelengths of the indicators found by using the two different instruments are in an acceptable range and similar differences have been reported in the literature, i.e. Offenbacher *et al.* (1986) reported for HPTS excitation maxima wavelength at 470 nm (in base form) and 405 nm (in acidic form) and emission maximum at 520 nm using an Aminco SPF 500 spectrofluorimeter; for the same indicator, Leiner and Hartmann (1993) reported excitation maxima at 475 nm (in base form) and 410 nm (in acidic form) and fluorescence emission maximum at 530 nm using a SPEX Fluorolog II fluorometer). The encountered disparities were much smaller for HPTS which presents a very sharp intensity peak, than tris(2,2'-bipyridyl)ruthenium(II) chloride hexahydrate which provides a very flat intensity curve in the peak region. This shape may cause

different instruments to pick a different maximum caused by random local variation in the flat peak region.

3.3 RESULTS

3.3.1 Spectroscopic Investigation of Glucose Oxidase

Glucose oxidase was dissolved in phosphate buffer to give a yellow coloured solution. The absorption spectrum of a 500 U/ml of this compound is shown in Figure 3.1. The spectrum extended from 200 nm to 700 nm and the maximum absorption occured at 268 nm (a = 1.91) in the UV region, with another peak at 240 nm (a = 1.85). The absorbance then decreased reaching a minimum value in the visible region at 379 nm (a = 0.38), before a final small peak was observed at 451 nm (a = 0.45).

The excitation and emission fluorescence spectra of glucose oxidase are shown in Figure 3.2, which illustrates that the excitation peaks occurred at 370 nm and 440 nm. Excitation with 440 nm radiation elicited a peak emission at 520 nm. Figure 3.3 and 3.4 show the fluorescence quenching of increasing enzyme concentrations in the range 1 - 100 U/ml with excitation wavelength at 370 nm and 440 nm, respectively. The corresponding graph of fluorescence intensity against concentrations of glucose oxidase (0 - 1000 U/ml), at an excitation wavelength of 440 nm, is shown in Figure 3.5, which indicates that the fluorescence intensity was directly proportional to enzyme concentration from 0 until about 200 U/ml and continued to increase to 500 U/ml. In addition, it was found out that the fluorescence of glucose did not vary significantly over the pH range from 4 to 8.

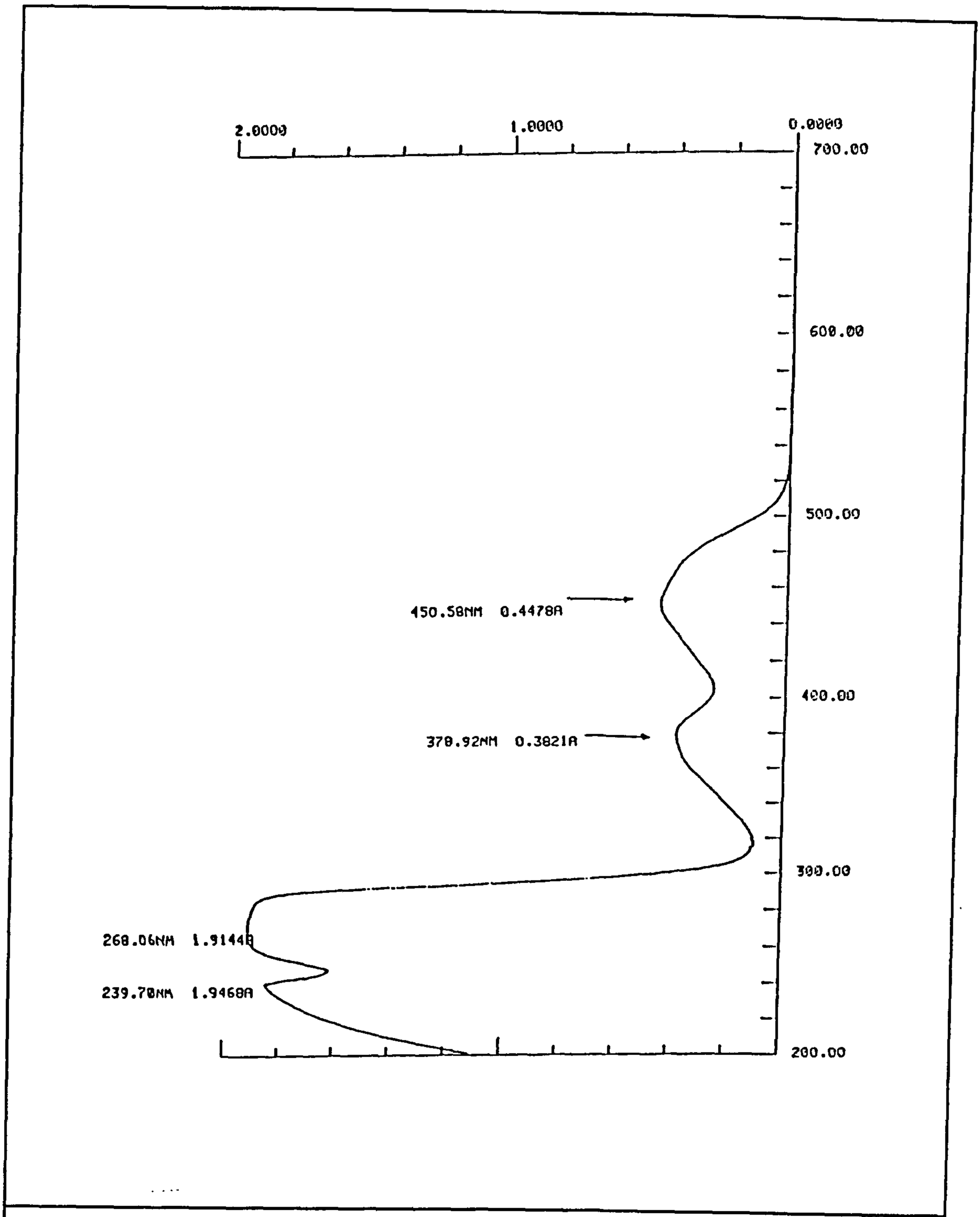

FIGURE 3.1 UV and Visible absorption spectrum of glucose oxidase (500 U/ml) in phosphate buffer pH 7.4 at 22 ^{0}C.

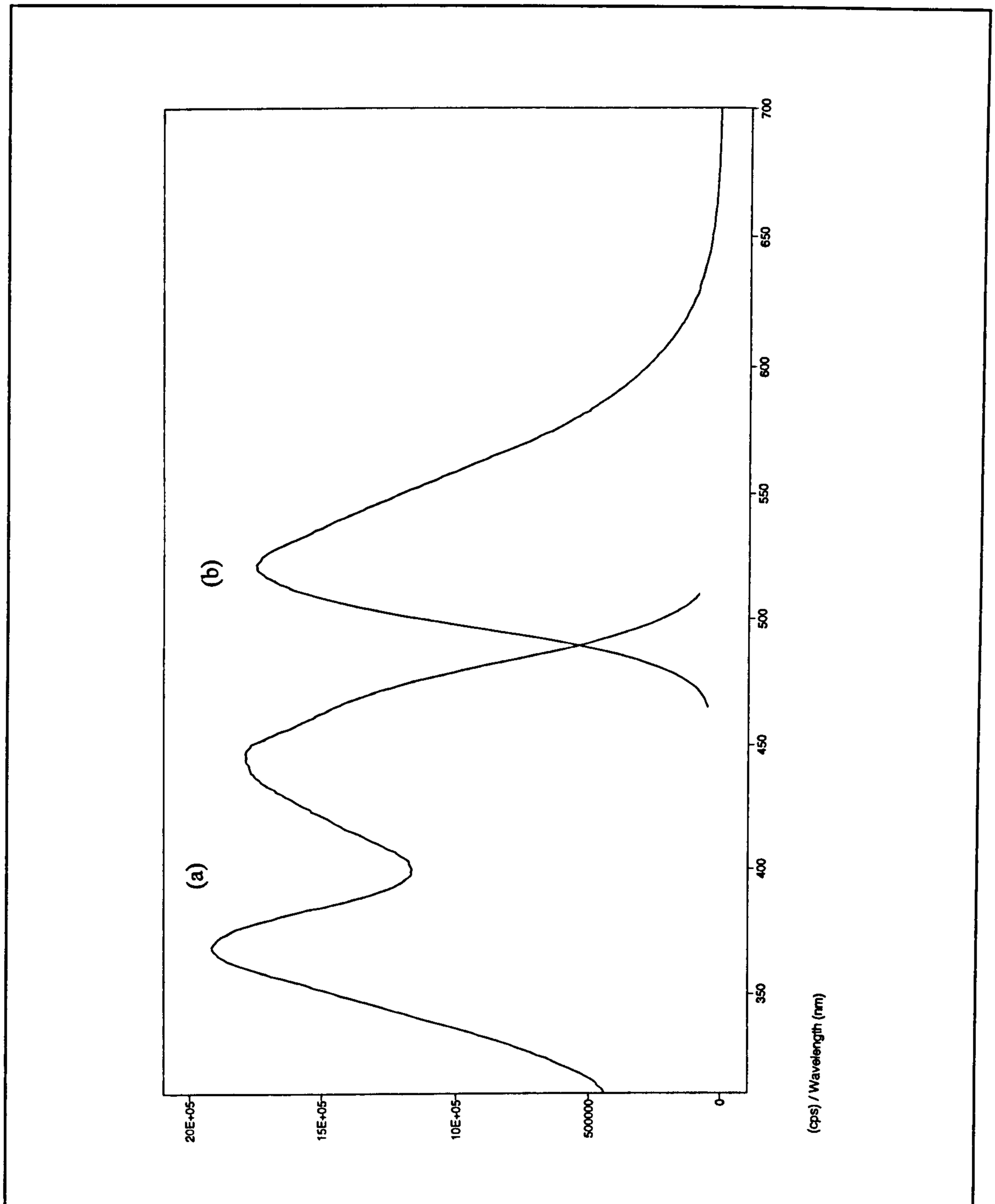

FIGURE 3.2 Excitation (a) and fluorescence (b) spectra of glucose oxidase (100 U/ml) with excitation wavelength at 440 nm and fluorescence monitored at 520 nm, in phosphate buffer pH 7.4 at 22 ^{0}C.

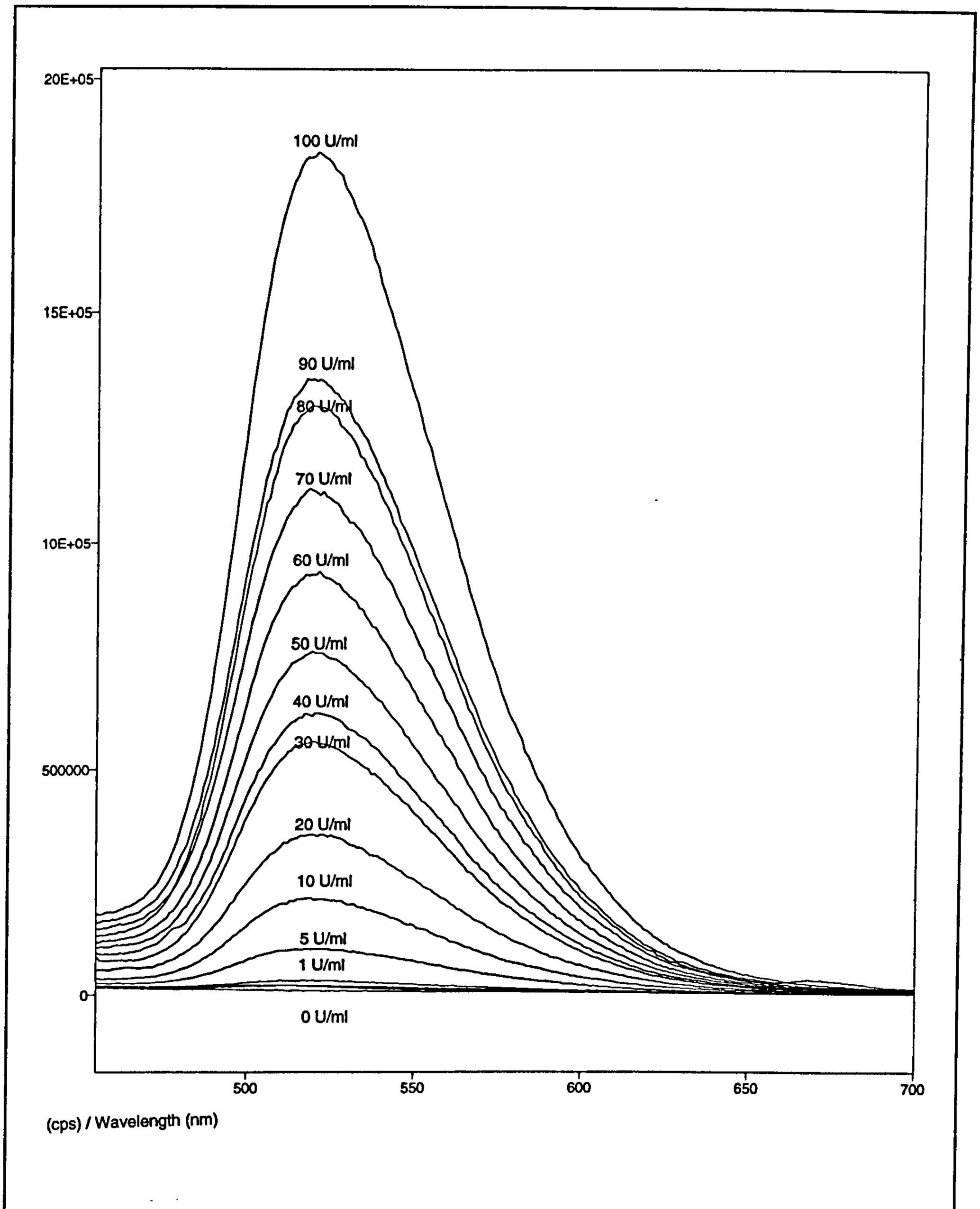

FIGURE 3.3 Fluorescence spectra of glucose oxidase (1-100 U/ml) in phosphate buffer pH 7.4 at 22 ^{0}C. Solutions were excited with a wavelength of 370 nm.

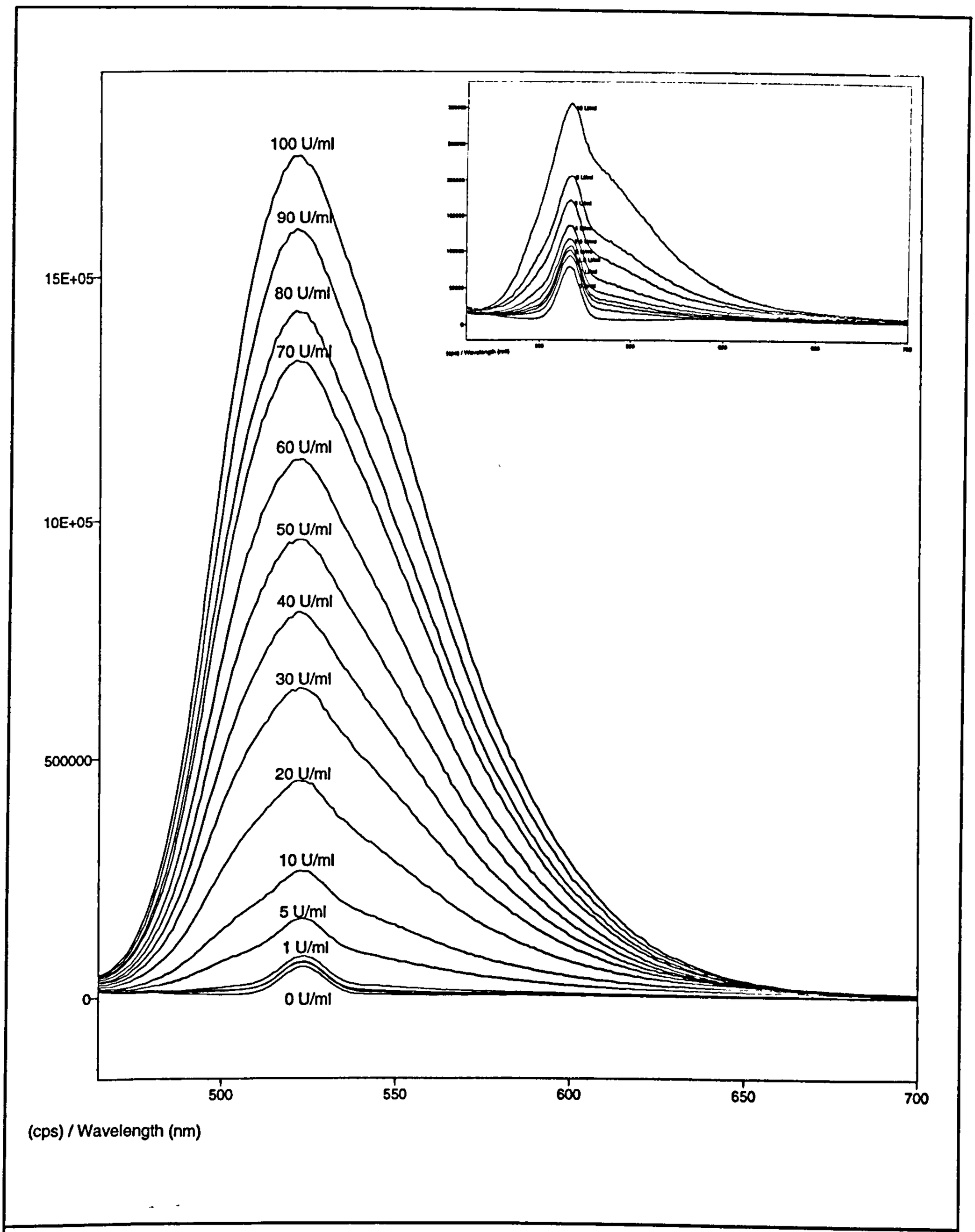

FIGURE 3.4 Fluorescence spectra of glucose oxidase (1-100 U/ml) in phosphate buffer pH 7.4 at 22 ^{0}C. Solutions were excited with a wavelength of 440 nm.

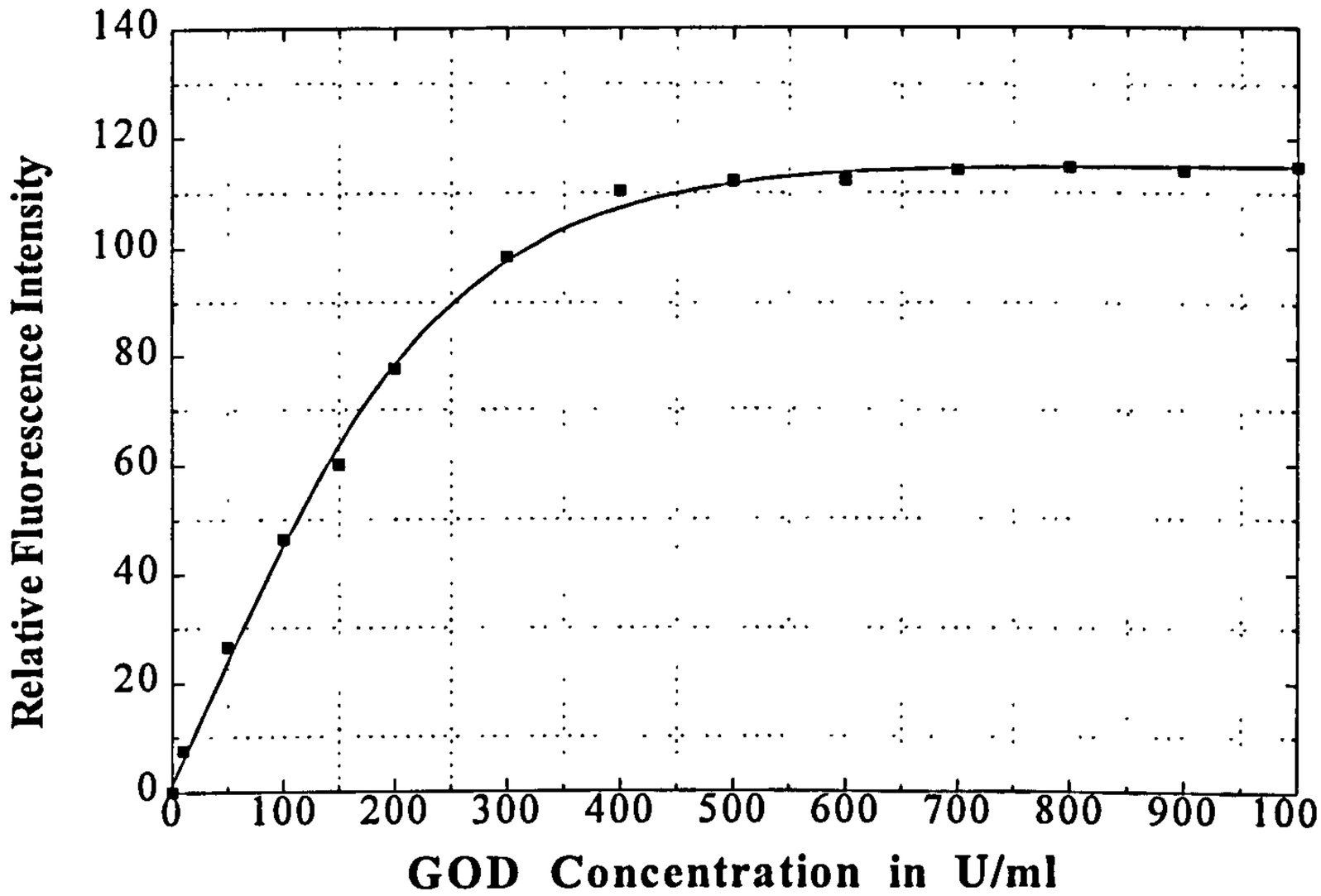

FIGURE 3.5 Relative fluorescence intensity versus concentration of glucose oxidase (10-1000 U/ml) in phosphate buffer pH 7.4 at 22 ^{0}C, excitation wavelength at 440 nm.

3.3.2 Kinetic Measurements of Glucose Oxidase Reaction

Kinetic experiments on the glucose oxidase reaction were divided into three sub-experiments, called "Experimental Modes", in order to establish the best choice of excitation and emission wavelengths for the indicators (HPTS and tris(2,2'-bipyridyl)ruthenium(II) chloride hexahydrate), and therefore light source and photodetector, respectively, for the design of an accurate fibre-optic glucose biosensor based on the fluorescence quenching of the pH-sensitive and oxygen-sensitive indicators, as discussed in Chapter 2. These Experimental Modes depend on changes in the fluorescence intensity at the maxima and common excitation and emission wavelengths of the indicators with time, during the biocatalytic oxidation of glucose by the enzyme glucose oxidase. Specifically, according to Reaction 3.a and the conclusions from Chapter 2, glucose can be measured by monitoring oxygen consumption with the oxygen-sensitive fluorescent indicator tris(2,2'-bipyridyl)ruthenium(II) chloride hexahydrate, and by changes in pH due to gluconic acid with the pH-sensitive fluorescent indicator HPTS.

From the previous section, it was found that glucose oxidase has a remarkable intrinsic fluorescence in aqueous solution, depending on its concentration. Its excitation wavelengths were at 370 nm and 440nm and the emission was monitored at 520 nm. It is important to note that glucose oxidase has an emission maximum wavelength at 520 nm (measured in quartz cuvettes), which is very close to the emission maximum of HPTS (507 nm), and can cause interference to the HPTS fluorescence, which is created by the strong overlap of the fluorescence emission bands of glucose oxidase and the indicators. Thus, the receiving signal during the oxidation of glucose, will not respond in

reality to the calibration curve of the indicator. Also, it would not be possible to use a standard concentration of the enzyme, with known fluorescence intensity, because changes in the fluorescence of the enzyme would be expected to occur during its interaction with glucose. Consequently, in order to avoid the above problems from the glucose oxidase, during the enzymatic oxidation of glucose, an optimum enzyme concentration of 1 U/ml was selected for the oxidation of glucose. The fluorescence intensity of the enzyme at this concentration was almost negligible in comparison with the corresponding fluorescence of 0.03 μM HPTS and 7 μM tris(2,2'-bipyridyl)ruthenium(II) chloride hexahydrate. In addition, the above enzyme concentration provided satisfactory reaction times for changes in the fluorescence intensity of the indicators responding to a glucose concentration range of 0 - 20 mM.

The following experiments (Experimental Modes) were carried out in quartz cuvettes (3ml total volume) containing: 1 U/ml glucose oxidase; 0.03 μM HPTS and 7 μM tris(2,2'-bipyridyl) ruthenium(II) chloride hexahydrate in buffer solution pH 7.4 (to reflect blood pH). Their experimental conditions were described in Section 3.2.1. Various concentrations of glucose were then added, and fluorescence was observed. The most interesting range of glucose is between 1 and 20 mM, which are typical values for patients with diabetes mellitus. The Experimental Modes can be described as follows:

Experimental Mode A

In this system, one excitation wavelength was used (the common wavelength of 410 nm) and changes in fluorescence intensity were followed with time, at two emission wavelengths (597 nm which is the maximum for tris(2,2'-bipyridyl)ruthenium(II)

chloride hexahydrate and 507 nm the maximum for HPTS), for different concentrations of glucose during the catalytic oxidation. This is based on the idea of constructing a glucose biosensor using a light source (i.e. LED) at a fixed excitation wavelength and monitoring the fluorescence simultaneously at two specific wavelengths probably using two photodetectors.

The results in terms of the rate of change of the fluorescence intensity of tris(2,2'-bipyridyl) ruthenium(II) chloride hexahydrate against the glucose concentration due to oxygen consumption are depicted in Figure 3.6. Details and an example of the raw data manipulation together with the reasons for choosing the values of rate of change of fluorescence intensity with time (dI/dt) instead of the actual values of fluorescence intensity itself for each glucose concentration, are reported in Appendix A. Similarly, the rate of change of the fluorescence intensity of HPTS due to pH changes in the microenvironment of the solution in the cuvette, during the production of gluconic acid by the oxidation, are illustrated in Figure 3.7.

The response time of the tris(2,2'-bipyridyl)ruthenium(II) chloride hexahydrate after the addition of glucose oxidase was around 1 to 4 minutes, depending on the glucose concentration, to reach a state where the changes of fluorescence intensity with time were negligible. Around 90% of the final intensity value was achieved in approximately 40 seconds to 3 minutes. Similarly, the corresponding response times of HPTS were 1 to 3 minutes for the state where the fluorescence intensity started remaining almost constant, and approximately 40 seconds to 2 minutes to reach 90% of this final value.

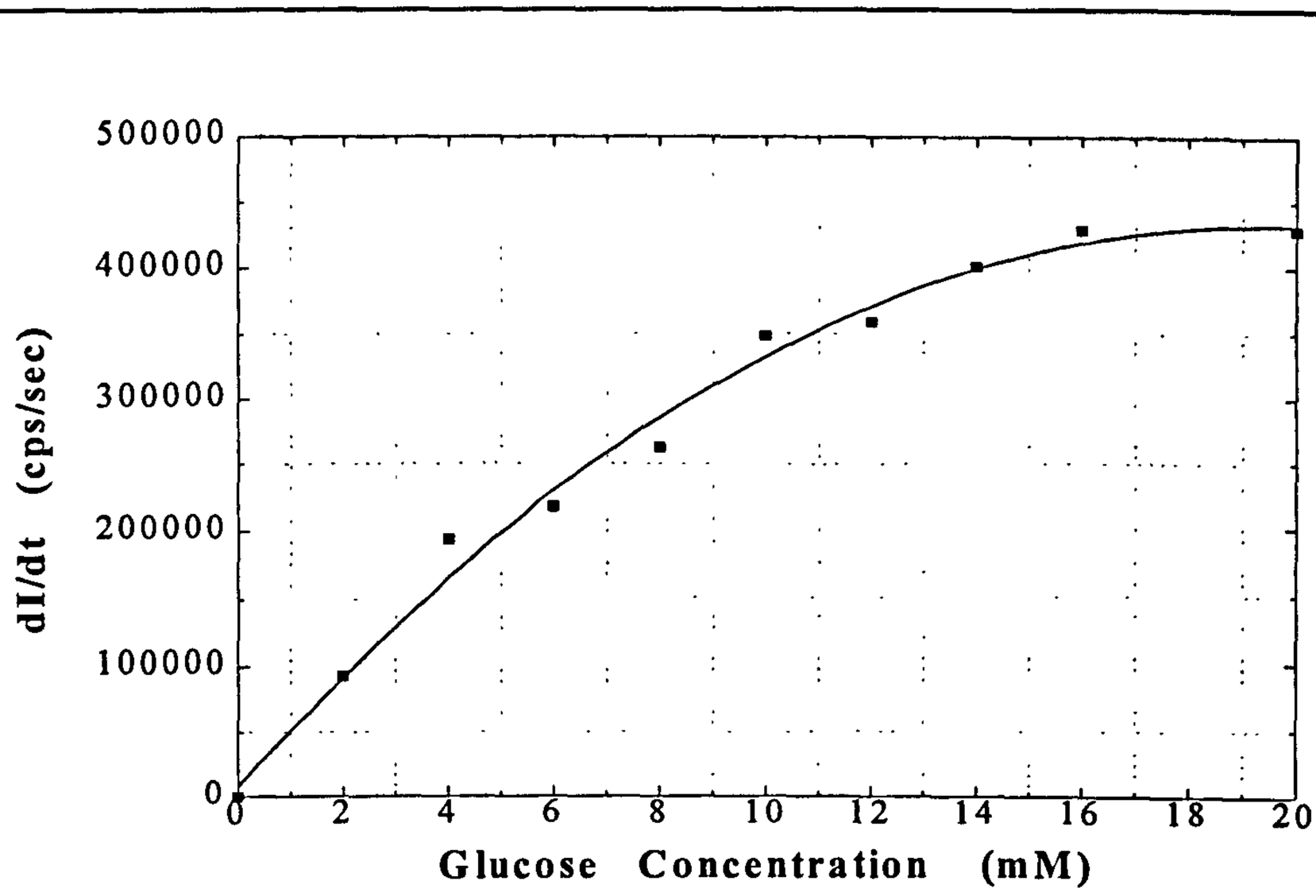

FIGURE 3.6 Rate of change of fluorescence intensity versus glucose concentration of tris(2,2'-bipyridyl)ruthenium(II) chloride hexahydrate, at fixed excitation wavelength of 410 nm and emission at 597 nm, during the catalytic oxidation of glucose.

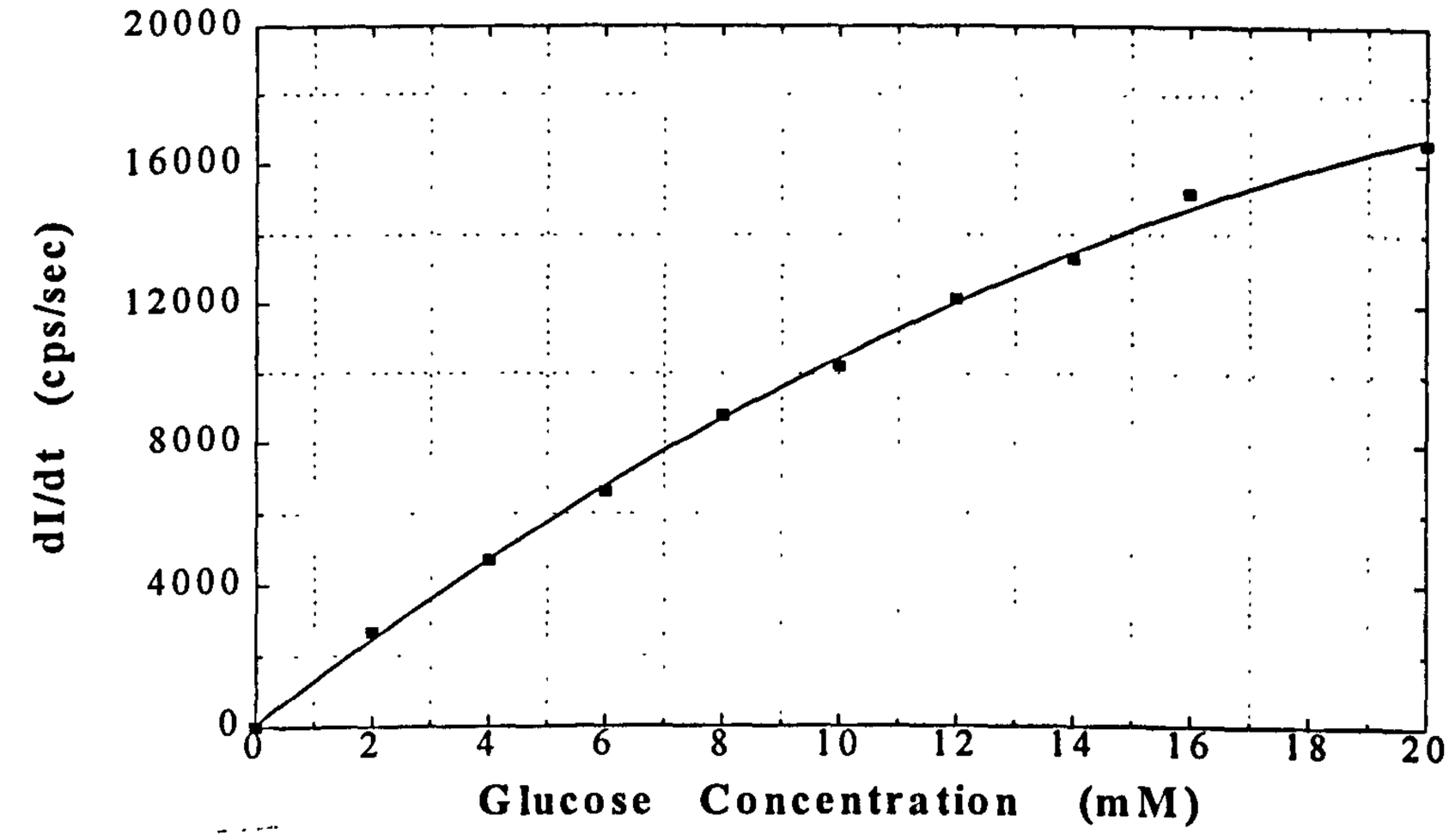

FIGURE 3.7 Rate of change of fluorescence intensity versus glucose concentration of HPTS, at fixed excitation wavelength of 410 nm and emission monitoring at 507 nm, during the catalytic oxidation of glucose.

For both indicators, lower glucose concentrations required longer response times (e.g. for 2mM glucose the response time was 3.3 minutes for tris(2,2'-bipyridyl)ruthenium(II) chloride hexahydrate and 2.5 minutes for HPTS), and vice versa for higher glucose concentrations (e.g. for 20 mM glucose the response times for tris(2,2'-bipyridyl) ruthenium(II) chloride hexahydrate and HPTS were 1 minute). Saturation appeared above 50 mM glucose and the lowest detectable glucose concentration was 1 μM for tris(2,2'-bipyridyl) ruthenium(II) chloride hexahydrate, and 100 μM for HPTS. In addition, Figures 3.6 and 3.7 show that these calibration curves of Experimental Mode A for glucose are hyperbolas following the Michaelis-Menten equation.

The kinetic parameters of 1 U/ml glucose oxidase in the presence of the indicators and concentrations of glucose were determined by using a Hanes plot (Cornish-Bowden, 1995). This plot is based on a transformation of the Michaelis-Menten equation for enzyme kinetics:

$$\nu = \frac{V \cdot \alpha}{K_m + \alpha} \qquad \text{(Michaelis-Menten equation)} \qquad (3.c)$$

into an equation that allows the results to be plotted as points on a straight line:

$$\frac{1}{\nu} = \frac{1}{V} + \frac{K_m}{V} \cdot \frac{1}{\alpha} \qquad \text{(eq. for Lineweaver-Burk or double-reciprocal plot)} \quad (3.d)$$

and if both sides are multiplied by α, the following equation is obtained:

$$\frac{\alpha}{\nu} = \frac{K_m}{V} + \frac{1}{V} \cdot \alpha \qquad \text{(eq. for Hanes or Woolf plot)} \qquad (3.e)$$

where K_m is the Michaelis constant, V the limiting rate of the reaction, α the glucose concentration, and ν the initial reaction rate.

The Hanes plots corresponding to Figures 3.6 and 3.7 are shown in Figures 3.8 and 3.9, respectively. From these plots and according to equation (3.e), the experimental value of the Michaelis constant K_m of the reaction was found to be equal to 13.3 mM for the case in which the reaction was monitored through the rate of change of fluorescence intensity of tris(2,2'-bipyridyl)ruthenium(II) chloride hexahydrate at excitation wavelength of 410 nm and fluorescence monitored at 597 nm. On the other hand, the Michaelis constant K_m was found to be equal to 33 mM when the reaction was monitored through the rate of change of fluorescence intensity of HPTS at excitation and fluorescence wavelengths of 410 nm and 507 nm, respectively.

Subsequent experiments were carried out in order to investigate the reproducibility and reliability of the above approach. Three glucose concentrations were chosen, in order to cover the critical range from 1 to 20 mM: 2 mM (hypoglycaemia); 5 mM (within normal range) and 20 mM (hyperglycaemia). Measurements were repeated 7 times for each concentration using the above system. The mean values of the rate of change of the

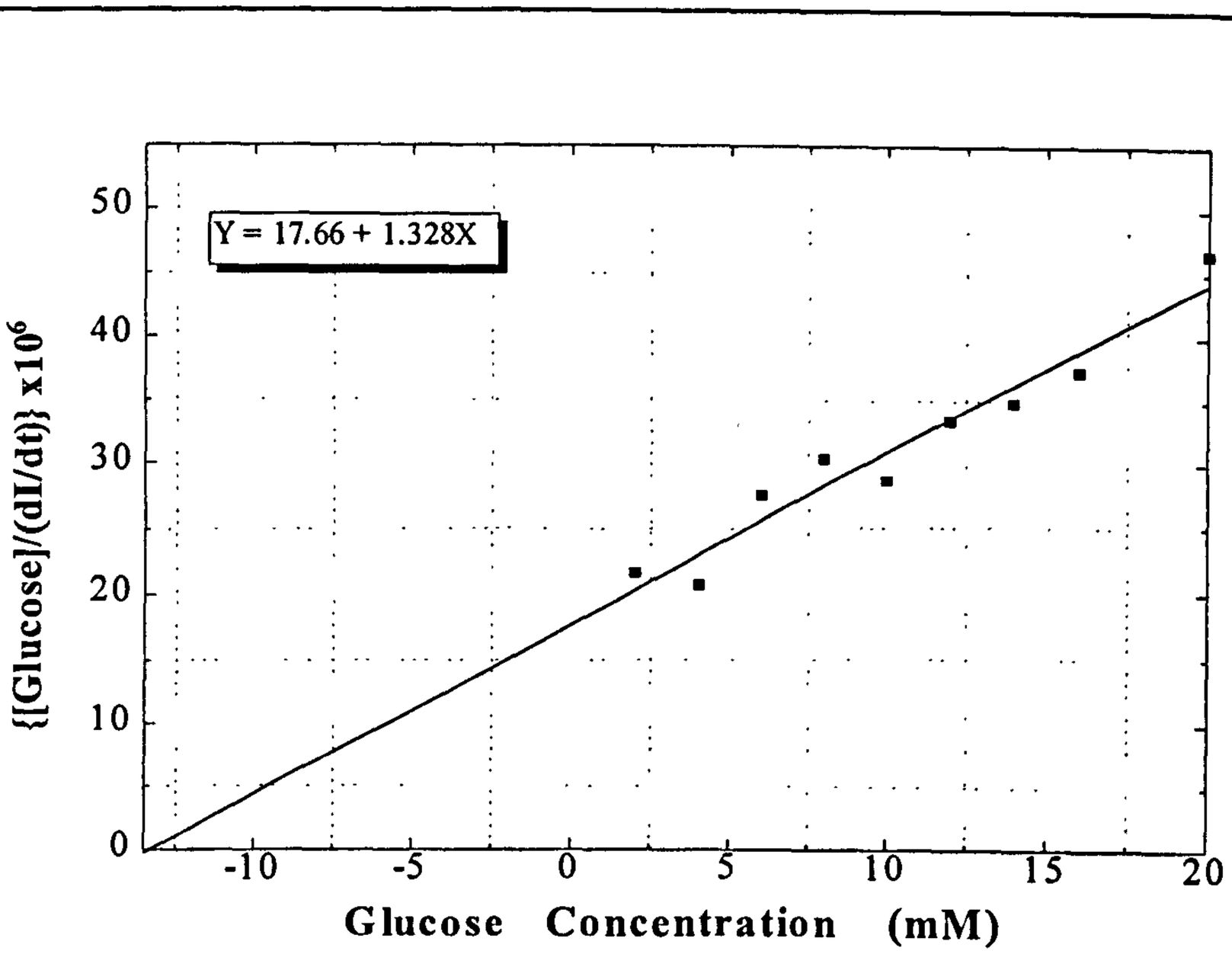

FIGURE 3.8 Hanes plot corresponding to Figure 3.6.

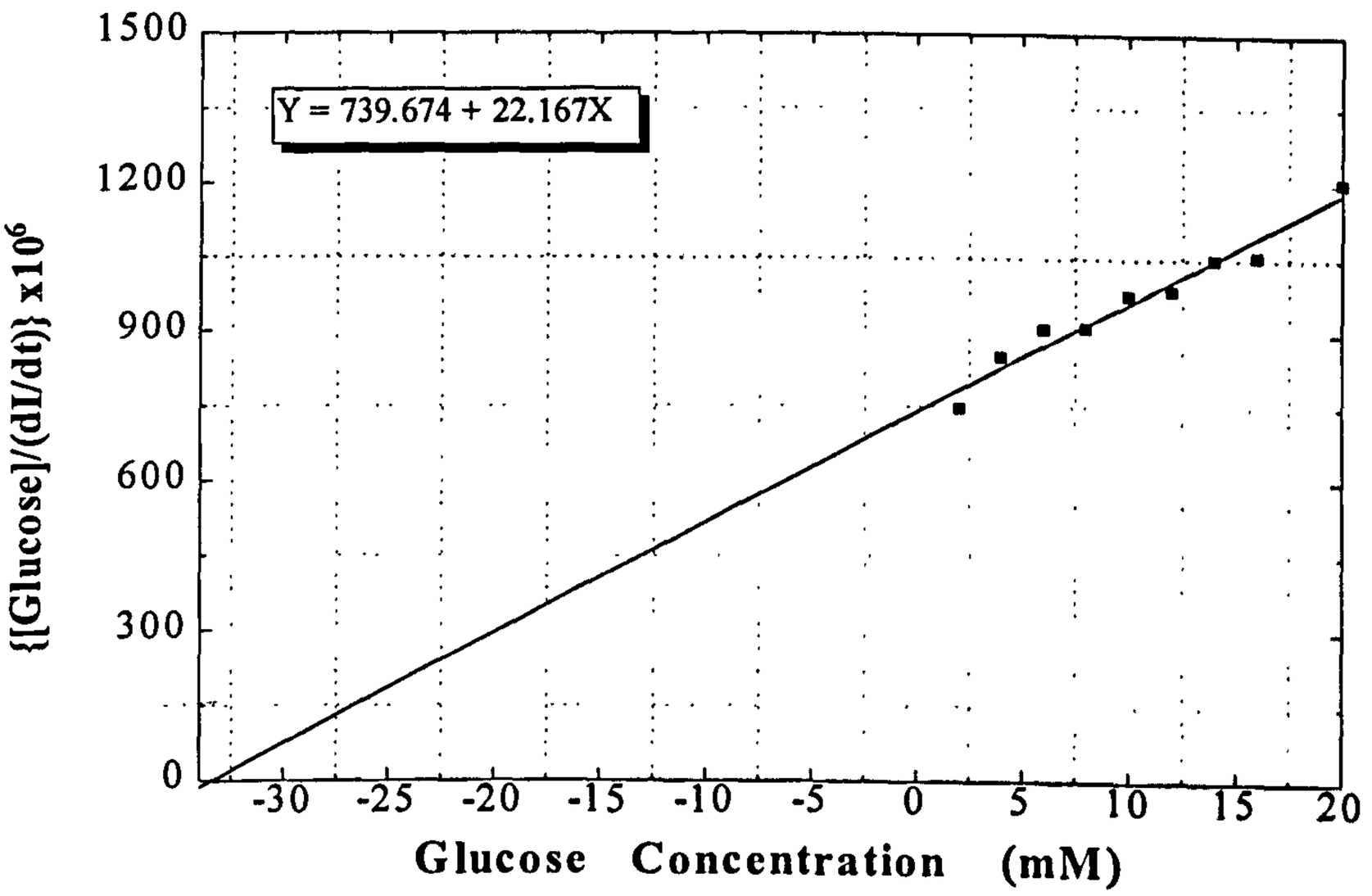

FIGURE 3.9 Hanes plot corresponding to Figure 3.7.

fluorescence intensity of tris(2,2'-bipyridyl)ruthenium(II) chloride hexahydrate, during the biocatalytic oxidation of glucose, against number of samples of 2 mM, 5 mM and 20 mM glucose and the coresponding coefficient of variations of these for each glucose concentration are presented in Table 3.1.

TABLE 3.1

Glucose Concentration	Mean Value	Coefficient of Variation (%)	R
2 mM	93	1.4	7
5 mM	207	1.8	7
20 mM	377	1.3	7

The results of the mean values for the rate of change in the fluorescence intensity of HPTS against number of samples of 2 mM, 5 mM and 20 mM of glucose during its oxidation, and the coresponding coefficient of variations of these concentrations are shown in Table 3.2.

TABLE 3.2

Glucose Concentration	Mean Value	Coefficient of Variation (%)	R
2 mM	2,65	0.87	7
5 mM	5,57	7.1	7
20 mM	17,21	4.6	7

In addition, experiments were performed to investigate the interference of substances usually found in biological samples, like ascorbic acid (0.5 mM), acetaminophen (0.3

mM), uric acid (1.5 mM), urea (4.2 mM) and lactate (4 mM), on the calibration curves of Experimental Mode A. A standard glucose concentration of 20 mM was used for the experiments. The response curve of the above glucose concentration was compared with the response curves taken in the same conditions but with the addition of one substance of the above reported chemicals. This experiment was repeated for all the above substances. The experimental results showed that all saturated solutions with the above substances did not interfere with the tris(2,2'-bipyridyl)ruthenium(II) chloride hexahydrate and HPTS responses. Therefore, the response curves of 20 mM glucose with or without the above substances were the same to those corresponding to Experimental Mode A.

Eventually, experiments were carried out in order to investigate the existence of any interference between the responses of the two indicators. Two glucose concentrations were chosen of 5 and 15 mM glucose and Experimental Mode A was applied using initially both indicators. For each glucose concentration, two curves of the changes in fluorescence intensity against time at two emission wavelengths (597 nm which is the maximum for tris(2,2'-bipyridyl) ruthenium(II) chloride hexahydrate and 507 nm the maximum for HPTS) were recorded, with excitation wavelength at 410 nm during the catalytic oxidation of glucose.

The above conditions were applied when only HPTS was used, and the response curves were obtained. Finally, tris(2,2'-bipyridyl)ruthenium(II) chloride hexahydrate was used only and the corresponding curves were recorded. The thorough comparison of the above curves proved that there was no interference between the responses of the two indicators.

Experimental Mode_B

The idea in this mode was to investigate the biocatalytic oxidation of glucose by measuring the sum of the changes in fluorescence intensity of both indicators against time, when the samples were excited at the common excitation wavelength of 410 nm and the fluorescence was monitored at the fixed common emission wavelength of 555 nm. This concept provides the basic principle for a simple design of an optical glucose biosensor using a light source (i.e. LED) in the fixed common excitation wavelength and a photodetector to monitor the fluorescence at the fixed common emission wavelength.

The results of the experimental data manipulation of the rate of change of the fluorescence intensity of both indicators against the glucose concentration during its catalytic oxidation are illustrated in Figure 3.10. These results were taken in a similar way to Experimental Mode A. The calibration curve in Figure 3.10 appears to be a hyperbola following Michaelis-Menten equation.The response time to reach a state where the changes of the fluorescence intensity with time were negligible, was approximately 1 to 4 minutes with 90% of the final intensity value being achieved in about 40 seconds to 3 minutes. This response time of the indicators was dependent on the glucose concentration; low glucose concentrations required longer times than larger concentrations. The lowest detectable glucose concentration was 80 μM, and saturation appeared above 50 mM glucose. The Hanes plot corresponding to the calibration curve of Figure 3.10 can be seen in Figure 3.11. The experimental Michaelis constant K_m from this Hanes plot, which was calculated according to equation (3.e), was equal to 15.54 mM.

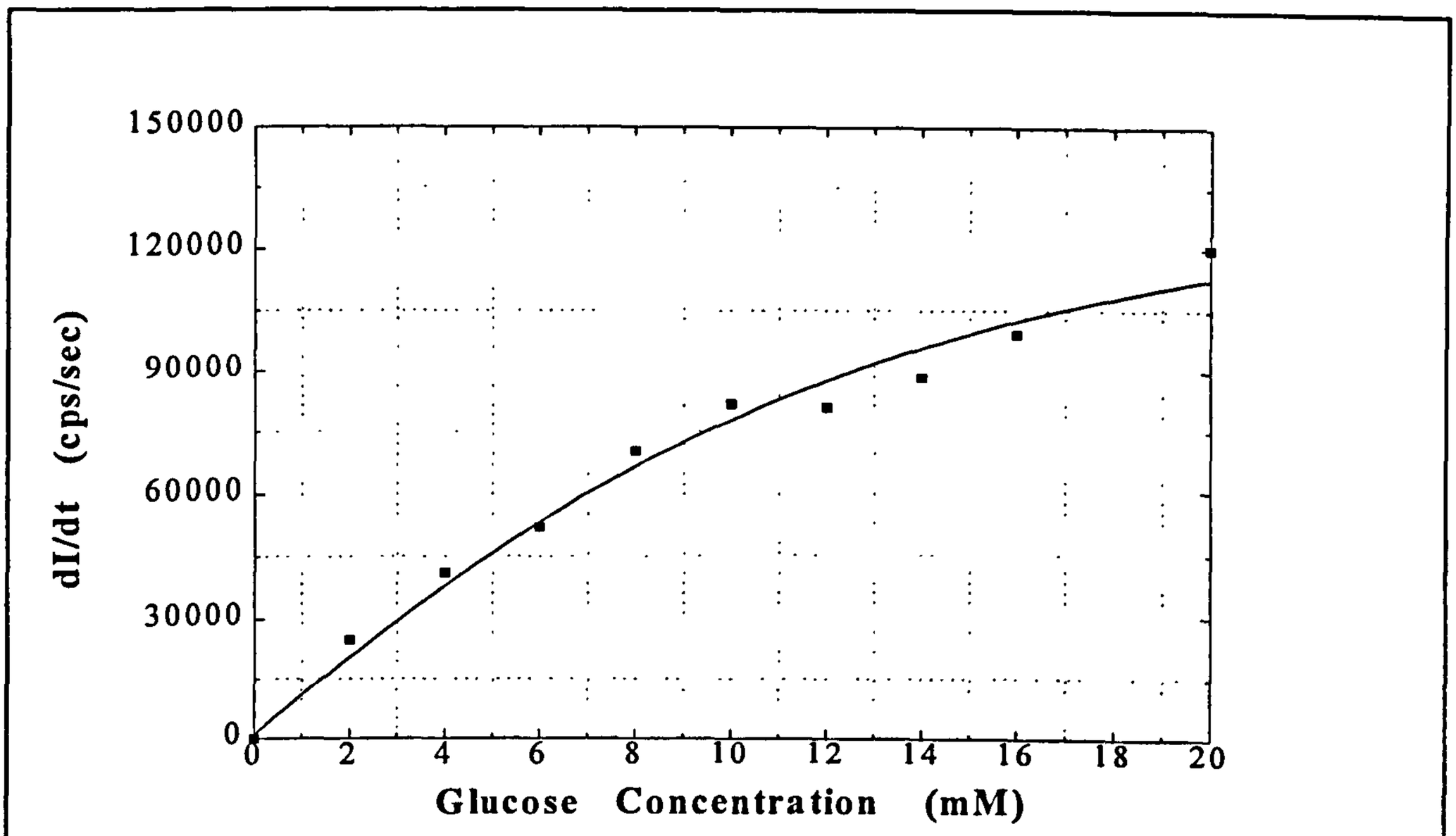

FIGURE 3.10 Rate of change of fluorescence intensity versus glucose concentration of the sum of tris(2,2'-bipyridyl)ruthenium(II) chloride hexahydrate and HPTS, at the excitation wavelength of 410 nm and monitoring the emission at 555 nm, during the catalytic oxidation of glucose.

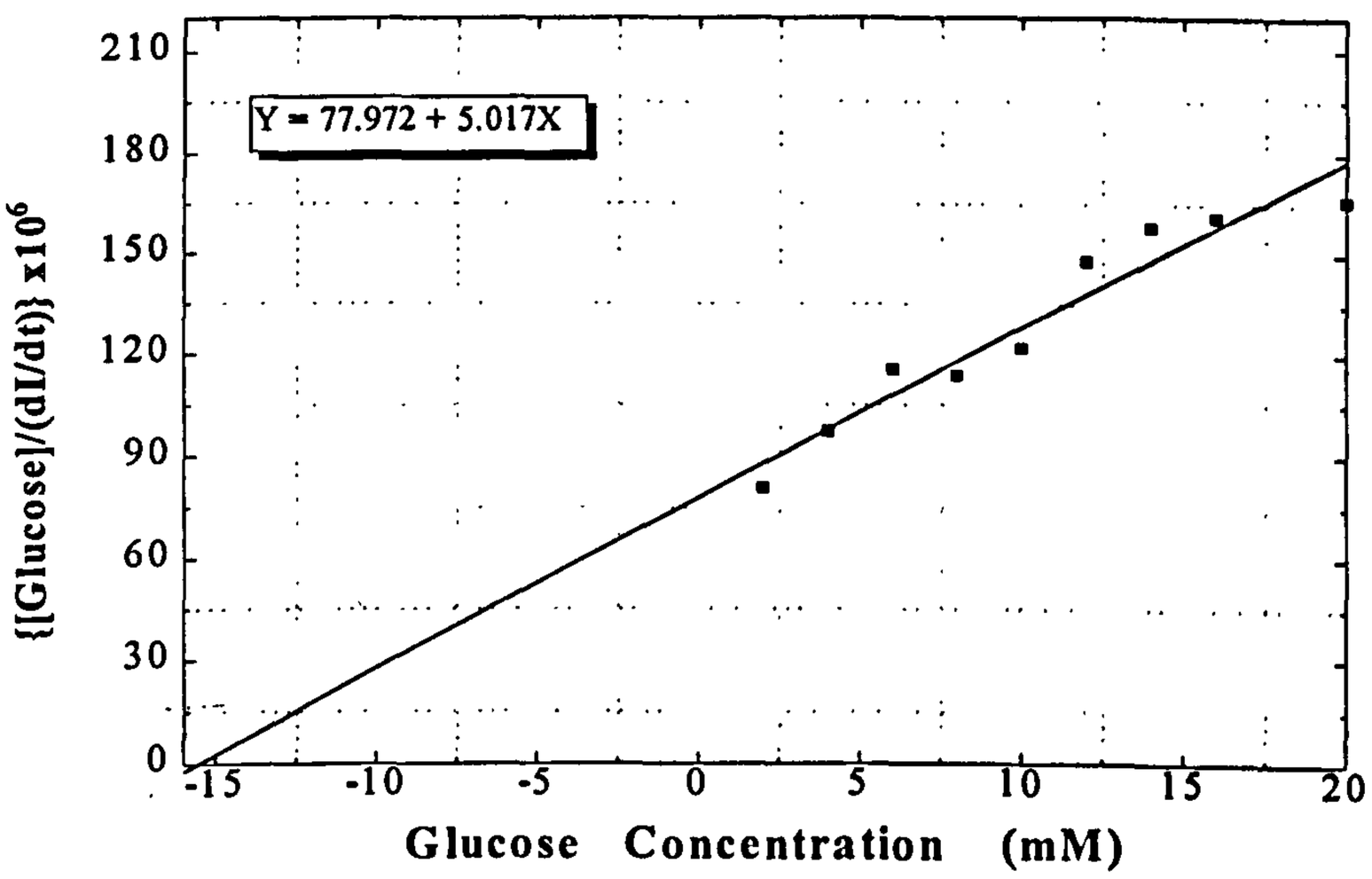

FIGURE 3.11 Hanes plot corresponding to Figure 3.10.

Experiments were carried out in order to determine the interference of substances usually found in biological samples, like ascorbic acid (0.5 mM), acetaminophen (0.3 mM), uric acid (1.5 mM), urea (4.2 mM) and lactate (1 mM) when Experimental Mode B was used. A standard glucose concentration of 20 mM was used, where the response curve of this concentration was taken as reference to compare the results from the solutions in cuvette containing in addition one of the above substances each time the experiment was repeated. The experimental results indicated that saturated solutions with the above substances did not interfere with the tris(2,2'-bipyridyl)ruthenium(II) chloride hexahydrate and HPTS responses similarly to Experimental Mode A.

Experimental Mode C

In this Experimental Mode, an investigation of the behaviour of the two indicators at their maxima excitation and emission wavelengths during the oxidation of glucose was carried out. Two calibration curves were established. In the first, the samples were excited at the maximum wavelength of tris(2,2'-bipyridyl)ruthenium(II) chloride hexahydrate of 452 nm and the emission intensity was measured at the maximum emission wavelength for this indicator which is 597 nm, in order to monitor the oxygen consumption during the reaction.

In the second curve, the excitation wavelength was fixed at the maximum of HPTS and the fluorescence was measured at 507 nm, which is the maximum emission wavelength for HPTS, in order to check the changes in pH during the reaction due to the production of gluconic acid. This idea results in a more complicated design for the glucose biosensor based on the simultaneous excitation of the sample at two specific

wavelengths and measuring the fluorescence from the sample separately at two particular wavelengths.

The results of the rate of changes of fluorescence intensity of tris(2,2'-bipyridyl) ruthenium(II) chloride hexahydrate and HPTS against glucose concentration during the oxidation are shown in Figures 3.12 and 3.13, similarly to Experimental Modes A and B. The response time of the tris(2,2'-bipyridyl)ruthenium(II) chloride hexahydrate was approximately 1 to 4 minutes to reach a state where the changes of fluorescence intensity with time were very small. A 90% of the final value of intensity was achieved in about 40 seconds to 3 minutes. Similarly, the response times of HPTS were 1 to 3 minutes to reach the above mentioned state, and approximately 40 seconds to 2.5 minutes to reach 90% of the final intensity value.

For both indicators, low glucose concentrations required large values of the above response times and vice versa. Saturation appeared above 50 mM glucose for both indicators and the lowest detectable glucose concentration was 1 μM for tris(2,2'-bipyridyl) ruthenium(II) chloride hexahydrate, and 80 μM for HPTS. Figures 3.12 and 3.13 show that these calibration curves are hyperbolas and follow the Michaelis-Menten equation. The corresponding Hanes plots for these calibration curves are illustrated in Figures 3.14 and 3.15, respectively. The experimental values of Michaelis constant K_m from these plots, according to equation (3.e), were found to be equal to 22 mM and 32.1 mM, respectively.

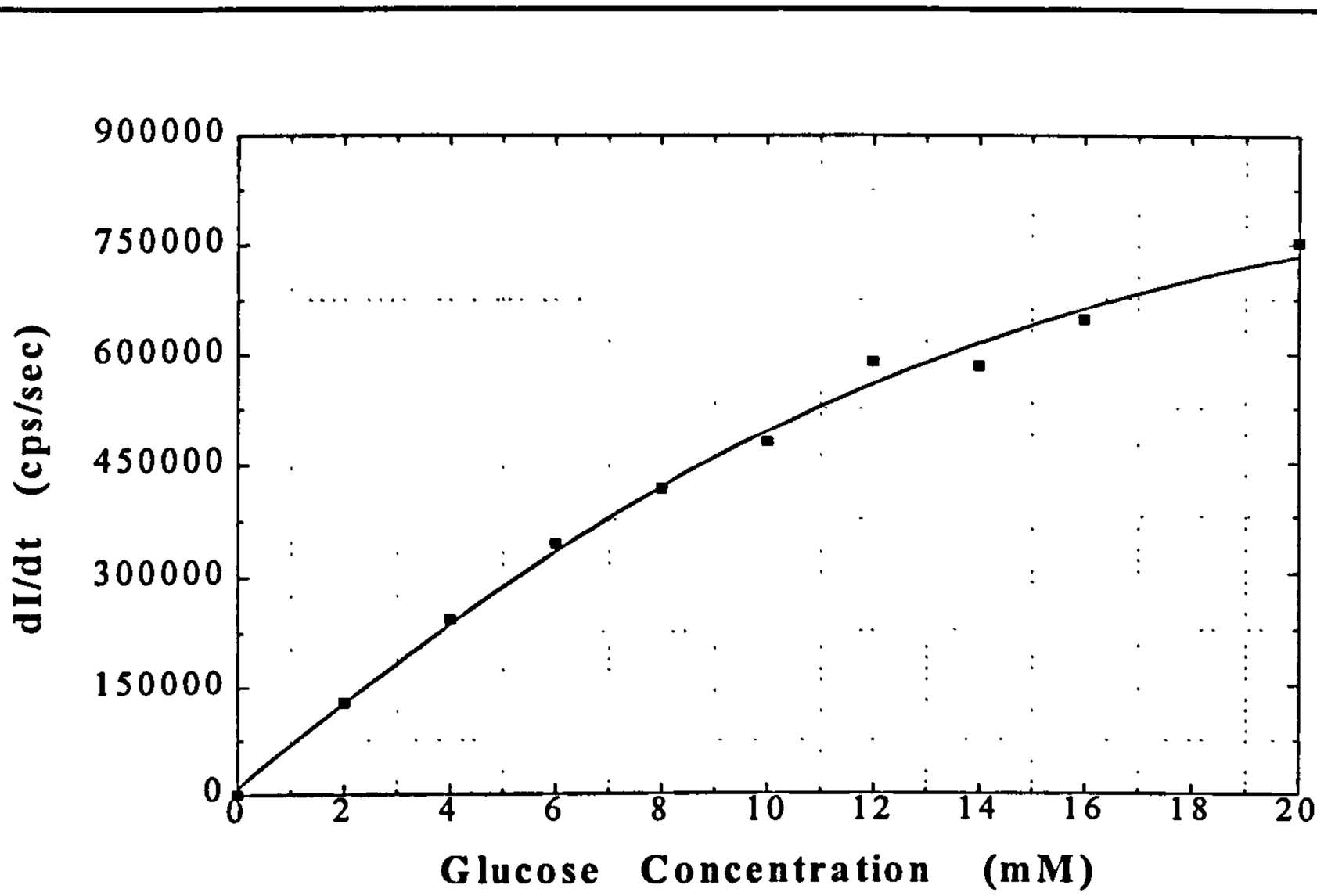

FIGURE 3.12 Rate of change of fluorescence intensity versus glucose concentration of tris(2,2'-bipyridyl)ruthenium(II) chloride hexahydrate, at fixed excitation wavelength of 452 nm and fluorescence monitoring at 597 nm, during the catalytic oxidation of glucose.

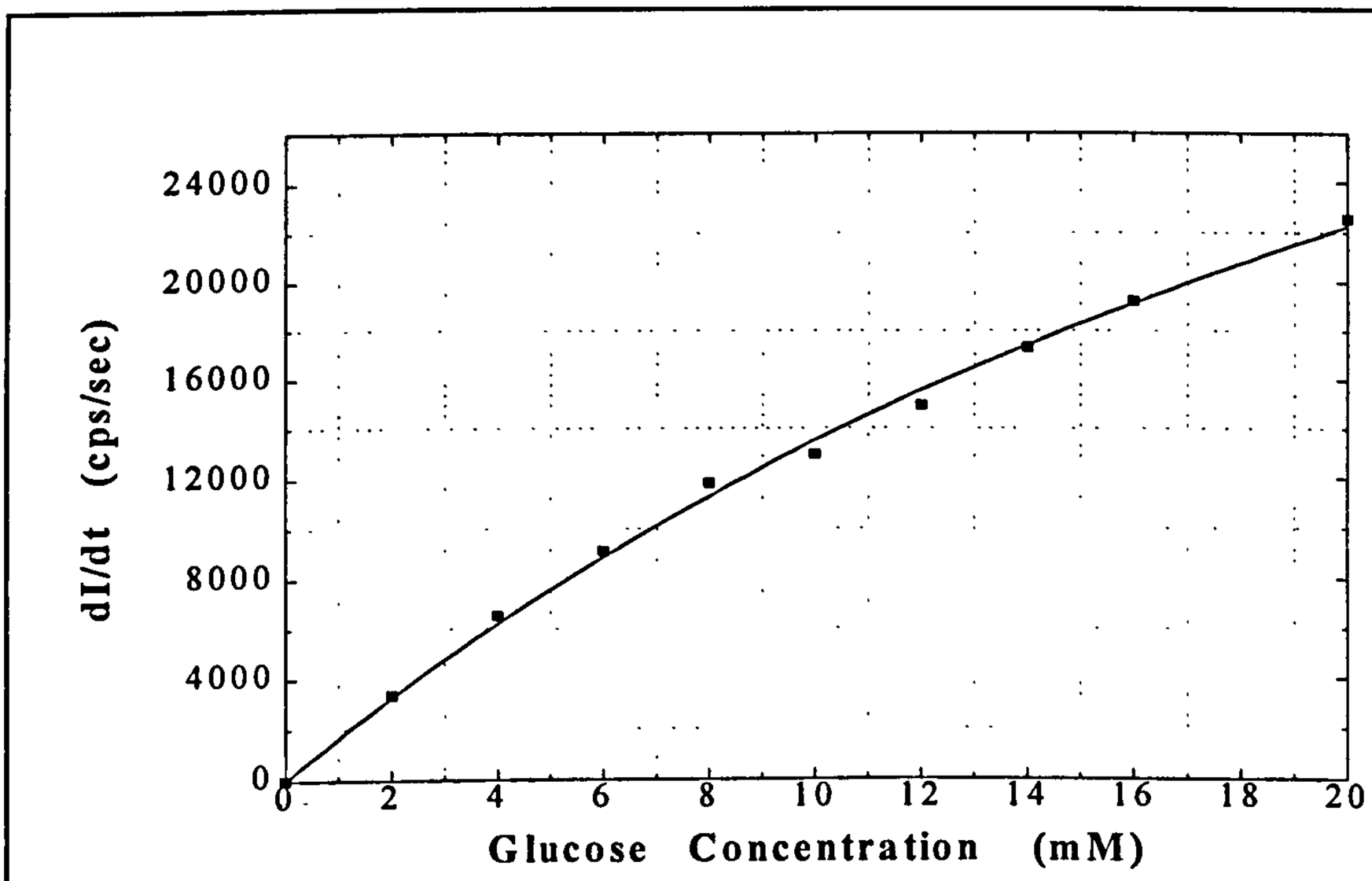

FIGURE 3.13 Rate of change of fluorescence intensity versus glucose concentration of HPTS, at fixed excitation wavelength of 401 nm and fluorescence monitoring at 507 nm, during the catalytic oxidation of glucose.

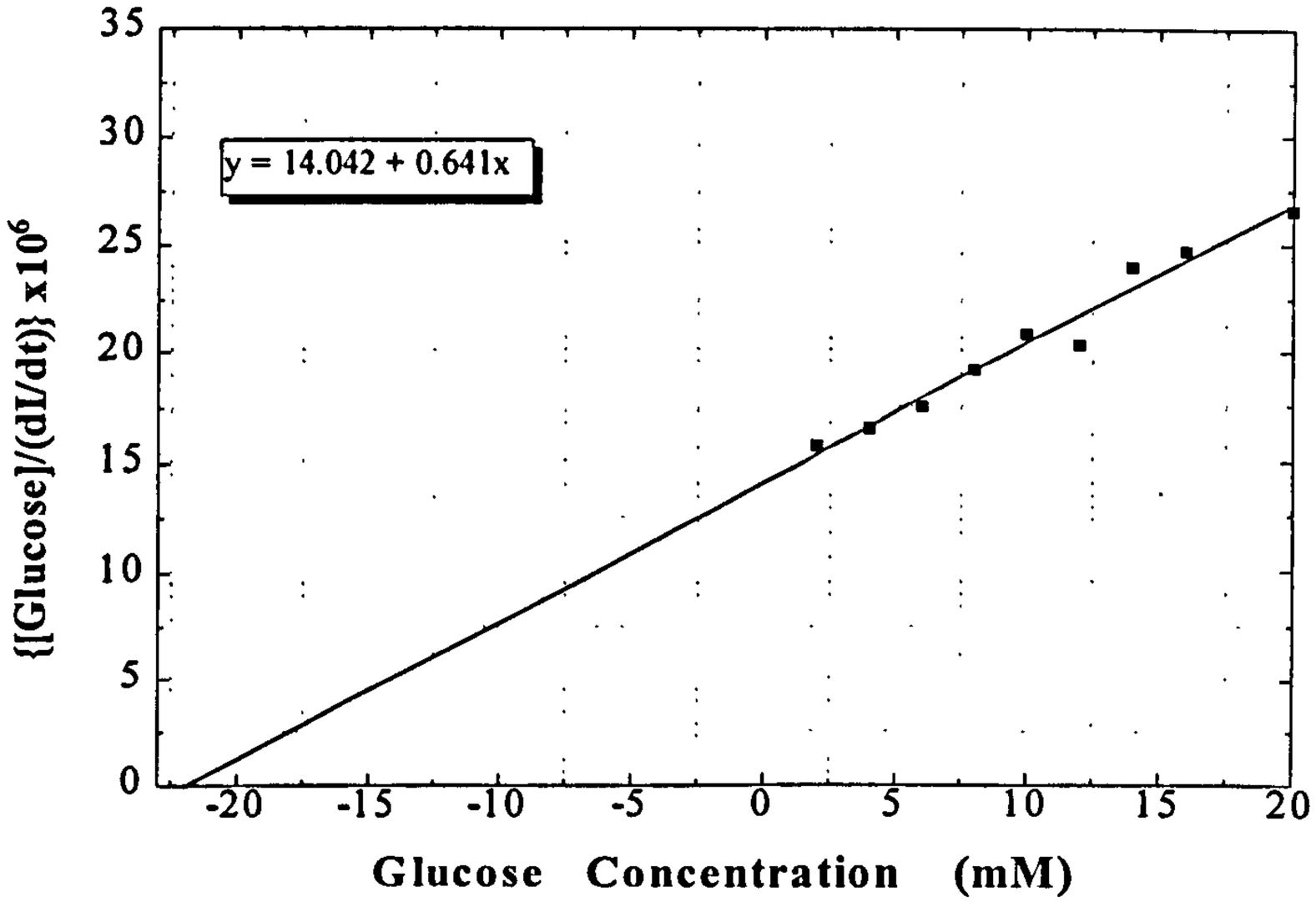

FIGURE 3.14 Hanes plot corresponding to Figure 3.12.

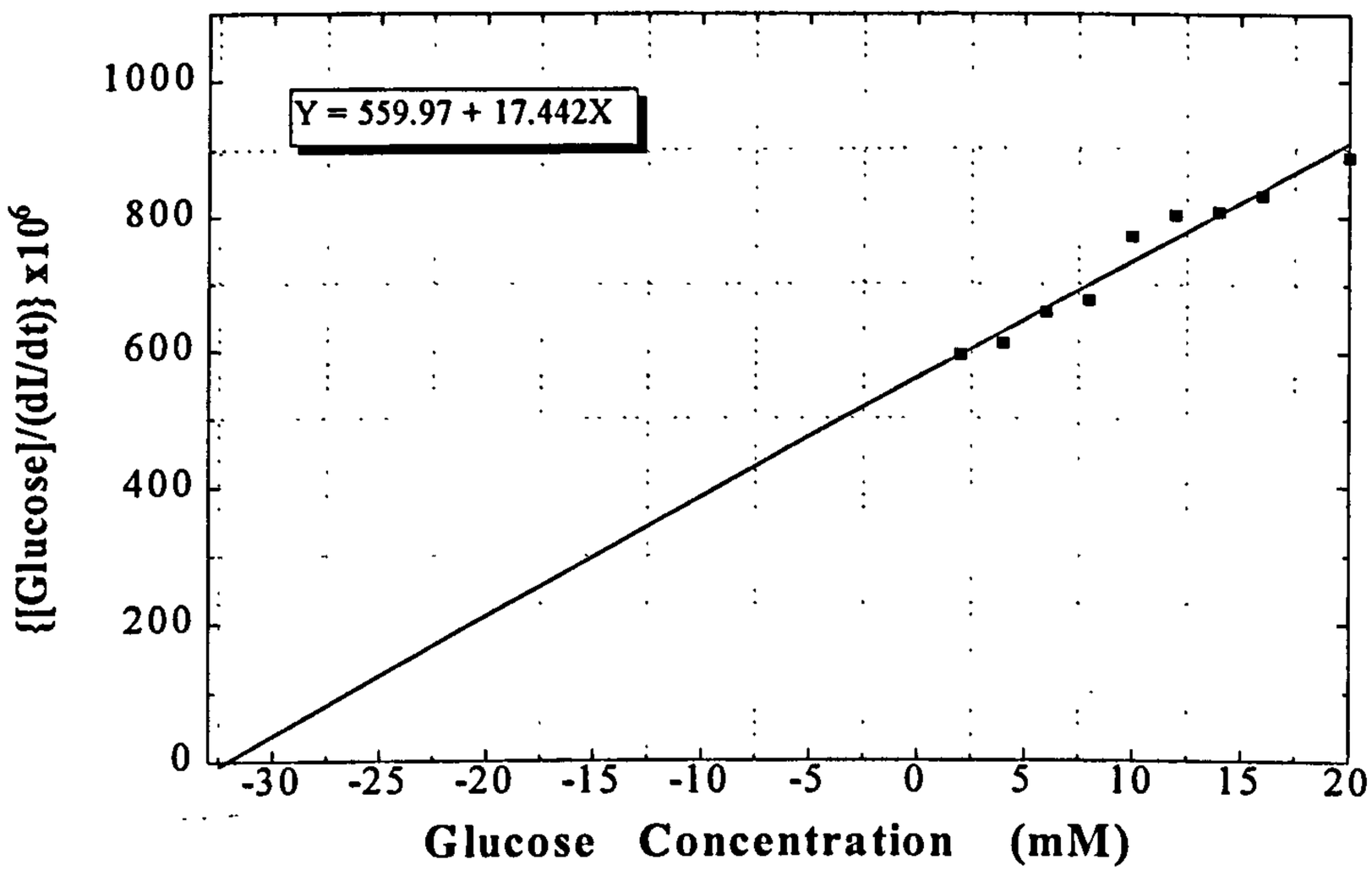

FIGURE 3.15 Hanes plot corresponding to Figure 3.13.

Experiments were carried out in order to investigate the interference of the substances of ascorbic acid (0.5 mM), acetaminophen (0.3 mM), uric acid (1.5 mM), urea (4.2 mM) and lactate (1 mM). These substances are usually present in biological samples in the above concentrations. For these experiments, a standard glucose concentrations of 20 mM was used. The experimental results showed that all saturated solutions with the above substances did not interfere with the responses from tris(2,2'-bipyridyl)ruthenium(II) chloride hexahydrate and HPTS under the conditions of Experimental Mode C.

3.4 DISCUSSION

The spectroscopic investigation of glucose oxidase (EC 1.1.3.4) demonstrated that the enzyme has a noticeable intrinsic fluorescence in aqueous solution, depending on its concentration, which is in agreement with published data in the literature (Wolfbeis, 1985; Wolfbeis & Trettnak, 1989). As it was discussed in Section 3.1.3, glucose oxidase, as a typical flavoprotein, has FAD as a coenzyme and this results in its intrinsic fluorescence properties.

According to Wolfbeis (1985), free FAD exhibits intrinsic fluorescence in aqueous solution, but it is known that this fluorescence can be almost completely quenched when bound to proteins, because amino acids can act as quenchers. In contrast to the oxidised flavins, reduced flavins show a variable absorption and emission behaviour, specially when bound to proteins. Also, Trettnak and Wolfbeis (1989b) reported that their finding that glucose oxidase-bound FAD was fluorescent was surpising because until then glucose oxidase had been described as non-fluorescent molecule in the oxidised or reduced state.

The present study showed that glucose oxidase has maxima excitation wavelengths of 370 nm and 440 nm and emisson maximum of 520 nm, which are close to the reported values by Trettnak and Wolfbeis (1989b), where absorption (excitation) maxima found to be at about 380 nm and 450 nm, and emission maximum approximately at 530 nm (measured in quartz cuvettes at pH 7.0). The above authors presented a fibre-optic glucose biosensor based on the intrinsic fluorescence of glucose oxidase using the same reaction, the oxidation of glucose, as in the present study. The authors justified that changes in the fluorescence of the enzyme could be expected to occur during its interaction with glucose, as reduced and oxidised flavins in the free form (FAD and $FADH_2$) were known to exhibit different fluorescence properties:

$$\text{GOD-FAD} + \text{glucose} \longrightarrow \text{GOD-FADH}_2 + \text{gluconolactone}$$

$$\text{GOD-FADH}_2 + \text{O}_2 \longrightarrow \text{GOD-FAD} + \text{H}_2\text{O}_2$$

A disadvantage of this biosensor was the use of large amount of enzyme in order to produce a sufficient fluorescence signal. In addition, the change in fluorescence intensity occurred within a small glucose concentration range (typically 1.5 to 2 mM), but at lower and higher glucose levels the signal was unaffected by changes in glucose concentration. The biosensor proposed in the present study, in contrast with the above biosensor, requires a small definite concentration of glucose oxidase (1 U/ml) with very low fluorescence intensity, in order to avoid the intrinsic fluorescence intensity from the molecule and the catalytic oxidation of glucose.

In addition, the proposed biosensor presents larger analytical range from 0.1 mM to 20 mM glucose, with saturation over 50 mM, in comparison with other published fluorescence-based optical glucose biosensors. For example, Rosenzweig and Kopelman (1996) presented a micrometer-sized optical fibre glucose biosensor using an oxygen indicator, as transducer, and the reported measurements of glucose levels were in the range of 1 to 10 mM. A noticeable deviation from linearity was observed at concentrations higher than 10 mM glucose, which could be attributed to enzyme saturation as well as to a depletion of oxygen within the sensing region. Moreno-Bondi *et al.* (1990b) described a fibre-optic glucose biosensor based on oxygen optrode with a small analytical range of 0.06 to 1 mM glucose.

Another fibre-optic glucose biosensor based on the consumption of oxygen via dynamic quenching of the fluorescence of an indicator by molecular oxygen, presented as a linear analytical range of 0.01 to 2 mM glucose (Schaffar & Wolfbeis, 1990). Also, a fibre-optic glucose sensor with a pH optode (using HPTS) as transducer exhibited a range of 0.1 to 2 mM glucose (Trettnak *et al.*, 1988a). All the previous described optical biosensors were based on the enzymatic reaction of glucose oxidase that catalyses the oxidation of glucose to gluconic acid and hydrogen peroxide while consuming oxygen, which is the same as in the proposed glucose biosensor.

In all Experimental Modes, the response time taken for 90% of the total signal change to occur, was approximately 40 seconds to 3 minutes depending on the glucose concentration. Also, a reproducibility analysis was performed in Experimental Mode A, which indicated the improved performance of the current approach over the previous

methods. The coefficient of variation for 7 replicate measurements of three different glucose concentrations, 2 mM (hypoglycaemia), 5 mM (within normal range) and 20 mM (hyperglycaemia) were found to be equal to ±0.7%, ±0.9% and ±0.7%, respectively, for tris(2,2'-bipyridyl)ruthenium(II) chloride hexahydrate at excitation wavelength of 410 nm and emission of 597 nm (Table 3.1); and ±0.45%, ±3.5% and ±2.3%, respectively for the above glucose concentrations, for HPTS at excitation wavelength of 410 nm and fluorescence monitored at 507 nm (Table 3.2).

The experimental values of the Michaelis constant from the kinetics experiments in all Experimental Modes were between 13 to 33 mM, which are close to published data in the literature. According to Kresse (1990) and Wilson and Turner (1991), the Michaelis constant of glucose oxidase with glucose lies approximately between 20 and 33 mM. In particular, in Experimental Mode A the calculated values for Michaelis constant were 13.3 mM (response from tris(2,2'-bipyridyl)ruthenium(II) chloride hexahydrate) and 33 mM (response from HPTS), this difference could be explained because of the slightly different response time of each indicator and also the added mathematical error due to the manipulation of the raw data. Also, the same phenomenon appears in Experimental Mode B, where the corresponding Michaelis constant took the values of 21. mM and 32.1 mM. In comparison with these data, Trettnak and Wolfbeis (1989b) reported for Michaelis constant the value of 110 mM for their fibre-optic glucose biosensor which was based on the intrinsic fluorescence of glucose oxidase.

All the Experimental Modes were also tested for their response to interfering substances usually found in biological samples, such as ascorbic acid (0.5 mM), acetaminophen (0.3

mM), uric acid (1.5 mM), urea (4.2 mM) and lactate (1 mM) (Bindra *et al.*, 1991; Atanasov & Wilkins, 1994). The first three compounds are known to be the major interferents in electrochemical measurements of glucose because they are oxidised at the same potential as hydrogen peroxide (Li & Walt, 1995). The experimental results indicated that all saturated solutions with the above substances did not interfere with the responses of tris(2,2'-bipyridyl) ruthenium(II) chloride hexahydrate and HPTS. This is in agreement with other published fluorescence-based optical glucose biosensors (Trettnak *et al.*, 1988a; Moreno-Bondi *et al.*, 1990a; Rosenzweig & Kopelman, 1996; Li & Walt, 1995). Therefore, the proposed optical glucose biosensor can be capable of biological measurements, such as in blood, but also, its dynamic range makes it adequate for glucose determinations in urine, where normal glucose levels are at approximately 0.8 mM.

The main difference between the above fluorescence-based glucose biosensors and the proposed biosensor is that all of these measure glucose concentration through one parameter of the catalytic oxidation of glucose, mainly, the oxygen consumption or the changes in pH due to gluconic acid. The proposed optical biosensor has scope to monitor the glucose through two simultaneous parameters of the reaction, the oxygen consumption and the changes in pH. This information obtained is expected to be more accurate and precise than in the conventional methods because of the double check in one optode using simultaneously two fluorescent indicators, tris(2,2'-bipyridyl) ruthenium(II) chloride hexahydrate and HPTS, without any interference between their responses.

3.5 CONCLUSIONS

The results obtained from the three Experimental Modes demonstrate that an optical fluorescence-based glucose biosensor using simultaneously an oxygen-sensitive and a pH-sensitive fluorescent indicators is feasible. In particular, the calibration curves in all Experimental Modes (Figures 3.6-3.7, 3.10 and 3.12-3.13) obey the Michaelis-Menten equation (3.c) and can be linearised using the Hanes plot (Figures 3.8-3.9, 3.11 and 3.14-3.15). The experimental values of Michaelis constant of the reaction appear to be close to the reported values in the literature (Kresse, 1990; Wilson & Turner, 1991).

As a conclusion, the reproducibility of the measurements of the rate of change of the fluorescence intensity with time of tris(2,2'-bipyridyl)ruthenium(II) chloride hexahydrate, during the oxidation of glucose, for different glucose concentrations, appears to be precise for the range of concentrations of glucose found in normal and diabetic patients (1-20 mM). On the other hand, HPTS assays were very precise for low concentrations (i.e. 2 mM glucose) and less so for higher concentrations (i.e. 20 mM glucose). A possible explanation for this fact is the general disadvantage of pH-based transducers in that they have strong dependence on the buffer capacity of the medium. A change in the pH, resulting from the catalytic reaction at the sensing layer, also modifies the kinetics of the enzyme reaction, and the dependence of the fluorescence intensity on the solution glucose concentration changes (Trettnak *et al.*, 1988a).

In addition, another disadvantage of HPTS was that the changes in the fluorescence intensity for different glucose concentrations, were slow and the signal slightly more unsteady in comparison with tris(2,2'-bipyridyl)ruthenium(II) chloride hexahydrate. As

can be observed in Modes A and C (Figures 3.6-3.7 and 3.12-3.13), the rate of change of fluorescence intensity for HPTS, during the oxidation of glucose was about 30 times lower than the equivalent changes for tris(2,2'-bipyridyl)ruthenium(II) chloride hexahydrate. The response time for 90% of the total signal change was 1-2 min for both indicators. All solutions contained 0.1 M NaCl in order to provide a constant ionic strength close to that appearing in blood, and also to provide high ionic strength so that small changes in ionic strength would not affect the pK_a of HPTS (see Chapter 2). The detection limit of glucose was 1 μM using the fluorescence intensity of the oxygen-sensitive indicator, tris(2,2'-bipyridyl)ruthenium(II) chloride hexahydrate (fluorescence monitoring at 597 nm), and 100 μM using the fluorescence intensity of the pH-sensitive indicator, HPTS (fluorescence monitored at 507 nm). It was also observed that the signal was saturated for glucose concentrations over 50 mM, for both indicators with the slope of the experimental curves (fluorescence intensity versus time) close to infinity.

One of the most important features of the proposed measuring system is that both indicators do respond to changes occurring in the solution environment during the oxidation of glucose. It is remarkable that both indicators present significant responses in the same dynamic range of the analyte, similar detectable lowest concentrations of the analyte and comparable response times.

The experimental results suggest that all three measurement modes could be utilised for glucose measurement. All Experimental Modes confirm the validity of the idea of using two indicators simultaneously for the analysis. Experimental Mode C presents the disadvantage of requiring the two simultaneously exciting beams with independent

wavelengths and as a consequence the use of two isolated light sources (e.g. LEDs). This complicates the design of the proposed biosensor device and increases its size and production cost.

Experimental Mode B appears to be the simplest design for the optical biosensor, but a small shift in the common excitation or emission wavelength, fluctuation in the light source or interference from the environment could produce errors because the measurements would be taken at the wrong wavelength. Experimental Mode A could offers the most attractive solution for the construction of the proposed optical glucose biosensor. It requires only one fixed excitation wavelength and the fluorescence can be measured at two separate wavelengths, where the maxima in emission of the two indicators occur, without interference and overlap between them, as discussed extensively in Chapter 2.

In the following chapters experiments are described to establish whether the proposed approach can be utilised to measure concentrations of other important analytes, such as lactate, xanthine and phenol by exploiting appropriate enzymatic oxidations.

CHAPTER 4

FLUORESCENCE-BASED OPTICAL BIOSENSORS FOR BLOOD-LACTATE MONITORING

4.1 INTRODUCTION

Reliable and rapid monitoring of lactate is essential in the areas of clinical diagnosis, sports medicine, biotechnology and food analysis. In the field of clinical analysis, blood lactate level determination plays an important role in diagnosis of lactic acidosis which may be a result of respiratory, hemodynamic, or metabolic disturbances like heart and liver diseases. In the food industry, lactic acid is an important parameter in a large variety of samples, for the control of dairy products and additives. It can be utilised in milk derivatives as an indicator of the quantity of fatty acids and bacterial contamination, and therefore of quality (Skladal *et al.*, 1993).

In sports, the increasing desire to naturally enhance the performance of sportsmen and athletes through evaluation of their training regime, requires an *in situ* estimation of physical and biochemical condition (Galban *et al.*, 1993). It is well known that the blood lactate concentration of an athlete undergoing exhausting exercise, such as a 100-meter sprint, increases. Once a certain level of lactate concentration is reached, however, exhaustion occurs and a rapid decline in exercise capacity follows. The concentration of blood lactate is therefore an important index for estimating physical condition. Previously, lactate concentration has been measured by taking blood samples from an athlete during exercise in an effort to improve performance (Wasserman *et al.*, 1987; Mattner, 1988). More information of an athlete's physical condition can be obtained from monitoring the fluctuations in blood lactate concentration depending on the type of exercise performed and the effort applied. Continuous collection of blood samples and the on-line analysis of the blood lactate concentration has been achieved mainly using amperometric biosensors (see Section 4.1.2).

In this chapter, a study of the fluorescence quenching of two indicators during the enzymatic oxidation of lactate is described. This method is based on the simultaneous detection of two parameters in the reaction in order to provide more accurate and reliable lactate measurements using a portable optical biosensor. The enzymatic oxidation of lactate to lactic acid proceeds as follows:

$$\text{L-Lactate} + H_2O + O_2 \xrightarrow{\text{LACTATE OXIDASE}} \text{Pyruvate} + H_2O_2 \qquad (4.a)$$

Lactate concentrations were measured by monitoring simultaneously the changes of fluorescence intensity of tris(2,2'-bipyridyl) ruthenium(II) chloride hexahydrate (due to oxygen consumption) and of HPTS due to changes pH resulting from pyruvate production. The same excitation and emission wavelengths were selected as in Experimental Modes A and B (Chapter 3).

4.1.1 Lactic Acid Formation

Reference lactate values in venous blood are 1-1.78 mM, but can increase through physical activity, stress, pregnancy, or in case of metabolic, respiratory, or hemodynamic disturbances (Trettnak & Wolfbeis, 1989a).

During very violent exercise, owing to relative anoxia of the muscles, lactic acid accumulates therein and diffuses out into the blood stream and throughout the body fluids (Stryer, 1995). The resting level of blood lactate is 10-20 mg/100ml (≅ 1.1 to 2.1 mM) (Keele & Neil, 1975). As a result of violent exercise the level may rise to 100 or even to 200 mg/100ml (≅ 11.1 to 22.2 mM). As lactate is freely diffusible, the blood

lactate levels represent the concentration in the muscles, the interstitial fluid, and possibly in the intracellular fluid generally. If the total volume of body fluid contains a lactate concentration of 200 mg/100ml (≅ 22.2 mM) (i.e., equal to that in the blood), the total lactate accumulation is 90 g. After the exercise is over this lactate is disposed of; the blood lactate concentration steadily diminishes and reaches the normal level after a variable period of time, sometimes after as long as 60 minutes (Keele & Neil, 1975).

4.1.2 Lactate Biosensors

An electrochemical sensor for lactate has been designed by constraining a dehydrogenase enzyme and nicotinamide adenine dinucleotide (NAD^+) at the surface of a platinum electrode (Blaedel & Engstrom, 1980). Efficient electrochemical regeneration of NAD^+ from the enzymatically produced NADH provided a current that was dependent on substrate concentration. Response of the sensor was influenced by product inhibition of the enzymatic reaction, causing nonlinearity to appear at substrate concentrations below the Michaelis constant. A few years later, lactate and pyruvate electrochemical sensors were constructed for control of an artificial pancreas (Mascini *et al.*, 1987). The sensors were realised by immobilising lactate oxidase and pyruvate oxidase from *Pediococcus* on polymeric membranes and fixing them on hydrogen peroxide electrochemical sensors. The sensors were coupled with an artificial pancreas to monitor the fate of lactate and pyruvate in human diabetic patients with the purpose of improving the dosage of insulin and other drugs.

ENFETs have been assembled by coimmobilising peroxidase and lactate oxidase onto a fluoride ion sensitive field effect transistor (Dransfeld *et al.*, 1990). These ENFETs for

lactate were based on the peroxidase-catalysed reaction liberating fluoride ions from organo-fluoro compound, the pentafluorophenol, in the presence of hydrogen peroxide, which was produced by the coupled oxidase reactions. Later, Yoshioka and colleagues reported the simultaneous determination of L-lactate and L-malate in wine by using flow injection analysis (FIA), which includes a parallel configuration of two enzyme reactors and a single oxygen electrode (Yoshioka *et al.*, 1992). L-lactate was determined by using lactate oxidase and monitoring oxygen consumption. NADH formed in the reaction catalysed by malate dehydrogenase (MDH) was regenerated to NAD^+ with dissolved oxygen, using vitamin K_3 and diaphorase (DI). The authors claim, the system may be applicable to the monitoring of malo-lactic fermentation during wine production. An amperometric lactate oxidase electrode has been designed for application to undiluted media by mathematical modelling, membrane screening and biochemical characterisation (Pfeiffer *et al.*, 1992). The lactate probe has been applied to lactate analysis via a catheter during exercise.

In 1989, Dremel and his colleagues developed a method for the determination of L-lactic acid using a fibre optic lactic acid biosensor in combination with a flow injection system (FIA) (Dremel *et al.*, 1989b). The biosensor was based on a fibre-optic oxygen optode which measured the oxygen consumption via dynamic quenching of the fluorescence of a dye by molecular oxygen. Lactic acid was immobilised onto the surface of the oxygen optode. Sample pre-treatment proved necessary for protection of the biosensor, during the detection of L-lactic acid in milk products, and as a consequence the samples were automatically diluted and buffered by means of a FIA-system. A different method has been described by Wolfbeis and Trettnak (1989) based on the finding that enzymes

having FAD as a prosthetic group change their fluorescence during interaction with a substrate. They designed a biosensor for lactate determination based on the intrinsic fluorescence of lactate monooxygenase (LMO). Its fluorescence was monitored via fiber optic light guides at wavelengths above 500 nm, following fluorescence excitation at 410 nm. These researchers found a very short linear response range (50-100 mg/L) of the biosensor.

Another optical sensor was described which was based on an enzymatic method for the determination of lactate (Rohen *et al.*, 1992). The enzyme used was cytochrome b_2, which was able to accept redox dyes as electron acceptors. The decolourisation of the dyes gave information about the lactate concentration. A linear calibration curve was obtained in the range from 0.05 to 0.3 mM lactate solutions. A problem was encountered with lack of long term stability caused by fast degradation of the enzyme.

Later, Galban and his colleagues presented a procedure for fluorometric-enzymatic lactate determination based on the modification of the fluorometric properties of the enzyme L-lactic dehydrogenase (cytochrome b_2), during the enzymatic oxidation of the analyte with ferricyanide (Galban *et al.*, 1993). During the reaction an irreversible fall in the intensity of the enzyme's fluorescence was observed, the rate of which was proportional to the concentration of lactate. A mathematical model was developed which made it possible to establish a linear response between the enzyme's fluorescence and the concentrations of the lactate, the cytochrome, and the ferricyanide. The procedure made it possible to determine lactate concentrations in the range 0.2 to 45 mg/L.

4.1.3 Lactate Oxidase

Four different kinds of enzymes are frequently reported for L-lactate determination: Lactate dehydrogenase or animal lactate dehydrogenase (LDH, EC 1.1.1.27), cytochrome b_2 or yeast lactate dehydrogenase (EC 1.1.2.3), lactate monooxygenase (LMO, EC 1.13.12.4) and lactate oxidase (EC 1.1.3.2) (Racek, 1987; Trettnak & Wolfbeis, 1989a).

Lactate oxidase (L-lactate: oxygen oxidoreductase) from *Pediococcus species* is a flavoenzyme which catalyses the oxidation of L-lactate in the presence of oxygen to pyruvate and hydrogen peroxide (reaction 4.a) (Schindler *et al.*, 1994). The enzyme is used in the determination of L-lactate (high specificity) and transaminase in biological fluids. Its molecular weight was determined by gel filtration on Sephadex G-150 and lies in the value of $80x10^3$ Da (Eichel & Rem, 1962; Mascini *et al.*, 1985).

The optimum pH range of the enzyme is between 6.0-7.0 in phosphate buffer and shows stability at pH range of 7.0-9.0 when kept for 60 min at 37°C; and its isoelectric point is 4.6 (Eichel & Rem, 1962). The stability of the enzyme was determined after incubation at temperatures below 40°C for 10 min in pH 7.0. It is recommended to be stored at -20°C in the presence of a desiccant (lyophilised powder) and the enzyme activity will be retained for at least one year under this condition. Lactate oxidase activity is higher in oxygen than in air and is little affected by chelating agents at a concentration of 10^{-3} M. *p*-Chloromercuribenzoic acid inhibits lactate oxidase activity completely at 10^{-3} M but has no effect at 10^{-4} M. The Michaelis constant of lactate oxidase with L-lactate lies at 0.7 mM (Eichel & Rem, 1962; Esders & Goodhue, 1980).

4.2 MATERIALS & METHODS

4.2.1 Chemicals

Lactate oxidase (L-lactate: oxygen oxidoreductase, EC 1.1.3.2) (142.3 units/mg protein at 37 ^{0}C, from Pediococcus species) was supplied by Genzymes Diagnostics (West Malling, Kent). One unit of activity of the enzyme is defined as the amount of enzyme that catalyses the oxidation of 1 μM of L-lactate per minute at 37 ^{0}C under the conditions specified in the assay procedure. L-lactate was purchased from Sigma Chemical Co. (Poole, Dorset). The purchase of the indicators, HPTS and tris(2,2'-bipyridyl)ruthenium(II) chloride hexahydrate, was mentioned in Sections 2.2.1.1 and 2.3.1.1. All other inorganic reagents were of analar grade and used as obtained from BDH Ltd. (Poole, Dorset).

The standard buffer solution was 10mM sodium phosphate buffer, pH 7.0 at 22 ^{0}C, containing 10mM $Na_2HPO_4 \cdot 12H_2O$ and 10mM $NaH_2PO_4 \cdot 2H_2O$. All experiments were performed at room temperature (22 ± 2 ^{0}C), using 7μM tris(2,2'-bipyridyl)ruthenium(II) chloride hexahydrate and 0.03 μM HPTS. For the measurement of kinetics the standard buffer solution was 0.1 mM sodium phosphate buffer containing 0.1 M NaCl in order to adjust the pH to 7.4. Stock solutions of indicators were prepared by bubbling 1 mM phosphate buffer with pure oxygen for at least 15 min. All components of the assay mixtures were freshly prepared.

4.2.2 Instrumentation

The instrumentation used was as described previously in Chapter 3 (see Section 3.2.2).

4.3 RESULTS

4.3.1 Spectroscopic Investigation of Lactate Oxidase

Lactate oxidase was dissolved in phosphate buffer pH 7.4 to give a yellow coloured solution. The excitation and emission fluorescence spectra of 20 U/ml lactate oxidase are illustrated in Figure 4.1, which shows that the peak excitation occurred at 370 nm followed by a second smaller peak at 440 nm. Excitation with 370 nm radiation gave a peak emission at 518 nm; similarly, with an excitation wavelength at 440 nm the fluorescence maximum occurred at 520 nm. The figure shows that lactate oxidase (20 U/ml) is a fluorescent molecule, but its fluorescence intensity was low in comparison with glucose oxidase (Chapter 3). The concentration of enzyme used in the following experiments for kinetic measurements of lactate was 0.1 U/ml, and because of its low fluorescence intensity it did not overlap with the distinct maximum peaks for each indicator.

4.3.2 Kinetic Measurements of Lactate Oxidase Reaction

Lactate concentration was measured by simultaneously monitoring the changes in fluorescence intensity against time of tris(2,2'-bipyridyl)ruthenium(II) chloride hexahydrate and HPTS, during the catalytic oxidation of lactate (Reaction 4.a). Two experimental setups were used. In the first, a common wavelength of 410 nm, was used as excitation wavelength, and the fluorescence was monitored at 597 nm and 507 nm, which correspond to the maxima emission of the tris(2,2'-bipyridyl)ruthenium(II) chloride hexahydrate and HPTS, respectively (Experimental Mode A, Chapter 3). In the second setup, common excitation and emission wavelengths at 410 nm and 555 nm, respectively, were utilised, (Experimental Mode B, Chapter 3).

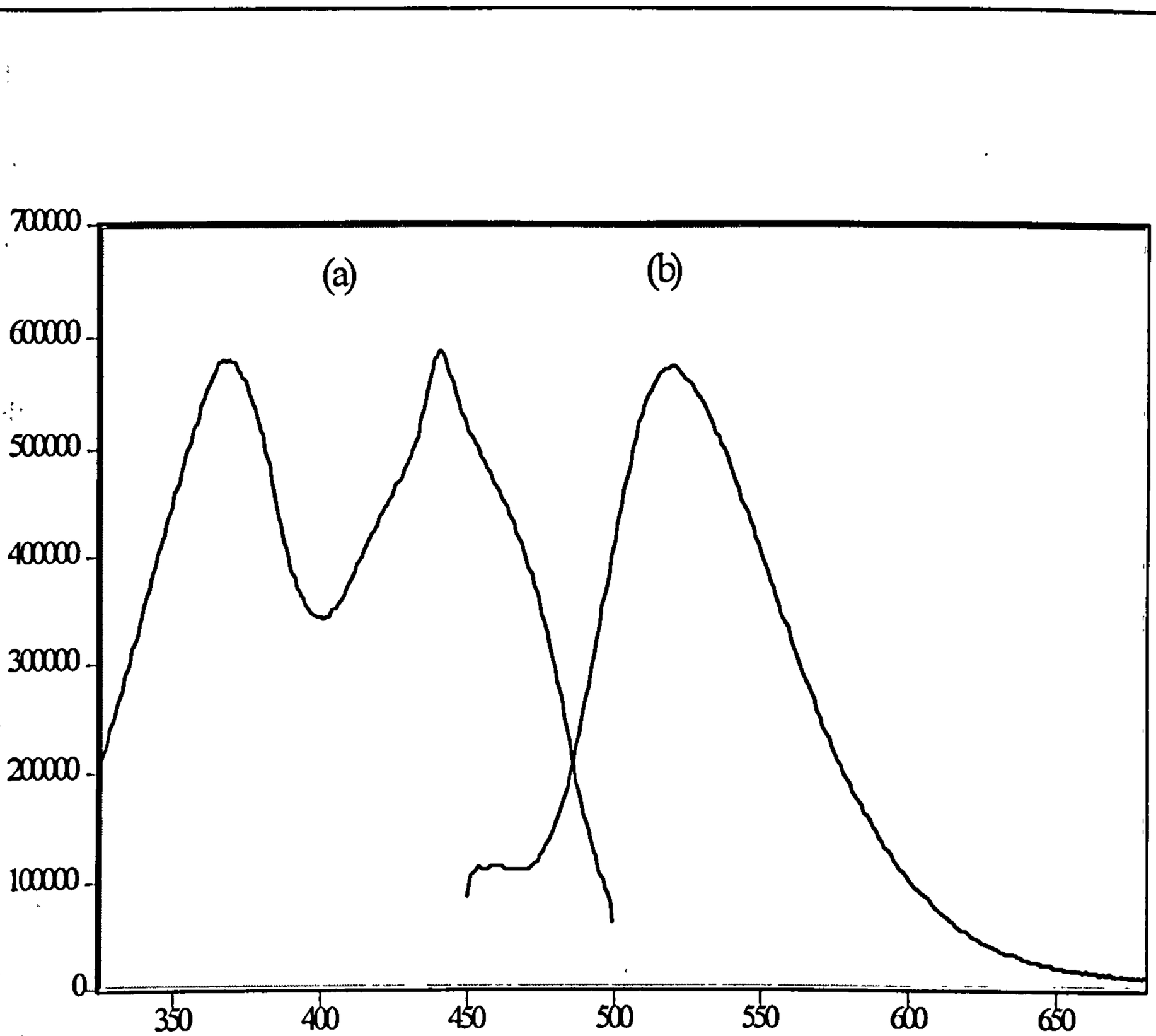

FIGURE 4.1 Excitation (a) and fluorescence (b) spectra of lactate oxidase (20 U/ml) with excitation wavelength at 440 nm and fluorescence monitored at 520 nm, in phosphate buffer pH 7.4 at 22 ^{0}C.

Kinetic measurements were carried out in quartz cuvettes (3 ml) with standard amounts of optimised enzyme and indicators concentrations, 0.1 U/ml lactate oxidase, 0.03 μM HPTS and 7 μM tris(2,2'-bipyridyl)ruthenium(II) chloride hexahydrate in buffer solution pH 7.4 (blood pH). The reaction was initiated by addition of lactate in the cuvette. A small magnetic stirrer bar was placed in the bottom of the cuvette and rotated at a constant speed in order to keep the solution homogeneous during the reaction. All additions of stock solutions (in the range of μl) were carried out outside of the instrument except the lactate which was added when the cuvette was placed in the instrument and the software was ready to run in order to monitor the reaction from the start.

The rate of change of the fluorescence intensity of tris(2,2'-bipyridyl)ruthenium(II) chloride hexahydrate against lactate concentration, due to oxygen consumption during the oxidation of lactate, is presented in Figure 4.2. This calibration curve follows the Michaelis-Menten equation (see below). The manipulation of the raw data in order to obtain values of rate of change of fluorescence intensity with time (dI/dt) (instead of the actual values of fluorescence intensity) was identical to the one used in the case of glucose (Chapter 3) and is described in Appendix A. In the same way, the variation in the rate of change of the fluorescence of HPTS due to pH changes resulting from the production of pyruvate, is illustrated in Figure 4.3 and Michaelis-Menten kinetics were again obeyed. In this approach (Experimental Mode A), the lowest detectable lactate concentration was 10 μM. Saturation occurred above 7 mM lactate for both indicators. The response of the indicators after the addition of lactate was rapid, and typically took 2 to 5 minutes to reach a point where the changes of fluorescence intensity with time were very small. About 90% of this final fluorescence intensity value was achieved in approximately 60 to 90 seconds.

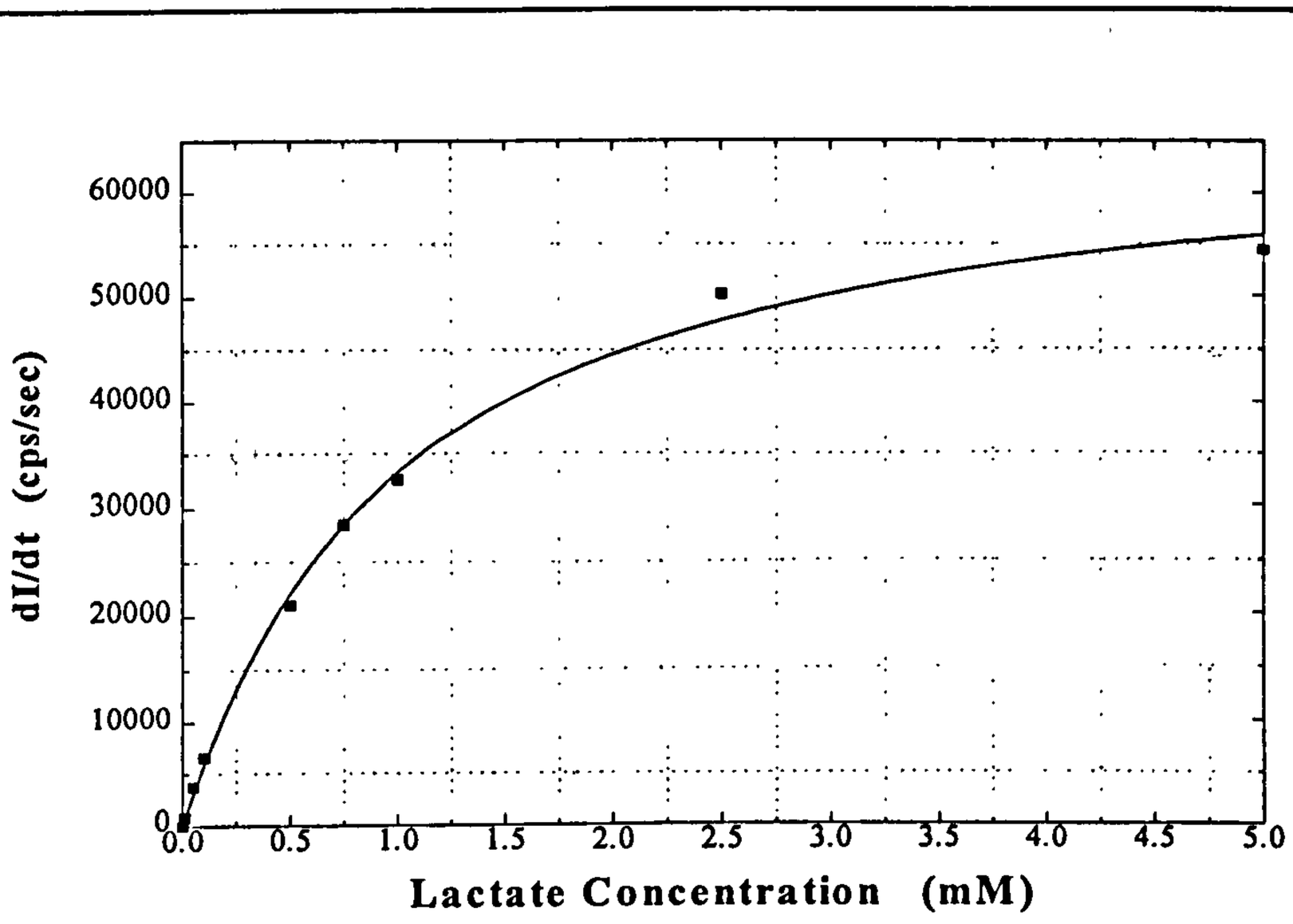

FIGURE 4.2 Rate of change of fluorescence intensity versus lactate concentration of tris(2,2'-bipyridyl)ruthenium(II) chloride hexahydrate, at fixed excitation wavelength of 410 nm and emission at 597 nm, during the catalytic oxidation of lactate.

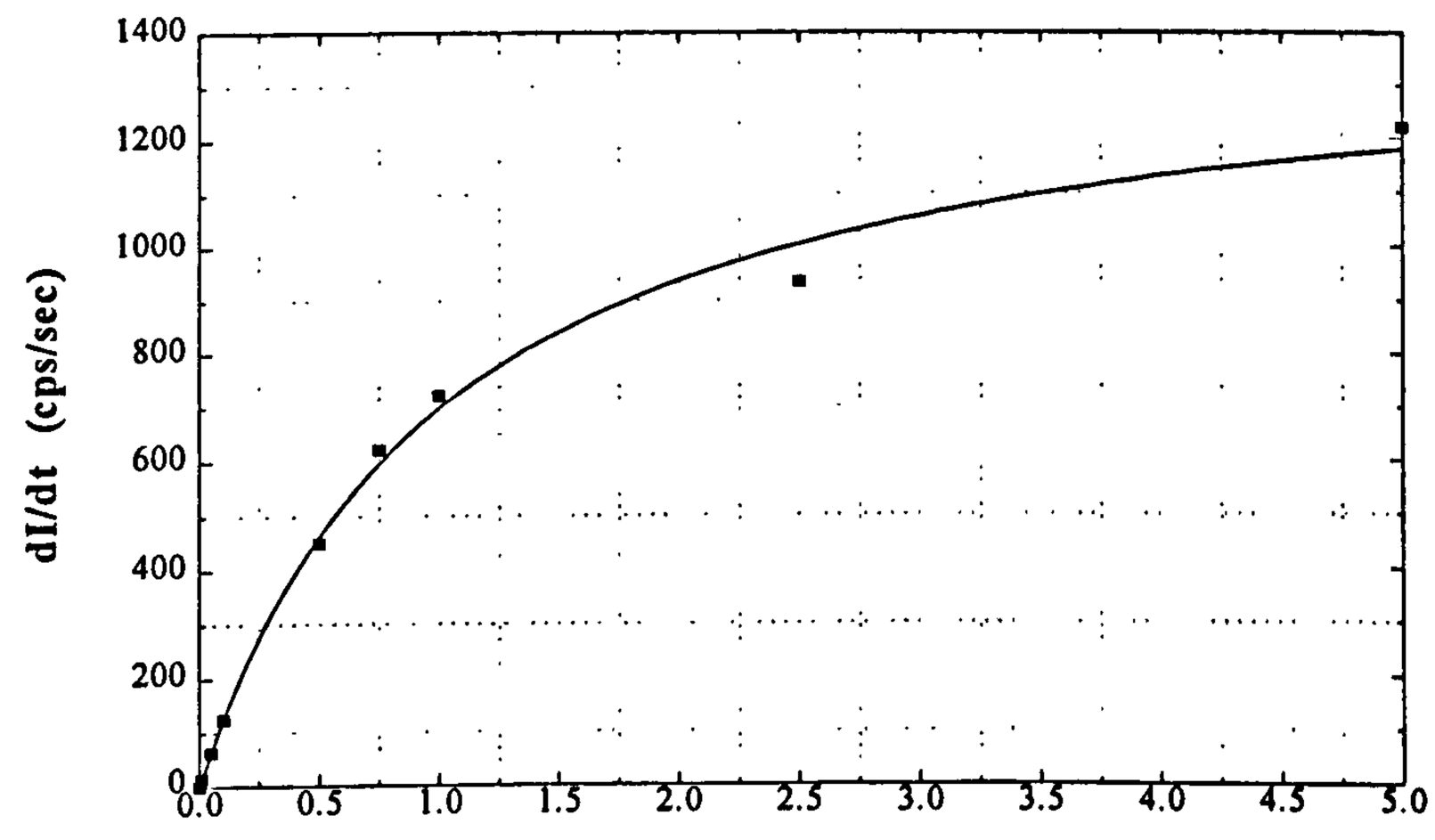

FIGURE 4.3 Rate of change of fluorescence intensity versus lactate concentration of HPTS, at fixed excitation wavelength of 410 nm and emission monitoring at 507 nm, during the catalytic oxidation of lactate.

The kinetic parameters of 0.1 U/ml lactate oxidase in the presence of the indicators and lactate, were determined using a Hanes plot. The Hanes plots corresponding to Figures 4.2 and 4.3 are illustrated in Figures 4.4 and 4.5, respectively. From these plots and according to equation (3.e), the experimental value of the Michaelis constant, K_m, of the reaction was found to be equal to 0.9 mM when the reaction was monitored through the rate of change of fluorescence intensity of tris(2,2'-bipyridyl)ruthenium(II) chloride hexahydrate at excitation wavelength of 410 nm and fluorescence monitored at 597 nm. K_m was found to be equal to 1.07 mM when the rate of change of fluorescence intensity of HPTS at excitation and fluorescence wavelengths of 410 nm and 507 nm, respectively, was monitored.

In a similar way, when the Experimental Mode B was used (common excitation wavelength 410 nm and fluorescence monitored at 555 nm), the rate of change of the fluorescence intensity of both indicators, in the common wavelength of 555 nm, against the lactate concentration are depicted in Figure 4.6. This setup gave a near linear response between 10 to 100 μM lactate at pH 7.4 in room temperature, and above 100 μM lactate the calibration curve was clearly non-linear saturating at 6 mM lactate. The response of the indicators after the addition of lactate took 2 to 5 minutes to reach a state where the changes in fluorescence intensity with time were negligible (lower concentrations of lactate needed more time to reach the above state than higher concentrations, e.g. 30 μM lactate needed 4.5 minutes, however 3 mM lactate required around 2 minutes), 90% of this final intensity value being achieved in approximately 60 to 90 seconds.

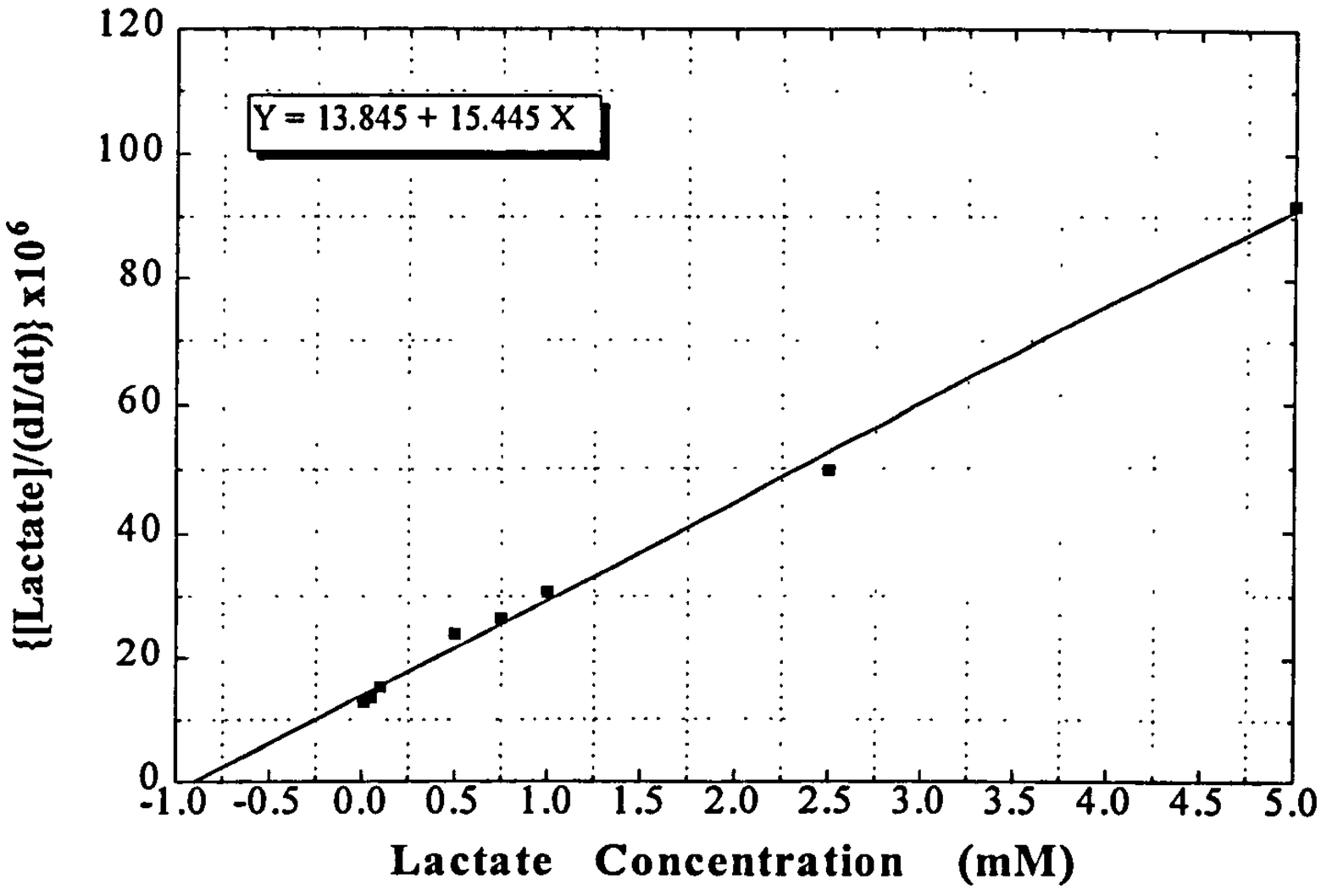

FIGURE 4.4 Hanes plot corresponding to Figure 4.2.

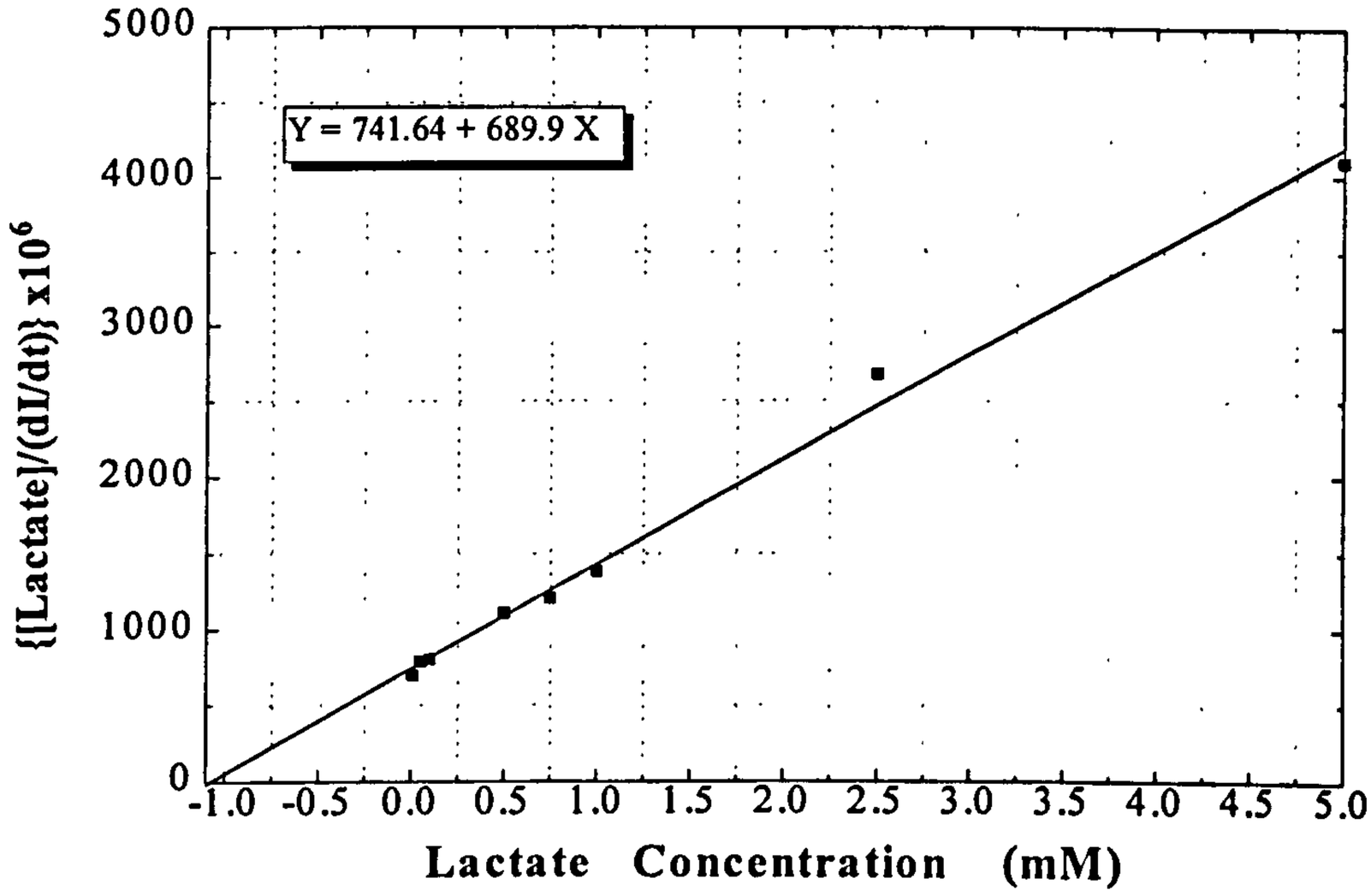

FIGURE 4.5 Hanes plot corresponding to Figure 4.3.

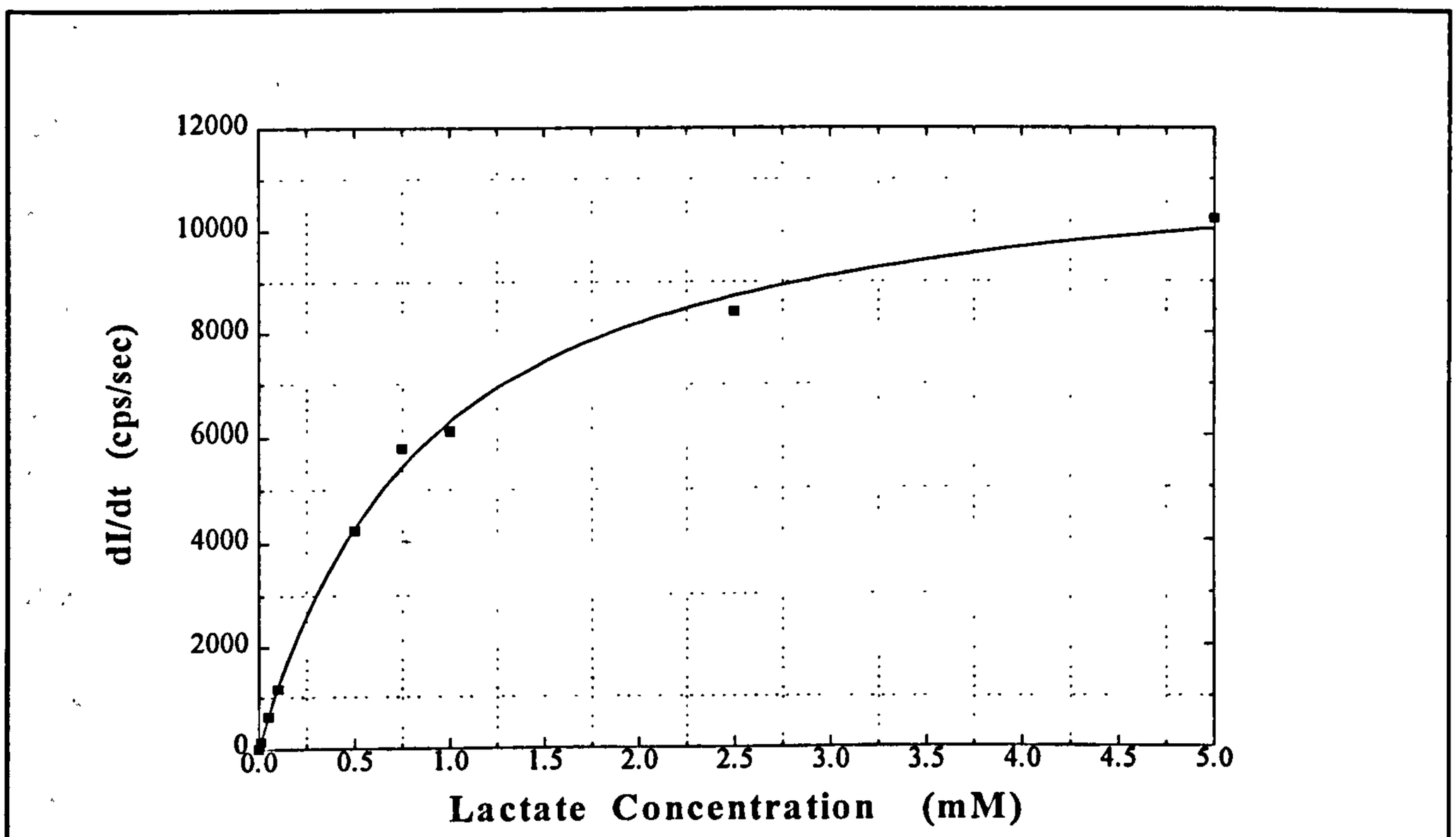

FIGURE 4.6 Rate of change of fluorescence intensity versus lactate concentration of the sum of tris(2,2'-bipyridyl)ruthenium(II) chloride hexahydrate and HPTS, at the excitation wavelength of 410 nm and monitoring the emission at 555 nm, during the catalytic oxidation of lactate.

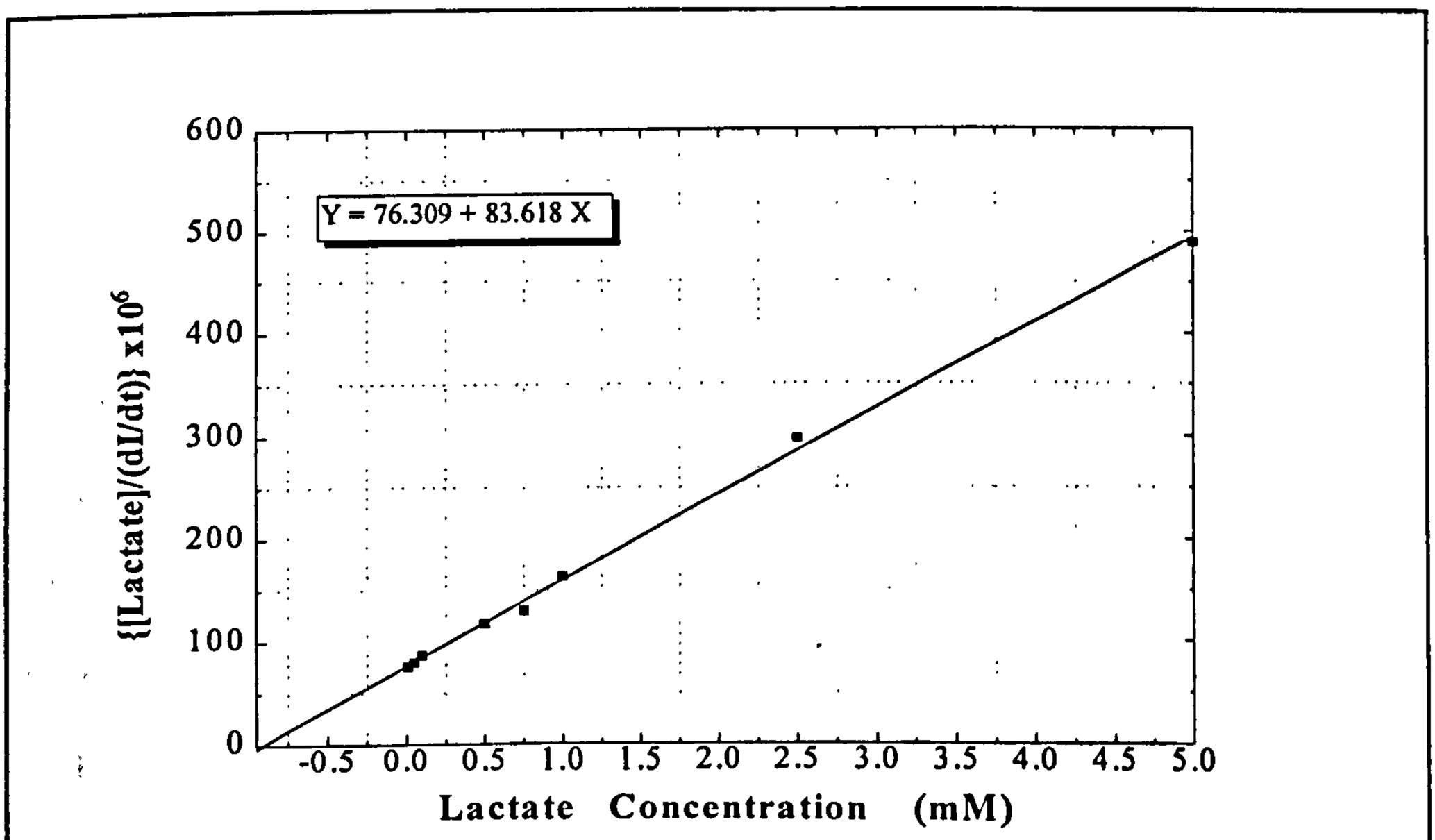

FIGURE 4.7 Hanes plot corresponding to Figure 4.6.

This approach (Experimental Mode B) offers a small amount of detection in the range of 15 μM lactate. As it can be observed, the calibration curve in the preceding figure obeyed the Michaelis-Menten equation, as well as in Experimental Mode A. The Hanes plot corresponding to this calibration curve is illustrated in Figure 4.7. The K_m from this Hanes plot was 0.91 mM.

4.4 DISCUSSION

The spectroscopic investigation of lactate oxidase (EC 1.1.3.2) showed that the enzyme presents fluorescence properties, with excitation wavelengths of 370 and 440 nm and emission monitored at 520 nm, which could be attributed to the structure of the enzyme which is a flavoprotein and possesses flavine adenine dinucleotide (FAD) as a prosthetic group in its molecule. The above results are in agreement with published data using typical enzymes having FAD as a prosthetic group in their molecule, like glucose oxidase, lactate monooxygenase and cholesterol oxidase (Wolfbeis & Trettnak, 1989).

Lactate oxidase did not show a noticeable increase in its fluorescence intensity during its interaction with the substrate, L-lactate, in contrast with the enzyme lactate monooxygenase which has been used by Wolfbeis and Trettnak (1989) for the construction of an optical biosensor for lactate. According to them, lactate monooxygenase showed an intrinsic fluorescence property, that could be explained in terms of different excitation spectra, emission spectra and quantum yields of oxidised and reduced enzyme. The biosensor had a detection limit of 0.5 mM lactate and a narrow dynamic range which did not exceed 3 mM lactate; the authors suggested no possible application of this method because of the problems associated with small

analytical range and long response times. However, lactate oxidase which was used in the present study, did not show similar behaviour to lactate monooxygenase, and therefore, it was not feasible to construct an optical biosensor based on the intrinsic fluorescence of the enzyme.

A fibre optic lactate biosensor with an oxygen optrode as the transducer using lactate monooxygenase has been presented by Trettnak and Wolfbeis (1989a). The authors suggested that an attractive alternative to lactate monooxygenase from *Mycobacterium smegmatis* could be provided by the enzyme lactate oxidase (EC 1.1.3.2) from *Pediococcus species*, which is the enzyme utilised in the present work. They explained that a disadvantage of lactate monooxygenase was the interference by chemicals or pH changes, in contrast with lactate oxidase which showed much less inhibitory effects and a very broad pH-optimum (Mascini *et al.*, 1985). The results from the kinetic measurements of lactate, in the present chapter, have proven the feasibility of the above suggestion for utilisation of lactate oxidase instead of lactate monooxygenase.

Experimental Modes A and B showed better analytical ranges of L-lactate detection in the blood, which were 10 μM to 5 mM, with smaller response times of 60 to 90 seconds (90%), in comparison with the previously reported optical biosensor (Trettnak and Wolfbeis, 1989a), where the analytical ranges were 0.3 to 6.0 mM and the response times (90%) 4.0 to 6.0 minutes. An alternative fibre-optic biosensor for lactate, based on fluorometric detection using confined macromolecular nicotinamide adenine dinucleotide derivatives, has been presented and it has shown analytical ranges of 11 to

150 mM lactate with response time 5 to 10 minutes (Scheper & Buckmann, 1990). This sensor does not appear to be suitable for blood lactate detection (1-1.78 mM).

As blood-lactate is a dynamic metabolite, frequent analyses are required to follow the course of this parameter. There are several automatic analysers commercially available, which can give results within a few minutes, but they are expensive, and also, under certain conditions, a small mobile analysis system would be desirable, e.g. for bedside monitoring or under conventional training conditions for athletes. Pfeiffer and his colleagues developed a wearable device for the continuous measurement of lactate in the blood by the combination of continuous blood sampling employing a double lumen catheter with an amperometric lactate sensor (Meyerhoff *et al.*, 1993). A problem in the above device was the lag time of about 4 minutes between a change in blood lactate concentration and its measurement by the lactate sensor. In comparison with the above device, the proposed optical biosensor looks to have simpler design and better response time, approximately 60 to 90 seconds, and finally it promises more accuracy because of the two measuring parameters in contrast with the above device which measures only hydrogen peroxide production.

Similarly to optical biosensors, most of the electrochemical lactate biosensors are based on an oxygen electrode, or on the detection of hydrogen peroxide, or the monitoring of the NADH produced from an enzymatic reaction, which are proportional to the substrate concentration, lactate (Blaedel & Engstrom, 1980; Mascini *et al.*, 1987; Dempsey *et al.*, 1993; Wang & Chen, 1994). The main difference between the present research work and the previous lactate optical and electrochemical biosensors is that Experimental Modes

A and B measure simultaneously two parameters of the lactate oxidation using two indicators (oxygen-sensitive indicator and pH-sensitive indicator) in order to detect more accurately the value of the lactate concentration.

4.5 CONCLUSIONS

Lactate oxidase, as a flavoprotein, appears to have fluorescent properties similar to those of glucose oxidase. An important consideration is that its fluorescence intensity is much lower than that of glucose oxidase for a similar range of concentrations, as can be observed in Figures 4.1 and 3.2. This is an advantage for the present approach because it allows no further investigation in order to define an optimum enzyme concentration which does not cause interference with the fluorescence intensities of the indicators used.

The results from the application of both Experimental Modes A and B have shown that, in principle, the proposed method works and can provide a measuring system for detection and measurement of lactate in the range of 0.01-5 mM. The calibration curves obtained were hyperbolas (Figures 4.2, 4.3, 4.6) and followed Michaelis-Menten kinetics. The calculation of the Michaelis'constant for the alternative experimental setups provided values which were in close agreement with literature values (Eichel & Rem, 1962; Esders & Goodhue, 1980). This means that the rate of change of fluorescence intensity of both indicators used in the above Experimental Modes, follow consistently the changes occurring during the catalytic oxidation of lactate.

Finally from a practical point of view, the above studies indicate that the construction of an optical lactate biosensor based on the above principles, is feasible. Further studies are required in order to confirm the applicability of the detection method when the indicators and the enzyme are immobilised, especially with the sol-gel method used in the case of phenol and glucose (Chapters 6 and 7).

CHAPTER 5

FLUORESCENCE-BASED OPTICAL BIOSENSORS FOR XANTHINE MONITORING

5.1 INTRODUCTION

Xanthine is one of the metabolites of adenine nucleotide degradation, which accumulates and can be used as a monitor of both the freshness of meat in food industry and some processes in human body. In the present work, the development of a new fibre-optic biosensor for the determination of xanthine is discussed. For this purpose, two different methods are presented, which are based on the phenomenon of fluorescence quenching. In principle, the first method is applied to design an intrinsic fibre-optic biosensor, where a product or a substrate can be determined directly by measuring its absorption or fluorescence (as in the present study), or even its chemiluminescence. The second method is applied to construct a transducer-based fibre-optic biosensor, where the substrate is determined indirectly by measuring changes in pH and in oxygen concentration during its catalytic oxidation.

In the first method, the intrinsic fluorescence of xanthine itself was used to provide the analytical information. No additional indicators were required, and therefore, the design of the optical biosensor could be kept very simple. The second method involved the well-defined fluorescent indicators, tris(2,2'-bipyridyl)ruthenium(II) chloride hexahydrate and HPTS (Chapters 2 and 3), for the simultaneous detection of oxygen consumption and the pH changes (due to uric acid production). A number of combinations of excitation and fluorescence wavelengths have been used in order to establish calibration curves with optimum performance. In particular, Experimental Modes A and B (Chapter 3) were applied in order to construct an optical biosensor for xanthine measurement, mainly for clinical purposes.

5.1.1 Diseases Related to Blood Xanthine and Uric Acid Concentrations

Nucleic acids and nucleotides are degraded to nucleosides or free bases before they are ingested. Nucleotides or their partial degradation products maybe reutilised for nucleic acid synthesis, or they may be further catabolised for excretion or for use in the synthesis of other products. Purine nucleotides are degraded via guanine, hypoxanthine and xanthine to uric acid, which in some species is degraded further before excretion. Inherited deficiencies in some of the enzymes involved in nucleotide degradation and salvage cause severe impairment of health, a fact testifying to the importance of the degradative pathways (Stryer, 1995). The immediate precursor of uric acid is xanthine, which arises from guanine or hypoxanthine.

At least 3 per 1,000 persons world-wide suffer from gout (Zubay, 1993). Gout is a painful chronic disease that affects the joints and kidneys. Inflammation of the joints is triggered by the precipitation of sodium urate crystals and their deposition may damage the kidneys too (Blackburn & Gait, 1990). Gout is also characterised by abnormally high uric acid concentration in the blood (above 5 mg/100ml), a condition which is called hyperuricemia. The reason for the deposition of sodium urate crystals is not known. Blood plasma is not saturated with uric acid, and in other diseases (e.g. leukaemia, polycythemia, pneumonia, hypertension and coronary thrombosis, chronic nephritis) there is greater hyperuricemia than in gout without the formation of urate crystals. Hyperuricemia in gout is not due to excess formation of uric acid, as normal amounts are excreted (Keele & Neil, 1975; Houssay *et al*, 1955). Sometimes uric acid excretion diminishes just before an attack and increases at the beginning of the attack. It

would seem that hyperuricemia is due to a selective retention of uric acid by the kidney. Uric acid clearance at the same level of blood uric acid is below normal in patients with gout. Uric acid injected intravenously into patients with gout is eliminated at a slower rate than in normal subjects (Stryer, 1995).

Another study had focused on patients who lacked the enzyme xanthine oxidase (Zubay, 1993). The amounts of xanthine and hypoxanthine excreted by these patients were compared with estimates of the amounts synthesised daily. The neurologic disorder of children called the Lesch-Nyhan syndrome is due to a congenital nearly total absence of the important enzyme hypoxanthine-guanine phosphoribosyltransferase (Stryer 1995). This disorder reveals abnormal behaviour such as aggressive behaviour, mental retardation, spastic cerebral palsy, and self-mutilation. Purine metabolism is profoundly disturbed, with greatly increased *de novo* biosynthesis of purines (200 times normal), overproduction of uric acid (6 times normal), and elevated blood uric acid levels, which lead to the kidney's stones early in life, followed by symptom of severe gout years later.

Consequently, the detection of hypoxanthine, or xanthine concentration in the blood is very important to the doctors in order to improve control or uric acid levels. Currently, they use expensive and lengthy methods to measure uric acid in the blood performed in a microbiology or hospital lab. The idea of developing an optical biosensor for this particular medical application has not been presented elsewhere in the literature.

5.1.2 Blood Xanthine and Uric Acid

Blood levels of xanthine and hypoxanthine are normally about 0.04 mM, which are maintained by release of purine bases from the liver. The normal limits of uric acid in serum are 1-5 mg/100 ml (about 0.2 mM) (Zubay, 1993; Green, 1976). It is raised in gout up to 8-15 mg/100 ml. Ingestion of purine-containing food has no effect on the blood uric acid in normal people, but raises it in cases of renal insufficiency. It is claimed that uric acid is the first nitrogenous constituent to be retained in nephritis, values of 8 mg/100 ml occurring before the other nitrogenous constituents are increased. In uraemia, values as high as 27 mg/100 ml may be obtained (Stryer 1995). In leukaemia and pneumonia considerable breakdown of nuclei of white blood corpuscles occurs, and the blood uric acid is raised. Although in these two diseases the kidneys are excreting a great deal of uric acid, they are unable to eliminate it as rapidly as it is formed.

5.1.3 Xanthine Biosensors

The measurement of xanthine and hypoxanthine is usually complicated and time consuming using techniques like HPLC (Halfpenny & Brown, 1985, Arin *et al.*, 1990), anion exchange chromatography (Burt, 1977) and HPLC with an immobilised enzyme reactor (Kito *et al.*, 1989, 1990). These compounds can also be quantified enzymatically by amperometric determination of the end products during their degradation by the enzyme xanthine oxidase:

$$\text{Hypoxanthine} + H_2O + 1/2\,O_2 \xrightarrow{\text{XANTHINE OXIDASE}} \text{Xanthine} + H_2O_2 \qquad (5.a)$$

$$\text{Xanthine} + H_2O + 1/2\,O_2 \xrightarrow{\text{XANTHINE OXIDASE}} \text{Uric Acid} + H_2O_2 \qquad (5.b)$$

The amount of the uric acid and hydrogen peroxide (H_2O_2) generated is proportional to the concentration of hypoxanthine (Mulchandani *et al.*, 1989). An amperometric sensor based on the detection of uric acid was developed by Gonzalez and his colleagues. The uric acid was oxidised electrochemically and hypoxanthine and xanthine were determined in the range of 5-100 μM at pH 7.2 (Gonzalez *et al.*, 1991).

Most of the biosensors which have been designed to determine the hypoxanthine or xanthine are used to measure the freshness of fish. Estimation of fish and meat freshness is very important in the fields of fresh food supplies and food processing industries. Hypoxanthine is one of the intermediates of the fish decomposition, and can be used as an indicator of fish freshness. Based on this principle, some enzyme biosensors have been developed. Burt and his colleagues determined hypoxanthine in fish extract spectrophotometrically by measuring hydrogen peroxide (Burt *et al.*, 1977).

Enzyme biosensors were constructed for assaying hypoxanthine, inosine and inosine-5'-monophosphate as indicators on fish freshness based on monitoring the oxygen consumption during oxidation of analytes (Watanabe *et al.*, 1983, 1984a & b, 1986, 1988). Another enzymatic assay was developed for hypoxanthine in fish extracts using soluble xanthine oxidase (Luong *et al.*, 1988, 1989). The reaction took place in a reaction chamber equipped with a polarographic electrode which amperometrically measured the products of degradation, uric acid and hydrogen peroxide. Another

technique has been demonstrated to measure xanthine and hypoxanthine in the range of 0.1-0.5 mM using xanthine oxidase (EC 1.1.3.22) (Satoh *et al.*, 1988). This technique was found to be suitable for continuous monitoring of xanthine in flow streams, although the stability of the enzyme column was comparatively low.

Later, a hypoxanthine biosensor for assaying fish freshness was constructed using immobilised xanthine oxidase and a Clark-type polarographic electrode (Mulchandani *et al.*, 1989). The polarographic electrode detected hydrogen peroxide and uric acid released during the enzymatic reaction. The electrode response was linear to hypoxanthine concentration in the range of 3.6-107 μM. Suzuki and his colleagues have described a disposable micro hypoxanthine sensor for the fish freshness measurement (Suzuki *et al.*, 1989). Xanthine oxidase was immobilised on the micro oxygen electrode with bovine serum albumin and glutaraldehyde. A linear calibration curve was obtained in the concentration range between 6.7-180 μM. Also, an enzymatic assay for hypoxanthine with a Clark oxygen electrode as sensor has been developed (Kim *et al.*, 1989). In the presence of sodium sulphite, oxidation of hypoxanthine by milk xanthine oxidase caused a very rapid increase in oxygen consumption in excess of the stoichiometric requirement for hypoxanthine oxidation.

In 1990, Haemmerli and his colleagues developed a biosensor using a polarographic electrode in combination with immobilised xanthine oxidase (Haemmerli *et al.*, 1990). The proposed electrodes responded linearly to hypoxanthine between 2.5 and 375 μM and were found to have longer lifetime and to be more sensitive than previously

described sensors. A mediated amperometric needle-type hypoxanthine biosensor for *in situ* monitoring of fish tissues has been also developed (Nguyen & Luong, 1993).

Recently, a fibre-optic biosensor was constructed for determination of hypoxanthine and xanthine (Hlavay *et al.*, 1994). Xanthine oxidase and peroxidase were immobilised on different preactivated membranes which were subsequently mounted onto the tip of a fibre-optic bundle. The hydrogen peroxide generated by the reaction of hypoxanthine and xanthine oxidase was measured by chemiluminescence detection using luminol and peroxidase. A linear calibration curve of the fibre-optic biosensor was obtained in the range of 1-316 μM hypoxanthine and 3.1-316 μM xanthine, respectively, with a detection limit of 0.55 μM. The developed method was found to be more sensitive and to have lower detection limit than the previously described electrochemical biosensors.

3.1.4 Xanthine Oxidase

Xanthine oxidase is one of the enzymes participating in the final steps of purine degradation (Zubay, 1993). In mammals, this enzyme is present in large amounts in liver, kidney and intestinal mucosa and in traces in other tissues, and catalyses the oxidation of hypoxanthine and xanthine to uric acid (Reaction 5.a and 5.b). The catalytic activity of serum is exclusively dependent on release of the enzyme from the liver. In sera of healthy persons, xanthine oxidase activity is normally absent or only present at very low levels, but it increases markedly in patients with viral hepatitis. The name xanthine oxidase was chosen because among the various substrates the oxidation rates

of xanthine and hypoxanthine to uric acid are the most rapid ones and the K_m values the lowest.

Most of the data for xanthine oxidase were derived from the enzyme isolated from cow's milk. Xanthine oxidase (xanthine: oxygen oxidoreductase, EC 1.2.3.2) is a complex metalloflavoprotein containing one molybdenum, one FAD and two iron-sulphur centres of the ferredoxide type in each of its two independent subunits (Heinz & Reckel, 1983). Low specificities towards both the substrate and the electron acceptor were reported. More than one hundred different compounds have been described as substrates, e.g. purines and pteridines, which are hydroxylated, and aldehydes, which are oxidised to the corresponding carbonic acids. Its molecular mass lies in the value of $283x10^3$ Da (Kresse, 1990). The optimum pH range of the enzyme is between 7.0-9.0 and the isoelectric point is 6.2. It is inhibited by allopurinol. Literature values for the Michaelis constant (K_m) of xanthine oxidase with xanthine are $1.7x10^{-6}$ M and with oxygen $2.4x10^{-5}$ M (Kresse, 1990).

5.2 MATERIALS & METHODS

5.2.1 Chemicals

The enzyme, xanthine oxidase (xanthine: oxygen oxidoreductase; EC 1.1.3.22) (1.3 units/mg protein, grade III, from Buttermilk) and xanthine (in sodium salt 99%, $C_5H_3N_4O_2Na$) were supplied by Sigma Chemical Co. (Poole, Dorset). One unit of activity of the enzyme is defined as the amount of the enzyme that will catalyse the oxidation of 1.0 μM of xanthine to uric acid per min at pH 7.5 at 25 ^{0}C. Approximately 50% of the

activity is obtained when hypoxanthine is used as substrate. The purchase of the indicators, HPTS and tris(2,2'-bipyridyl)ruthenium(II) chloride hexahydrate, was reported in Chapter 2. All other inorganic reagents were of analar grade and used as obtained from BDH Ltd. (Poole, Dorset).

The standard buffer solution was 10mM sodium phosphate buffer, pH 7.4 at 21^0C, containing 10mM $Na_2HPO_4 \cdot 12H_2O$ and 10mM $NaH_2PO_4 \cdot 2H_2O$. All experiments were performed at room temperature ($22 \pm 2\ ^0$C), using 7μM tris(2,2'-bipyridyl)ruthenium(II) chloride hexahydrate and 0.03 μM HPTS. For the kinetic measurements the standard buffer solution was 0.1 mM sodium phosphate buffer containing 0.1 M NaCl in order to adjust the pH to 7.4. Stock solutions of indicators were prepared by bubbling 1 mM phosphate buffer with pure oxygen for at least 15 min. All components of the assay mixtures were freshly prepared.

In the kinetic experiments, a small stirrer bar was placed in the bottom of the cuvette in order to keep the solution homogeneous during the reaction and was rotated at a standard rate for all experiments; the motor was fixed under the cuvette holder inside the spectrofluorometer. All additions of stock solutions (in the range of μl) were made outside the instrument and only xanthine oxidase was added when the cuvette was in the instrument, in order to monitor the reaction from time zero.

5.2.2 Instrumentation

The instrumentation used was as described in Chapter 3 (see Section 3.2.2).

5.3 RESULTS

5.3.1 Spectroscopic Investigation of Xanthine

Xanthine or 2,6-Dihydroxypurine is an aromatic compound with structural formula $C_5H_4N_4O_2$, and molecular weight of 152. It appears in the form of fine white crystals and yields yellowish solution in the water. In the following experiments, xanthine in sodium salt was used in order to be dissolved easily in phosphate buffer pH 7.4 to give a colourless limpid solution.

The excitation and emission fluorescence spectra of xanthine for 1 mM concentration are shown in Figure 5.1, which illustrates that the peak excitation occurs at 335 nm. Excitation with 335 nm radiation elicits a peak emission at 435 nm. Figures 5.2, 5.3 and 5.4 show the fluorescence quenching of increasing xanthine concentrations in the ranges of 1-10 mM, 0.1-1 mM, and 10-100 μM, respectively. The small peak in Figure 5.3 at 376 nm is due to the Raman scattering from the solvent (water in the present study) because the sample was excited at a selected wavelength of 335 nm.

The corresponding graphs of concentration versus fluorescence intensity for the above concentrations of xanthine are shown in Figures 5.5, 5.6 and 5.7, respectively. They indicate that the fluorescence intensity increased when the xanthine concentration increased, and more importantly they show a linear relationship in the analytical ranges of 10 μM to 10 mM. Above 10 mM xanthine, the fluorescence intensity against xanthine concentration followed a curve rather than a linear regression fit. Below 10 μM the fluorescence intensity of xanthine was not clearly detectable.

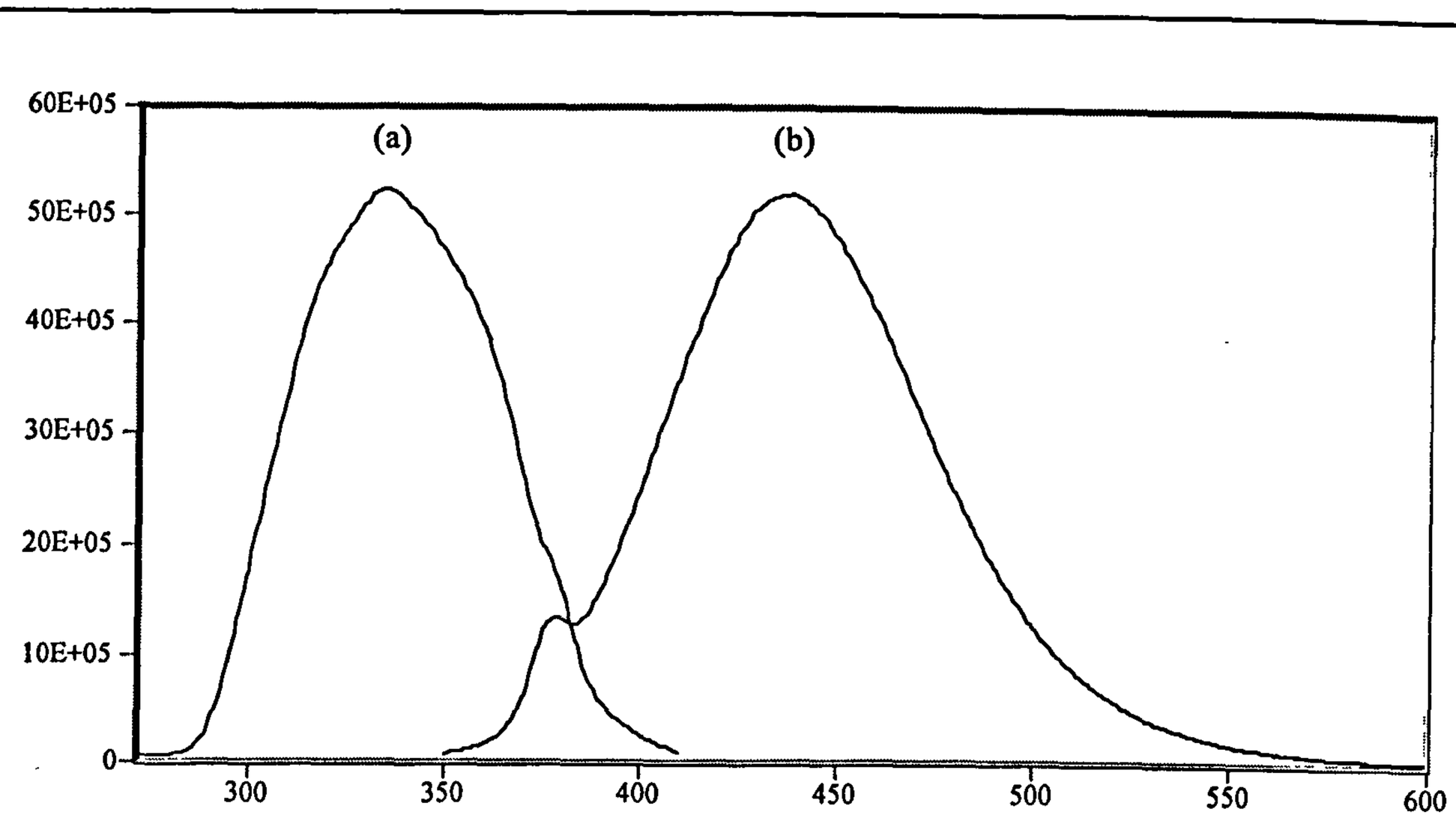

FIGURE 5.1 Excitation (a) and fluorescence (b) spectra of xanthine (1 mM) with excitation wavelength at 335 nm and fluorescence monitored at 435 nm, in phosphate buffer pH 7.4 at 22 ^{0}C.

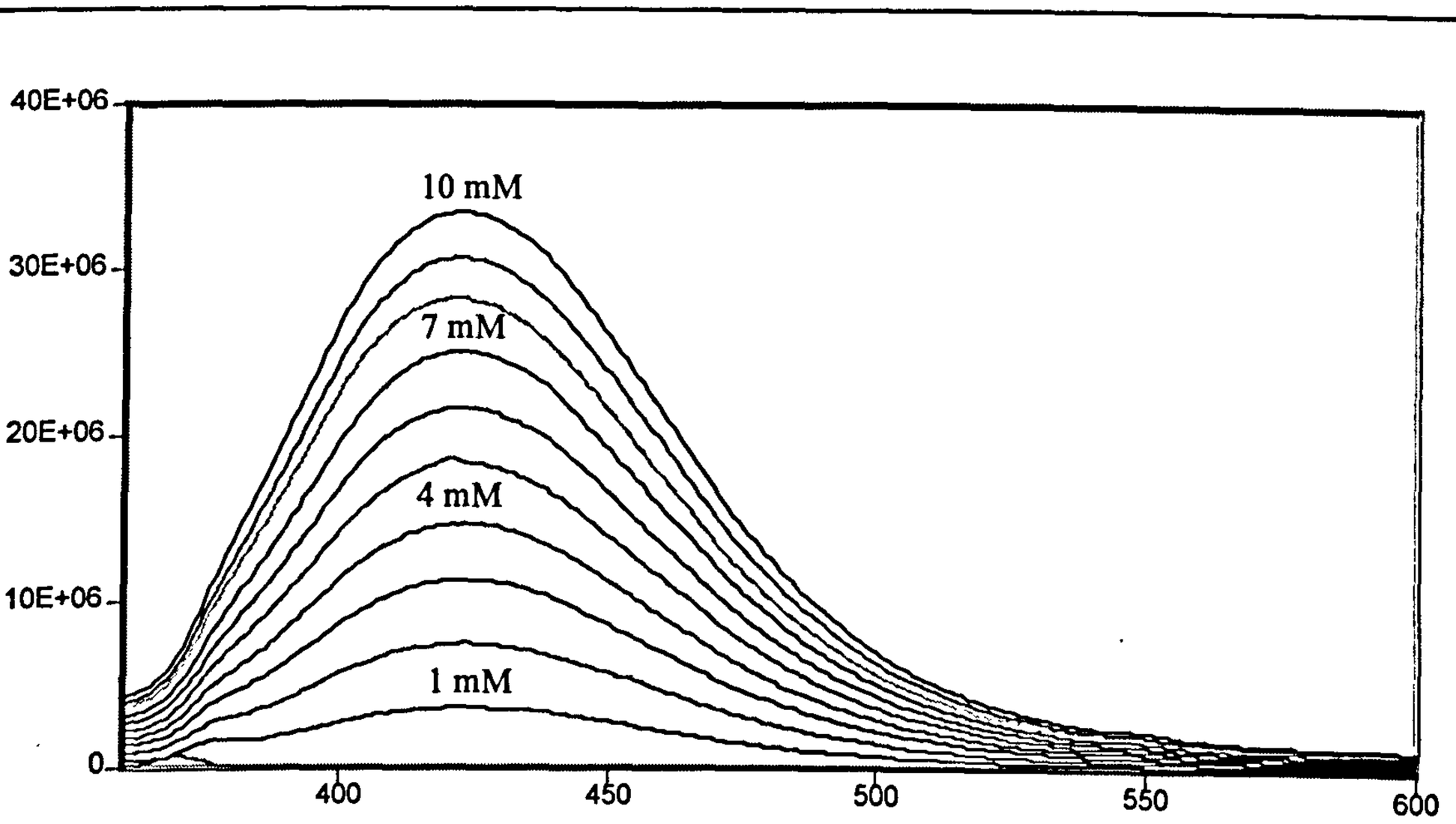

FIGURE 5.2 Fluorescence spectra of xanthine (1-10 mM) in phosphate buffer pH 7.4 at 22 ^{0}C. Solutions were excited at a wavelength of 335 nm.

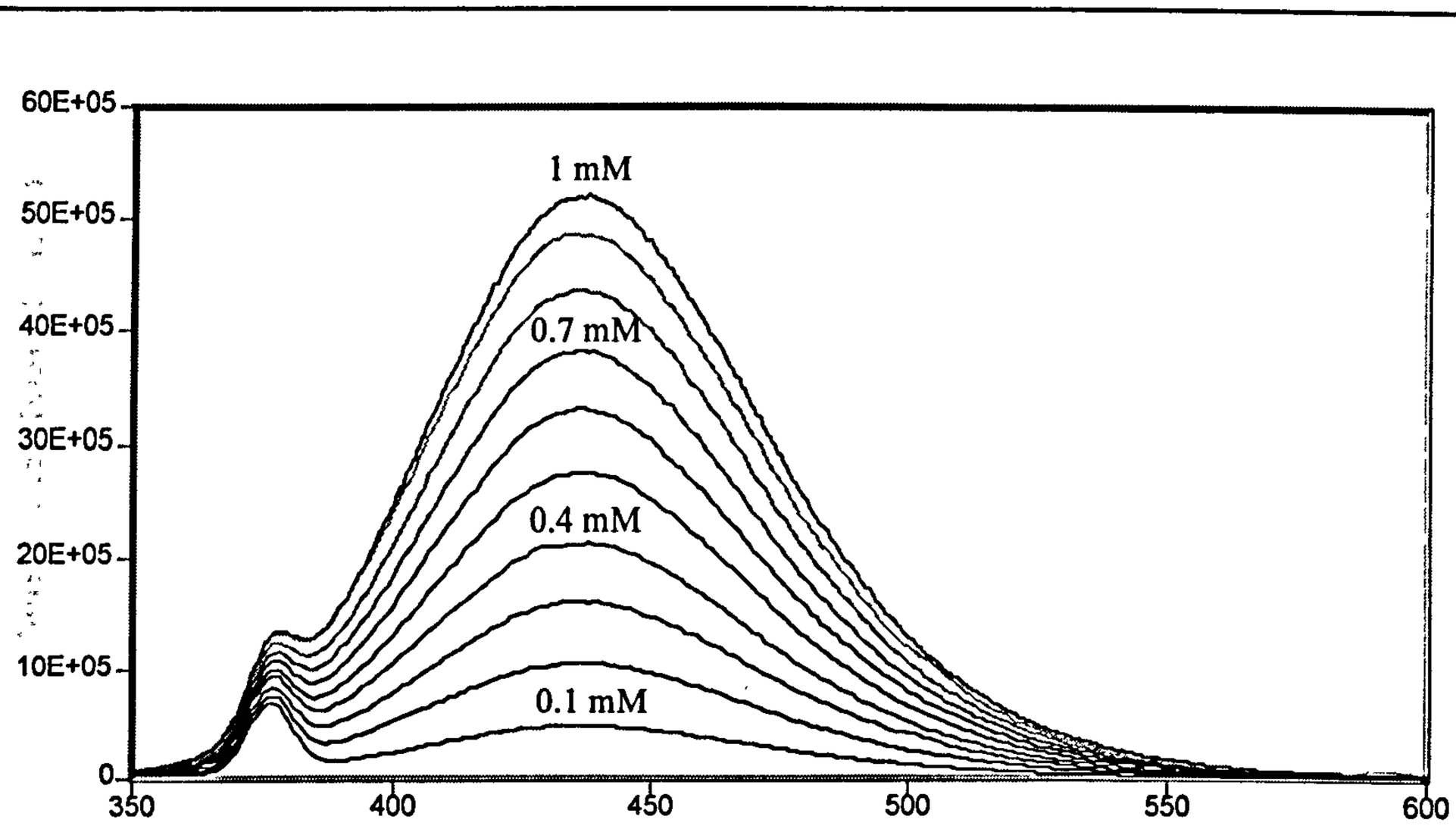

FIGURE 5.3 Fluorescence spectra of xanthine (0.1-1 mM) in phosphate buffer pH 7.4 at 22 ^{0}C. Solutions were excited at a wavelength of 335 nm.

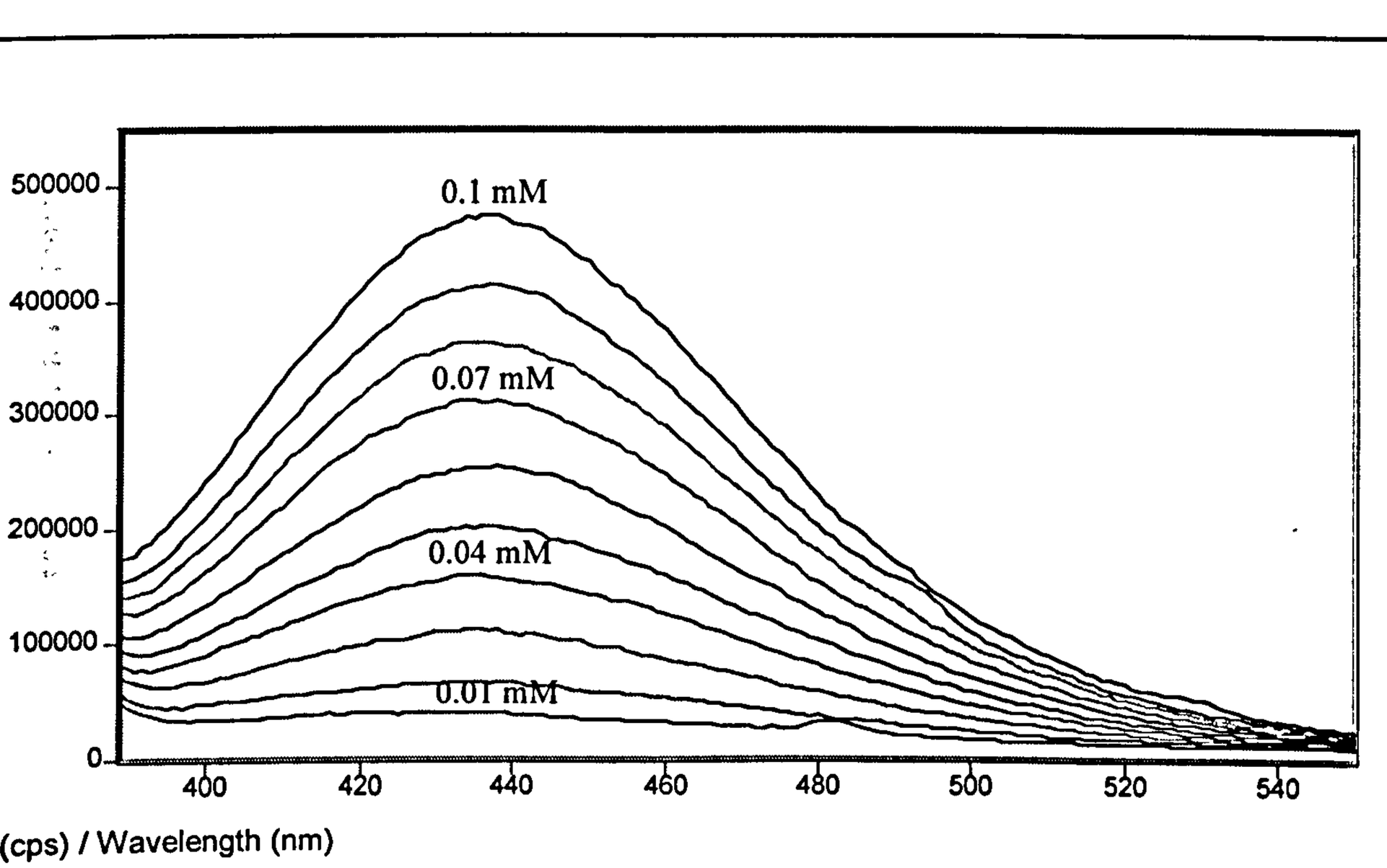

FIGURE 5.4 Fluorescence spectra of xanthine (0.01-0.1 mM) in phosphate buffer pH 7.4 at 22 ^{0}C. Solutions were excited at a wavelength of 335 nm.

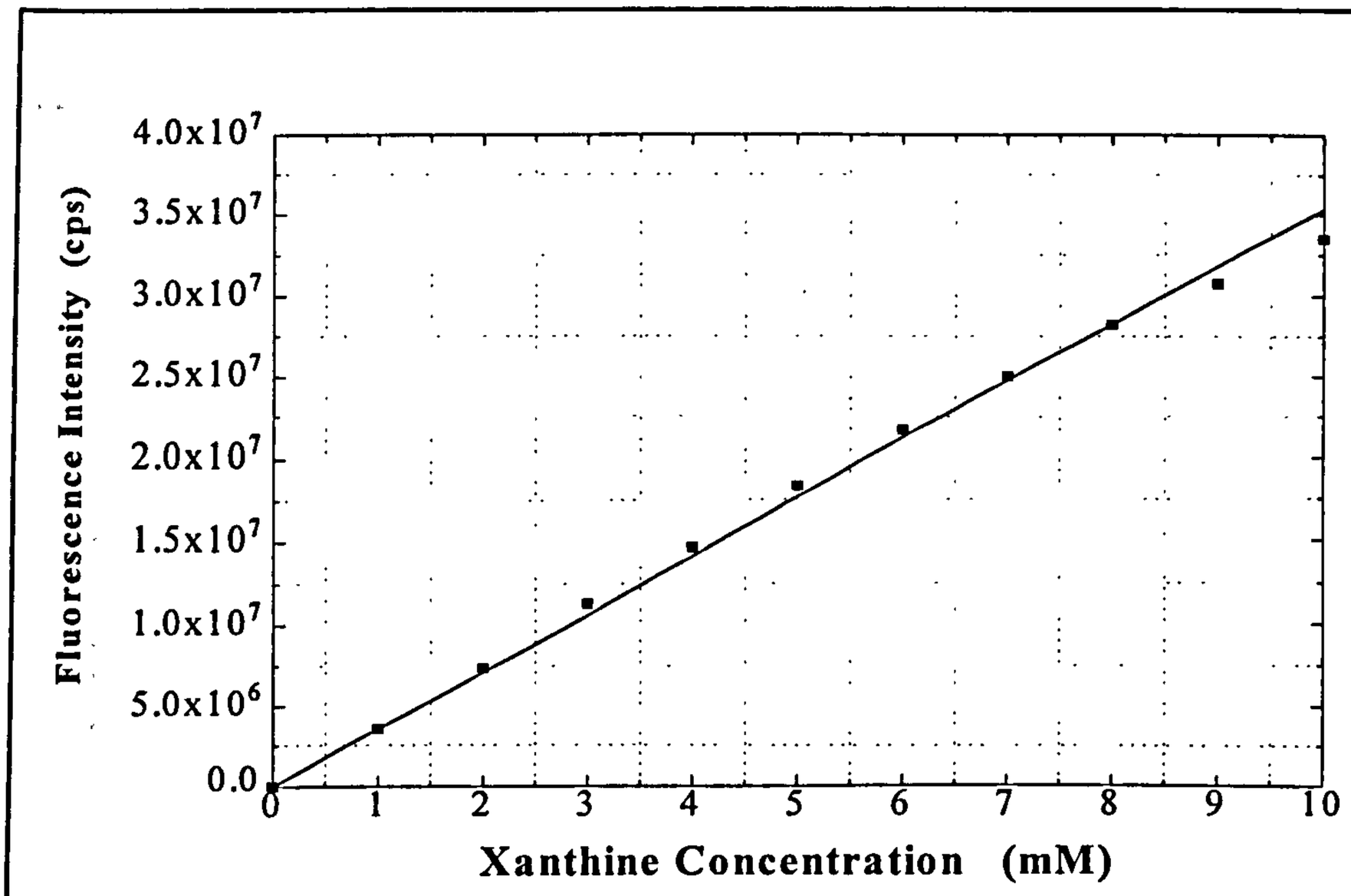

FIGURE 5.5 Fluorescence intensity versus concentration of xanthine (1-10 mM) in phosphate buffer pH 7.4 at 22 ^{0}C, excitation wavelength 335 nm.

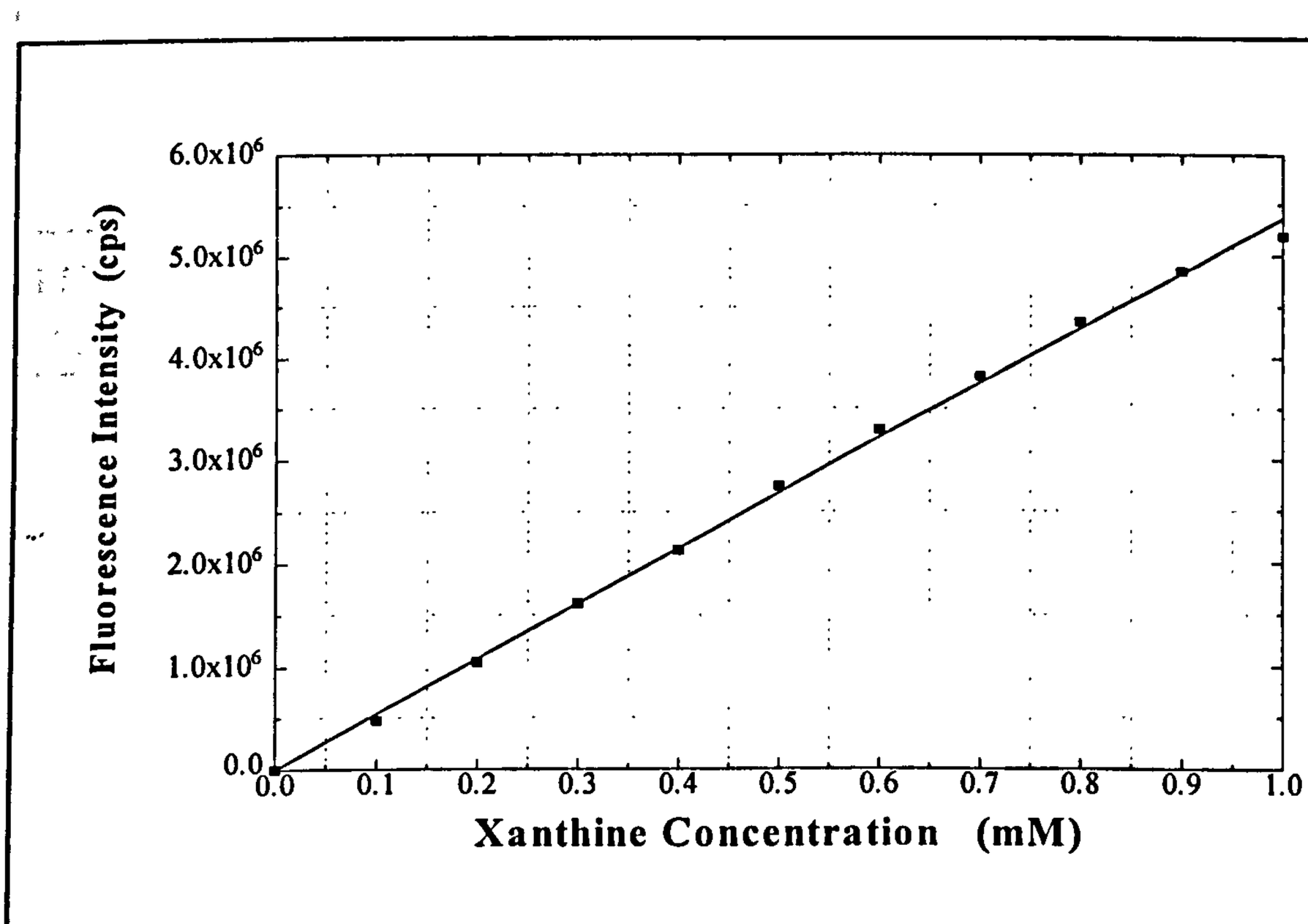

FIGURE 5.6 Fluorescence intensity versus concentration of xanthine (0.1-1 mM) in phosphate buffer pH 7.4 at 22 ^{0}C, excitation wavelength 335 nm.

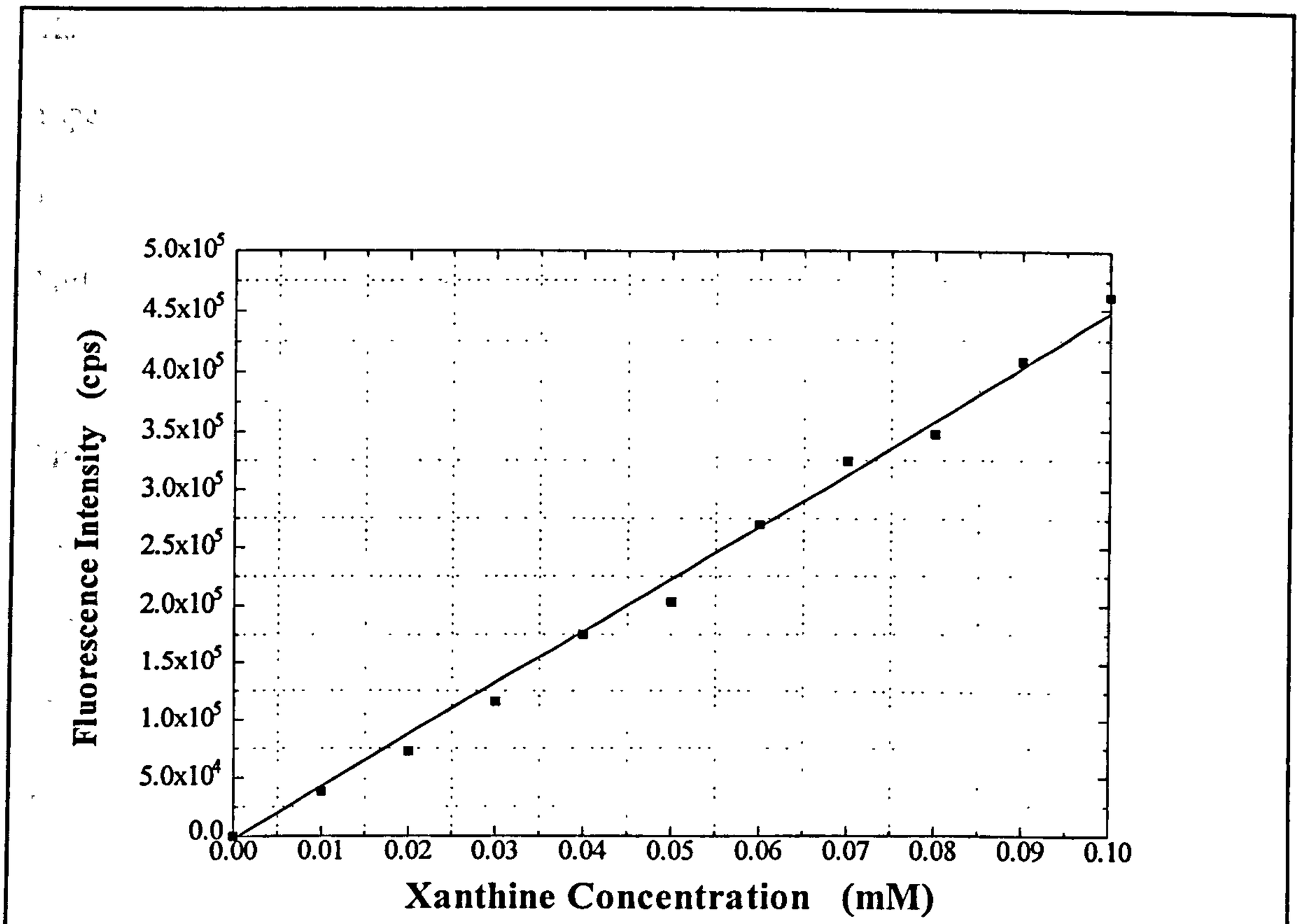

FIGURE 5.7 Fluorescence intensity versus concentration of xanthine (0.01-0.1 mM) in phosphate buffer pH 7.4 at 22 ^{0}C, excitation wavelength 335 nm.

5.3.2 Spectroscopic Investigation of Xanthine Oxidase

Xanthine oxidase is mainly used for the determination of xanthine, hypoxanthine and superoxide dismutase. In the experiments described below, xanthine oxidase has been used for the measurement of xanthine. Xanthine oxidase was dissolved in phosphate buffer pH 7.4 to give a yellow coloured solution.

Figure 5.8 shows the excitation and emission fluorescence spectra of 0.4 U/ml xanthine oxidase, which illustrates that the peak excitation occurred at 370 nm followed by a second smaller peak at 440 nm. Excitation with 370 nm radiation gave a peak emission at 518 nm, similarly, with excitation wavelength at 440 nm the maximum of fluorescence occurred again at 518 nm. Figure 5.9 and 5.10 show the fluorescence quenching of increasing enzyme concentrations in the range of (0.01-0.4) U/ml with excitation wavelength fixed at 370 and 440 nm, respectively.

As can be observed in Figure 5.8, in the excitation spectrum the peak at 370 nm is slightly higher than the peak at 440 nm, and the same trend was followed by Figures 5.9 and 5.10. Therefore, the fluorescence intensities at the peak of 518 nm of different xanthine oxidase concentrations at excitation wavelength of 370 nm are slightly higher than the fluoerescence intensities of the corresponding xanthine concentrations in the peak of 518 nm when are excitated at wavelength of 440 nm.

The corresponding graphs of fluorescence intensity against concentration of xanthine oxidase for the above two excitation wavelengths are shown in Figures 5.11 and 5.12.

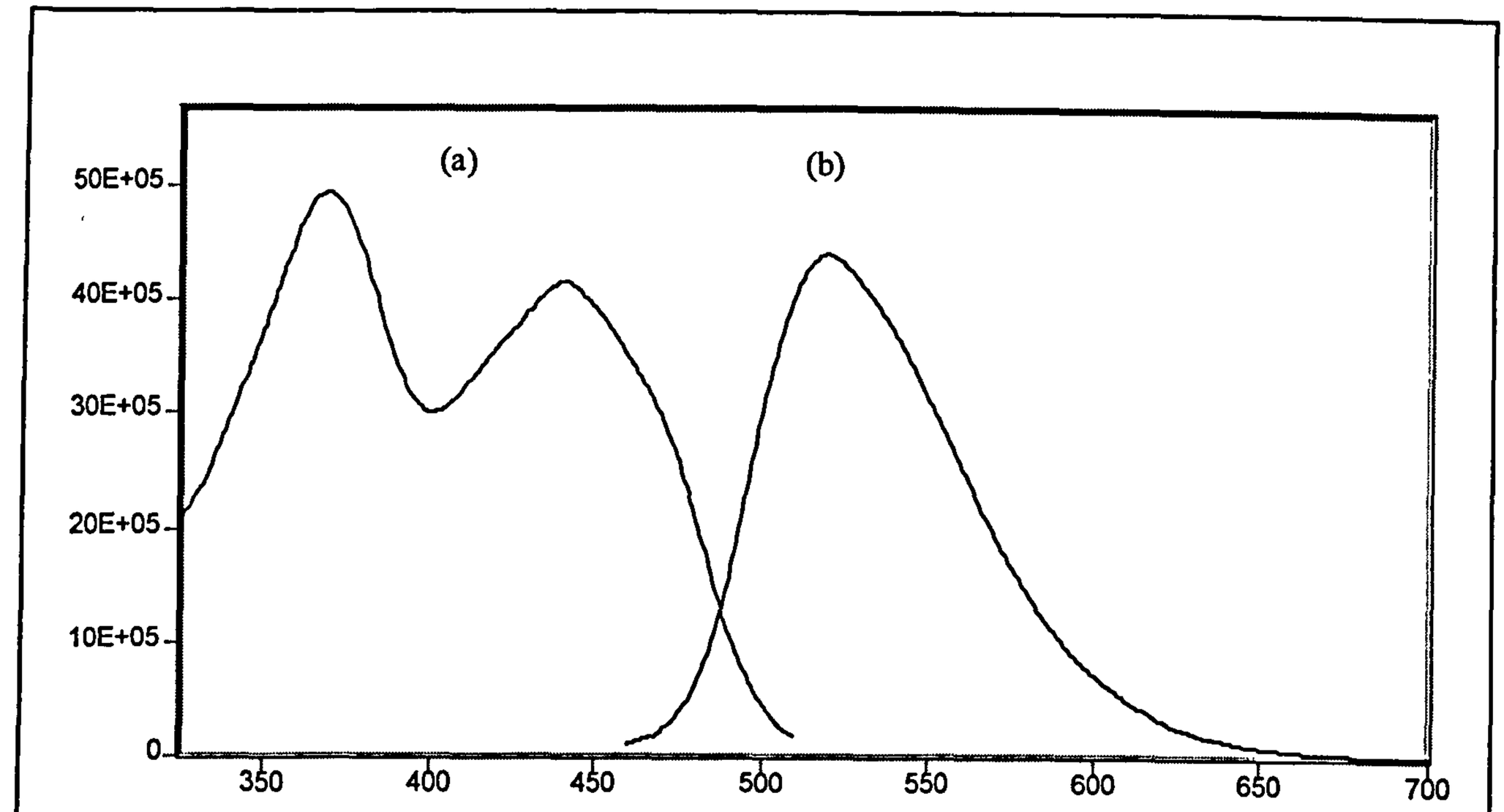

FIGURE 5.8 Excitation (a) and fluorescence (b) spectra of xanthine oxidase (0.4 U/ml) with excitation wavelength at 440 nm and fluorescence monitored at 518 nm, in phosphate buffer pH 7.4 at 22 ^{0}C.

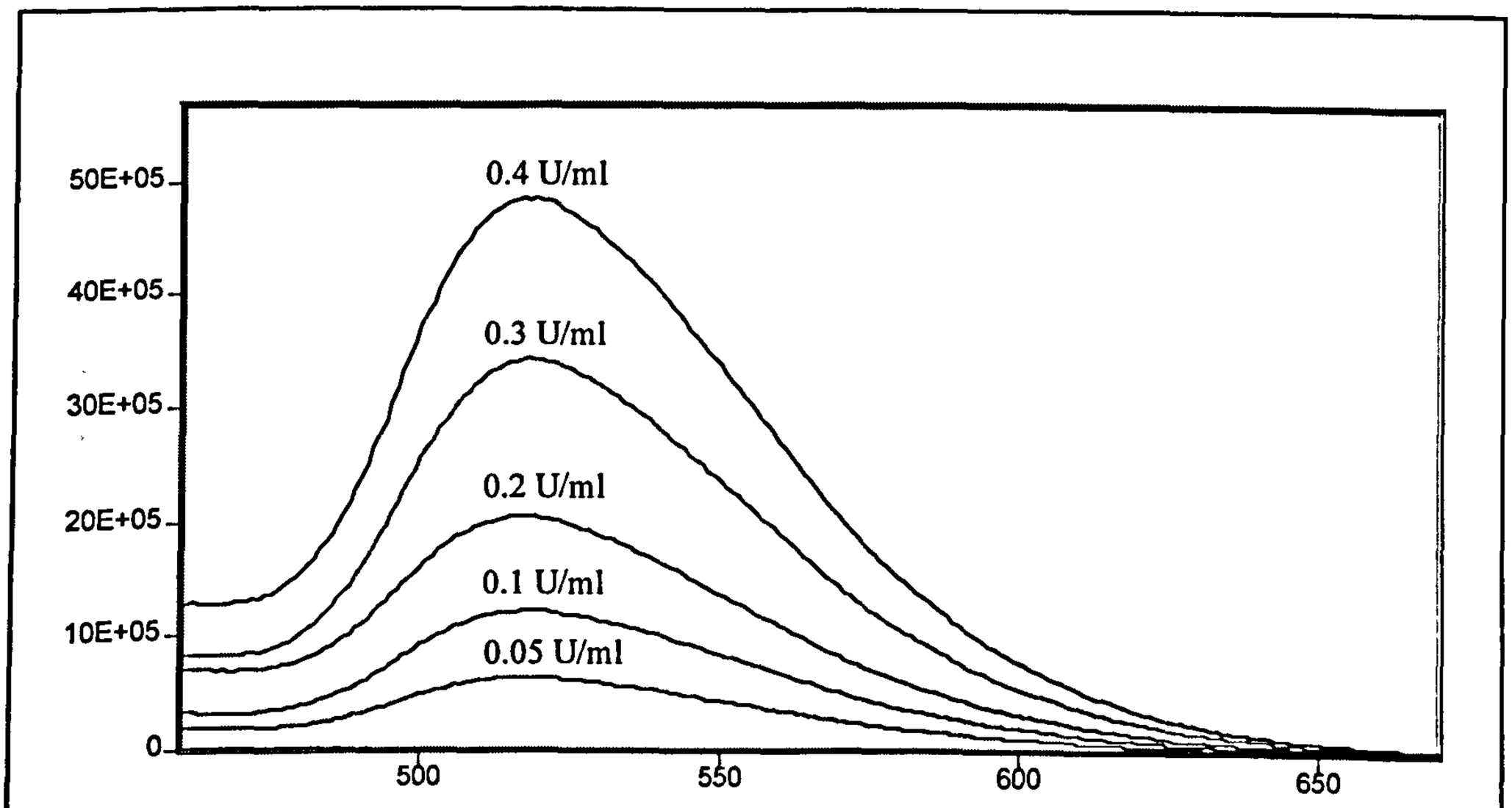

FIGURE 5.9 Fluorescence spectra of xanthine oxidase (0.05-0.4 U/ml) in phosphate buffer pH 7.4 at 22 ^{0}C. Solutions were excited at a wavelength of 370 nm.

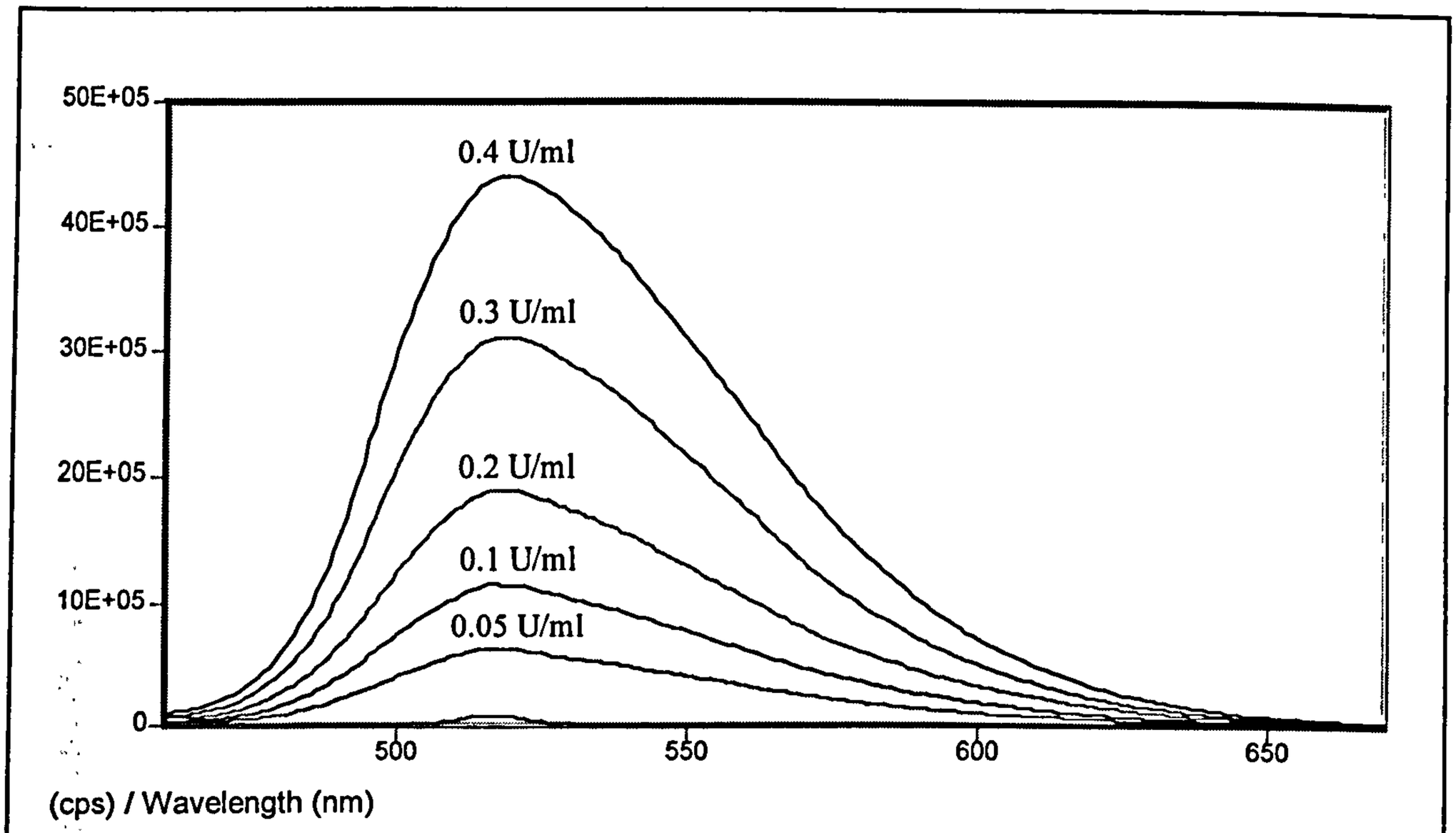

FIGURE 5.10 Fluorescence spectra of xanthine oxidase (0.05-0.4 U/ml) in phosphate buffer pH 7.4 at 22 ^{0}C. Solutions were excited at a wavelength of 440 nm.

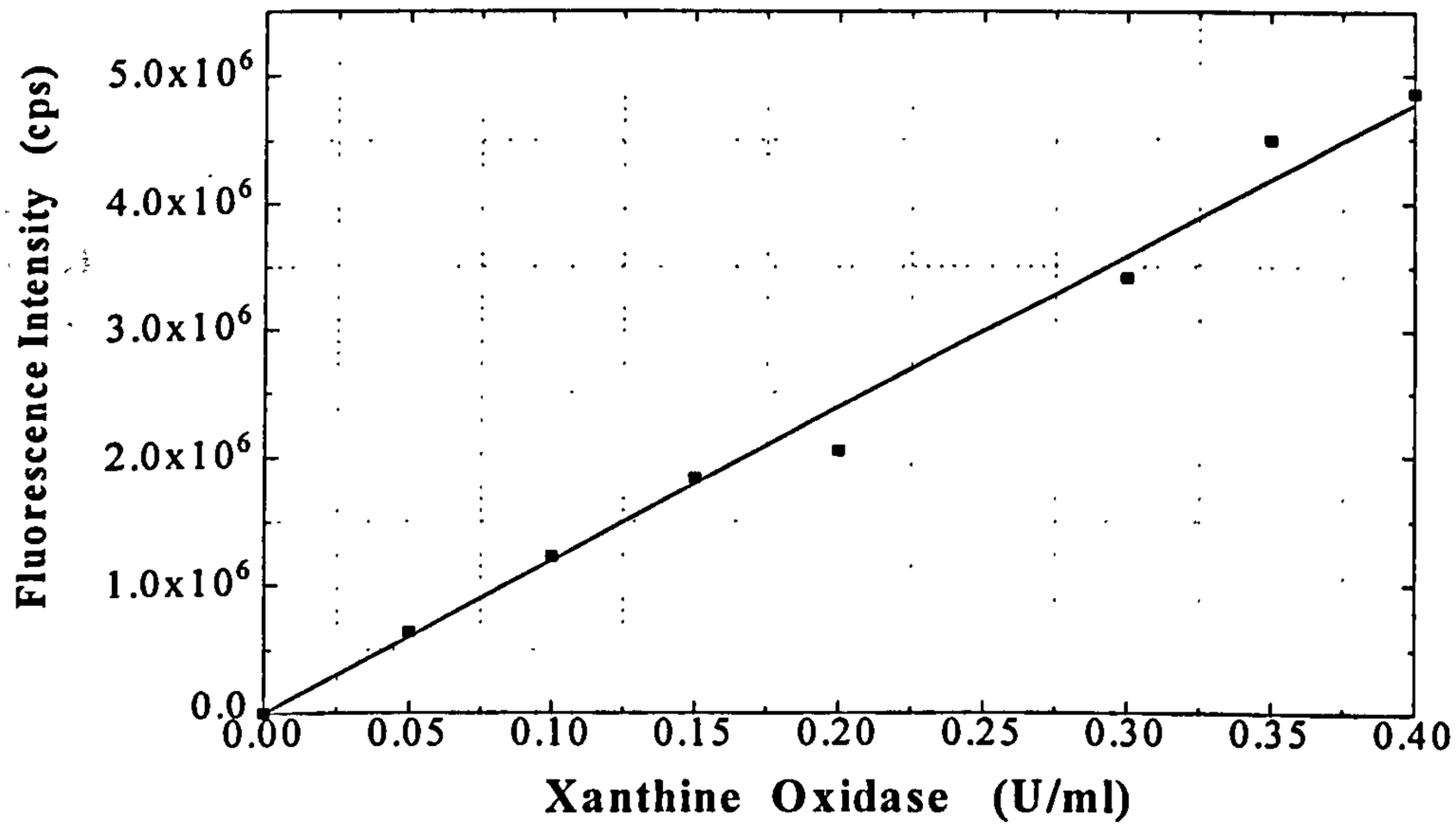

FIGURE 5.11 Fluorescence intensity versus concentration of xanthine oxidase (0.05-0.4 U/ml) in phosphate buffer pH 7.4 at 22 ^{0}C, excitation wavelength 335 nm.

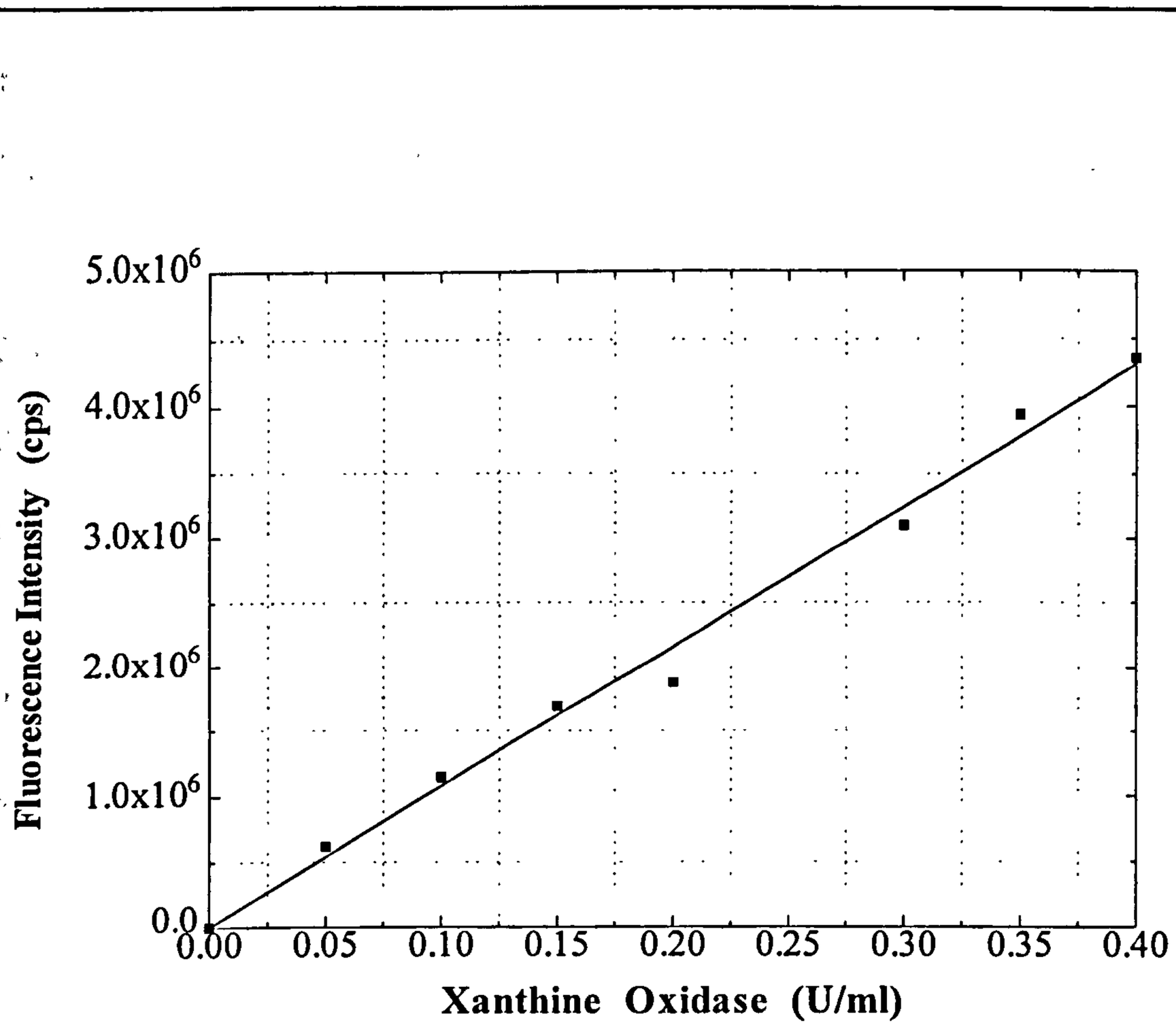

FIGURE 5.12 Fluorescence intensity versus concentration of xanthine oxidase (0.05-0.4 U/ml) in phosphate buffer pH 7.4 at 22 ^{0}C, excitation wavelength 440 nm.

These Figures (5.11 and 5.12) indicate that xanthine oxidase, like glucose oxidase, had a significant fluorescence intensity with maximum at 518 nm, when it was excited at 370 nm or 440 nm. This fluorescence intensity increased when the enzyme concentration increased, and it followed a linear relationship in the analytical range of 0-0.4 U/ml.

5.3.3 Kinetic Measurements of Xanthine Oxidase Reaction

According to Reaction 5.b, xanthine can be measured by monitoring oxygen consumption, or/and pH changes due to uric acid, or/and hydrogen peroxide production. As mentioned in Chapter 3, this research aimed to use fluorescent indicators, in order to detect two parameters simultaneously which may enable more accurate detection of xanthine concentrations in a single biosensor. This was again achieved using tris(2,2'-bipyridyl)ruthenium(II) chloride hexahydrate for oxygen consumption, and HPTS to monitor pH changes during the oxidation of xanthine.

As indicated in the previous section, xanthine oxidase is a strong fluorescent flavoprotein, with maxima excitation wavelengths of 370 nm and 440 nm and maximum fluorescence wavelength at 518 nm, which is closer to the emission maximum of HPTS (507 nm). Consequently, an enzyme concentration of 0.2 U/ml was used in the reaction with xanthine in order to avoid fluorescence quenching by the enzyme, which would prevent observation of distinct maximum peaks for each indicator. In addition, this enzyme concentration provides satisfactory reaction time for the changes in the fluorescence intensity of both indicators, tris(2,2'-bipyridyl)ruthenium(II) chloride

hexahydrate and HPTS, to be detected during the catalytic oxidation of xanthine at concentrations between 1 μM to 0.5 mM xanthine.

Experiments were performed in quartz cuvettes (3 ml) with standard amounts of optimised enzyme and indicators, 0.2 U/ml xanthine oxidase, 0.03 μM HPTS and 7 μM tris(2,2'-bipyridyl)ruthenium(II) chloride hexahydrate in buffer solution pH 7.4. The reaction was initiated by addition of xanthine. The most interesting range of xanthine in the blood is between 1 and 100 μM, where abnormalities appear related to diseases as described in Sections 5.1.2 and 5.1.3.

Two series of experiments were devised in order to determine how different concentrations of xanthine affected fluorescence intensity of the indicators during the enzymatic oxidation of xanthine oxidase. The first series of experiments were carried out in order to design a fibre-optic biosensor with one source at a fixed excitation wavelength and two photodetectors fixed to the emission wavelengths of the two indicators respectively. Two sub-experiments were executed in which the common excitation wavelength of the indicators at 410 nm, was used as excitation wavelength. In the first experiment, the emission wavelength of the first indicator tris(2,2'-bipyridyl) ruthenium(II) chloride hexahydrate at 597 nm, was used as emission wavelength. In the second experiment, the emission wavelength of the second indicator HPTS at 507 nm, was used as emission wavelength. This is the implementation of Experimental Mode A (Chapter 3) to enzymatic oxidation of xanthine oxidase.

The results in terms of the rate of change of the fluorescence intensity of tris(2,2'-bipyridyl)ruthenium(II) chloride hexahydrate against the xanthine concentration because of the oxygen consumption during the oxidation are illustrated in Figure 5.13. Details and an example (the case of glucose substrate, Chapter 3) of the raw data manipulation together with the reasons for choosing the values of rate of change of fluorescence intensity with time (dI/dt) instead of the actual values of fluorescence intensity itself for each concentration, are presented in Appendix A.

Similarly, the changes of the rate of the fluorescence of HPTS because of the pH changes in the cuvette, during the production of uric acid by the oxidation, are presented in Figure 5.14. The response of the tris(2,2'-bipyridyl)ruthenium(II) chloride hexahydrate after the addition of xanthine took around 4 to 7 minutes to reach a condition where the changes in fluorescence intensity with time were very small. About 90% of this almost constant intensity value was achieved in approximately 3 to 4 minutes. The corresponding response times of HPTS were 3 to 5 minutes, and approximately 2 to 3 minutes to reach 90% of the final value.

For both indicators, lower xanthine concentrations required longer response times, and vica versa for higher xanthine concentrations. Saturation appeared above 0.55 mM xanthine and the lowest detectable concentration was 1 μM for both indicators. Finally, Figures 5.13 and 5.14 show that these calibration curves of Experimental Mode A for xanthine are hyperbolas and they follow the Michaelis-Menten equation.

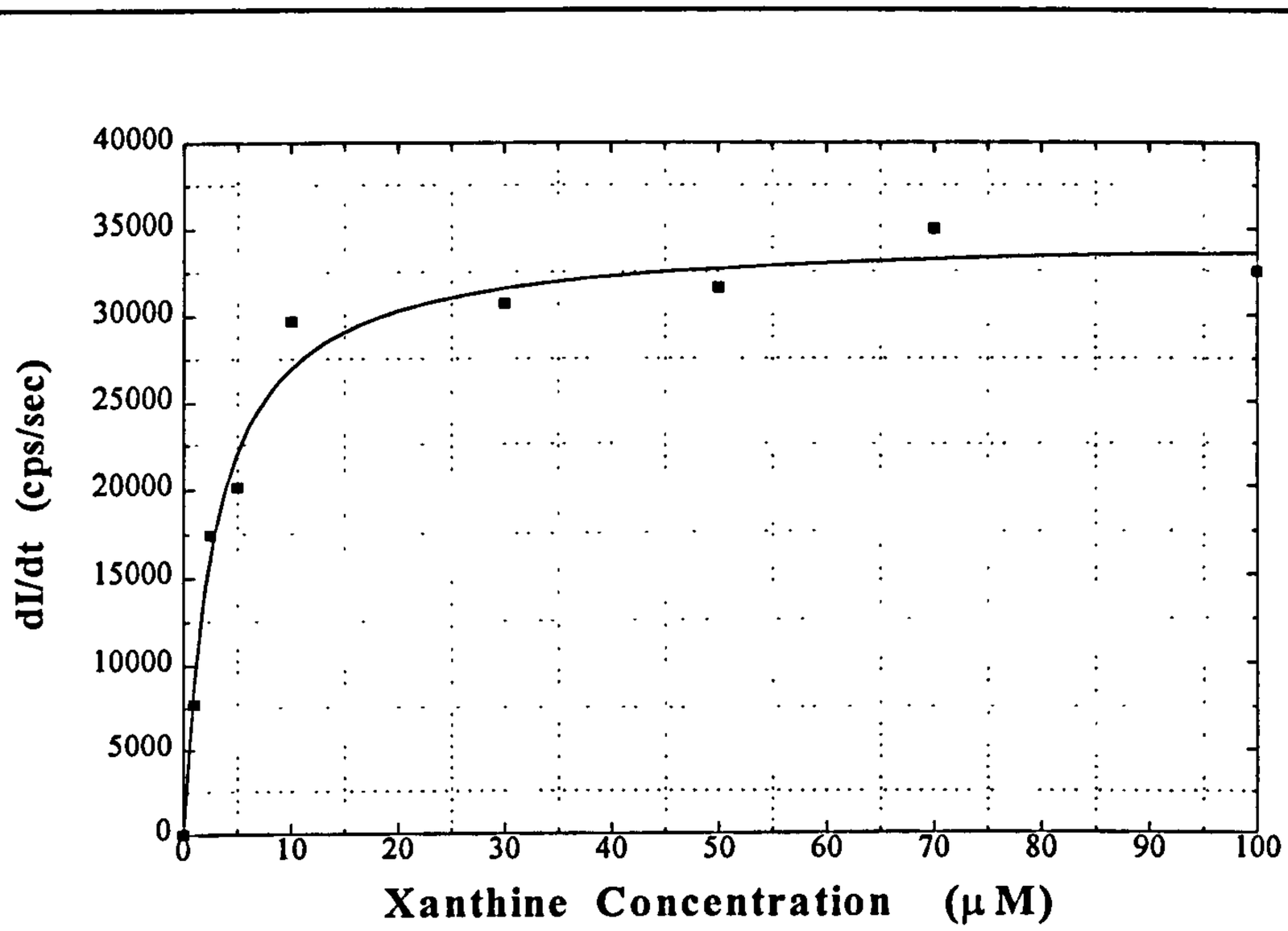

FIGURE 5.13 Rate of change of fluorescence intensity versus xanthine concentration of tris(2,2'-bipyridyl)ruthenium(II) chloride hexahydrate, at excitation wavelength of 410 nm and emission at 597 nm, during the catalytic oxidation of xanthine.

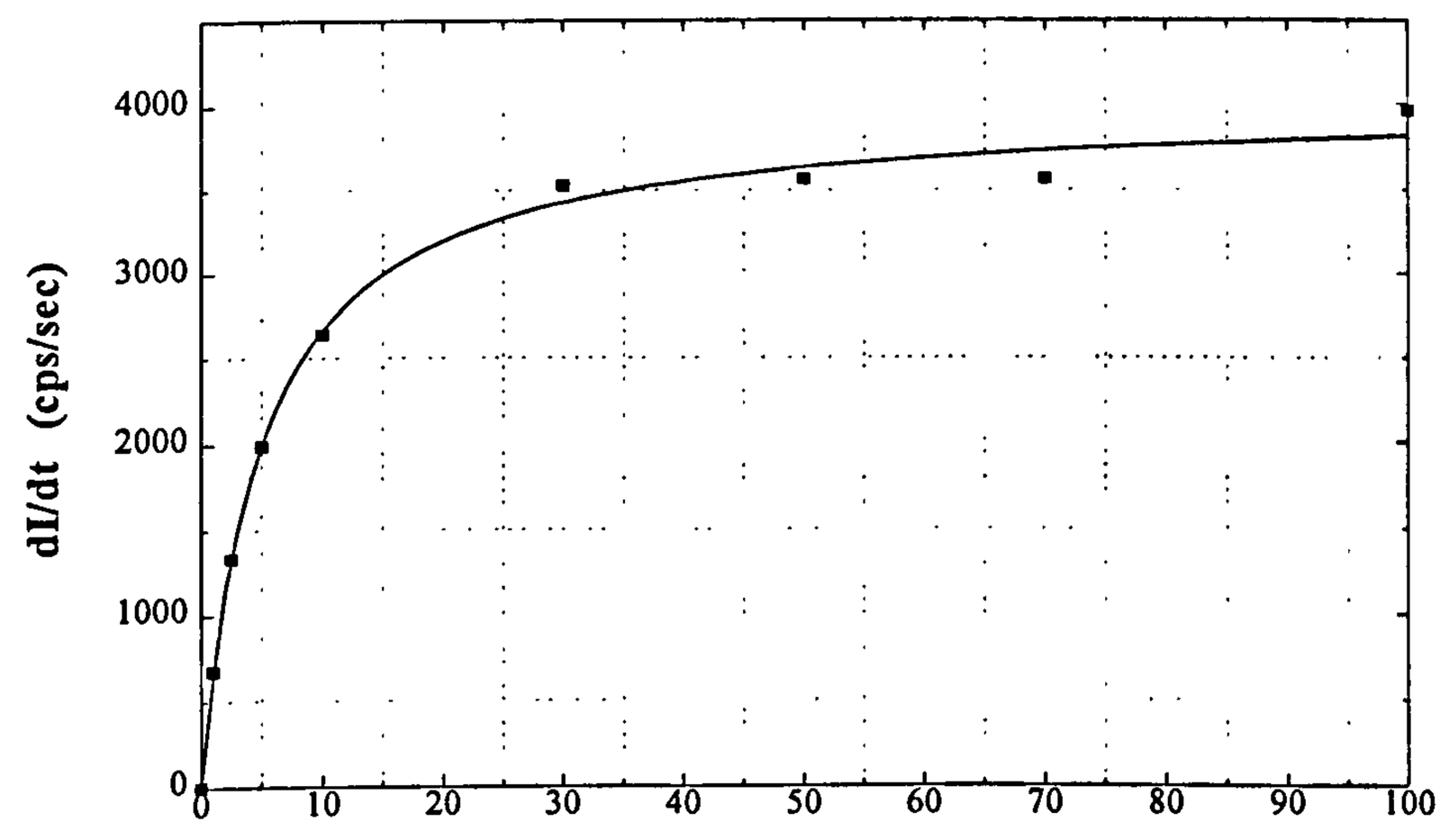

FIGURE 5.14 Rate of change of fluorescence intensity versus xanthine concentration of HPTS, at excitation wavelength of 410 nm and emission monitoring at 507 nm, during the catalytic oxidation of xanthine.

The Hanes plots corresponding to Figures 5.13 and 5.14 are presented in Figures 5.15 and 5.16, respectively. The experimental value of the Michaelis constant, K_m, of the reaction was found to be equal to 3.07 μM for the case in which the reaction was monitored through the rate of change of fluorescence intensity of tris(2,2'-bipyridyl) ruthenium(II) chloride hexahydrate at excitation wavelength of 410 nm and fluorescence monitored at 597 nm. However, the K_m was found out to be equal to 5.46 μM when the reaction was monitored via the rate of change of fluorescence intensity of HPTS at excitation and fluorescence wavelengths of 410 nm and 507 nm respectively.

The second series of experiments were performed under the following conditions: the common excitation wavelength of the indicators at 410 nm, was used as excitation wavelength and the common emission wavelength of the indicators at 555 nm, was considered as emission wavelength. The reason for using only one excitation and emission wavelength was to facilitate the construction of a simpler biosensor design with only one source at a fixed excitation wavelength and one photodetector at a fixed emission wavelength, which is capable to detect xanthine by monitoring simultaneously two parameters through the sum of the changes in fluorescence intensity of both indicators against time. This constituted the application of Experimental Mode B to the enzymatic oxidation of xanthine oxidase in the same way as in the enzymatic oxidation of glucose oxidase, described in Chapter 3. The results, after manipulation of the raw experimental data, of the rate of change of the fluorescence intensity of both indicators against xanthine concentration during its catalytic oxidation are depicted in Figure 5.17.

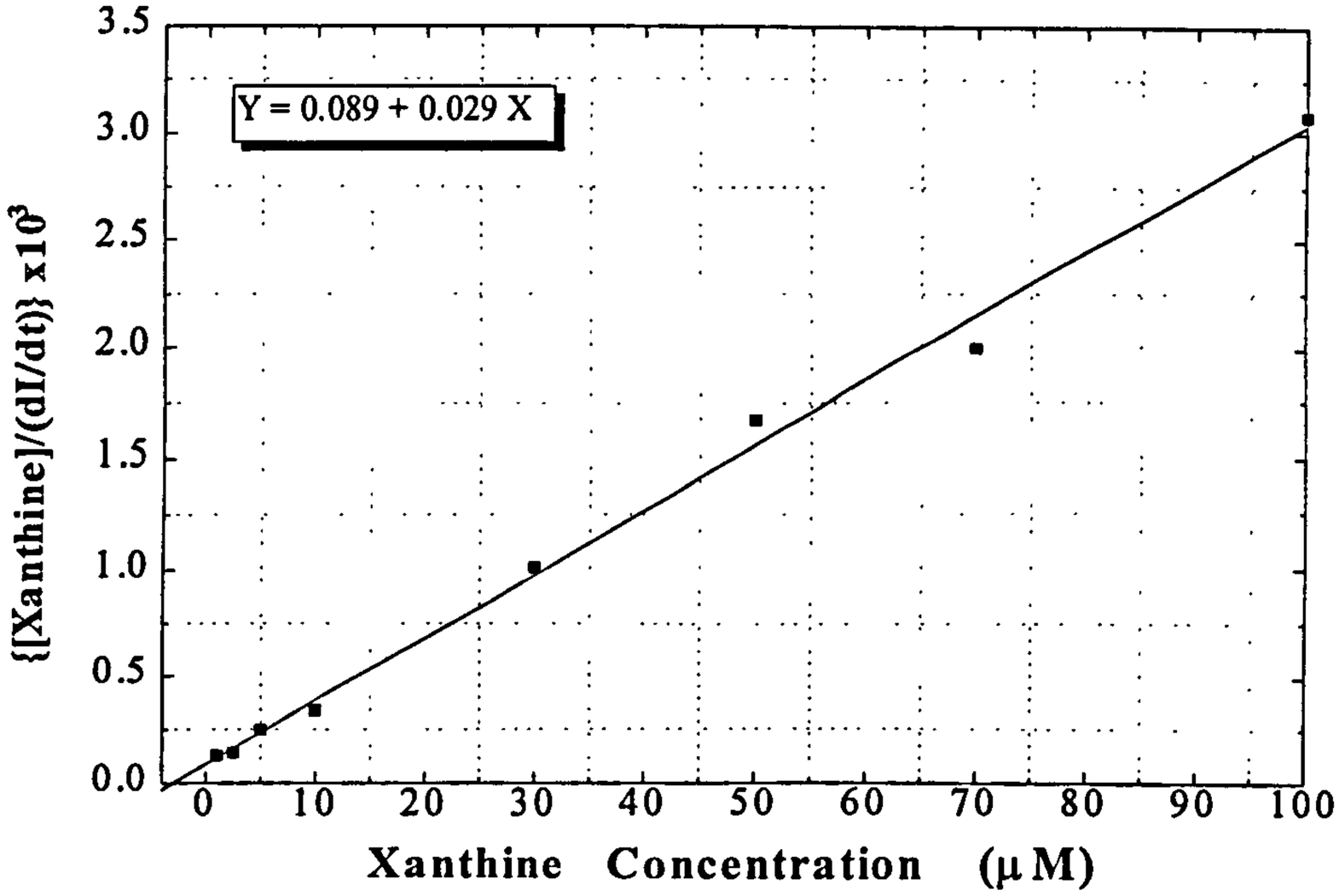

FIGURE 5.15 Hanes plot corresponding to Figure 5.13.

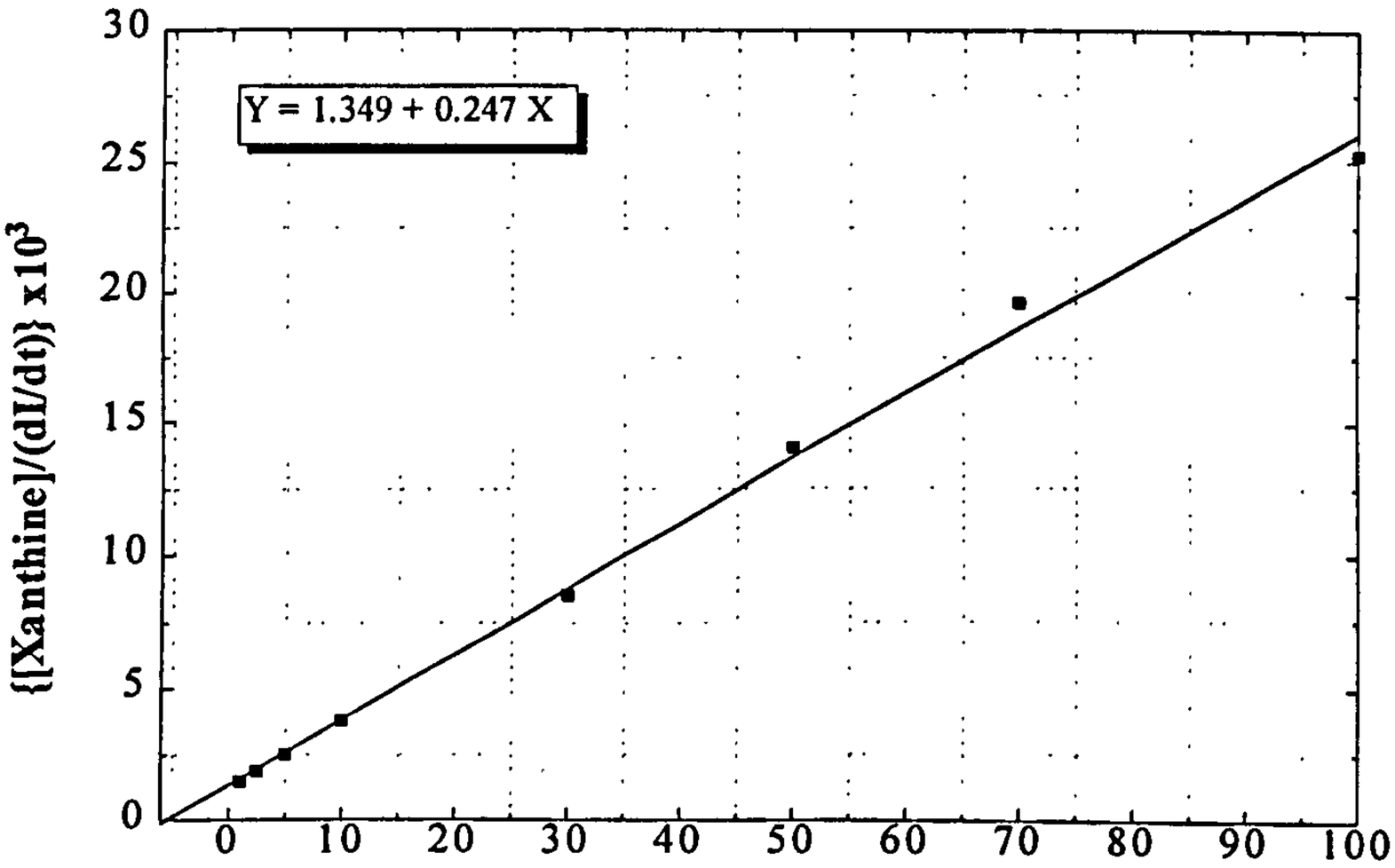

FIGURE 5.16 Hanes plot corresponding to Figure 5.14.

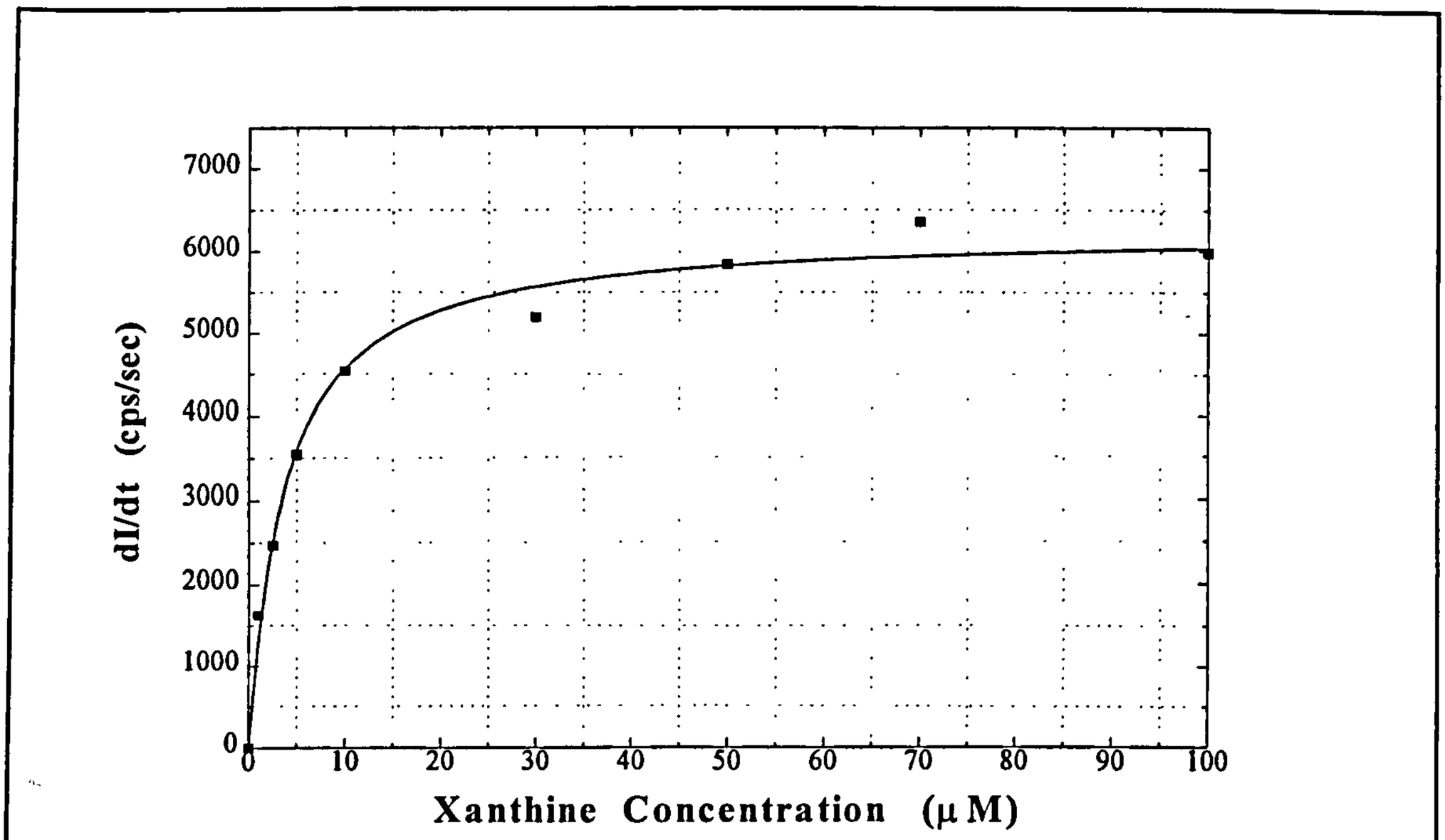

FIGURE 5.17 Rate of change of fluorescence intensity versus xanthine concentration of the sum of tris(2,2'-bipyridyl)ruthenium(II) chloride hexahydrate and HPTS, at excitation wavelength of 410 nm and monitoring the emission at 555 nm, during the catalytic oxidation of xanthine.

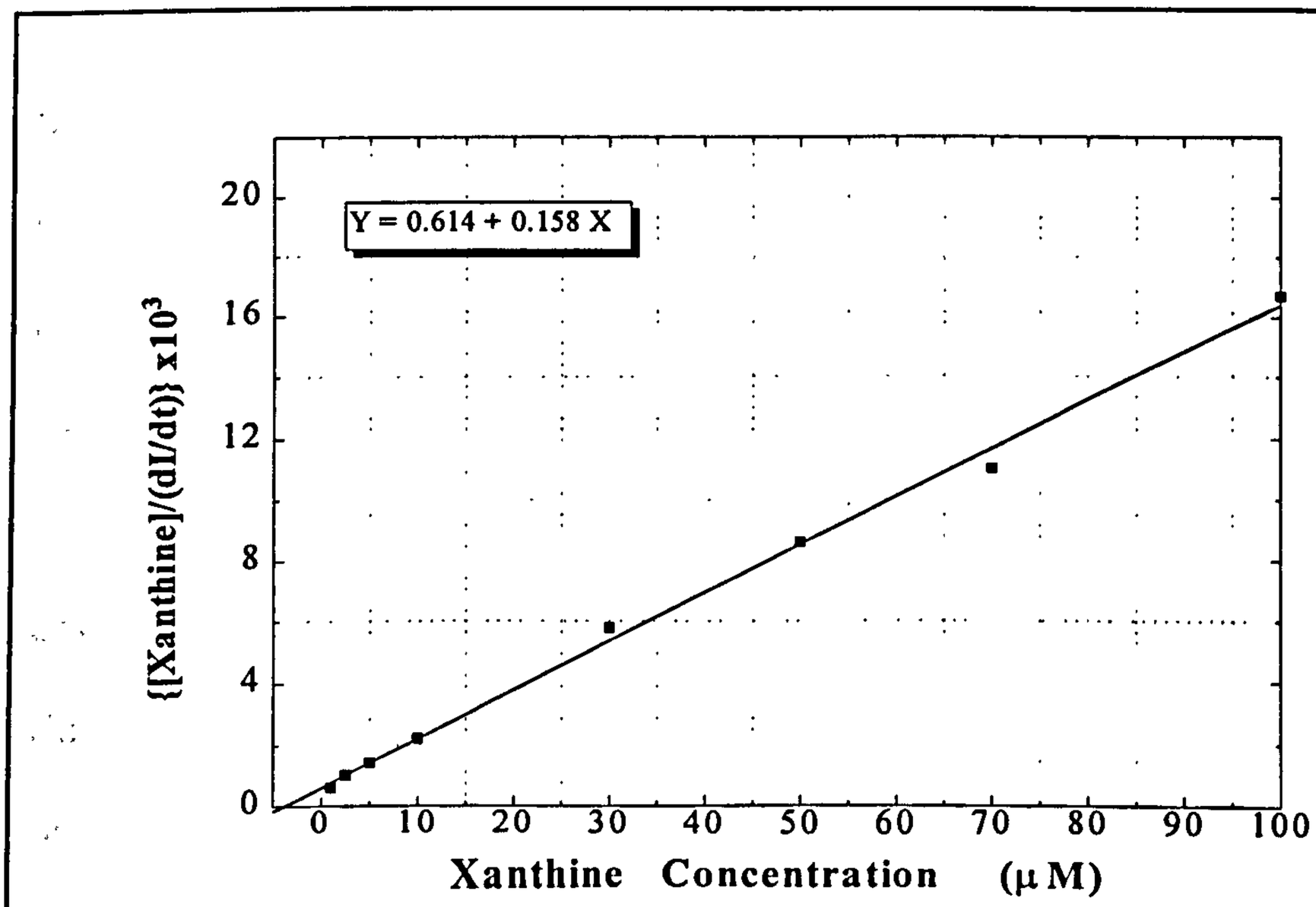

FIGURE 5.18 Hanes plot corresponding to Figure 5.17.

This mode offered the lowest detectable concentration of xanthine (1.5 μM) and a response time of 3.5 to 6 minutes to reach a state after which the flurescence intensity remained almost constant, and 90% of the final value was achieved within 2 to 4 minutes. Saturation occurred above 0.55 mM xanthine. According to Michaelis-Menten equation, the Hanes plot corresponding to the previous calibration curve (Figure 5.17) is illustrated in Figure 5.18. The K_m from this Hanes plot according to equation (3.e), was found to be equal to 3.89 μM.

5.4 DISCUSSION

Xanthine oxidase belongs to the category of flavoproteins and has shown fluorescence properties like glucose oxidase and lactate oxidase (excitation wavelengths 370 nm and 440 nm, fluorescence 518 nm), which are in agreement with available data in the literature (Wolfbeis & Trettnak, 1989).

Most of the xanthine biosenors presented in the literature are electrochemical and measure hypoxanthine instead of xanthine because it is proportional to the xanthine concentration, and therefore a known xanthine concentration implies a specific hypoxanthine concentration and vice versa (Mulchandani *et al.*, 1989; Nguyen & Luong, 1993; Hlavay *et al.*, 1994). In addition, most xanthine sensors were mainly developed for the determination of fish-meat freshness. In the present study, xanthine (instead of hypoxanthine) was used as substrate in order to test the feasibility of an optical biosensor for blood xanthine measurements with the intention of improving the accuracy and precision.

In the Experimental Modes A and B, the analytical ranges (1 μM to 0.5 mM) compare favourably with other biosensors described in the literature. Hlavay *et al.*, (1994) reported a linear calibration curve of 3.1-316 μM xanthine for a fibre optic biosensor based on a chemiluminescence reaction (see Section 5.1.3). An amperometric xanthine minibiosensor gave linearity in the range of 20 μM to 1 mM xanthine (Rehak *et al.*, 1994). Mulchandani *et al.*, (1989) reported a linear calibration curve of 3.6 - 107 μM using a hydrogen peroxide electrode and pre-activated membranes.

Also, linear relationships were obtained for hypoxanthine in different ranges, the most sensitive was 62.5-1500 μM with an oxygen base electrode and cellulose acetate membranes (Watanabe *et al.*, 1988). A disposable micro enzyme electrode in the linear range of 6.7-180 μM hypoxanthine was described (Suzuki *et al.*, 1989). A biosensor based on a Clark type electrode for the determination of hypoxanthine at concentrations of 2.5-275 μM was also developed (Haemmerli *et al.*, 1990).

An advantage of the present study is that the proposed biosensor works at room temperature, at pH 7.4 (ideal for blood xanthine monitoring) and is not subject to interferences from other chemicals present in the oxidation of xanthine. This compares favourably with the xanthine biosensor published by Rehak *et al.*, (1994) for possible environmental and medical applications, where the temperature should be between 30 and 37 °C, the pH between 7.5 and 7.7, and there was interference from ascorbic acid and hypoxanthine.

Similarly, as in the case of the lactate assay, the main difference between the present research work and the published xanthine biosensors is that Experimental Modes A and B monitor simultaneously two parameters of xanthine oxidation (oxygen consumption and changes in pH) using the two indicators in order to measure with more accuracy and precision the xanthine value.

5.5 CONCLUSIONS

The first method, for determination of xanthine using an optical sensor, was based on the fluorescence properties of xanthine itself. For xanthine concentrations in the range of 0.01-10 mM, the measured fluorescence intensity against xanthine concentration appears to be linear as presented in Figures 5.2, 5.3 and 5.4. This type of linear response is remarkable and proves that in principle the proposed approach can be used for the direct measurement of xanthine using an isolated light source with fixed excitation at 335 nm and a photodetector with selective wavelength at 435 nm, in order to construct a simple optical sensor.

One of the main drawbacks in this type of sensor is that the excitation wavelength belongs to the UV range and thus requires very good isolation of the light source and the sample from the user. Also, possible interference problems could be present in real samples, and this sensor has no specificity in contrast with the second proposed method which has the advantage of high specificity due to enzyme xanthine oxidase.

From the experimental study of the enzyme, it was found that xanthine oxidase has a significant intrinsic fluorescence intensity in aqueous solution, depending on its concentration, as can be observed in Figures 5.9 and 5.10. The reason for these intrinsic fluorescence properties is the presence of FAD as coenzyme in its molecule, as described in Section 3.3.2 for glucose oxidase. One important conclusion was that the optimum concentration of the enzyme, which was used for the purpose of kinetic measurements, did not interfere with the fluorescence intensity from the specific concentrations of both indicators. Figures 5.11 and 5.12 illustrate that the fluorescence that occurred at 518 nm with excitation wavelengths of 370 nm and 440 nm appeared to provide similarly significant values, with linearity in the range of 0.05 - 0.4 U/ml.

From the experimental investigation using the second method based on the indirect determination of xanthine through the simultaneous detection of pH changes and oxygen consumption, during its oxidation, it seems that in principle the system provides detection capabilities and can be used for practical applications. It was found that the uric acid which appears as a product of the oxidation, was not fluorescent and thus its presence did not affect the resulting signal. The study of the kinetics of the reaction, provided a Michaelis constant which was close to the values reported in the literature for both modes (Kresse, 1990). It is worth mentioning, that this constant is very small and this implies that the reaction was completed very rapidly, as was observed during the spectroscopic measurements of fluorescence against time.

This approach can be used to detect small amounts of xanthine in the range of 1-100 μM. When the concentration exceeded 0.5 mM the rate of change of fluorescence intensity against time remained almost constant as a consequence of saturation of the reaction. As far as the two different Experimental Modes A and B are concerned, it was found that both modes could be used for the measurement of xanthine and would offer similar characteristics in a fluorescence-based optical biosensor for xanthine.

CHAPTER 6

FLUORESCENCE-BASED OPTICAL BIOSENSORS FOR MONITORING PHENOL IN ENVIRONMENTAL SAMPLES

6.1 INTRODUCTION

The impacts of industrialisation and its associated environmental pollution have expanded to virtually all communities and nations; consequently, environmental protection is receiving global attention. Each national and international protection issue ultimately necessitates environmental monitoring. The scope of the monitoring efforts ranges from quick response, single parameter, localised measurement tasks to planned, multiparameter, long-term programmes of regional, national, or international scale. Assessing the nature and quantity of chemicals in the environment is often central to the mandated monitoring programmes, and many of the techniques and instruments used in these assessments have been developed in response to specific regulatory requirements. The application of fibre optic chemical sensors to environmental monitoring is a significant example of technology driven by regulation. The ideal monitoring system would provide *in situ* determination of the levels of potential contaminants at low concentrations (e.g. phenols). Instrumentation would be inexpensive to install and maintain, would be capable of automatic operation with small size, and would give reliable results when used by operators who have only modest technical training.

In the present study, a fluorescence-based optical phenol biosensor using polyphenol oxidase is described. Polyphenol oxidase catalyses the oxidation of phenols to catechols and then to quinones, and therefore, phenol concentrations can be measured by monitoring oxygen consumption during the above oxidation utilising an oxygen-sensitive fluorescent indicator, the well-known, tris(2,2'-bipyridyl)ruthenium(II) chloride hexahydrate. The oxidation of phenol belongs to the few exceptional oxidations where there is no production of hydrogen peroxide during the reaction. In addition, the

production of quinones does not significantly affect pH, in contrast with the previously studied oxidations of glucose, lactate and xanthine where the production of an acid occurred. For the above reasons, it is not possible to use the same experimental Modes as in previous chapters (Chapters 3, 4, and 5) for the detection of phenol. Hence, it was proposed to use only the oxygen-sensitive indicator, tris(2,2'-bipyridyl)ruthenium(II) chloride hexahydrate, and not the pH-sensitive indicator, HPTS.

Initial experiments were carried out in solution where measurements of the kinetics of the polyphenol oxidase reaction were carried out in the presence of tris(2,2'-bipyridyl) ruthenium(II) chloride hexahydrate. They were followed by additional experiments with polyphenol oxidase and the oxygen-sensitive indicator tris(2,2'-bipyridyl) ruthenium(II) chloride hexahydrate immobilised using the sol-gel encapsulation method.

6.1.2 Phenols in the Aquatic Environment - Health Effects

Phenols from a variety of sources may be found in the aquatic environment. Some of them have a natural origin, others are related to agricultural and industrial processes. Phenolic compounds abound in nature and make up the backbone of lignin, one of the main components of wood. Lignins are often responsible for imparting the brown coloration in waters of lakes, dams and puddles in forested areas. Natural leaching of wood products by either the action of rain or the continuous action of water courses release lignins into the aqueous environment which are then available to be further broken down to a range of phenolic compounds (Symons, 1990). Agricultural sources of phenols mainly arise from the breakdown of pesticides and herbicides containing the phenolic skeleton. Phenol is one of the most important and widely used chemicals,

being used in the manufacture of products such as coke production, paper and pulp processing, oil refineries, coal gas liquefaction, polyurethanes, phenolformaldehyde resins, disinfectants, pesticides, drugs, photographic developers, plasticisers, surfactants, explosives, antioxidants, dyes etc. (Tesarova & Pacakova, 1983; Arana *et al.*, 1994).

The inadequate disposal or misuse of the above compounds brings them into the aquatic environment in concentrations of up to more than 20 g/L (Arana *et al.*, 1994). Phenols can be toxic even in low concentrations (above 2 mg/L), with their toxicity increasing as their acid strength increases. They have a relatively high oxygen demand (about 2 mg O_2/mg phenol) (Lanouette, 1977). They cause bad taste in chlorinated water, even at low concentrations, because of the formation of chlorinated phenols, some of which are suspected to be carcinogenic (Fawell & Hunt, 1988). Because of their toxic effect upon aquatic organisms, phenolic substances also have a unique ability to impact on the taste and odour of food (e.g. fish). Studies have shown the existence of phenols as pollutants of air, water and soil (Shah & Singh, 1988; Drugon & Muraveva, 1991; Ciccoli *et al.*, 1992). Often soil and surface waters of areas around former production and processing plants are contaminated by phenolic compounds with risk to ground water sources. For all these reasons, the separation and/or elimination of these compounds from waste streams is necessary. Therefore, screening, monitoring and control of these pollutants are of great importance.

6.1.3 Methods for Phenol Monitoring

At present the most commonly used laboratory analytical methods for phenols analysis are based on gas chromatographic techniques. Gas chromatography (GC) with electron-

capture detector (ECD) and flame ionization detector (FID), high-performance liquid chromatography (HPLC), and gas chromatography - mass spectrometry (GC/MS) have been traditionally used to determine phenolic compounds (Tesarova and Pacakova, 1983; Lee *et al*, 1987b). Also, spectrophotometric detection of phenols has been accomplished by a variety of means. Ultraviolet-visible absorption detectors are the most widely used detectors in liquid chromatography (Realini, 1981; Ogan & Katz, 1981). Additionally, analysis of phenols in water by fluorometry has been published (Uchiyama & Yamaguchi, 1977; John *et al*., 1982; Naley, 1983). Since phenol is acidic it can be determined by acid-base titration with electrochemical indication of the stoichiometric end point. Several researchers have reported direct amperometric electrochemical detection of phenols in aqueous environmental samples consisting basically of wastewater at bare carbon-based and other solid electrodes (Shoup and Mayer, 1982; Ortiz *et al*, 1993).

All the methods mentioned above are in current use. They are all non-specific, i.e. they can be used for the measurement of different substances. This lack of selectivity necessitates a great deal of sophistication and quite expensive instrumentation, and thus elevates the size and fragility of the equipment required. These instruments have been evolved from laboratory analytical devices. They still retain their need for highly specialised conditions which are maintained within the casing of the instrument. All the developments of the instruments have been centred around the preservation of this environment from external changes. The cost of these instruments is also a prohibitive factor in their widespread use.

As was mentioned previously, biosensors offer a number of important advantages over conventional analytical techniques including: specificity, low cost, and portability. Their biological base also makes them exquisitely sensitive to toxins and ideal for health and safety applications, and also for pollution monitoring. Tyrosinase-based enzyme electrodes for biosensors monitoring various phenols have been reported. They are based on the immobilisation of the enzyme, or an appropriate plant tissue, onto graphite surfaces (Hall *et al.*, 1988; Ortega *et al.*, 1992) or within carbon paste matrices (Wang & Lin, 1988; Bonakdar *et al.*, 1989; Wang *et al.*, 1992).

In 1993, a solid-state fibre-optic luminescent oxygen sensor for flow-through measurements of phenols was described (Papkovsky *et al.*, 1993a). It was consisted of a flow path, sample injector, micro-column with the immobilised enzyme, oxygen membrane and fibre-optic connector joined together to form an integral unit. Laccase enzyme was used as a recognition system which provided specific oxidation of the substrate with the dissolved oxygen being monitored. The sensor was applied to the determination of polyphenol content in tea, brandy, beer, etc. (quality control), and to monitor important phenolic compounds in industrial wastewater.

Wang and colleagues have demonstrated a sensitive biosensor for phenolic compounds, based on the incorporation of the enzyme tyrosinase within ruthenium-dispersed carbon paste matrices (Wang *et al.*, 1994). Later, a methylphenazonium-zeolite-modified enzyme sensor based on a planar, screen-printed, two-electrode arrangement was described for the subnanomolar detection of phenols (Kotte *et al.*, 1995). The detection limit of phenols was 0.25 nM. The development of a microbiosensor, which used

polyphenol oxidase incorporated in a water-retaining gel with a microelectrode functioning as transducer, for measuring phenol directly in the vapour phase has been reported (Dennison *et al.*, 1995). Parts per billion phenol vapour could be detected with this method.

6.1.4 Plant Tyrosinase (Polyphenol Oxidase)

Enzymes which use molecular oxygen to oxidise phenols and polyphenols have been prepared from various sources. Certain of these enzymes contain copper as an integral part of their structure, and one type of copper oxidase which has received a great deal of study is that referred to as tyrosinase, polyphenol oxidase and "phenolase complex" (Sizer, 1948; Duckworth & Coleman, 1970). Tyrosinase (monophenol monooxygenase; polyphenol oxidase; catechol oxidase; monophenol dihydroxyphenylalanine: oxygen oxidoreductase; EC 1.14.18.1) is of central importance in vertebrate pigmentation (Rodriguez-Lopez *et al.*, 1994). It is directly responsible for the conversion of the amino acid, tyrosine (which was the first experimental substrate), to one of several types of melanin pigments. Also, the darkening of mushrooms, apples, potatoes and many others plants and plant products on injury to the tissue is the result of the enzymatic oxidation of certain monohydric and *o*-dihydric phenols by tyrosinase (Gauillard *et al.*, 1993).

Tyrosinase has the unique property of catalysing two ostensibly different types of enzymatic oxidations; namely, the *ortho*-hydroxylation of phenols to give catechols, and the dehydrogenation of catechols to *o*-quinone stage. These latter products are unstable in aqueous solution, and break down over a period of minutes to hours by a combination of nucleophilic reactions and further oxygen-mediated oxidations, not all of which are

understood (Estrada *et al.*, 1991). In addition, these types of activity have generally been referred to as the cresolase and catecholase activity, since the substrates most commonly employed were *p*-cresol and catechol. Catechol oxidase, also referred to as polyphenol oxidase, contains little or no cresolase activity depending of the preparation of tyrosinase (Gauillard *et al.*, 1993).

In the oxidation of pyrocatechol and dopa by catechol oxidase a relatively constant activity between pH 5.5 and 8.0 and a decrease in rate at lower pH values has been observed (Duchworth & Coleman, 1970). Assays at higher pH were unreliable because of instability of both substrates and the quinone products. Benzoic acid and cyanide are inhibitors of the activity of tyrosinase. Benzoic acid is competitive with catechol and non-competitive with oxygen. Cyanide is non-competitive with catechol and competitive with oxygen. Literature values for the Michaelis constant (K_m) of mushroom tyrosinase with phenol lie around 1.70 ± 0.15 mM using 3-methyl-2-benzothiazolinone hydrazone (MBTH) adduct formation and around 11.65 ± 3.40 mM using benzoquinone formation. Reported K_m with catechol are around 0.80 ± 0.08 mM using MBTH adduct formation and around 0.76 ± 0.12 mM using benzoquinone formation (Rodriguez-Lopez *et al.*, 1994; Estrada *et al.*, 1991).

The purified enzyme is commonly prepared from the edible mushroom, *Psalliota campestris*, which exhibits both types of activity, cresolase and catecholase, and the ratios depending on the source and the method of fractionation (Smith & Krueger, 1962); also some other sources are from potato tubers, *Neurospora crassa*, broad bean and mammalian melanoma tumors. Activity can be measured by oxygen consumption

either with the Warburg technique or with an oxygen electrode, by spectrophotometric estimation of the product formation, by the coupled oxidation of an added reducing agent in "chronometric assays", or by the use of a complexing agent in "chronometric assays". Recently, two methods for following phenol consumption have been proposed: differential spectrophotometry with chlorogenic acid as substrate and electrochemical determination using HPLC (Gauillard *et al.*, 1993). The lowest molecular weight of mushroom tyrosinase observed corresponds to about $32x10^3$ Da and the highest to about $118x10^3$ Da (Duckworth & Coleman, 1970).

6.2 MATERIALS & METHODS

6.2.1 Chemicals

Mushroom polyphenol oxidase (EC 1.14.18.1) with an activity of 6300 units/mg and hydrochloric acid 0.5N were supplied by Sigma Chemical Co. (Poole, Dorset). One unit of polyphenol oxidase caused an increase in absorbance of 0.001 per minute at pH 6.5 at 25 ^{0}C in a 3 ml reaction mix containing L-tyrosine. Tris(2,2'-bipyridyl) ruthenium(II) chloride hexahydrate and phenol were purchased from Fluka Chemie AG (CH-9470 Buchs-Switzerland); tetramethoxysilane (TMOS) from Aldrich (Poole, UK). All other chemical reagents were of analytical reagent quality and used as obtained from BDH Ltd. (Poole, Dorset). The standard buffer solution was 10 mM sodium phosphate buffer, pH 6.5 at 21^{0}C, containing 10 mM $Na_2HPO_4 \cdot 12H_2O$ and 10mM $NaH_2PO_4 \cdot 2H_2O$. All kinetic experiments were performed at room temperature (21 ± 2 ^{0}C), using 7μM tris(2,2'-bipyridyl)ruthenium(II) chloride hexahydrate.

6.2.2 Immobilisation Procedure

Enzyme "gel". The silica sol was prepared by sonication of tetramethoxysilane (TMOS, 15.22 g), deionized water (3.38 g) and 0.04N aqueous hydrochloric acid (0.22 g) in an ice-cooled ultrasonic bath for approximately 20 min. The sol was then buffered to create more favourable pH conditions for the enzyme polyphenol oxidase at 10 mM sodium phosphate buffer pH 6.5. Enzyme stock solution was prepared by dissolving 0.86 mg of polyphenol oxidase in 3 ml buffer pH 6.5, and the indicator stock solution was prepared by mixing 43 μM of 10 mM tris(2,2'-bipyridyl)ruthenium(II) chloride hexahydrate with 8.28 ml of 10 mM sodium phosphate buffer pH 7.0. For these samples, 4.05 ml of TMOS sol was mixed with 4.95 ml of buffer pH 6.5 and then 3 ml of the enzyme mixture and 8.32 ml of the indicator solution were added to this solution. All of the additions were carried out on ice. The doped sol was quickly transferred to polystyrene cuvettes (1 ml sol-gel was spreaded in one face-side of each cuvette, homogeneously), and sealed with parafilm. All samples were stored at 4 ^{0}C for ageing and drying (Dave *et al*, 1994).

6.2.3 Instrumentation

The instrumentation used was as described in Chapter 3 (see Section 3.2.2).

6.3 RESULTS

Polyphenol oxidase was dissolved in phosphate buffer pH 6.5 and its spectroscopic characteristics were investigated. The absorption spectrum of 500 U/ml polyphenol oxidase gave a maximum peak in ultraviolet range at 281 nm, and a secondary peak at 263 nm. Also, it was found that the enzyme did not have any excitation or fluorescence spectra in the visible range. Therefore, no interference from the enzyme was expected

with the fluorescence spectra of the indicator tris(2,2'-bipyridyl)ruthenium(II) chloride hexahydrate. Similar experiments were carried out for phenol, the substrate in polyphenol oxidase reaction, in order to establish its spectroscopic properties. Phenol did not show any excitation or fluorescence spectra in the visible range, and once again no interference was expected in the response of the indicator due to the phenol substrate.

Kinetic experiments were devised to determine how different concentrations of phenol affected the quenching of tris(2,2'-bipyridyl)ruthenium(II) chloride hexahydrate, when phenol was added to a quartz cuvette (3ml volume) containing a mixed solution of: 7μM tris(2,2'-bipyridyl)ruthenium(II) chloride hexahydrate, and 150 U/ml polyphenol oxidase in 10mM sodium phosphate buffer pH 6.5. The reaction was initiated by addition of phenol. A small magnetic stirrer bar was placed in the bottom of the cuvette and rotated at a constant speed in order to keep the solution homogeneous during the reaction. All additions of stock solutions (in the range of μl) were carried out outside of the instrument except the phenol, which was added when the cuvette was placed in the instrument and the software was ready to run, in order to monitor the reaction from the start.

The rate of change of the fluorescence intensity of tris(2,2'-bipyridyl)ruthenium(II) chloride hexahydrate against phenol concentration, due to oxygen consumption during the oxidation of phenol, is displayed in Figure 6.1. This calibration curve follows the Michaelis-Menten equation (see below). The manipulation of the raw data in order to obtain values of rate of change of fluorescence intensity with time (dI/dt) (instead of the actual values of fluorescence intensity) was identical to the one used in the case of glucose (Chapter 3) and is described in Appendix A.

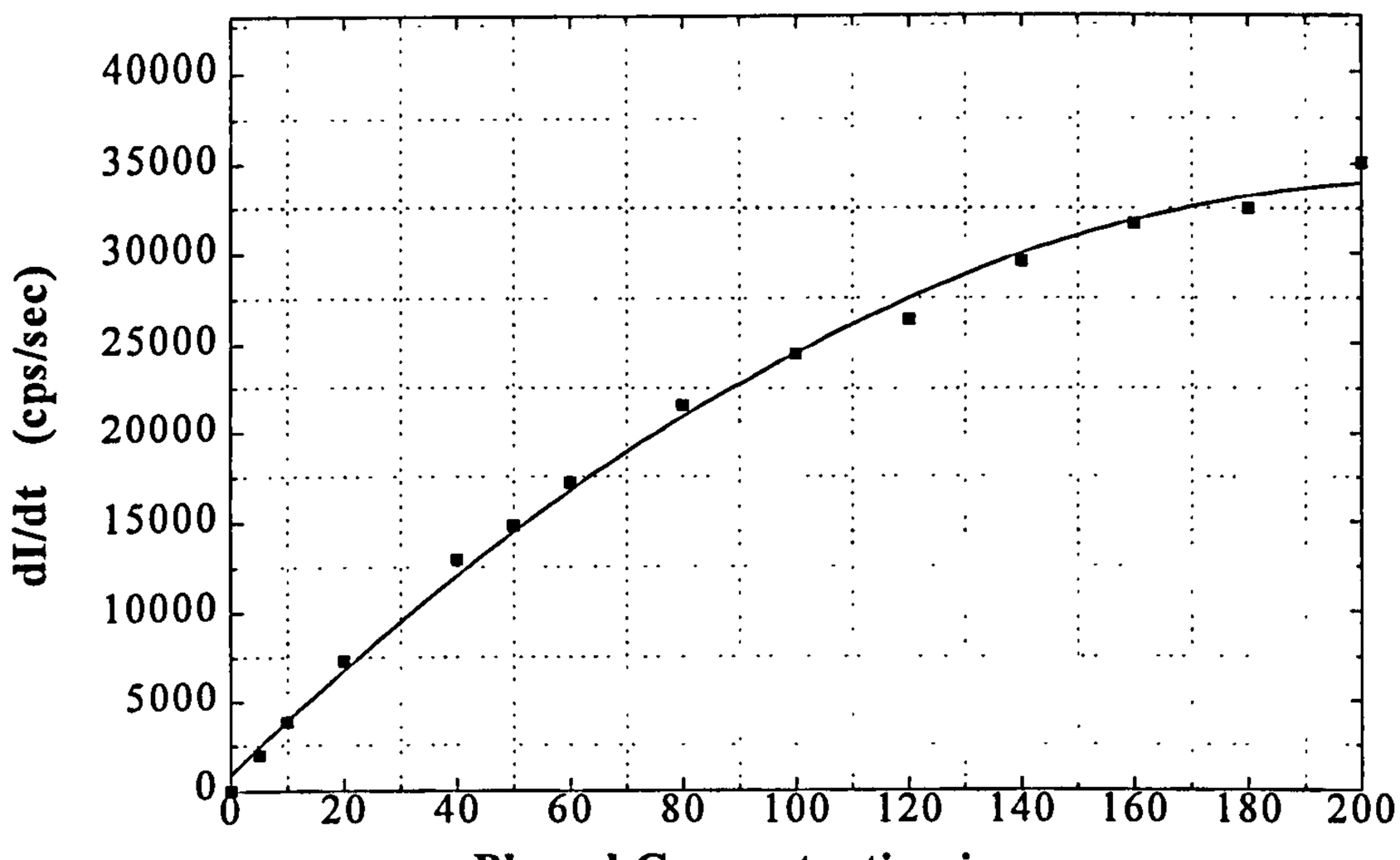

FIGURE 6.1 Rate of change of fluorescence intensity versus phenol concentration of tris(2,2'-bipyridyl)ruthenium(II) chloride hexahydrate, at fixed excitation wavelength of 452 nm and emission at 597 nm, during the catalytic oxidation of phenol.

In this approach the lowest detectable phenol concentration was 1 ppb. Saturation occurred above 220 ppm phenol. The response time of the indicator after the addition of phenol took around 2 to 5 minutes to reach a state where the changes in fluorescence intensity with time were negligible. About 90% of the final intensity value was achieved in approximately 90 to 170 seconds. Lower phenol concentrations required longer response times, and vice versa for higher phenol concentrations.

The kinetic parameters of 150 U/ml polyphenol oxidase in the presence of tris(2,2'-bipyridyl) ruthenium(II) chloride hexahydrate and phenol, were determined using a Hanes plot. The Hanes plot corresponding to Figures 6.1 is illustrated in Figure 6.2. From this plot and according to equation (3.e), the experimental value of the Michaelis constant, K_m, of the reaction was found to be equal to 148.16 ppm (≈ 1.57 mM).

The calibration curve of the biosensor, in terms of the rate of change of the fluorescence intensity of tris(2,2'-bipyridyl)ruthenium(II) chloride hexahydrate against phenol concentration, when the enzyme was immobilised in sol-gel matrix is presented in Figure 6.3. In addition, the stability and repeatability of the biosensor have been investigated. In terms of stability it was found that the biosensor response remained approximately constant over a period of 4 months, when it was stored in temperature of 4 ^{0}C. Subsequent experiments were carried out in order to investigate the reproducibility and reliability of the sol-gel immobilisation method on the proposed optical phenol biosensor. Three phenol concentrations were chosen: 10 ppm, 50 ppm and 100 ppm, and measurements were repeated 7 times for each concentration.

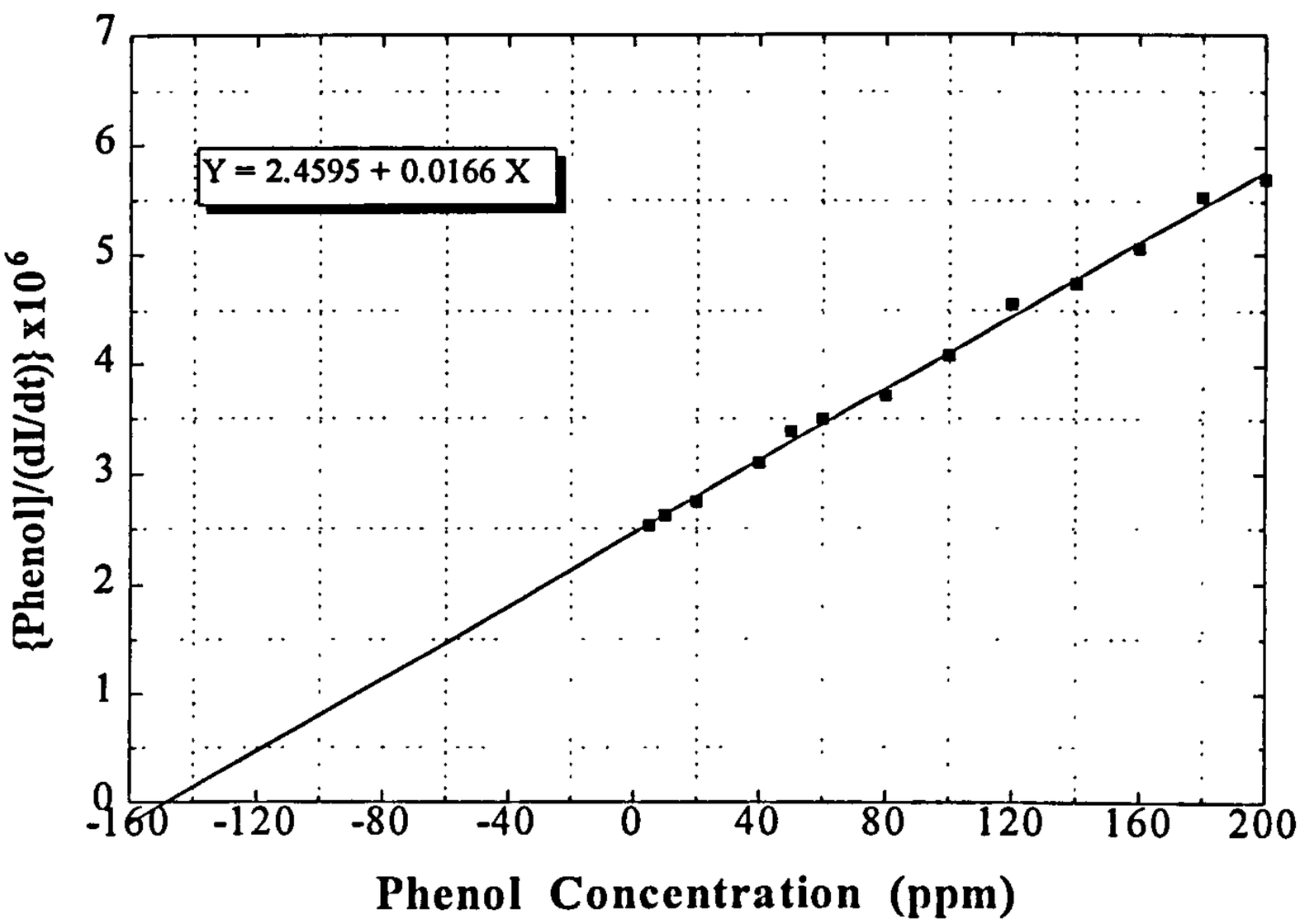

FIGURE 6.2 Hanes plot corresponding to Figure 6.1.

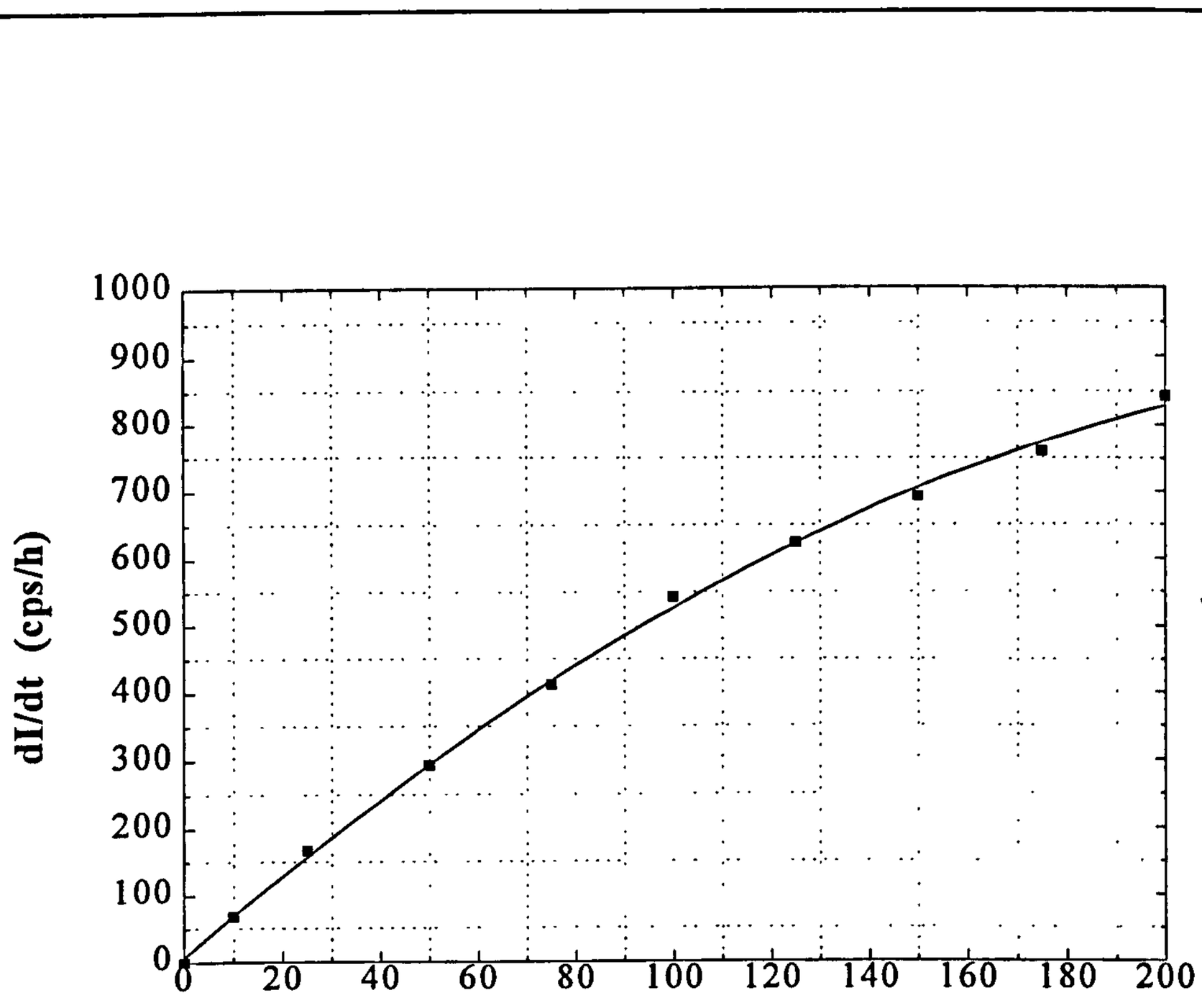

FIGURE 6.3 Rate of change of fluorescence intensity versus phenol concentration of tris(2,2'-bipyridyl)ruthenium(II) chloride hexahydrate at excitation wavelength of 452 nm and fluorescence monitored at 597 nm, during the catalytic oxidation of phenol using sol-gel immobilisation.

The mean values of the rate of change of the fluorescence intensity of tris(2,2'-bipyridyl)ruthenium(II) chloride hexahydrate, during the oxidation of phenol, for each phenol concentration and the corresponding standard deviations are presented in Table 6.1.

TABLE 6.1

Phenol Concentration	Mean Value	Standard Deviation	R
10 ppm	68	1.8	7
50 ppm	292	8	7
100 ppm	542	13	7

The reproducibility of the biosensor for seven different samples under the same conditions for 10 ppm phenol concentration was approximately 2.6% deviation from the mean value. This was repeated for 50 ppm and 100 ppm phenol concentrations and the standard deviations were around 2.7% and 2.4%, respectively.

Regarding the response of the indicator immobilised with polyphenol oxidase in sol-gel matrix, it took around 20 to 25 minutes to reach a state where the fluorescence intensity of the indicator obtained an almost constant value after the addition of phenol. About 90% of this constant value was achieved in approximately 10 to 15 minutes.

The selectivity of the proposed biosensor was studied, applying 11 phenolic substrates, namely phenol, L-DOPA, catechol, , *o*-cresol, *m*-cresol, *p*-cresol, *m*-hydroxybenzoic acid, *p*-hydroxybenzoic acid, L-tyrosine, *m*-chlorophenol and *p*-chlorophenol. The biosensor

responded markedly to five phenolic substrates, including phenol, L-DOPA, pyrocatechol, L-tyrosine, *p*-cresol. Compared with phenol (100%) the highest sensitivities were observed for L-DOPA (215%), pyrocatechol (185%) and *p*-cresol (150%), as apparent from their calibration plots. Generally, the proposed biosensor was insensitive to *ortho*- and *meta*-substituted phenolic compounds.

6.4 DISCUSSION

The spectroscopic investigation of polyphenol oxidase (EC 1.14.18.1) showed that the enzyme had no detectable fluorescence properties and the absorption spectrum gave a maximum peak in ultraviolet range at 281 nm, and a smaller peak at 263 nm; which are in agreement with published data by Duckworth and Coleman (1970) in their report about the physicochemical and kinetic properties of muchroom tyrosinase.

In the present study, the analytical range of the proposed optical biosensor was approximately up to 220 ppm of phenol concentration, and saturation was observed above this concentration. The lowest detectable amount of phenol concentration was 1 ppb. In 1989, a bioamperometric sensor for phenol based on carbon paste electrodes was presented with a dynamic range of up to 2.5 ppm and with a detection limit of 14 ppb (w/v) (Bonakdar *et al.*, 1989). Wang *et al.* (1994) reported a tyrosinase-based ruthenium dispersed carbon paste biosensor for phenols with analytical range of 0.1 to 0.6 mM phenol (9.4 to 56.5 ppm), and detection limit of 0.8 μM (approximately equal to 7.5 ppb). Kotte *et al.* (1995) published for the detection of phenols a methylphenazonium-modified enzyme sensor based on polymer thick films with a detection limit of 0.25 nM phenol (approximately equal to 0.023 ppb) and a linear response range between 0.05 to 14 μM

(4.7 ppb to 1.32 ppm). Later, Dennison *et al* (1995) described a gas-phase microbiosensor for monitoring phenol vapour with a detection limit of 30 ppb. Based on the above discussion, it appears that the proposed optical biosensor presents more favourable characteristics in comparison with the reviewed phenol sensors, in terms of analytical concentration range and detection limit.

The repeatability and stability of the proposed optical biosensor were investigated in seven different samples under the same conditions and with the same phenol concentration, 2.6% deviation from the mean value was observed. This was repeated for 3 different phenol concentrations. In terms of stability it was found that the biosensor response remained approximately constant over a period of 4 months at temperature of 4 ^{0}C. Papkovsky *et al.* (1993a) described a flow-cell fibre-optic enzyme sensor for phenols and reported 5% reproducibility of this system using hydroquinone as substrate. Another biosensor based on the incorporation of the enzyme tyrosinase within metal-dispersed carbon paste matrices gave a relative standard deviation of 2.4% for phenol detection (Wang *et al.*, 1994). Navaratne *et al.* (1990) reported an eggplant-based bioamperometric catechol sensor with a lifetime of at least 3 weeks at temperature of 4 ^{0}C. On the other hand, Kotte *et al.* (1995) presented a storage stability of more than 100 days at 5 ^{0}C and dry at -18 ^{0}C for a methylphenazonium-modified phenol sensor.

The experimental value of the Michaelis constant from the kinetic solution experiments was 148 ppm (≈1.57 mM), which is close to published data in the literature. According to Rodriguez-Lopez *et al.* (1994) the Michaelis constant for the oxidation of phenol by mushroom tyrosinase is approximately 1.70 ± 0.15 mM using the method MBTH adduct

formation. In addition, in the present study using the sol-gel method, the apparent Michaelis constant K_m app was found to be around 2-fold higher (≈ 288 ppm) than that of the enzyme in solution. These results are similar to the published results by Yamanaka *et al.* (1992) using another enzyme, glucose oxidase, where the apparent Michaelis constant $K_{m,app}$ with β-D-glucose using sol-gel immobilisation was found to be approximately 2-fold higher than the corresponding $K_{m,app}$ in solution.

6.5 CONCLUSIONS

The spectroscopic analysis of polyphenol oxidase showed that both the enzyme, and the substrate, phenol, did not present fluorescence properties in the visible range. This is an advantage for the proposed biosensor since no interference with the indicator tris(2,2'-bipyridyl)ruthenium(II) chloride hexahydrate from the enzyme and the substrate during the oxidation of phenol would be expected. The pH-sensitive indicator HPTS was not utilised as in the previous chapters because there was no significant pH change during the oxidation of phenol.

From the experimental work described in this chapter, it can be concluded that the sol-gel immobilisation technique presents certain advantages for the construction of the proposed optical biosensor including easy preparation, enhanced stability features and utility for optical methods because of its transparency and porosity. The above characteristics of the sol-gel technique will be discussed in more detail in the following chapter.

The advantages of the proposed phenol optical biosensor in comparison to conventional chromatographic techniques are the low cost of its construction, the quick time and simplicity to obtain results and also the possibility of taking measurements near to the source (FID-GC chromatographic techniques require complicated and time consuming procedures with the use of expensive instrumentation and highly trained personnel). The major disadvantage of the biosensor is the absence of high specificity and selectivity which does not allow the classification of a detected phenolic compound. Therefore, the present biosensor could be used only for measuring very low levels of phenols (ppb) in aquatic environmental samples and not to determine exactly the particular type of phenol.

The design of the proposed biosensor will be based on an optoelectronic circuit which would offer potential application in the field of health and safety monitoring. Its ease of use, low cost, small size, and portability are attractive properties for a device which could monitor phenol pollution near to its source in real-time, and could provide personnel with accurate data. The design of the biosensor should be based on a optoelectronic circuit with a light emitting diode (LED) at 456 nm as source, and p-n diode as photodetector and a single mode fibre optic as the connecting cable between the source the photodetector and the measuring probe, which should be placed the environmental sample. The result could be shown on a digital display in ppb or ppm units, and the power supply could be a lithium battery.

CHAPTER 7

FLUORESCENCE-BASED OPTICAL BIOSENSORS FOR BLOOD-GLUCOSE MONITORING: IMMOBILISED CONFIGURATIONS AND SOLUTION STUDIES OF HUMAN SERUM

7.1 INTRODUCTION

This chapter presents the application and characterisation of immobilisation techniques for the fluorescence-based optical blood-glucose biosenor which was described in Chapter 3 (solution studies). It was based on the biocatalytic oxidation of glucose using the two fluorescent indicators, HPTS and tris(2,2'-bipyridyl)ruthenium(II) chloride hexahydrate simultaneously, relating their changes in fluorescence to glucose concentration.

Four different immobilisation procedures (covalent, adsorption, aggregation and sol-gel encapsulation) were employed for the enzyme glucose oxidase. In the first three procedures only glucose oxidase was immobilised, but in the last the enzyme was immobilised with both indicators. All the three Experimental Modes, which were extensively studied in Chapter 3, were applied in order to establish calibration curves with the optimum performance for the proposed biosensor. The above approaches could be used for the construction of an optical biosensor for the measurement of blood-glucose to meet urgent requirements in medicine. In addition, the advantages of the microcapsulation sol-gel method in place of conventional immobilisation techniques for application in an optical biosensor was investigated.

Finally, additional solution studies were conducted in order to evaluate the implementation and performance of Experimental Mode A when used for the detection and measurement of glucose concentration in biological samples such as human serum, instead of the buffer solution as extensively discussed in Chapter 3 (Section 3.3.2).

7.1.1 Glucose Biosensors Based on a Sol-Gel-Derived Matrix

The encapsulation of enzymes, other proteins and organic molecules in sol-gel glass matrices has been actively studied and evaluated for use in various applications including chemical biosensors, biocatalysts, and new optical materials (Dave *et al.*, 1994; Browne *et al.*, 1996; Dunn & Zink, 1991). Sol-gel encapsulation is a method that involves the trapping of enzymes or other molecules within a gel as its polymerises, resulting in a uniform distribution of the trapped molecules throughout the bulk inorganic glass matrix (see Chapter 1, Section 1.2.5). The sol-gel glass-encapsulation process does not require heating, and the resulting glass matrix is transparent and porous. The encapsulated species are accessible to low molecular weight reagents, and their interactions may frequently be monitored by spectroscopic means. Therefore, sol-gel glasses are almost ideal host matrices for optical chemical biosensors.

There are several literature reports on the immobilisation of enzymes, and glucose oxidase in particular, within a sol-gel-derived matrix. Yamanaka *et al.* (1992) demonstrated the feasibility of glucose oxidase-doped sol-gel processed materials for glucose sensing. In this work, the activity of the encapsulated enzyme glucose oxidase was investigated by use of a photometric detection scheme. Activity information on the immobilised glucose oxidase was provided by grinding glucose oxidase-doped sol-gel monoliths (10x5x2 mm) into a fine powder. In order to quantify glucose oxidase activity, the ground sol-gel material was incubated with reagent solution and glucose added. The apparent turnover number (k_{cat} = 250 ± 80) was similar to the value for native glucose oxidase in solution. However, the recovered dissociation constant ($K_m \geq$ 0.05 ± 0.05 M) was two-fold greater than native glucose oxidase in solution (0.026 M),

suggesting that glucose binding to the sol-gel-encapsulated glucose oxidase was weaker. The authors showed that the response was strongly dependent on the storage conditions and was 5-10-fold slower compared to native glucose oxidase solution.

Tatsu *et al.* (1992) reported the preparation and properties of glucose oxidase-entrapped silica gel and its application to glucose sensor in human serum using a flow injection analysis scheme. Saturation of the signal response was observed over 400 mg/dl, and the glucose oxidase activity was shown to vary over time, depending on the actual storage temperature. The activity of the entrapped glucose oxidase was found to be approximately 20-fold greater when stored at -20 ^{0}C compared to room temperature. The sol-gel-encapsulated glucose oxidase was reported to remain active for at least 2 months when stored desiccated at 4 ^{0}C.

Glezer and Lev (1993) prepared platinum electrodes coated with sol-gel-derived films of V_2O_5 doped with glucose oxidase. Cyclic voltammetry was used as the detection mode for glucose. Saturation of signal was observed beyond 10 mM β-D-glucose. The vanadium pentaoxide biosensor was reported to remain stable without any loss of activity during 10 days of storage at 4 ^{0}C. Also, Audebert *et al.* (1993) used cyclic voltammetry to study the activity of glucose oxidase doped within a TMOS-derived sol-gel matrix. In this scheme the sol-gel was doped with glucose oxidase and a mediator, (hydroxymethyl)ferrocene. This mixture was then coated onto the distal end of a glassy carbon electrode. Enzyme activity was 70-80% in the polymeric silica sol compared to the activity in solution.

The characterisation of thin sol-gel films derived from TEOS that were doped with glucose oxidase as a prototype for sol-gel-based biosensor development was reported (Narang *et al.*, 1994). Immobilisation of glucose oxidase was carried out in three ways: physisorption of glucose oxidase onto the precast sol-gel film; microencapsulation within the sol-gel film matrix; and, a sol-gel: glucose oxidase: sol-gel sandwich configuration. Sensor performance was compared for each immobilisation scheme, and the sandwich configuration showed the better results due to high loading of the enzyme and a relatively fast response time. Photometric (absorbancy) and amperometric detection modes were used to study the glucose oxidase and quantify β-D-glucose. The authors claimed that the preparations of the sandwich configuration were between 2- and 6-fold more active than previous sol-gel glucose oxidase preparations, and the stability of the glucose-glucose oxidase complex was at least 3-fold greater than other sol-gel entrapment schemes. Detection limits were in the order of 0.2 mM, and working curves were linear from 5 to 35 mM. Precision was in the order of 5%, and the sensors were stable for at least 2 months under dry ambient conditions.

7.2 MATERIALS & METHODS

7.2.1 Chemicals

Peroxidase (hydrogen-peroxide oxidoreductase, EC 1.11.1.7, 200 units/mg, type II, from Horseradish), glutaraldehyde (grade I: 25% aqueous solution), L(+)lactic acid (98%), bovine serum albumin (BSA, 98-99% albumin, fraction V powder), acrylamide (40% solution), N,N'-methylene-bis-acrylamide (2% solution), sodium persulfate, agarose (type VI-A), N,N,N',N'-tetramethylethylenediamine (TMEDA or TEDEM, 99%), human serum (frozen liquid) and Sigma Diagnostic glucose (HK) kit (enzymatic, hexokinase, procedure

N_o 16-UV) were all obtained from Sigma Chemical Co. (Poole, Dorset). Also, glucose oxidase (β-D-Glucose, oxygen 1-oxidoreductase; EC 1.1.3.4) (176 units/mg type VII, from *Aspergillus niger*) and β-D(+)Glucose (97+%, containing up to 3% α-anomer) were purchased from Sigma Chemicals.

Tetramethoxysilane (TMOS) and cellulose acetate (CA, with 39.8% acetyl content) were purchased from Aldrich Chemicals Ltd. (Gillingham, Dorset). Pure *p*-benzoquinone (PBQ) was obtained from Merck Ltd. (Poole, Dorset). Collagen (30% w/v solids) (type IV, from human placenta) was purchased from Fluka Chemie AG (CH-9470 Buchs-Switzerland). The purchase of the indicators, HPTS and tris(2,2'-bipyridyl)ruthenium(II) chloride hexahydrate, was mentioned in Chapter 2. All other chemical reagents were of analytical reagent quality and used as obtained from BDH Ltd. (Poole, Dorset).

All experiments were performed at room temperature (22±2 ^{0}C) and buffers were prepared with doubly-distilled, deionized water. The standard buffer solution was 0.1 mM sodium phosphate buffer containing 0.1 M NaCl, pH at 7.4. Stock solutions of indicators were prepared by bubbling 1 mM phosphate buffer with pure oxygen for at least 15 min. All components of the assay mixtures were freshly prepared except for stock solutions of glucose for kinetic measurements of immobilisation configurations, which were freshly prepared daily and stored in the refrigerator for 12 hours before use to allow equilibration of mutarotation between α-D-glucose and β-D-glucose.

7.2.2 Instrumentation

The instrumentation used was as described in Chapter 3 (see Section 3.2.2).

7.2.3 Immobilisation Techniques

Four different techniques were implemented for the immobilisation of glucose oxidase: covalent immobilisation to cellulose acetate, inclusion in a polyacrylamide-agarose gel, adsorption-noncovalent collagen membrane impregnation and encapsulation in transparent glass using sol-gel immobilisation. In the last technique, namely the sol-gel method, the two indicators, HPTS and tris(2,2'-bipyridyl)ruthenium(II) chloride hexahydrate, were immobilised in the same system.

METHOD 1. Covalent immobilisation of glucose oxidase to cellulose acetate membranes (Sternberg *et al.*, 1988; Wilson & Thevenot, 1990).

Step 1. Cellulose acetate membrane preparation. Cellulose acetate (1.8 g) was dissolved in 15.8 g acetone with stirring, and 2.8 ml of distilled water was added. After homogenisation, this solution was cast on a glass plate and evaporated for 60 sec at 22 ^{0}C to form a thin membrane (0.015 mm in the wet state and 0.010 mm in the dry state). The cellulose acetate membrane was removed from the glass plate by immersing the plate in distilled water. The membrane was cut into smaller pieces and stored in distilled water.

Step 2. Cellulose acetate membrane activation. Four cellulose acetate membranes (each 2.5 cm^2) were suspended for 20 min in 100 ml of 0.1 M sodium periodate at room temperature. Then the membranes were washed in distilled water for 5 min and were immersed in 10 ml of 10 mg/ml solution of BSA in 0.1 M borate buffer, pH 9 for 2 hours. Most of the BSA (9 ml) was removed and 4 mg of sodium cyanoborohydride was added and the membranes were incubated at room temperature for 2 hours. After a second washing of 5 min in distilled water, the membranes were stored in 0.1 M phosphate

buffered saline solution (PBS), pH 7.4, at room temperature until the GOD coupling reaction was performed.

Step 3. Glucose oxidase activation. Recrystallized *p*-benzoquinone from petroleum ether was used for the preparation of a solution of 15 mg/ml in ethanol. Then, 100 µl of the freshly prepared *p*-benzoquinone was added to 0.5 ml of 20 mg/ml solution of glucose oxidase in 0.1 M phosphate buffer, pH 7.4 in a tube covered with aluminium foil. After 30 min of incubation at 37^{0}C, the mixture was filtered through a G-25 Sephadex column (1x10 cm) coupled to a peristaltic pump (20 ml/h) and equilibrated with 0.15 M sodium chloride. The first fraction, a pink-brown band of 2-3 ml, was collected and used as the enzyme coupling solution.

Step 4. Coupling reaction. The BSA-cellulose acetate membranes were suspended in 2-3 ml of the activated glucose oxidase solution, whose pH was adjusted to 8.0-9.0 with 0.25 ml of 1 M sodium carbonate. After 38 hours of incubation at room temperature, the membranes were removed, washed in stirred 0.15 M potassium chloride solution for 24 hours and finally were stored in 0.1 M PBS, pH 7.4, containing 1.5 mM sodium azide. The azide was added in order to limit microbial contamination and catalyse activity.

METHOD 2. Inclusion in a gel of soluble aggregated glucose oxidase molecules (Broun, 1976).

Step 1. Aggregation in a solution. A 1 mg/ml (176 IU/ml) GOD solution in 20 mM phosphate buffer, pH 6, was mixed in a test tube with an equal volume of 2.5% glutaraldehyde solution in the same buffer. Aggregation proceeded at 4 ^{0}C for 10 hours.

The cross-linking process was then interrupted by the addition of ethanolamine up to a concentration of 0.1 M.

Step 2. Inclusion. In order to obtain 10 cm^2 of a 1.5 mm-thick gel, 0.1 ml of a solution of 60% acrylamide and 1.6% bisacrylamide were mixed with 5 ml of enzyme oligomer solution. The mixture was heated at 37 ^{0}C (solution A). A gel containing 9.6 mg agarose in 0.6 ml of water was boiled for 5 min, then cooled to 40 ^{0}C with constant stirring (solution B). To solution B was added 0.5 ml of N,N,N',N'-tetramethylethylenediamine solution, 0.36 mg of sodium persulfate, followed immediately by the bulk of the solution A. The entire mass was spread between two glass plates. The gel was allowed to polymerise 30 min at 4 ^{0}C, removed and then rinsed with distilled water until the rinse water no longer absorbed at 280 nm.

METHOD 3. Adsorption-noncovalent collagen membrane-impregnation immobilisation method.

(Vieth & Venkatasubramanian, 1976; Kierstan & Coughlan, 1991)

Step 1. Membrane-impregnation method. Hide collagen (60 mg; 30% solids) was dispersed in 4 ml of distilled water. The pH was adjusted to 3.0 by dropwise addition of lactic acid. The pulp was homogenised in a stirrer overnight, where the temperature was maintained below 25^{0}C. The dispersion was then degassed and a membrane was cast by pouring 0.5 ml of the dispersion onto one inside (horizontal) face of a glass cuvette (10 mm^3) and spreading it out uniformly with a glass rod.

After 3 hours, while the rest of the pulp was still stirred, and the horizontal side of the cuvette had been dried, the cuvette was turned to the next inside face and another 0.5 ml aliquot of the dispersion poured uniformly and left to dry at room temperature. The membrane was allowed to swell for 2 hours in 0.1 M phosphate buffer, pH 6 and this was repeated for another 2 hours in new phosphate buffer. Then, the cast membranes on the two faces of the cuvette were immersed fully in an enzyme impregnation bath, containing 10 mg/ml of glucose oxidase in 0.1 M phosphate buffer solution pH 6, for 36 hours, at room temperature. After impregnation the cuvette was allowed to dry at room temperature prior to tanning.

Step 2. Tanning. Tanning was carried out by adjusting the glutaraldehyde solution (2.5 w/v) to pH 6 (at which the immobilised glucose oxidase is more stable). This was achieved by addition of solid sodium bicarbonate. The enzyme membranes in the cuvette were immersed in the tanning solution at room temperature for 2 min followed immediately by washing with running cold tap water for 1 hour.

METHOD 4. Encapsulation in transparent glass by the Sol-Gel Immobilisation method (Yamanaka *et al.*, 1992).

Step 1. Silica sol preparation. The silica sol was prepared by sonication of 15.22 g tetramethoxysilane (TMOS), 3.38 g of deionized water and 0.22 g of 0.04 N aqueous hydrochloric acid in an ice-cooled ultrasonic bath for approximately 20 min. The sol was then buffered to create more favourable pH conditions for the enzyme glucose oxidase, in particular, a volume of 4.05 ml of the sol was mixed with 4.95 ml of 10 mM sodium phosphate buffer pH 6.

Step 2. Addition of glucose oxidase and indicators to the sol-gel. Enzyme stock solution was prepared by dissolving 1 mg of glucose oxidase in 1 ml of 10 mM sodium phosphate buffer pH 6. Then, 0.35 ml of glucose oxidase stock solution was mixed with 2.65 ml of buffer yielding 3 ml of enzyme mixture to be used for the encapsulation. Enzyme mixture (3 ml) and 8.32 ml of the indicator solution (containing: 18 µl of 100 µM HPTS, 43 µl of 10 mM tris(2,2'-bipyridyl)ruthenium(II) chloride hexahydrate, and 8.26 ml of 10 mM sodium phosphate buffer, pH 6) were added immediately to the buffered sol (4.05 ml of TMOS sol mixed with 4.95 ml of buffer). Thus, the resulting sol-gels contained the glucose oxidase and the two fluorescent indicators components. All steps were carried out on ice. The resulting sol was transferred homogeneously to one inside face of polystyrene cuvettes (10 mm^3) (1 ml in each cuvette) and sealed with Parafilm. All samples were stored at 4 ^{0}C for aging and drying for at least 48 hours.

7.2.4 Assay Method for Glucose Oxidase Activity

Glucose oxidase catalyses the oxidation of D-glucose and the products are D-gluconate and hydrogen peroxide. The formation of hydrogen peroxide was determined using a peroxidase assay system, which resulted in the formation of a quinoneimine dye measured spectrochemically at 436 nm. The reagents used were 24 ml of the dye, o-dianisidine dihydrochloride (1 ml of a 6 mg/ml solution added to 100 ml 0.1 M phosphate buffer pH 7.0), 5 ml peroxidase (60 U/ml), 5 ml glucose (10% w/v), the enzyme solution glucose oxidase in distilled water (1 mg/ml), and 0.1 M potassium phosphate pH 7.0 as enzyme diluent. The dye/buffer was oxygenated with pure oxygen, for at least 5 minutes before use, and the glucose solution was allowed 2 hours to mutarotate.

o-Dianisidine dihydrochloride (2.4 ml), 0.1 ml peroxidase and 0.5 ml glucose were pipetted into a cuvette (quartz, 3 ml), stirred and equilibrated to 25 ^{0}C. Then, 0.1 ml enzyme was added to the cuvette and the absorbance (ΔA/min) was measured at a wavelength of 436 nm with light path 1 cm. From the absorbance values the activity of glucose oxidase was determined using the following equation:

$$U/mg = \frac{\Delta A/min \times \text{total volume (ml)} \times \text{dilution factor}}{E436 \times \text{sample volume (ml)} \times \text{enzyme concentration (mg/ml)}} \quad (7.a)$$

where: Total volume = 3.10 ml

Sample volume = 0.10 ml

E436 = Extinction coefficient at 436 nm = 8.3 cm^2/μmole.

7.2.5 Reference Assay Method for the Determination of Glucose in Human Serum

The initial glucose concentration in the serum sample was determined using Sigma Diagnostic Glucose (HK) reagent. This method was based on the catalytic oxidation of glucose with hexokinase and the use of a spectrophotometer to measure the increase in absorbance of reduced NADH at 340 nm. Glucose (HK) reagent (1 ml) was dissolved in 10 ml of distilled water. The spectrophotometer was set at a wavelength of 340 nm and zeroed with distilled water as reference.

Blank and sample were pipetted into two separate cuvettes (quartz, 1 ml and light path 1 cm), where in each of them 1 ml Glucose (HK) reagent was pipetted firstly, and then 10

µl distilled water was added to cuvette labelled Blank and 10 µl sample (human serum) to appropriately labelled cuvette and mixed by gentle inversion. Both cuvettes were incubated for 5 minutes at ambient temperature and then the absorbance (A) of blank and sample cuvettes was read and recorded at 340 nm using distilled water as reference. From the absorbance values the original glucose concentration in the human serum sample was determined using the following equation:

$$\text{Glucose Concentration (mg/dl) of Sample} = \frac{\Delta A \times TV \times MW \times 100}{6.22 \times LP \times SV \times 1000} \qquad (7.b)$$

where: ΔA = change in absorbance at 340 nm

TV = total volume (ml)

MW = molecular weight of glucose (180.16)

100 = converts millilitres to decilitres

6.22 = millimolar absorptivity of NAD at 340 nm

LP = lightpath in centimeters

SV = sample volume (ml)

1000 = converts micrograms to milligrams

7.3 RESULTS

7.3.1 Immobilisation Procedures

Four different immobilisation techniques, covalent to cellulose acetate, inclusion in an polyacrylamide-agarose gel, adsorption-noncovalent collagen membrane impregnation, and encapsulation in transparent glass using sol-gel immobilisation, were applied to the

previously studied fluorescence-based optical glucose biosensor (Chapter 3) using the three well-defined Experimental Modes (see Section 3.3.2). As was mentioned, these Experimental Modes depend on changes in the fluorescence intensity at the maxima and common excitation and emission wavelengths of the fluorescent indicators with time, during the biocatalytic oxidation of glucose by the enzyme glucose oxidase.

The same principles and experimental set-ups (Experimental Modes A, B and C) used in the solutions studies were applied to the immobilisation configurations. In the first three immobilisation configurations only glucose oxidase was immobilised, while in the last the enzyme was immobilised together with both indicators tris(2,2'-bipyridyl) ruthenium(II) chloride hexahydrate and HPTS, as described in Section 7.2.3. Also, in all immobilisation techniques the supports were checked in the specific wavelengths used in Experimental Modes for any interference without and with immobilisation of the enzyme (blank).

In the first procedure, covalent immobilisation, stored cellulose acetate membranes were cut into smaller pieces (7 mm-diameter) and were placed firmly on the bottom surface of the cuvette under a fine stirrer bar. The experimental procedure described in Section 3.3.2 was followed, except that in the cases with immobilised enzyme, the last reagent added was glucose instead of glucose oxidase. The results from this procedure were poor with very small signals and the reaction proved to be very slow, taking several hours (around 5 hours) to detect change in the fluorescence intensity of the indicators. The smallest detectable concentration of glucose was 15 mM.

The same procedure was also carried out for the polyacrylamide-agarose gel, but without the use of a stirrer bar on the bottom surface of the cuvette in order to avoid desecration of the gel. Instead the cuvette was given a good shake (for approximately 1 min) before running the instrument. Again the results were very poor with small and irreproducible signals. Another problem was the leakage of the enzyme from the gel which created interference to the fluorescence of the indicators because of its high concentration.

Slightly better results were obtained using glass cuvettes with the glucose oxidase immobilised on their two inside surfaces using the membrane impregnation method with collagen (higher signals in comparison with the previous immobilisation methods). However the reaction was still very slow. It required few hours (approximately 4.5 hours) in order to detect obvious changes in the fluorescence intensity of the indicators in different glucose concentrations, and the smallest detectable concentration of glucose was 10 mM.

The sol-gel method gave very interesting results. For each sample a different polystyrene cuvette was used with the immobilised enzyme glucose oxidase and the two indicators tris(2,2'-bipyridyl)ruthenium(II) chloride hexahydrate and HPTS, on one inside surface of the cuvette, with this side facing the excited beam. All sol-gel cast films in polystyrene cuvettes were optically transparent with no visible surface cracks. Initial experiments checked the spectroscopic properties of the immobilised indicators in comparison with the corresponding properties in solution. The excitation and emission maxima of both indicators were at the same wavelengths as in solution (Section 3.2.3).

The sol-gel technique was also applied to the three Experimental Modes as described in Section 3.3.2. The results for Experimental Mode A, can be observed in Figures 7.1 and 7.2. Details of the mathematical analysis of the experimental data and the use of rate change of fluorescence intensity (dI/dt) instead of fluorescence intensity itself, for each glucose concentration, are explained in Appendix A. The results for Experimental Mode B, are depicted in Figure 7.3, and finally, the results for the Experimental Mode C, are illustrated in Figures 7.4 and 7.5.

The experimental values of the apparent Michaelis constant, K_m, of the reaction in the case where glucose oxidase and the two fluorescent indicators were immobilised in sol-gel matrices, were calculated using the Hanes plots corresponding to Figures 7.1 and 7.2 for Experimental Mode A, to Figure 7.3 for Experimental Mode B, and to Figures 7.4 and 7.5 for the Experimental Mode C, and according to equation (3.e); these the apparent K_m's were 39 mM and 64 mM, 37 mM, and, 47 mM and 63 mM, respectively for the above Experimental Modes.

The lowest detectable glucose concentration in all Experimental Modes was around 0.3 mM. For glucose concentrations up to 50 mM (experiments were carried out for the three Experimental Modes for glucose concentrations 50-100 mM), a saturation in the fluorescence intensity was observed in all situations in the polystyrene cuvettes, where the enzyme and the indicators were immobilised in sol-gel matrices. For the above experiments, the enzyme immobilised in polystyrene cuvettes maintained the same sensitivity and stability for at least 4 months storage at 4 ^{0}C.

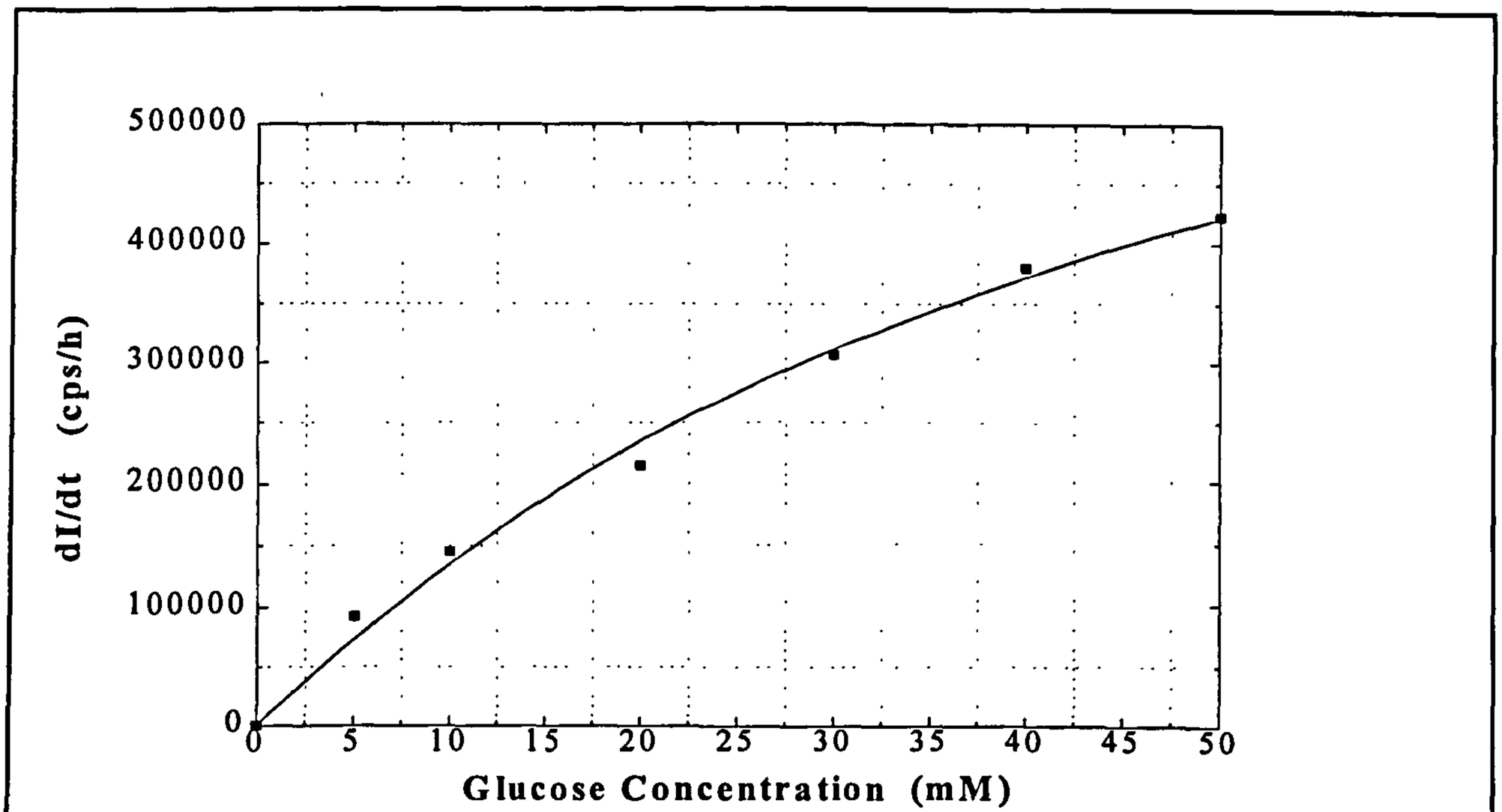

FIGURE 7.1 Rate of change of fluorescence intensity versus glucose concentration of tris(2,2'-bipyridyl)ruthenium(II) chloride hexahydrate, at fixed excitation wavelength of 410 nm and fluorescence monitored at 597 nm, during the catalytic oxidation of glucose using sol-gel immobilisation (Experimental Mode A).

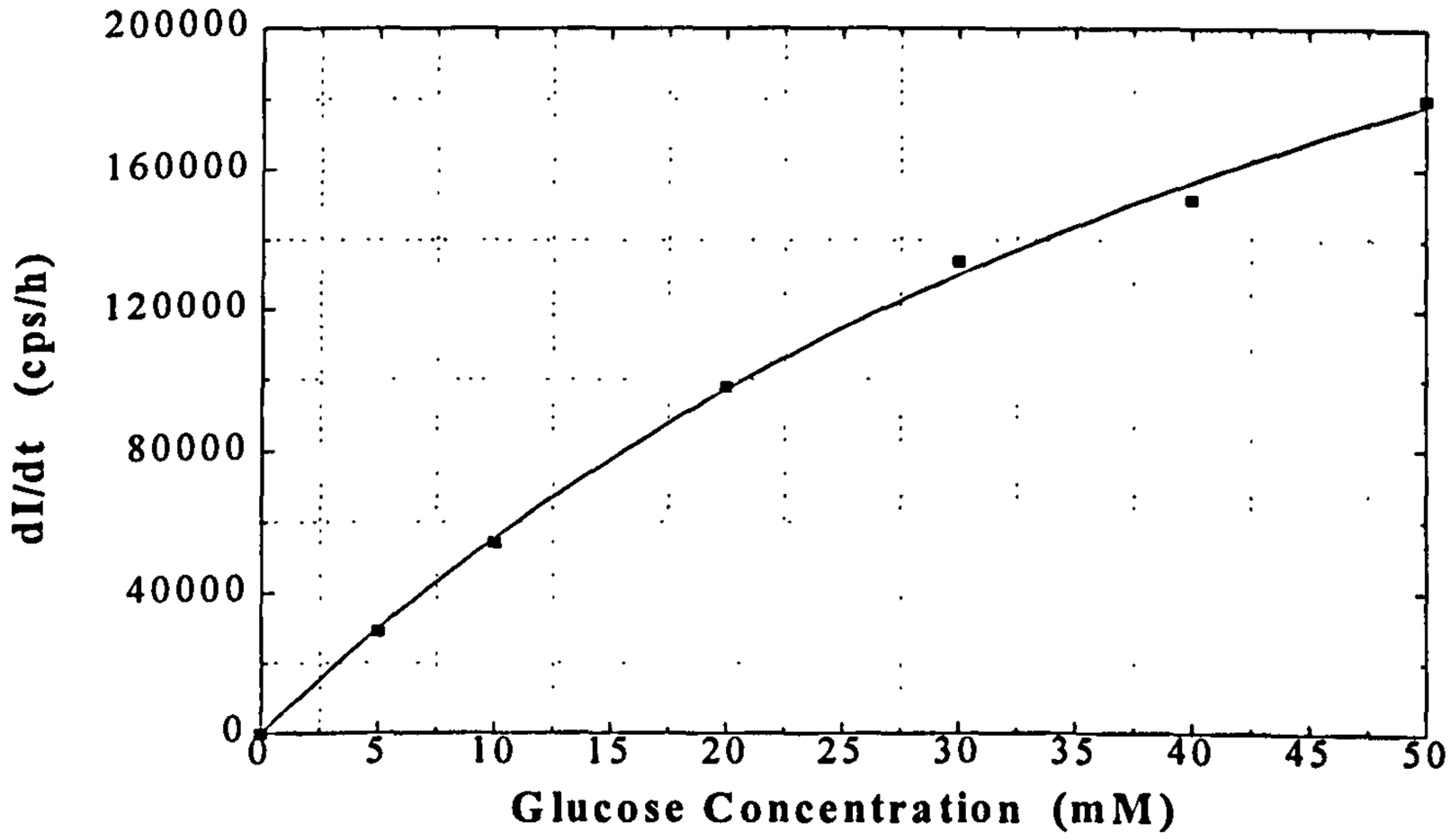

FIGURE 7.2 Rate of change of fluorescence intensity versus glucose concentration of HPTS, at fixed excitation wavelength of 410 nm and emission monitored at 507 nm, during the catalytic oxidation of glucose using sol-gel immobilisation (Experimental Mode A).

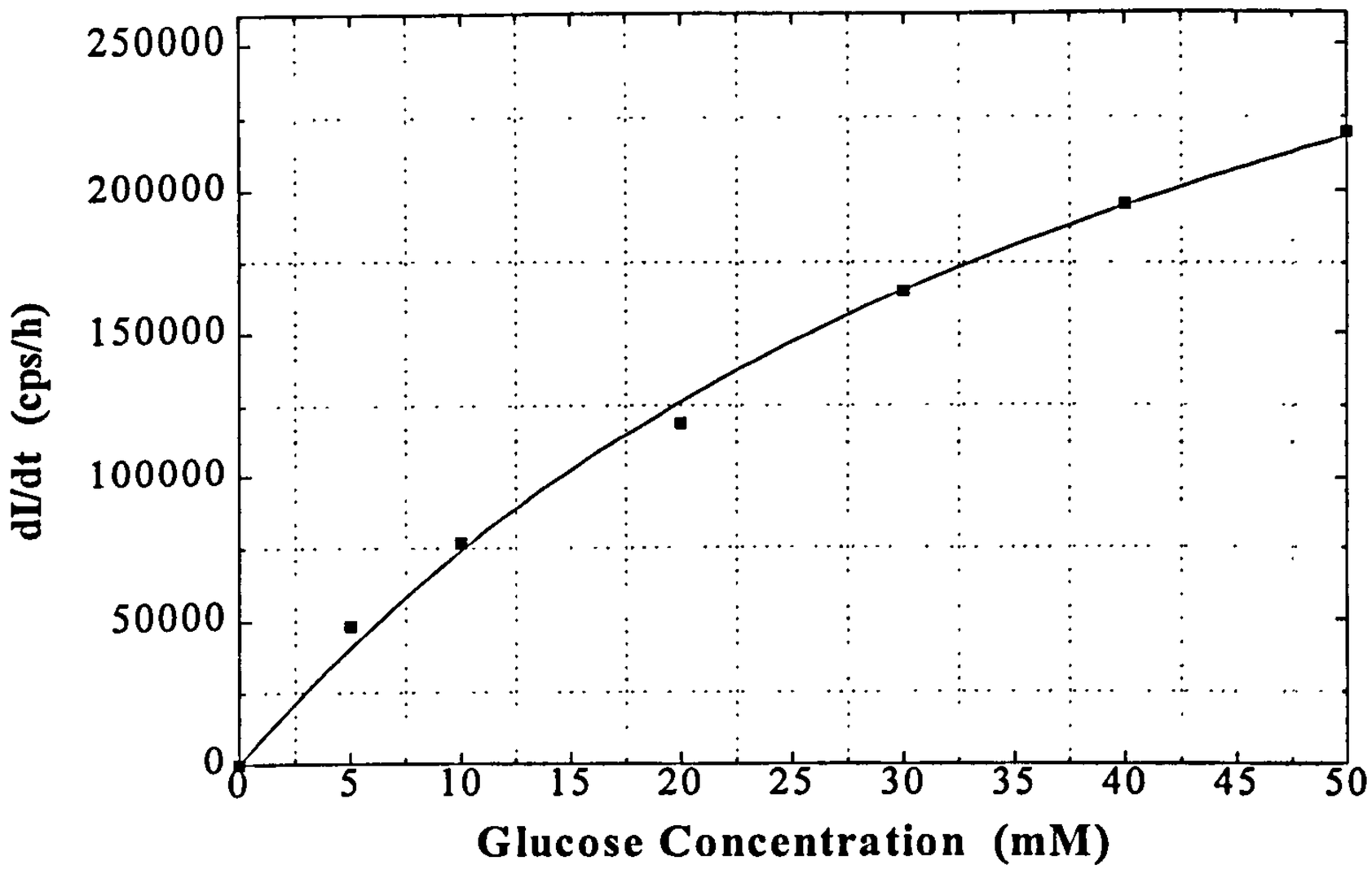

FIGURE 7.3 Rate of change of fluorescence intensity versus glucose concentration of the sum of tris(2,2'-bipyridyl)ruthenium(II) chloride hexahydrate and HPTS, at the excitation wavelength of 410 nm and monitoring the emission at 555 nm, during the catalytic oxidation of glucose using sol-gel immobilisation (Experimental Mode B).

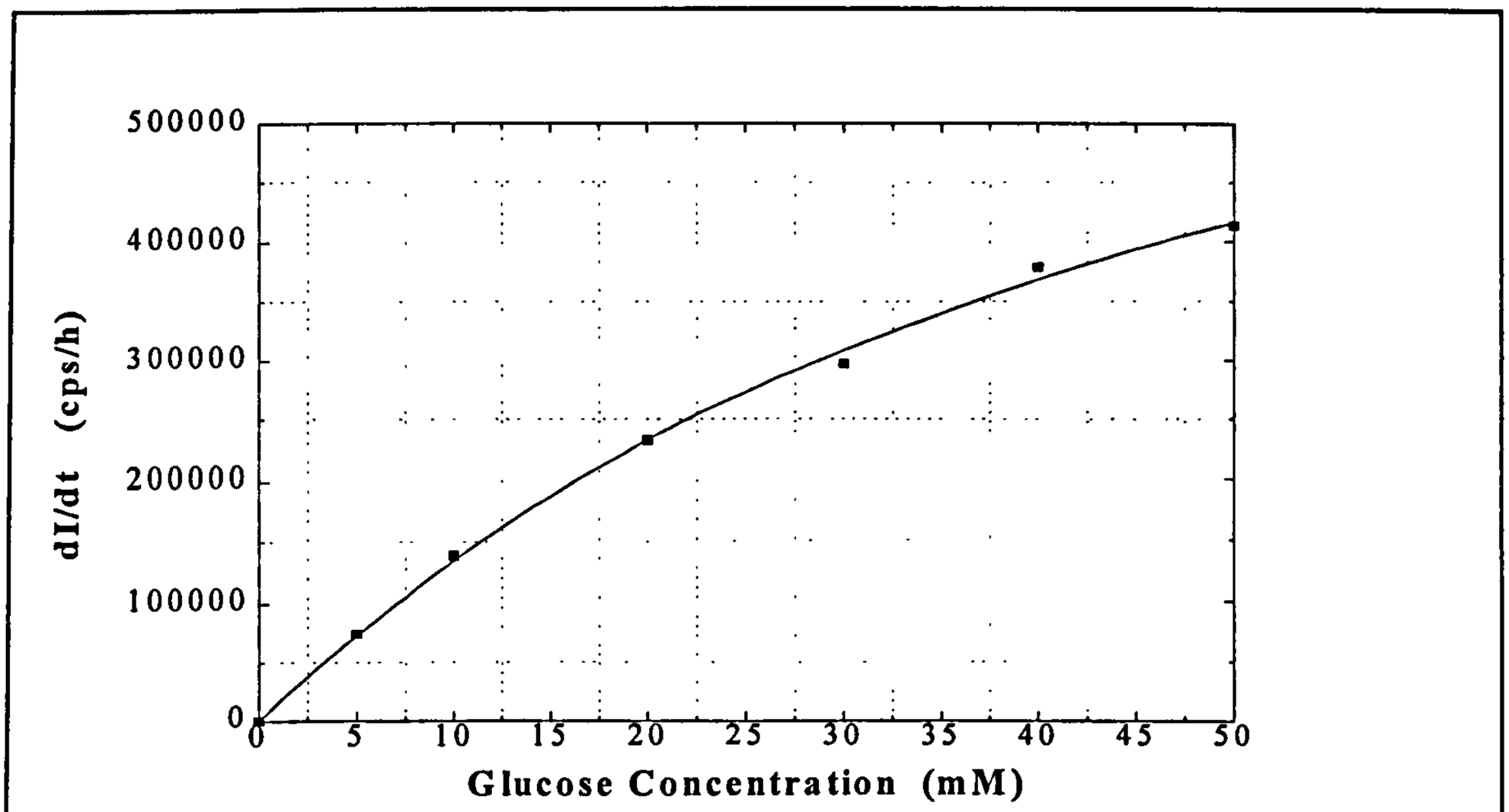

FIGURE 7.4 Rate of change of fluorescence intensity versus glucose concentration of tris(2,2'-bipyridyl)ruthenium(II) chloride hexahydrate, at fixed excitation wavelength of 452 nm and fluorescence monitored at 597 nm, during the catalytic oxidation of glucose using sol-gel immobilisation (Experimental Mode C).

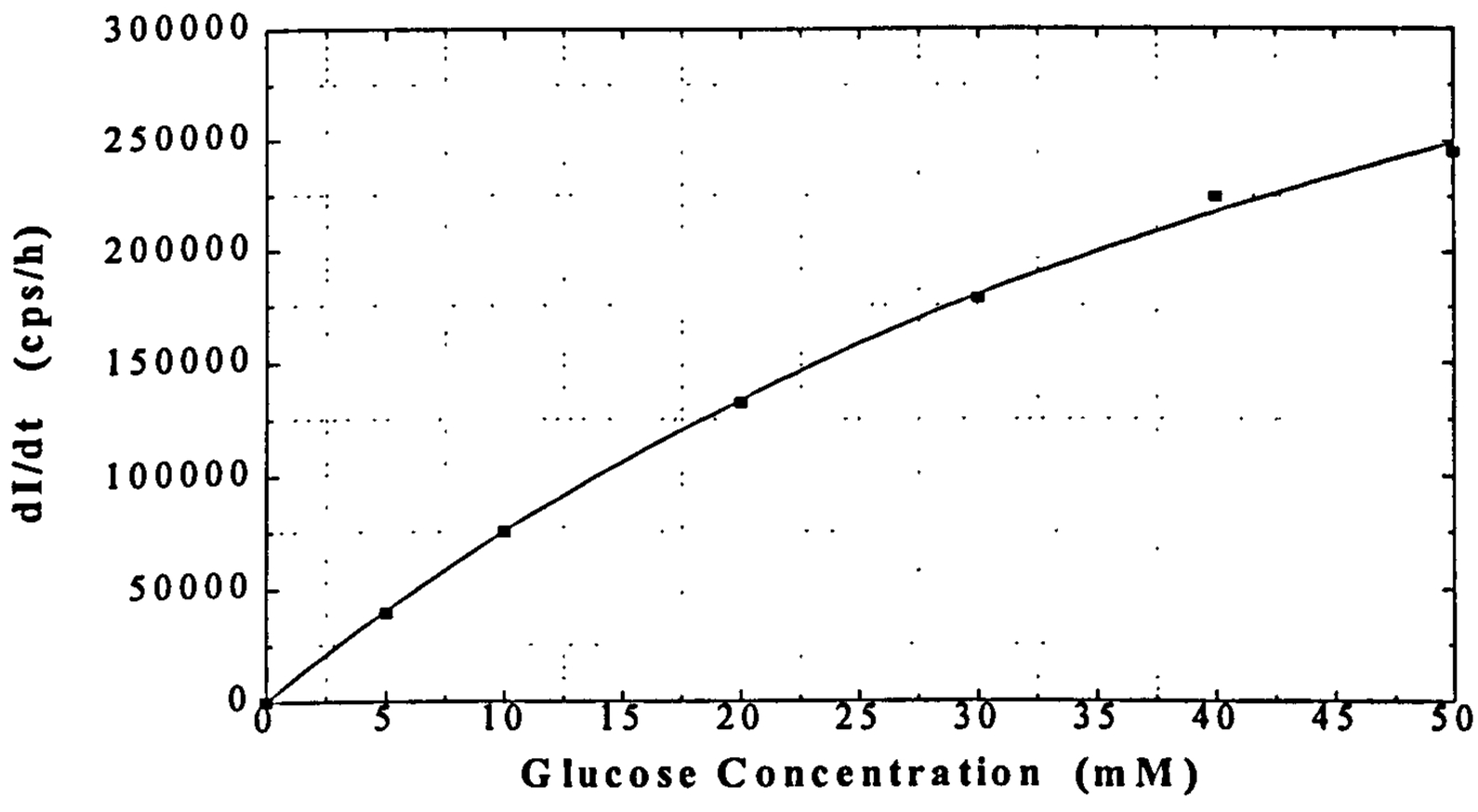

FIGURE 7.5 Rate of change of fluorescence intensity versus glucose concentration of HPTS, at fixed excitation wavelength of 401 nm and fluorescence monitored at 507 nm, during the catalytic oxidation of glucose using sol-gel immobilisation (Experimental Mode C).

Subsequent experiments were carried out in order to investigate the reproducibility and reliability of the sol-gel immobilisation method for the proposed optical glucose biosensor using the Experimental Mode A. Three glucose concentrations were chosen: 5 mM, 15 mM and 30 mM, and measurements were repeated 5 times for each concentration. The mean values of the rate of change of the fluorescence intensity of tris(2,2'-bipyridyl) ruthenium(II) chloride hexahydrate, during the biocatalytic oxidation of glucose, for each glucose concentration and the corresponding standard deviations are presented in Table 7.1.

TABLE 7.1

Glucose Concentration	Mean Value	Coefficient of Variation (%)	R
5 mM	91,6	3.2	5
15 mM	185,1	2.7	5
30 mM	309,6	2.9	5

Similarly, the mean values of the rate of change of the fluorescence intensity of HPTS, of samples of 5 mM, 15 mM and 30 mM of glucose during the oxidation, for each glucose concentration, and their corresponding standard deviations are shown in Table 7.2.

TABLE 7.2

Glucose Concentration	Mean Value	Coefficient of Variation (%)	R
5 mM	28,1	4.1	5
15 mM	74,3	3.5	5
30 mM	127,7	3.7	5

A series of experiments were carried out in order to determine the activity of glucose oxidase in the solution. The assay described in Section 3.2.4 was used with three concentrations of glucose oxidase, 0.15 U/ml, 0.2 U/ml and 0.4 U/ml and the experimental values of the rate of change in the absorbance (ΔA/min) were applied to Equation (7.a). From these calculations it was found that the mean value of the activity of glucose oxidase was equal to 173 U/mg with coefficient of correlation 1.000, which is close to the manufacturer's value of 176 U/mg.

Subsequent experiments were conducted in order to find out the activity of glucose oxidase when it was encapsulated alone on sol-gel matrices on one inside surface of a polystyrene cuvette. These sol-gel samples were aged for 4 months stored at 4 ^{0}C. Comparison was made with the activity of the enzyme in solution and also with another immobilisation method, i.e. the enzyme impregnation procedure of collagen membranes on the two inside surfaces of a glass cuvette (freshly made). The same enzyme assay method was followed for different glucose oxidase concentrations (0.15 U/ml - 3 U/ml) in solution, in order to establish a calibration curve (Figure 7.7). An example of the experimental data for 1 U/ml glucose oxidase can be seen in Figure 7.6. The experimental data from the immobilised sol-gel polystyrene cuvette and collagen membrane in a glass cuvette are shown in Figures 7.8 and 7.9, respectively.

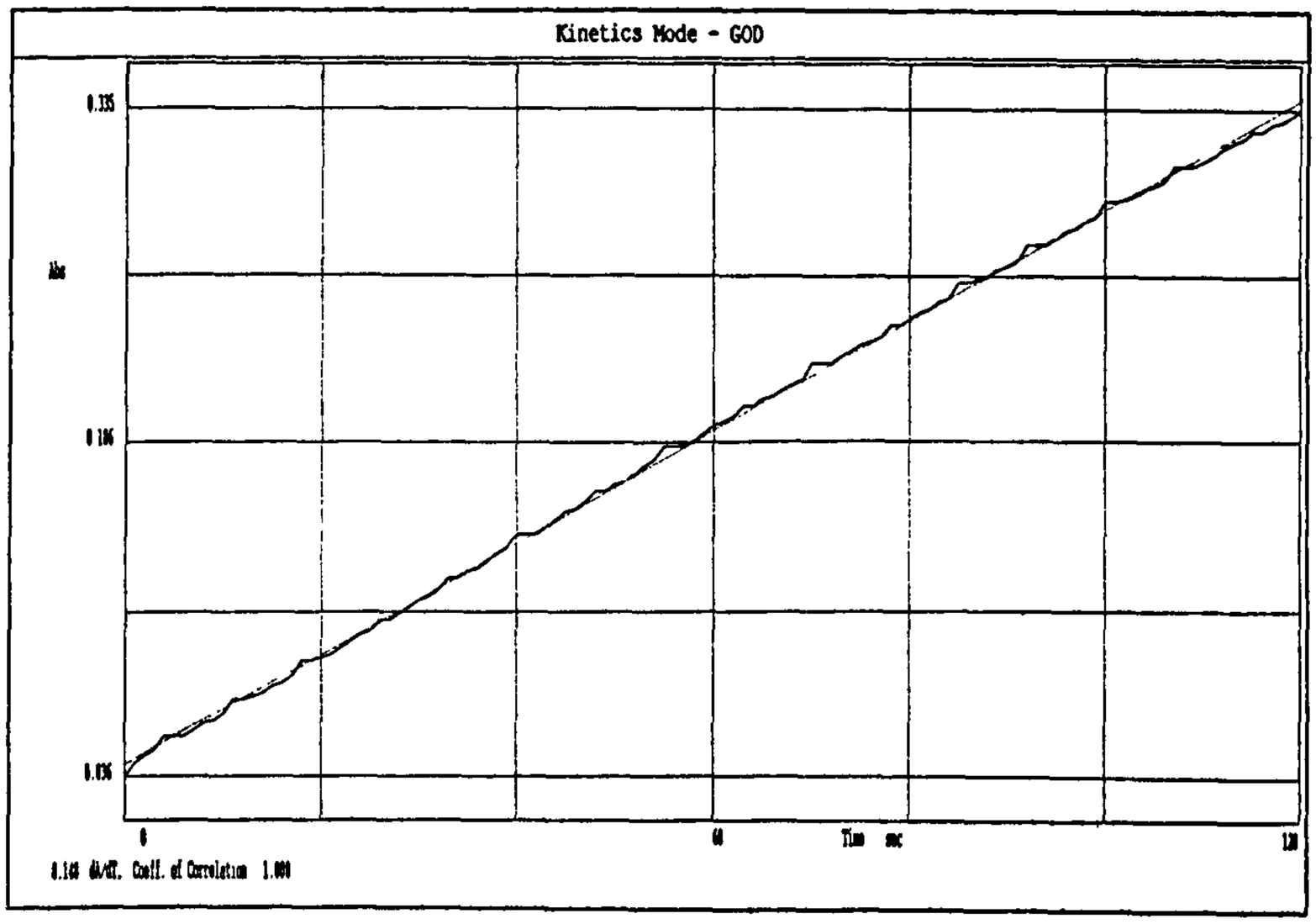

FIGURE 7.6 Absorbance versus time of glucose oxidase (1 U/ml), during the assay procedure at 22 ^{0}C.

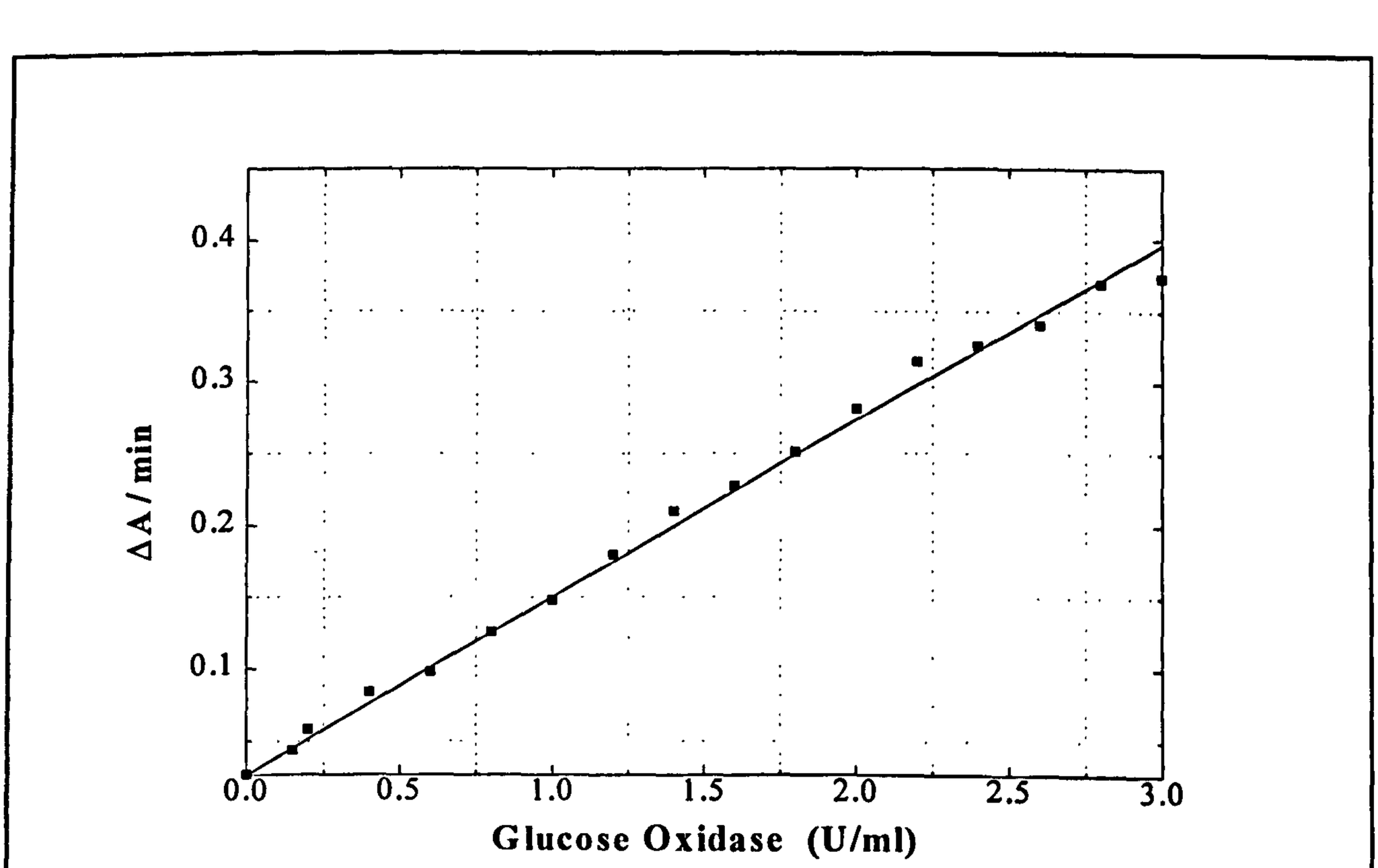

FIGURE 7.7 Calibration curve of ΔA/min of absorbance versus glucose oxidase concentrations (U/ml), resulting from the assay procedure.

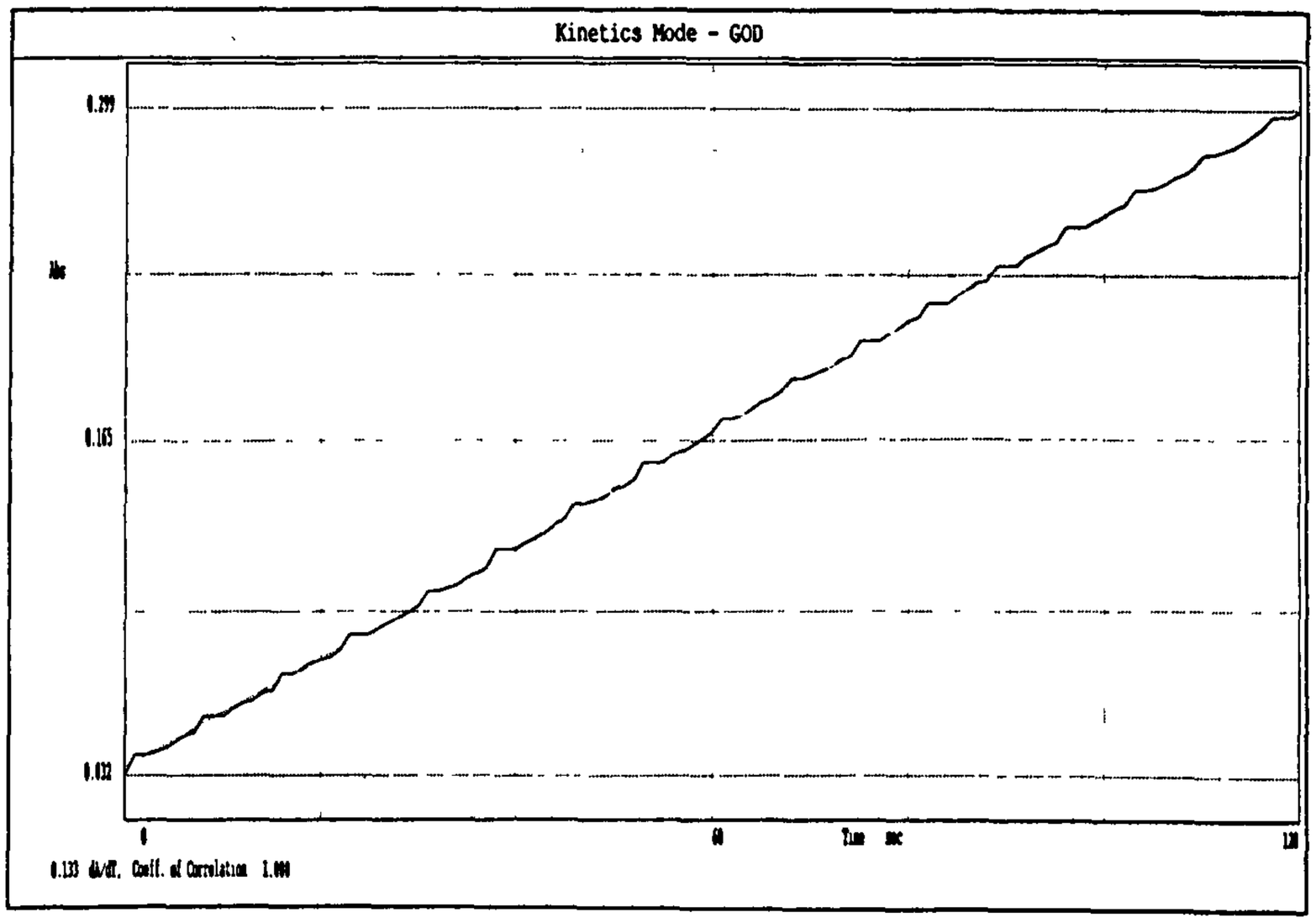

FIGURE 7.8 Absorbance versus time of glucose oxidase immobilised in sol gel using the assay procedure at 22 ^{0}C.

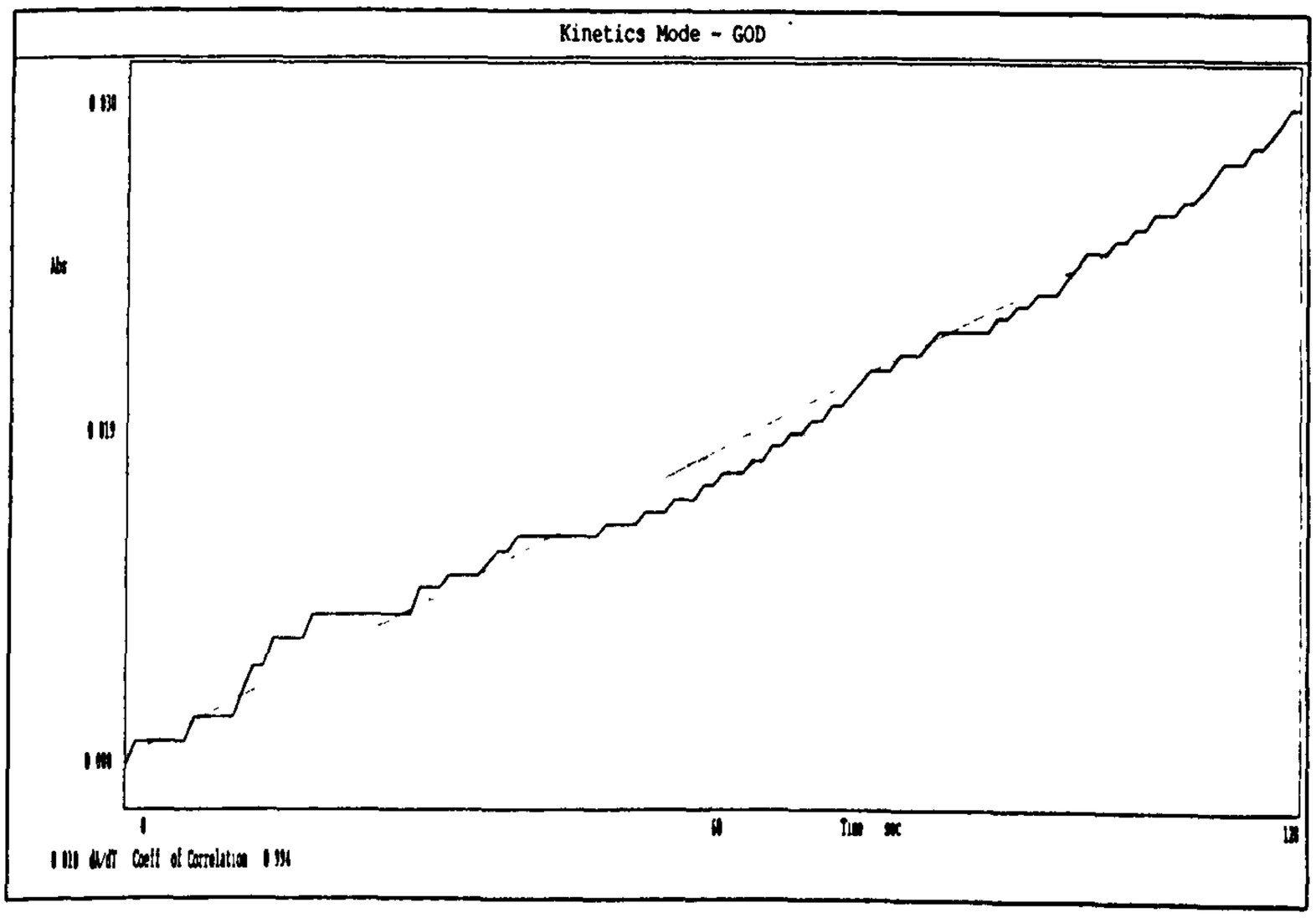

FIGURE 7.9 Absorbance versus time of glucose oxidase immobilised in collagen membrane using the assay procedure at 22 ^{0}C.

7.3.2 Kinetic Measurements in Human Serum

The following experiment was performed using real biological samples, human serum, instead of the phosphate buffer solution in the cuvette. Specific amounts of the indicators, glucose oxidase and various glucose concentrations were added in the cuvette as described in Section 3.3.2, using Experimental Mode A.

Initial experiments were carried out in order to investigate the spectroscopic characteristics of the human serum. The excitation and emission fluorescence spectra are shown in Figure 7.10, which indicates that the peak excitation is located at 365 nm and the peak emission fluorescence at 455 nm, which appears to be very strong. This intense fluorescence overlaps the fluorescence from HPTS. In order to avoid this interference, a higher concentration of 0.6 μM (about 20 times more than the 0.03 μM used previously) of this indicator was chosen which is still within the linear range (Chapter 2). Interference with the second indicator, tris(2,2'-bipyridyl)ruthenium(II) chloride hexahydrate, was negligible.

The initial glucose concentration in the serum sample was determined using Sigma Diagnostic glucose (HK) reagent. The method detailed in Section 7.2.5 was repeated for 24 times for the same human serum and the mean value of the glucose in this human serum was found to be 5.7 mM, with a standard deviation of 0.83.

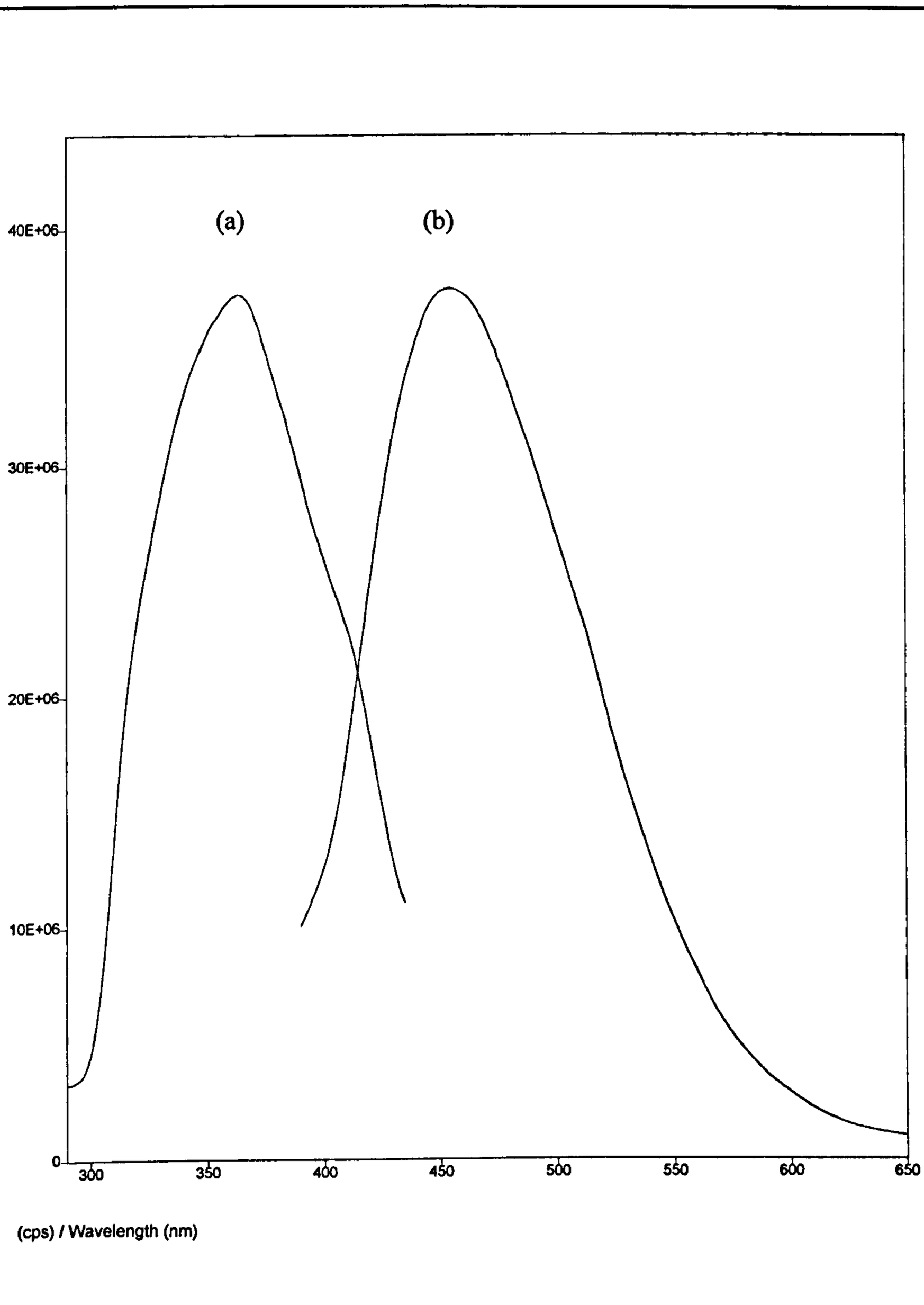

FIGURE 7.10 Excitation (a) and fluorescence (b) spectra of human serum with excitation wavelength at 365 nm and fluorescence monitored at 455 nm, at 22 ^{0}C.

For the kinetic measurements, the cuvette contained human serum with the addition of 7 μM tris(2,2'-bipyridyl)ruthenium(II) chloride hexahydrate, 0.6 μM HPTS and various concentrations of glucose. The reaction was started by the addition of glucose oxidase (1 U/ml) as described in the previous section. The human serum in these experiments was not dilluted in order to maintain its substances and to identify any interference of them. The excitation wavelength was selected to be common at 410 nm, and the changes in fluorescence intensity with time were monitored at 597 nm (the maximum for tris(2,2'-bipyridyl)ruthenium(II) chloride hexahydrate), and 507 nm (the maximum for HPTS), respectively. The experiment was carried out several times for different concentrations of glucose and the variations in fluorescence intensity were measured.

The rates of change in the fluorescence intensity of tris(2,2'-bipyridyl)ruthenium(II) chloride hexahydrate and HPTS against the added glucose concentration in human serum are shown in Figures 7.11 and 7.12. The corresponding Hanes plots for these calibration curves are illustrated in Figures 7.13 and 7.14, respectively, where the glucose concentration values shown are the values of total glucose concentrations in the human serum, measured (5.742 mM) plus the glucose concentration added. The experimental values of the Michaelis constants K_m from these plots and according to equation (3.e) were found to be 15.6 mM with tris(2,2'-bipyridyl)ruthenium(II) chloride hexahydrate at excitation wavelength of 410 nm and fluorescence monitored at 597 nm, and 30.3 mM with HPTS at excitation and fluorescence wavelengths of 410 nm and 507 nm, respectively.

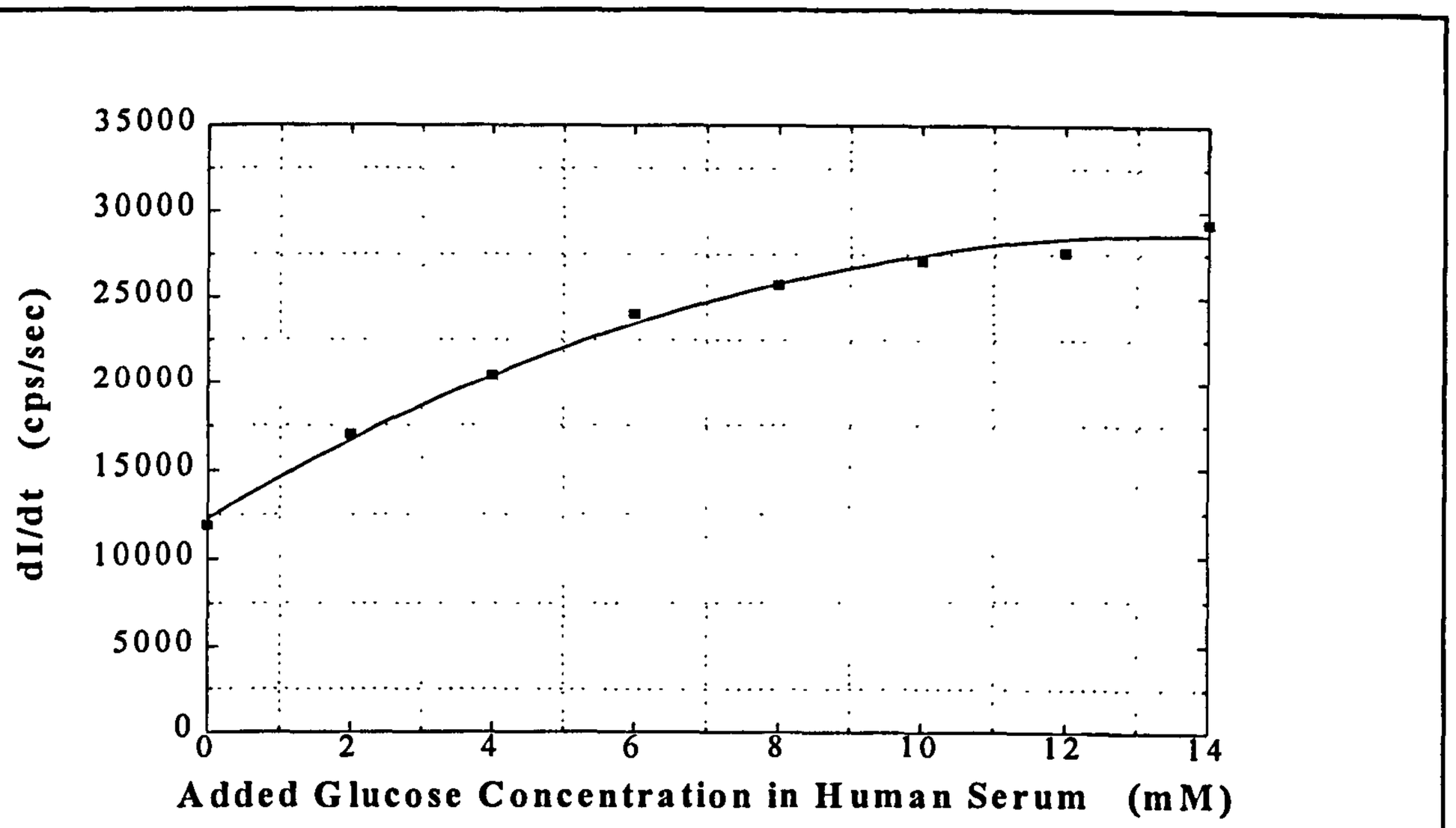

FIGURE 7.11 Rate of change of fluorescence intensity versus glucose concentration in human serum of tris(2,2'-bipyridyl)ruthenium(II) chloride hexahydrate, at fixed excitation wavelength of 410 nm and fluorescence monitored at 597 nm, during the catalytic oxidation of glucose (Experimental Mode A).

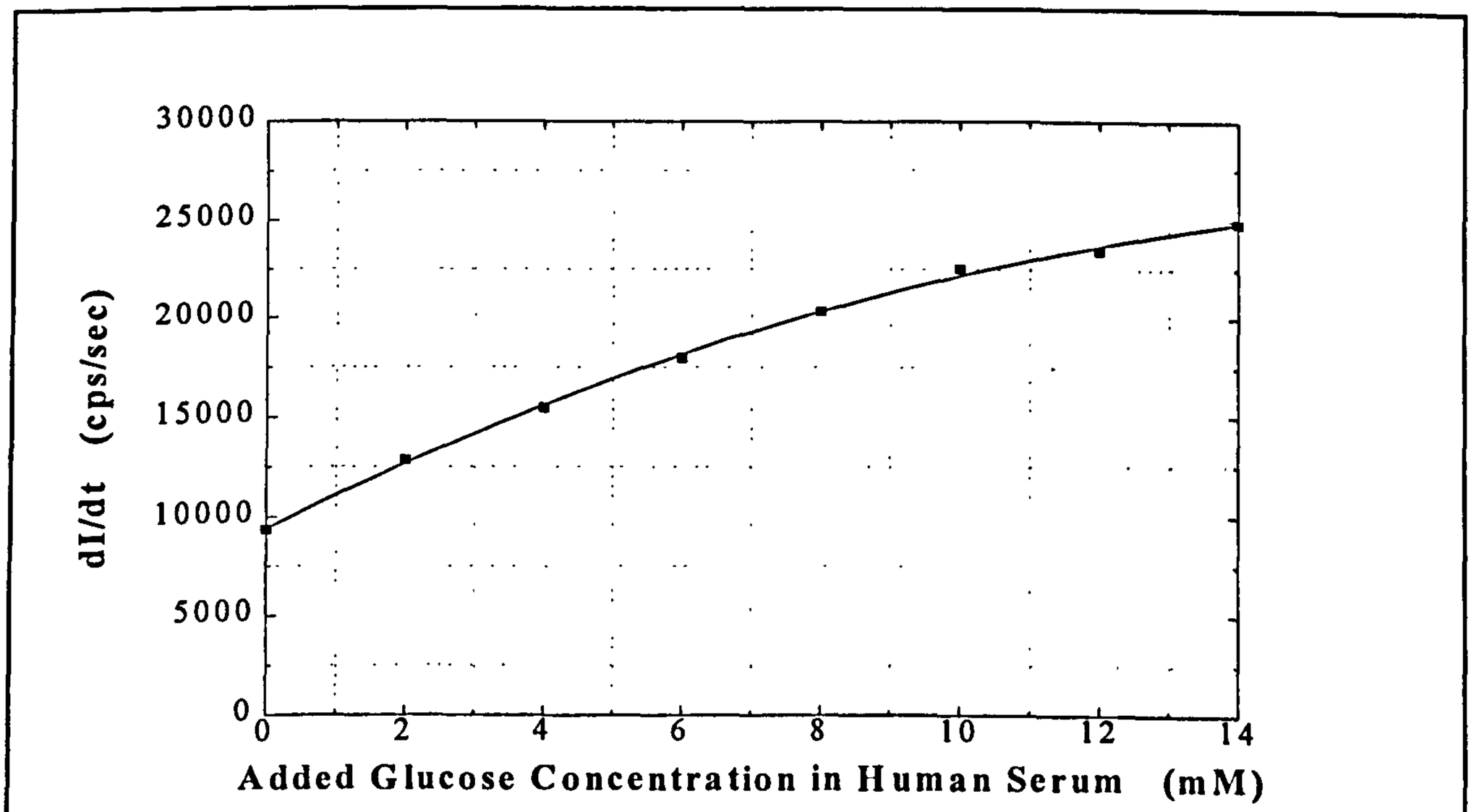

FIGURE 7.12 Rate of change of fluorescence intensity versus glucose concentration of human serum HPTS, at fixed excitation wavelength of 410 nm and fluorescence monitored at 507 nm, during the catalytic oxidation of glucose (Experimental Mode A).

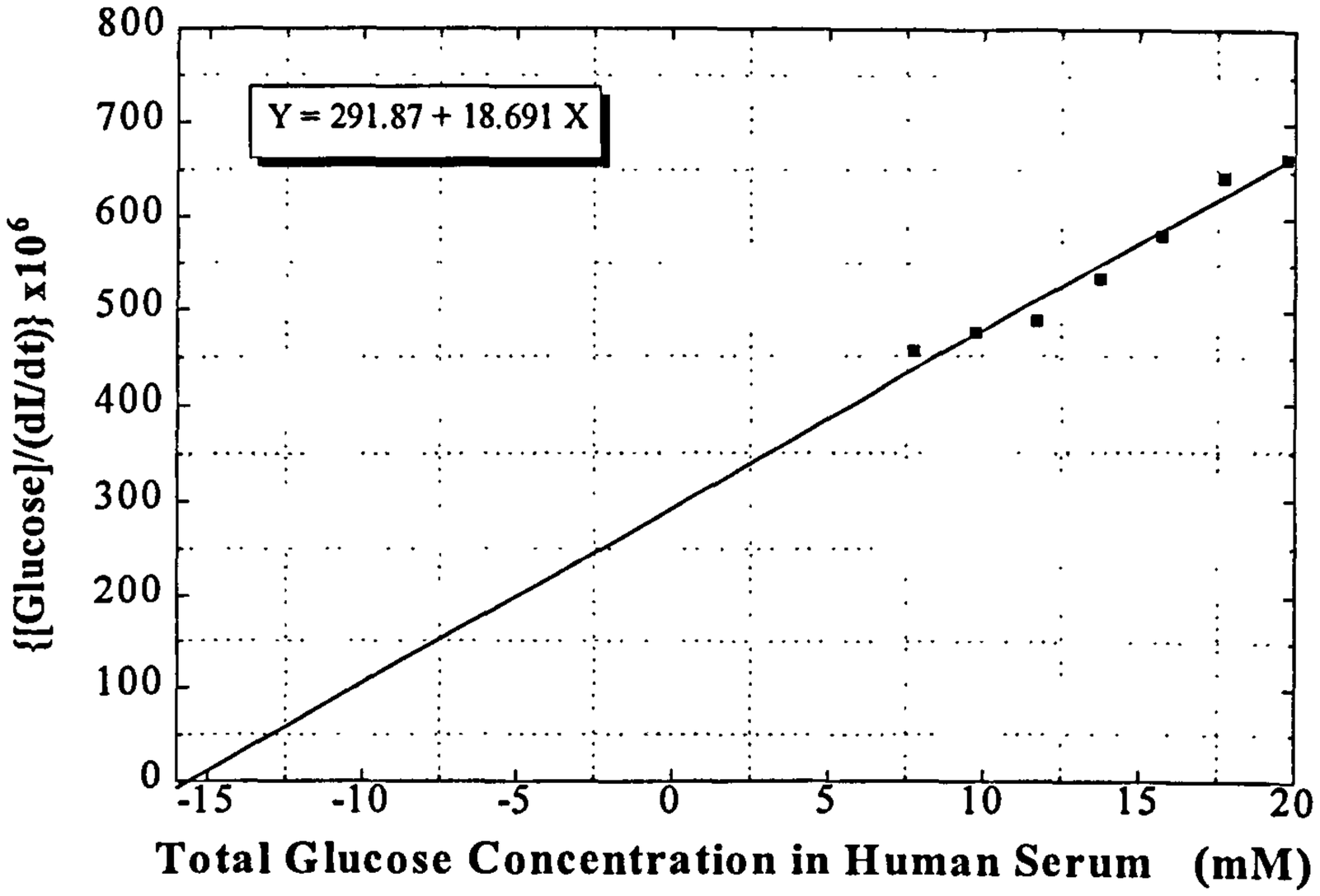

FIGURE 7.13 Hanes plot corresponding to Figure 7.11.

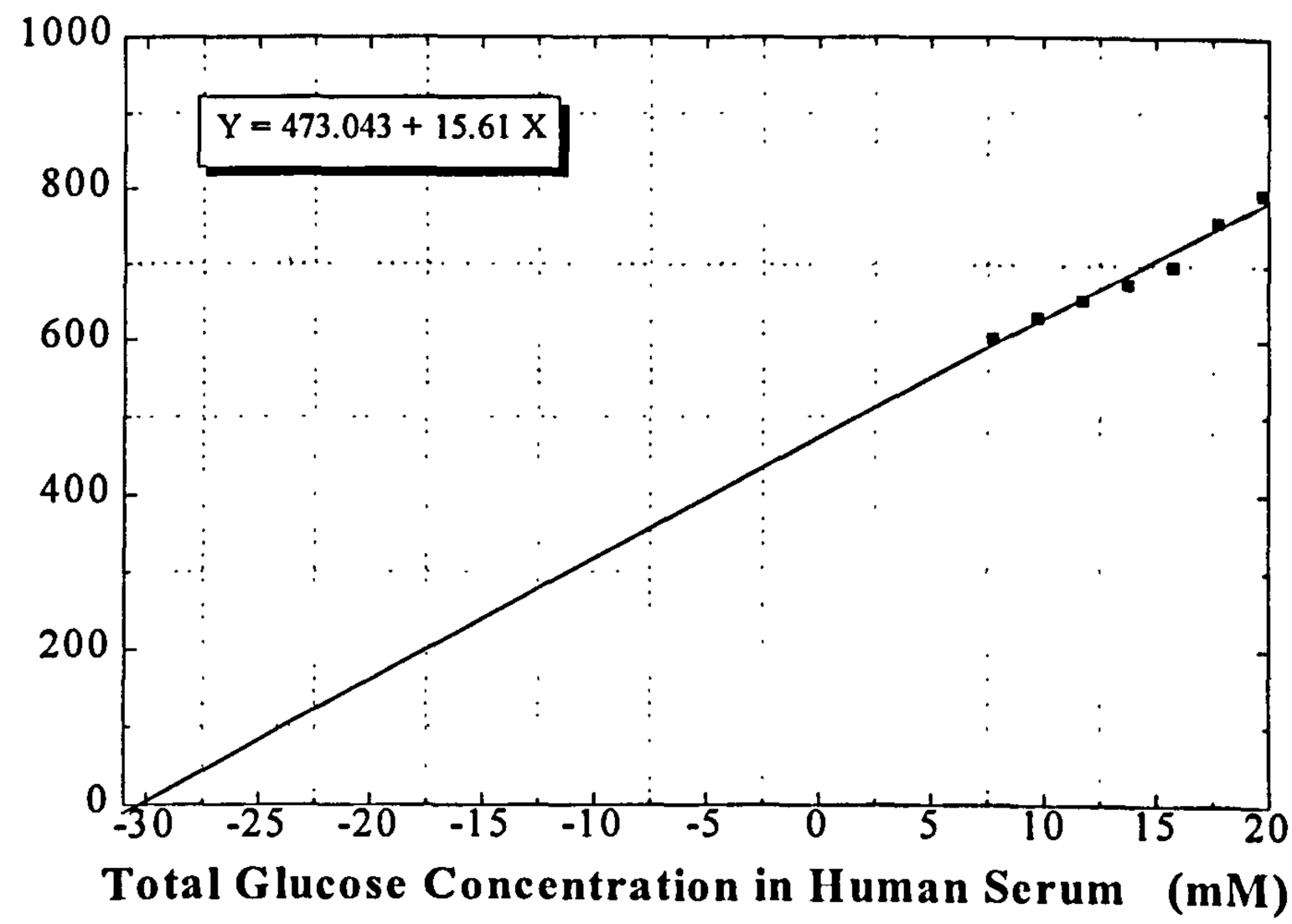

FIGURE 7.14 Hanes plot corresponding to Figure 7.12.

A series of experiments were carried out in order to investigate the reproducibility and reliability of the above approach. Three added glucose concentrations to the human serum were chosen: 2 mM, 6 mM and 12 mM, and measurements were repeated 5 times for each concentration. The mean values of the rate of change of the fluorescence intensity of tris(2,2'-bipyridyl) ruthenium(II) chloride hexahydrate, during the biocatalytic oxidation of glucose, for each glucose concentration in the human serum and the corresponding standard deviations are showed in Table 7.3.

TABLE 7.3

Glucose Concentration (added to the the human serum)	**Mean Value**	**Coefficient of Variation (%)**	**R**
2 mM	16,7	1.9	5
6 mM	24,3	2.1	5
12 mM	27,7	1.9	5

Similarly, the mean values of the rate of change of the fluorescence intensity of HPTS, of samples of 2 mM, 6 mM and 12 mM of glucose during the reaction, for each added glucose concentration in the human serum and their corresponding standard deviations are presented in Table 7.4.

TABLE 7.4

Glucose Concentration (added to the the human serum)	**Mean Value**	**Coefficient of Variation (%)**	**R**
2 mM	11,1	2.5	5
6 mM	18,4	1.7	5
12 mM	23,3	2.4	5

7.4 DISCUSSION

The investigation of the spectroscopic behaviour of the two fluorescent indicators tris(2,2'-bipyridyl)ruthenium(II) chloride hexahydrate and HPTS in sol-gel bulk glass was carried out and the results showed that the excitation and fluorescence maxima of both indicators were the same as in buffer solution. This is in agreement with published data presented in the literature. Wolfbeis and colleagues (1988) utilised the same indicators as in the present study, in order to construct a fibre-optic fluorosensor for simultaneous measurement of oxygen and carbon dioxide. The indicators used as the oxygen-sensitive (tris(2,2'-bipyridyl)ruthenium(II) dichloride) and carbon dioxide-sensitive (HPTS) materials, were entrapped in a gas-permeable polymer matrix. They reported no difference in the excitation and emission spectra and their maxima for both indicators immobilised or in solution.

Reisfeld (1990) presented work about tris(2,2'-bipyridyl)ruthenium(II) chloride hexahydrate in sol-gel glasses that showed similar absorption and emission spectra with similar corresponding maxima as in water solution. The author claimed that essentially the mechanisms of absorption, internal conversion and intersystem crossing for this indicator were similar in sol-gel films as well as in solution at room temperature, and therefore the surroundings have little or no effect on the shape and on the molar absorptivity of the spectroscopic properties of the indicator. For HPTS, Offenbacher *et al.* (1986) presented the similarity in excitation and emission spectra of free and covalent bound HPTS, and the observation of complete photodissociation even in the immobilised state which indicated that there was hardly any electronic interaction between HPTS and a glass surface. Also, Trettnak *et al.* (1988a) reported that HPTS retained the same

spectroscopic properties when physically immobilised in QA 52 cellulose fibres and in buffer solution. On the other hand, Schulman *et al.* (1995) showed that the immobilised indicator HPTS (covalently immobilised on cellulose attached to a plastic strip) demonstrated acid-base chemistry qualitatively similar to that of its freely diffusing progenitor; but, the fluorescence of immobilised HPTS varied in the low pH region from about pH 3 to below pH 1.

In the present work, immobilisation of glucose oxidase was carried out in four different ways, namely, covalent in cellulose acetate membranes, crosslinked in polyacrylamide-agarose gel, adsorption-noncovalent in collagen membranes and encapsulation in sol-gel glass. The first three methods gave poor results with small and/or irreproducible signals during the the experimental conditions of the three Experimental Modes. One explanation could be the way the measurements were carried out, the cuvette environment. Thin cellulose acetate membranes, small pieces polyacrylamide-agarose gels and very thin collagen membranes were immersed at the bottom of a cuvette (3 ml) containing the fluorescent indicators and the glucose injection. A serious problem appeared to be the inhomogeneity of the solution and therefore the response of the indicators.

In the literature, various solid supports such as cellulose, starch, glass, polyacrylamide and polystyrene have been reported as supports for immobilisation (Offenbacher *et al.*, 1986). In particular; cellulose was a much less rigid support than glass. Also, they claimed that immobilising HPTS on crosslinked polyacrylamide provided sensors with extremely long response times, as found in the present study as well, possibly because

of a large amount of carboxylate groups with their inherent buffer capacity being present at the polymer surface. Their presence results from the treatment of the surface with strong alkali prior to immobilisation. Poly(chloromethyl-styrene was rejected as a support because of its hydrophobic surface and certain difficulties in the reproducibility of the immobilisation step and starch as a polymeric support has the disadvantage of being easily attacked by bacteria.

In the present study, the sol-gel encapsulation technique was favoured over the other methods, where the glucose oxidase and the two fluorescent indicators were immobilised in the same matrix. By placing the enzyme close to the indicators, the diffusional barrier for the protons produced by the enzyme was kept small. Figures 7.1-7.5 illustrated that the catalytic oxidations that occured normally in solution for the three Experimental Modes (Section 3.3.2), were readily carried out in the pores of the glass matrix, and appeared to follow similar trends. These results suggest that the sol-gel matrix did not affect the ability of the immobilised glucose oxidase to influence the response of the indicators during the oxidation of glucose, and therefore, there was essentially no difference in the behaviour of the indicators whether the glucose oxidase was immobilised in sol-gel matrix or present as native enzyme in buffer. Also, the sol-gel glass offered very little resistance to diffusion effects responsible for the kinetic behaviour of the immobilised enzyme.

The above results are in agreement with published literature reports. Narang *et al.* (1994) proved that entrapped enzymes in different sol-gel matrices behaved as free enzymes dissolved in an aqueous medium such as buffer or water. Such results are in

complete agreement with conclusions previously reported on the basis of optical measurements (Audebert *et al.*, 1993; Yamanakana *et al.*, 1992; Braun *et al.*, 1990).

In the three Experimental Modes using the sol-gel method, the apparent Michaelis constant, $K_{m,app}$, was found to be around 2-fold higher (≈ 50 ± 13 mM) than that of the enzyme in solution (≈ 23 ± 10 mM) (see Section 3.3.2 and 7.3.1). These results are similar to the published results by Yamanaka *et al.* (1992) where K_m with β-D-glucose in solution was determined equal to 28 ± 3 mM and the apparent K_m in sol-gel was ≥ 50 ± 50 mM. Also, the above results can be compared to the value reported by Narang *et al.* (1994) using sol-gel-sandwich films for the development of a glucose biosensor where the apparent K_m was found to be 15 ± 5 mM. The published literature value of K_m for glucose oxidase with β-D-glucose with the conventional methods in solution was found to be around 26 mM (Gibson *et al.*, 1964; Bright & Gibson, 1967; Rogers & Brandt, 1971).

In the current study, the analytical range of glucose for the proposed optical glucose biosensor was found around 0.3 to 50 mM. For glucose concentrations up to 50 mM (experiments were carried out for the three Experimental Modes for glucose concentrations 50-100 mM), a saturation in the fluorescence intensity was observed in all situations in the polystyrene cuvettes (Experimental Modes A, B and C), where the enzyme and the indicators were immobilised in sol-gel matrices. Narang *et al.* (1994) reported smaller analytical range of 5 to 35 mM for their glucose biosensor based on a sol-gel-derived platform using absorbance measurements. The absorbance values for glucose

concentration beyond 35 mM were not accurately determined introducing significant errors in the measurements.

The immobilised sol gel in polystyrene cuvettes utilised in the present study maintained its stability for at least 4 months in storage conditions 4 ^{0}C. These results offer certain advantages in comparison with other glucose sol-gel-based biosensors. For example, in a sol-gel vanadium pentaoxide glucose biosensor was only stable for 10 days at 4 ^{0}C (Glezer & Lev, 1993). Tatsu *et al.* (1992) presented a stability of at least 2 months for their glucose biosensor based on sol-gel method when stored desiccated at 4 ^{0}C. Also, Narang *et al.* (1994) reported a stability of 2 months for their glucose biosensor based on a sol-gel-sandwich platform. They presented a data table comparing the stability of their sensor in comparison with previous literature reports using different techniques for glucose oxidase immobilisation, e.g. covalent attachment with poly(vinylbutyral) gave 3 weeks stability, covalent attachment with cellulose acetate offered 3 months stability and an entrapment scheme with ferrocene-modified pyrrole polymer provided 2 days stability.

A reproducibility analysis was performed in Experimental Mode A, which indicated the improved performance of the current approach. The coefficient of variation for 5 replicate measurements of three different glucose concentrations of 5 mM, 15 mM and 30 mM were found to be equal to 3.2%, 2.7% and 2.9%, respectively, for tris(2,2'-bipyridyl) ruthenium(II) chloride hexahydrate at excitation wavelength of 410 nm and emission of 597 nm (Table 7.1); and 4.1%, 3.55% and 3.7%, for HPTS at excitation wavelength of 410 nm and fluorescence monitored at 507 nm (Table 7.2). In comparison with these values, Narang *et al.* (1994) reported 5% (n=5) reproducibility for a glucose biosensor

based on a sol-gel-glass matrix. In addition, other optical glucose biosensors gave similar reproducibility results such as Rosenzweig and Kopelman (1996) reported the reproducibility of an optical glucose biosensor, and in particular that the deviation between 10 consecutive measurements at a given glucose concentration was around 3%. Also, Schaffar and Wolfbeis (1990) reported approximately 5% reproducibility for their fibre-optic glucose biosensor.

In the present study using the sol-gel method, the response times of the biosensor appeared to be long (around 1 to 2 hours). This problem could be minimised using thinner sol-gel glass in the range of μm instead of approximately 3 mm used in the present immobilisation technique. A report has been published by Narang *et al.* (1994) using sol-gel films with thicknesses ranging from 0.10 to 1.00 μm and they observed that the response times became longer when the sol-gel films were made thicker.

Figures 7.6-7.9 showed that the activity of glucose oxidase in sol-gel matrix was close to its activity in the solution for the same concentration of the enzyme. For example, the experimental value ΔA/min (0.133) of 1 U/ml enzyme, immobilised with the sol-gel method in polystyrene cuvette, was close to the corresponding value of ΔA/min (0.148) of 1 U/ml glucose oxidase in solution following the same assay method (Figures 7.6-7.8). This was in contrast to results obtained with the glass cuvette with collagen membranes impregnation immobilisation method (Figure 7.9), where ΔA/min appeared to be very small (0.010) according to the calibration curve shown in Figure 7.7 especially considering the large amount of immobilised glucose oxidase. The activity of

glucose oxidase in sol-gel matrices after 4 months ageing in 4 ^{0}C remained 89% of the enzyme activity in a fresh solution, in comparison with the corresponding activity in collagen membranes during the ageing, which was found around 7% of the enzyme activity in solution. These results are close to previous literature reports. Audebert *et al.* (1993) reported that about 90% of the commercial glucose oxidase was active in water and this proportion fell to about 70-80% in polymeric silica sol matrix. Yamanaka *et al.* (1992) described lower activity of glucose oxidase in the sol-gel samples; approximately 20% activity was measured in comparison with that of a reference solution.

Finally, an analysis of precision was performed with human serum using Experimental Mode A in solution, which indicated the improved performance of the proposed approach. The coefficient of variation for 5 replicate measurements of three different added glucose concentrations of 2 mM, 6 mM and 12 mM in human serum were found to be 1.9%, 2.1% and 1.95%, respectively, for tris(2,2'-bipyridyl)ruthenium(II) chloride hexahydrate at excitation wavelength of 410 nm and emission of 597 nm (Table 7.3); and 2.5%, 1.7% and 2.4%, for HPTS at excitation wavelength of 410 nm and fluorescence monitored at 507 nm (Table 7.4).

Dubowski (1962) described an o-toluidine method for body-fluid glucose determination using absorbance and reported reproducibility of this method to within 4.5%. Also, an electrochemical blood-glucose sensor, the satellite G, in the low-normal and hypoglycaemic range, was described and the examination of repeatability of this sensor gave as mean coefficient of variation 7.2% (Tieszen *et al.*, 1993). The satellite G was a development from the ExacTech sensor (MediSense Inc, Abingdon, Oxon), which is a

portable pocket-sized and battery-operated commercial blood-glucose biosensor based on the measurement of blood-glucose as an electric current generated from a glucose oxidase reaction using ferrocene as a mediator; the magnitude of the current is proportional to the amount of glucose in the blood (Matthews *et al.*, 1987; Cardosi & Turner, 1990; Matthews *et al.*, 1991).

7.5 CONCLUSIONS

The results showed that the best immobilisation procedure was the sol-gel method. The study on cuvettes containing glucose oxidase and the fluorescent indicators immobilised using the sol-gel method, proved that both the enzyme and the indicators were securely immobilised, and confirmed recent reports that small molecules such as glucose diffused readily through the porous glass. This method differs from conventional methods for immobilisation of enzymes that require adsorption or covalent bonding to a glass surface. The sol-gel glass-encapsulation process does not require heating, it is easy and quick in preparation and the resulting glass matrix is transparent and porous with a high loading of enzyme, and chemical, thermal and dimensional stability. The encapsulated species are accessible to low molecular weight analytes, and their interactions may be monitored frequently by spectroscopic means.

Experimental Mode A provided meaningful results in human serum. The plots in Figures 7.11 and 7.12 were hyperbolas and obeyed the Michaelis-Menten equation (3.c) similarly to the results obtained in the solutions with glucose as described in Chapter 3 (Figures 3.6 and 3.7). In the experiments with human serum, the HPTS concentration was successfully modified in order to solve the problem of overlap of fluorescence from

the human serum. The Michaelis constants K_m appeared to be very close to those obtained for the solution experiments described in Section 3.3.2 and to those published in the literature (Gibson *et al.*, 1964; Bright & Gibson, 1967; Rogers & Brandt, 1971). The results from human serum analysis were promising and established the basis for the design of an accurate glucose biosensor, with two parameters contributing to the results of the measurement of glucose, based on the Experimental Mode A, as described in Sections 3.3.2 and 7.3.2.

Following the experimental work and analysis described in this chapter, it was concluded that the sol-gel immobilisation technique presents certain advantages for the construction of the proposed optical glucose biosensor for accurate measurements of blood-glucose concentrations using simultaneously two fluorescent indicators. This study has established the immobilisation of the glucose oxidase and the two fluorescent indicators in sol-gel films, for the construction of an optode and it merely requires to add "off the self" optoelectronics to realise a device, an optical blood-glucose biosensor.

A conceptual design of the optoelectronic circuit for implementation of Experimental Mode A is illustrated schematically in Figure 7.15 and can be described as follows: a light emitting diode (blue-LED) at 410 nm would be used as source, and two *p-n* diode as photodetectors for signals at 597 nm and 507 nm respectively. A single mode bifurcated fibre optic would be the connecting cable between the source, the photodetectors and the measuring probe (the distal end of the fibre where the sol-gel films are attached). After the manipulation and analysis of the signals and comparison with calibration curves in order to provide the value for glucose concentration, the result

would be shown on a digital display in mM units. The power supply could be a low cost lithium battery. The above assembly can be easily contained in a pocked-size portable device with low cost and easy operation.

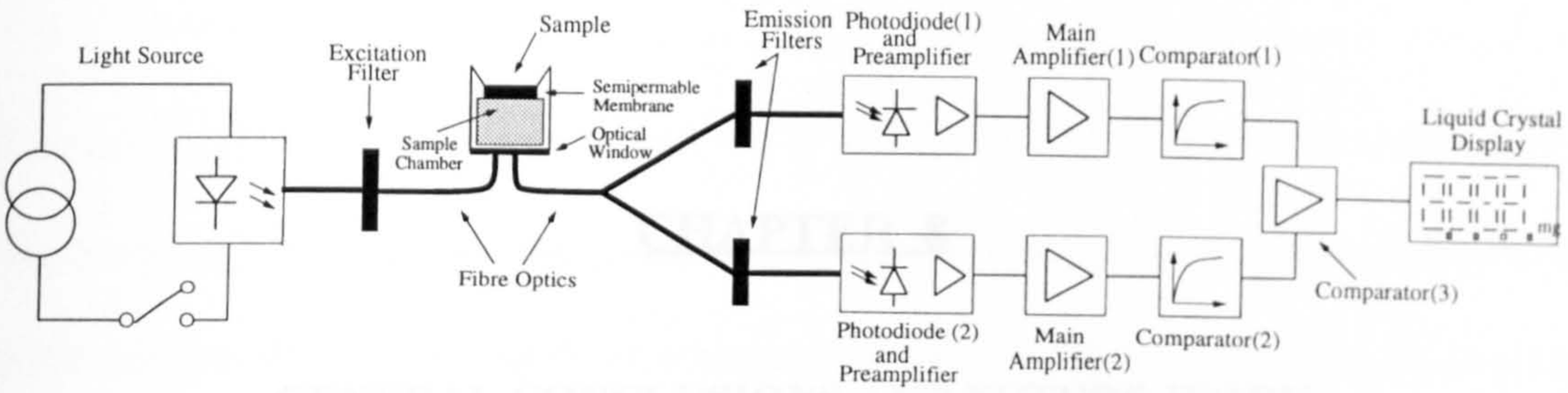

FIGURE 7.15 Block diagram of the optoelectronic circuit of the proposed biosensor (Experimental Mode A).

CHAPTER 8

GENERAL CONCLUSIONS AND FUTURE WORK

8.1 GENERAL CONCLUSIONS

The primary concern of this work was to progress the development of a fluorescence-based portable optical biosensor with improved operating range, stability and accuracy by measuring simultaneously changes in two indicator species (pH- and oxygen-dependent) generated by a single enzyme-catalysed reaction in response to one analyte; and the implementation of the above system using the sol-gel immobilisation technique.

The current approach differs from previously published work where only one indicator was employed per analyte. The measurement of two quantities simultaneously for the determination of the same analyte offers a novel feature and can contribute to the accuracy of the measurements by automatically cross-checking the two independent readings. The immobilisation of both fluorescent indicators and enzyme in the same support material is another novel feature which contributes towards the construction of a simpler and smaller portable biosensor. The general applicability of the proposed approach to a number of enzyme-catalysed oxidations was also demonstrated. The obtained characteristics of the proposed biosensor in terms of dynamic range, minimum detectable amount, repeatability, stability and absence of interference were similar or better than those previously reported for biosensors for the same substrates.

In Chapter 1, fluorescence-based pH and oxygen optical biosensors were discussed together with their advantages and disadvantages over conventional biosensors, and their applications. A recently published immobilisation technique appropriate for application in optical biosensors, the sol-gel method, was highlighted. In order to achieve the objective of this project, HPTS (1-hydroxypyrene-3,6,8-trisulfonic acid) and tris(2,2'-bipyridyl)

ruthenium(II) chloride hexahydrate were identified as the target fluorescent indicators. The catalytic oxidation of glucose by the enzyme glucose oxidase, and other biocatalysed oxidations of analytes such as lactate, xanthine and phenol were reviewed.

In Chapter 2, it was concluded that the two indicators proposed had no cross sensitivity when measured either separately or in the same solution, and would therefore be appropriate for the construction of the proposed biosensor based on an enzymatic oxidation. Substrate concentration may be assessed by simultaneously measuring two parameters: oxygen consumption, through the reduction of the fluorescence intensity of tris(2,2'-bipyridyl)ruthenium(II) chloride hexahydrate; and the production of acid, through pH changes affecting the fluorescence intensity of HPTS. The sensing method was based on the simultaneous excitation of the two fluorescent indicators with well-separated emission bands. The indicators, HPTS and tris(2,2'-bipyridyl)ruthenium(II) chloride hexahydrate, have shown quite different emission maxima (510 nm and 610 nm, respectively), where the spectral overlap and the efficiency of energy transfer of the two indicators appeared to be negligible. The utilisation of a common excitation wavelength offers the possibility to excite at one particular wavelength and to receive information for the fluorescence intensity of both indicators. It was found that there was no spectral interference between the separate indicators present in the same solution. Another important feature of the mixed solution containing both indicators, was that each indicator was specific for a given analyte (HPTS for pH changes and tris(2,2'-bipyridyl) ruthenium(II) chloride hexahydrate for oxygen) and they retained the same behaviour as when they were separate.

Chapter 3 describes the simultaneous utilisation of the two fluorescent indicators, HPTS and tris(2,2'-bipyridyl)ruthenium(II) chloride hexahydrate, in solution studies, in order to develop a novel optical fluorescence biosenor for the measurement of blood-glucose. This biosensor was based on the enzymatic oxidation of glucose using the enzyme glucose oxidase (GOD). Initial experiments were carried out in order to determine the fluorescence quenching of glucose oxidase itself due to the FAD (flavin adenine dinucleotide) coenzyme, and define the optimum concentration of this enzyme to be used in the kinetic measurement experiments.

A thorough spectroscopic study of the enzymatic oxidation of glucose was performed using glucose oxidase in solution in a cuvette, in the presence of both indicators. A number of combinations of excitation wavelengths were utilised (Experimental Modes A, B and C), in order to establish calibration curves with the optimum performance for glucose detection using kinetic measurements of the glucose oxidase reaction. The results obtained demonstrated that an optical fluorescence-based glucose biosensor using simultaneously oxygen-sensitive and pH-sensitive fluorescent indicators is feasible. The calibration curves in all Experimental Modes (Figures 3.6-3.7, 3.10 and 3.12-3.13) obeyed the Michaelis-Menten equation (3.c) and could be linearised using the Hanes plot (Figures 3.8-3.9, 3.11 and 3.14-3.15). The experimental values of Michaelis constant of the reaction appear to be close to the reported values in the literature.

The reproducibility of the measurements of the rate of change of the fluorescence intensity with time of tris(2,2'-bipyridyl)ruthenium(II) chloride hexahydrate, during the oxidation of

glucose, for different glucose concentrations, was very good for the range of concentrations of glucose found in normal and diabetic patients (1-20 mM). HPTS assays were very precise for low concentrations (i.e. 2 mM glucose) and less so for higher concentrations (i.e. 20 mM glucose). Another disadvantage of HPTS was that the changes in the fluorescence intensity for different glucose concentrations, were slow and the signal much lower in comparison with tris(2,2'-bipyridyl)ruthenium(II) chloride hexahydrate. The responce time for 90% of the total signal change was 1-2 min for both indicators. The lowest detectable amount of glucose was 1 μM using the fluorescence intensity of the oxygen-sensitive indicator, tris(2,2'-bipyridyl)ruthenium(II) chloride hexahydrate (fluorescence monitoring at 597 nm), and 100 μM using the fluorescence intensity of the pH-sensitive indicator, HPTS (fluorescence monitored at 507 nm). It was also observed that the signal was saturated for glucose concentrations over 50 mM, for both indicators.

The experimental results suggest that all three measurement modes could be utilised for glucose measurement. All Experimental Modes confirm the validity of the idea of using two indicators simultaneously for the analysis. Experimental Mode C presents the disadvantage of being complicated to construct because it requires the use of two simultaneously excited beams with independent wavelengths and as a consequence the use of two isolated light sources (e.g. LEDs). Experimental Mode B appears to offer the simplest design for the optical biosensor, but a small shift in the common excitation or emission wavelength, fluctuation in the light source or interference from the environment could produce errors because the measurements would be taken at the wrong wavelength. Experimental Mode A offers the most attractive solution for the construction of the proposed optical glucose biosensor as it requires only one fixed

excitation wavelength and the fluorescence can be measured at two separate wavelengths, where the maxima in emission of the two indicators occur, without interference and overlap between them.

In Chapter 4, a study of the fluorescence quenching of two indicators during the enzymatic oxidation of lactate is described. Lactate concentrations were measured by monitoring simultaneously the changes of fluorescence intensity of tris(2,2'-bipyridyl) ruthenium(II) chloride hexahydrate (due to oxygen consumption) and of HPTS due to changes in pH resulting from pyruvate production. The same excitation and emission wavelengths were selected as in Experimental Modes A and B (Chapter 3). Lactate oxidase, as a flavoprotein, appears to have fluorescent properties similar to those of glucose oxidase. An important consideration is that its fluorescence intensity was much lower than that of glucose oxidase for a similar range of concentrations.

The results from the application of both Experimental Modes A and B have shown that, in principle, the proposed method works and can provide a measuring system for detection and measurement of lactate in the range of 0.01-5 mM. The calibration curves obtained followed Michaelis-Menten kinetics.

In Chapter 5, the development of a new fibre-optic biosensor for the determination of xanthine was discussed. For this purpose, two different methods were presented, which were based on the phenomenon of fluorescence quenching. In the first method, the intrinsic fluorescence of xanthine itself was used to provide the analytical information without the use of indicators. The second method involved the fluorescent indicators,

tris(2,2'-bipyridyl)ruthenium(II) chloride hexahydrate and HPTS (Chapters 2 and 3), for the simultaneous detection of oxygen consumption and the pH changes (due to uric acid production). Experimental Modes A and B (Chapter 3) were applied in order to construct an optical biosensor for xanthine measurement, mainly for clinical purposes.

The first method, for determination of xanthine using an optical sensor, was based on the fluorescence properties of xanthine itself. For xanthine concentrations in the range of 0.01-10 mM, the measured fluorescence intensity against xanthine concentration appeared to be linear (Figures 5.2, 5.3 and 5.4). This type of linear response is remarkable and proves that in principle the proposed approach can be used for the direct measurement of xanthine using an isolated light source with fixed excitation at 335 nm and a photodetector with selective wavelength at 435 nm. One of the main drawbacks in this type of sensor is that the excitation wavelength belongs to the UV range and thus requires very good isolation of the light source and the sample from the user. Also, possible interference problems could be present in real samples, and this sensor has no specificity in contrast with the second proposed method which has the advantage of high specificity due to the enzyme xanthine oxidase.

From the experimental study of the enzyme, it was found that xanthine oxidase has a significant intrinsic fluorescence intensity in aqueous solution, depending on its concentration, due to the presence of FAD as coenzyme in its molecule. One important conclusion was that the optimum concentration of the enzyme, which was used for the purpose of kinetic measurements, did not interfere with the fluorescence intensity from the specific concentrations of both indicators.

From the experimental investigation using the second method, it was found that the uric acid which appears as a product of the oxidation, was not fluorescent and thus its presence did not affect the resulting signal. The study of the kinetics of the reaction, provided a Michaelis constant which was close to the values reported in the literature for both modes. The reaction was completed very rapidly, as was observed during the spectroscopic measurements of fluorescence against time. This approach could be used to detect small amounts of xanthine in the range of 1-100 μM. When the concentration exceeded 0.5 mM saturation of the reaction occurred. Both Experimental Modes A and B could be used for the measurement of xanthine and would offer similar characteristics in a fluorescence-based optical biosensor for xanthine.

In Chapter 6, a fluorescence-based optical phenol biosensor using polyphenol oxidase was described. Polyphenol oxidase catalyses the oxidation of phenols to catechols and then to quinones, and therefore, phenol concentrations can be measured by monitoring oxygen consumption during the above oxidation utilising an oxygen-sensitive fluorescent indicator, the well-known, tris(2,2'-bipyridyl)ruthenium(II) chloride hexahydrate. The oxidation of phenol belongs to the few exceptional oxidations where there is no production of hydrogen peroxide during the reaction. In addition, the production of quinones does not significantly affect pH, in contrast with the previously studied oxidations of glucose, lactate and xanthine where the production of an acid occurred. For the above reasons, it was not possible to use the same experimental Modes as in previous chapters (Chapters 3, 4, and 5) for the detection of phenol. Hence, it was proposed to use only the oxygen-sensitive indicator, tris(2,2'-bipyridyl)ruthenium(II) chloride hexahydrate, and not the pH-sensitive indicator, HPTS.

Initial experiments were carried out in solution where measurements of the kinetics of the polyphenol oxidase reaction were carried out in the presence of tris(2,2'-bipyridyl) ruthenium(II) chloride hexahydrate. They were followed by additional experiments with polyphenol oxidase and the oxygen-sensitive indicator tris(2,2'-bipyridyl) ruthenium(II) chloride hexahydrate immobilised using the sol-gel encapsulation method. The sol-gel immobilisation technique presented certain advantages for the construction of the proposed optical biosensor including easy preparation, enhanced stability features and utility for optical methods because of its transparency and porosity.

The spectroscopic analysis of polyphenol oxidase showed that both the enzyme, and the substrate, phenol, did not present fluorescence properties in the visible range and no interference with the indicator from the enzyme and the substrate during the oxidation of phenol would be expected. The major disadvantage of this biosensor was the absence of high specificity and selectivity which did not allow the classification of a detected phenolic compound. Therefore, the present biosensor could be used only for measuring very low levels of phenols (ppb) in aquatic environmental samples and not to determine the particular type of phenol.

In Chapter 7, the application and characterisation of immobilisation techniques for the fluorescence-based optical blood-glucose biosenor described in Chapter 3 (solution studies) was presented. Four different immobilisation procedures such as covalent, adsorption, aggregation and sol-gel encapsulation were employed to produce the appropriate supports for the enzyme glucose oxidase and the two indicators. In the first three procedures only glucose oxidase was immobilised, and in the last the enzyme was

immobilised together with both indicators. All three Experimental Modes studied in Chapter 3, were applied in order to establish calibration curves with the optimum performance for the proposed biosensor. In addition, the advantages of the microcapsulation sol-gel method over conventional immobilisation techniques for application in an optical biosensor were presented. The results showed that the best immobilisation procedure was the sol-gel method. The study of the optically transparent silica glass polystyrene cuvettes, containing glucose oxidase and the two fluorescent indicators, synthesised using the sol-gel method, proved that both the enzyme and the indicators were securely immobilised, and that small molecules such as glucose diffused readily through the porous glass. The sol-gel glass-encapsulation process offers easy and quick preparation and the resulting glass matrix is transparent and porous with high loading of enzyme and chemical, thermal and dimensional stability.

Finally, additional solution experiments were conducted in order to evaluate the implementation and performance of Experimental Mode A when used for the detection and measurement of glucose concentration in biological samples such as human serum, instead of the buffer solution. In the experiments with human serum, the HPTS concentration was successfully modified in order to solve the problem of overlap of fluorescence from the human serum. The results from human serum analysis were promising and established the basis for the design of an accurate glucose biosensor, with two parameters contributing to the results of the measurement of glucose, based on Experimental Mode A.

Following the experimental work and analysis, it was concluded that the sol-gel immobilisation technique presents certain advantages for the construction of the proposed optical glucose biosensor for accurate measurements of blood-glucose concentrations using simultaneous measurement of two fluorescent indicators. This study has established the immobilisation of the glucose oxidase and the two fluorescent indicators in sol-gel films, for the construction of an optode. Finally a design for the optoelectronic biosensor was proposed.

8.2 FUTURE WORK

Further studies on the precise construction of the proposed fluorescence-based optical biosensor are obviously required, followed by construction of a prototype and a detailed evaluation of its performance. In addition, other types of pH-dependent fluorescent indicators could be envisaged. In particular as mentioned in Chapter 3, HPTS has the disadvantage that the changes in the fluorescence intensity during an oxidation, are slow and the signal slightly more unsteady in comparison with tris(2,2'-bipyridyl)ruthenium(II) chloride hexahydrate. An alternative solution would be the investigation of another pH-dependent fluorescent indicator with better characteristics, i.e. fluorescein, instead of HPTS. Like HPTS, fluorescein has an excitation maximum at 480 and emission maximum at 510 nm, which do not overlap the emission band of tris(2,2'-bipyridyl)ruthenium(II) chloride hexahydrate.

As was mentioned in Chapter 3, Experimental Mode B offers the simplest instrumental design, using one light source and one photodetector. However, there are still uncertainties concerning this Mode because only one measurement is taken (in the common emission

wavelength) instead of two as in the case of Experimental Modes A and C. As a consequence, it is not clear whether this approach is superior than using only one indicator as in most applications of fluorescence-based optical biosensors. For the above reason, further experimental and theoretical investigation is required in order to assess the feasibility of this Mode.

Also, further studies are required in cases of lactate and xanthine, in order to confirm the applicability of the detection method when both the indicators and the enzyme are immobilised using the Experimental Modes A, B and C, especially with the implementation of the sol-gel method used in the case of phenol and glucose.

During the sol-gel immobilisation experiments, certain advantages of this method were identified. However, long response times (1 to 2 hours) were required which is not a favourable characteristic for the design of a portable biosensor. Future experiments can be performed to investigate this problem by using sol gel layers of different thickness, or by improving the immobilisation method itself (i.e. using a sol-gel sandwich technique taking as reference the one reported by Narang *et al.*, 1994).

REFERENCES

Abdel-Latif, M.S. & Guilbault, G.G. (1988). Fiber-optic sensor for the determination of glucose using micellar enhanced chemiluminescence of the peroxyoxalate reaction. *Anal. Chem.* **60,** 2671-2674.

Abdel-Latif, M.S., Suleiman, A.A. & Guilbault, G.G. (1988). Enzyme-based fiber optic sensor for glucose determination. *Analytical Letters* **21,** 943-951.

Adams, E.C., Mast, R.L. & Free, A.H. (1960). Specificity of glucose oxidase. *Arch. Biochem. Biophys.* **91,** 230-234.

Albisser, A.M. (1982). Insulin delivery systems: Do they need a glucose sensor? *Diabetes Care* **5,** 166-173.

Albisser, A.M., Ellman, J., Hanna, A., Goriya, Y. & Minuk, H. (1978). Continuous blood sampling and glucose analysis in vitro and in vivo. *Diabetologia* **15,** 303-308.

Andres, K.-D., Wehnert, G., Thordsen, O., Scheper, T., Rehr, B. & Sahm, H. (1993). Biotechnological applications of fiber-optic sensing: multiple uses of a fiber-optic fluorimeter. *Sensors and Actuators B* **11,** 395-403.

Angel, S.M. (1987). Optrodes: Chemically selective fiber-optic sensors. *Spectroscopy* **2,** 38-48.

Arana, G., Etxebarria, N. & Fernandez, L.A. (1994). Potentiometric determination of the protonation constants of some phenols in 1.0 mol/L NaCl at 25 ^{0}C. *Fresenius'Journal of Analytical Chemistry* **349,** 703-707.

Arin, M.J., Diez, M.T., Resines, J.A. & Alemany, M.T. (1990). Quantitative estimation of urinary metabolites in ruminants by high-performance liquid chromatography. *J. Liq. Chromatogr.* **13,** 2465-2473.

Arnold, M.A. (1990). Fiber-optic biosensors. *Journal of Biotechnology* **15,** 219-228.

Arnold, M.A. & Small, G.W. (1990). Determination of physiological levels of glucose in an aqueous Matrix with digitally filtered fourier transform near-infrared spectra. *Anal. Chem.* **62,** 1457-1464.

Atanasov, P. & Wilkins, E. (1994). Biosensor for continuous glucose monitoring. *Biotechnology and Bioengineering* **43,** 262-266.

Atkinson, M.A. & Maclaren, N.K. (1990). What causes diabetes? *Scientific Am.* **7,** 62-71.

Audebert, P., Demaille, C. & Sanchez, C. (1993). Electrochemical probing of the activity of glucose oxidase embedded sol-gel matrices. *Chemistry of Materials. American Chemical Society.* **5,** 911-913.

Aussenegg, F.R., Lippitsch, M.E. & Riegler, M. (1986). Picosecond spectroscopy of photoreceptor molecules. *Laser Chem.* **6,** 269-289.

Bacon, J.R. & Demas, J.N. (1987). Determination of oxygen concentrations by luminescence quenching of a polymer-immobilized transition metal complex. *Anal. Chem.* **59,** 2780-2785.

Bambot, S.B., Holavanahali, R., Lakowicz, J.R., Carter, G.M. & Rao, G. (1994). Phase fluorometric sterilizable optical oxygen sensor. *Biotechnology and Bioengineering* **43,** 1139-1145.

Bates, R.G. & Bower, V.E. (1956). Alkaline solutions for pH control. *Anal. Chem.* **28,** 1322-1324.

Bennetto, H.P., Box, J., Delaney, G.M., Mason, J.R., Roller, S.D., Stirling, J.L. & Thurston, C.F. (1987). Redox-mediated electrochemistry of whole micro-organisms: from fuel cells to biosensors. In: *Biosensors: Fundamentals and Applications,* pp 303-314. Eds. A. P. F. Turner, I. Karube and G. S. Wilson. Oxford University Press, New York.

Bergman, I. (1968). Rapid-response atmospheric oxygen monitor based on fluorescence quenching. *Nature* **218,** 396-399.

Berlman, I.B. (1971). *Handbook of fluorescence spectra of aromatic molecules.* pp 67-95. Second Edition. Academic Press, Inc., New York.

Betts, P., Buckley, M., Davies, R., McEvilly, E. & Swift, P. (1996). The care of young people with diabetes. *Diabetic Medicine* **13,** S54-S59.

Bhattacharya, P. (1994). *Semiconductor optoelectronics devices.* pp 466-495. Prentice-Hall International Inc., Englewood Cliffs, New Jersey.

Bindra, D.S., Zhang, Y., Wilson, G.S., Sternberg, R., Thevenot, D.R., Moatti, D. & Reach, G. (1991). Design and *in vitro* studies of a needle-type glucose sensor for subcutaneous monitoring. *Anal. Chem.* **63,** 1692-1696.

Blackburn, G.M. & Gait, M.J. (1990). *Nucleic acids in chemistry and biology.* pp 142-148. IRL Press, Oxford.

Blaedel, W.J. & Engstrom, R.C. (1980). Reagentless enzyme electrodes for ethanol, lactate, and malate. *Anal. Chem.* **52,** 1691-1697.

Blair, T.L., Yang, S.-T., Smith-Palmer, T. & Bachas, L.G. (1994). Fiber optic sensor for Ca^{2+} based on induced change in the conformation of the protein calmodulin. *Anal. Chem.* **66,** 300-302.

Blum, L.J. & Gautier, S.M. (1991). Bioluminescence- and chemiluminescence-based fiberoptic sensors. In: *Biosensor principles and applications,* pp 213-247. Eds. L. J. &. C. Blum P.R. Marcel Dekker Inc., New York.

Blum, L.J., Gautier, S.M. & Coulet, P.R. (1989). Design of luminescence photobiosensors. *Journal of Bioluminescence and Chemiluminescence* **4,** 543-550.

Bock, C.R., Meyer, T.J. & Whitten, D.G. (1975). Photochemistry of transition metal complexes. The mechanism and efficiency of energy conversion by electron-transfer quenching. *J. Am. Chem. Soc.* **97,** 2909-2911.

Boisde, G., Blanc, F. & Perez, J.-J. (1988). Chemical measurements with optical fibers for process control. *Talanta* **35,** 75-82.

Boisde, G. & Perez, J.J. (1987). Miniature chemical optical fiber sensors for pH measurements. *SPIE, Fiber Optic Sensors II* **798,** 238-245.

Bonakdar, M., Vilchez, J.L. & Mottola, H.A. (1989). Bioamperometric sensors for phenol based on carbon paste electrodes. *J. Electroanal. Chem.* **266,** 47-55.

Borman, S.A. (1981). Optrodes. *Anal. Chem.* **53,** 1616A-1620A.

Bower, V.E. & Bates, R.G. (1955). pH Values of the Clark and Lubs buffer solutions at 25^0C. *Journal of Research of the National Bureau of Standards.* **55,** 197-200.

Braun, S., Rappoport, S., Zusman, R., Avnir, D. & Ottolenghi, M. (1990). Biochemically active sol-gels glasses: the trapping of enzymes. *Materials Letters* **10,** 1-5.

Bright, H.J. & Gibson, Q.H. (1967). The oxidation of 1-deuterated glucose by glucose oxidase. *The Journal of Biological Chemistry* **242,** 994-1003.

Brinker, C.J. & Scherer, G.W. (1990). *Sol-gel science. The physics and chemistry of sol-gel processing.* pp 839-870. Academic Press, Inc., San Diego.

Brooks, S.L., Higgins, I.J., Newman, J.D. & Turner, A.P.F. (1991). Biosensors for process control. Review. *Enzyme Microb. Technol.* **13,** 946-955.

Broun, G.B. (1976). Chemically aggregated enzymes. In: *Immobilized enzymes.,* pp 272-273. Eds. K. Mosbach. Academic Press, Inc., New York.

Browne, C.A., Tarrant, D.H., Olteanu, M.S., Mullens, J.W. & Chronister, E.L. (1996). Intrinsic sol-gel clad fiber-optic sensors with time-resolved detection. *Anal. Chem.* **68,** 2289-2295.

Buchholz, K. & Klein, J. (1987). Characterization of immobilized biocatalysts. In: *Methods in Enzymology,* pp 3-30. Eds. K. Mosbach, S. P. Colowick and N. O. Kaplan. Academic Press, San Diego.

Burstall, F.H. (1936). Optical activity dependent on co-ordinated bivalent ruthenium. *J. Chem. Soc.* , 173-175.

Burt, J.R. (1977). Hypoxanthine: a biochemical index of fish quality. *Process Biochem.* **12,** 32-35.

Caraway, W.T. (1976). Carbohydrates. In: *In Fundamentals of Clinical Chemistry.,* pp 234-263. Ed. N. W. Tietz. Saunders Co., Philadelphia.

Cardosi, M.F. & Turner, A.P.F. (1990). Recent advances in enzyme-based electrochemical glucose sensors. In: *The Diabetes Annual.* pp 254-272. Eds. K.G.M.M. Alberti and L.P. Krall. Elsevier, Amsterdam.

Carr, P.W. & Bowers, L.D. (1980). *Immobilized enzymes in analytical and clinical chemistry. Fundamentals and applications.* Volume 56, pp 148-191. John Wiley & Sons, New York.

Carraway, E.R., Demas, J.N., DeGraff, B.A. & Bacon, J.R. (1991). Photophysics and photochemistry of oxygen sensors based on luminescence transition-metal complexes. *Anal. Chem.* **63,** 337-342.

Chaimowicz, J.C.A. (1989). *Lightwave technology: An introduction.* pp 89-118. Butterworth & Co. Ltd, London.

Chibata, I. (1978). *Immobilized enzymes. Research and development.* pp 9-92. John Wiley & Sons, New York.

Chung, K.E., Lan, E.H., Davidson, M.S., Dunn, B.S., Valentine, J.S. & Zink, J.I. (1995). Measurement of dissolved oxygen in water using glass-encapsulated myoglobin. *Anal. Chem.* **67,** 1505-1509.

Ciccoli, P., Cecinato, A., Brancaleoni, E. & Frattoni, M. (1992). Identification and quantitative evaluation of C4-C14 volalite organic compounds in some ubran, suburban and forest sites in Italy. *Fresenius Environmental Bulletin* **1,** 73-78.

Claremont, D.J. (1987). Biosensors: clinical requirements and scientific promise. *Journal of Medical Engineering & Technology* **11,** 51-56.

Clark, D.J., Blake-Coleman, B.C. & Calder, M.R. (1987). Principles and potential of piezo-electric transducers and acoustical techniques. In: *Biosensors: Fundamentals and Applications.*, pp 551-571. Eds. A. P. F. Turner, I. Karube and G. S. Wilson. Oxford University Press, New York.

Collison, M.E. & Meyerhoff, M.E. (1990). Chemical sensors for bedside monitoring of critically III patients. *Anal. Chem.* **62,** 425A-437A.

Connolly, P. (1995). Clinical diagnostics opportunities for biosensors and bioelectronics. *Biosensors & Bioelectronics* **10,** 1-6.

Cordier, D., Dumaine-Bouaziz, M. & Coulet, P.R. (1995). Toward biomimetic sensors: A fluorescent artificial macrocyclophanic receptor for the quantification of Zn(II). *Analytical Letters* **28,** 959-969.

Cornish-Bowden, A. (1995). *Fundamentals of enzyme kinetics.* pp 30-37. Second Edition. Portland Press Ltd., London.

Coughlan, M.P., Kierstan, M.P.J., Border, P.M. & Turner, A.P.F. (1988). Analytical applications of immobilised proteins and cells. *Journal of Microbiological Methods* **8,** 1-50.

Coulet, P.R. (1991). Electrochemical and fiber optic biosensors for highly selective molecular targeting. *Analytical Letters* **24,** 1333-1345.

Coulet, P.R. (1992). Polymeric membranes and coupled enzymes in the design of biosensors. *Journal of Membrane Science* **68,** 217-228.

Coulet, P.R. & Bardeletti, G. (1991). Biosensors: Biosensor-based instrumentation. *Biochemical Society Transactions* **19,** 1-4.

Coulet, P.R., Blum, L.J. & Gautier, S.M. (1993). Luminescence-based fibre-optic probes. *Sensors and Actuators B* **11,** 57-61.

Coulthard, C.E., Michaelis, R., Short, W.F., Skrimshire, G.E.H., Standfast, A.F.B., Birkinshaw, J.H. & Raistrick, H. (1945). An antibacterial glucose aerohydrogenes from *Penicillium notatum* Westling. *Nature* **150,** 634-635.

Cox, M.E. & Dunn, B. (1985). Detection of oxygen by fluorescence quenching. *Applied Optics* **24,** 2114-2120.

Cullen, D.C., Sethi, R.S. & Lowe, C.R. (1990). Multi-analyte miniature conductance biosensor. *Analytica Chimica Acta* **231,** 33-40.

Dave, B.C., Dunn, B., Valentine, J.S. & Zink, J.I. (1994). Sol-gel encapsulation methods for biosensors. *Anal. Chem.* **66,** 1120A-1127A.

DCCT Research Group. (1993). The effect of intensive treatment of diabetes on the development and progression of long-term complications in insulin-dependent diabetes mellitus. *The New England Journal of Medicine* **329,** 977-986.

DeGraff, B.A. & Demas, J.N. (1994). Direct measurement of rotational correlation times of luminescent ruthenium(II) molecular probes by differential polarized phase fluorimetry. *J. Phys. Chem.* **98,** 12478-12480.

Dempsey, E., Wang, J. & Smyth, M.R. (1993). Electropolymerised *o*-phenylenediamine film as means of immobilising lactate oxidase for a L-lactate biosensor. *Talanta* **40,** 445-451.

Denney, R.C. & Sinclair, R. (1987). *Visible and ultraviolet spectroscopy.* pp 1-55. John Wiley & Sons, Chichester.

Dennison, M.J., Hall, J.M. & Turner, A.P.F. (1995). Gas-phase microbiosensor for monitoring phenol vapor at ppb levels. *Anal. Chem.* **67,** 3922-3927.

Dill, K.A. (1990). Dominant forces in protein folding. *Biochemistry. American Chemical Society* **29,** 7133-7155.

Downey, T.M. & Nieman, T.A. (1992). Chemiluminescence detection using regenerable tris(2,2'-bipyridyl)ruthenium(II) immobilized in nafion. *Anal. Chem.* **64,** 261-268.

Dransfeld, I., Hintsche, R., Moritz, W., Pham, M.T., Hoffman, W. & Hueller, J. (1990). Biosensors for glucose and lactate using fluoride ion sensitive field effect transistors. *Analytical Letters* **23,** 437-450.

Draxler, S. & Lippitsch, M.E. (1996). Lifetime-based sensing: Influence of the microenvironment. *Anal. Chem.* **68,** 753-757.

Draxler, S., Lippitsch, M.E., Klimant, I., Kraus, H. & Wolfbeis, O.S. (1995). Effects of polymer matrices on the time-resolved luminescence of a ruthenium complex quenched by oxygen. *J. Phys. Chem.* **99,** 3162-3167.

Draxler, S., Lippitsch, M.E. & Leiner, M.J.P. (1993). Optical pH sensors using fluorescence decay time. *Sensors and Actuators B* **11,** 421-424.

Dremel, B.A.A., Li, S.-Y. & Schmid, R.D. (1992). On-line determination of glucose and lactate concentrations in animal cell culture based on fibre optic detection of oxygen in flow-injection analysis. *Biosensors & Bioelectronics* **7,** 133-139.

Dremel, B.A.A., Schaffar, B.P.H. & Schmid, R.D. (1989a). Determination of glucose in wine and fruit juice based on a fibre-optic glucose biosensor and flow-injection analysis. *Analytica Chimica Acta* **225,** 293-301.

Dremel, B.A.A., Trott-Kriegeskorte, G., Schaffar, B.P.H. & Schmid, R.D. (1989b). L-lactic acid determination in milk products based on a fibre optic biosensor and Flow Injection Analysis (FIA). In: *Biosensors Applications in Medicine, Environmental Protection and Process Control.*, pp 225-228. Eds. R. D. Schmid and F. Scheller. VCH, Braunschweig.

Drugov, Y.S. & Muraveva, G.V. (1991). Analysis of air pollutants of a typical industrial region. *Zhurnal Analititicheskoi Khimi* **46,** 2014-2020.

Dubowski, K.M. (1962). An o-toluidine method for body-fluid glucose determination. *Clinical Chemistry* **8,** 215-235.

Duckworth, H.W. & Coleman, J.E. (1970). Physicochemical and kinetic properties of mushroom tyrosinase. *The Journal of Biological Chemistry* **245,** 1613-1625.

Duke, F.R., Weibel, M., Page, D.S., Bulgrin, V.G. & Luthy, J. (1969). The glucose oxidase mechanism: enzyme activation by substrate. *J. Am. Chem. Soc.* **91,** 3904-3909.

Dunbar, R.A., Jordan, J.D. & Bright, F.V. (1996). Development of chemical sensing platforms based on sol-gel-derived thin films: origin of film age vs performance trade-offs. *Anal. Chem.* **68,** 604-610.

Dunn, B. & Zink, J.I. (1991). Optical properties of sol-gel glasses doped with organic molecules. Feature article. *J. Mater. Chem.* **1,** 903-913.

Edmonds, T.E., Flatters, N.J., Jones, C.F. & Miller, J.N. (1988). Determination of acid-base indicators: implications for optical fibre probes. *Talanta* **35,** 103-109.

Eichel, H.J. & Rem, L.T. (1962). Respiratory enzyme studies in Tetrahymena pyriformis. *The Journal of Biological Chemistry* **237,** 940-945.

Eisenthal, R. & Danson, M.J. (1993). *Enzyme assays. A practical approach.* pp 1-53. Oxford University Press Inc., New York.

Ellerby, L.M., Nishida, C.R., Nishida, F., Yamanaka, S.A., Dunn, B., Valentine, J.S. & Zink, J.I. (1992). Encapsulation of proteins in transparent porous silicate glasses prepared by the sol-gel method. *Science* **255,** 1113-1115.

Esders, T.W. & Goodhue, C.T. (1980) Process and composition for the quantification of glycerol ATP and triglycerides. United States Patent 4,241,178. Dec. 23. Eastman Kodak Company, Roschester, New York.

Estrada, P., Sanchez-Muniz, R., Acebal, C., Arche, R. & Castillon, M.P. (1991). Characterization and optimization of immobilized polyphenol oxidase in low-water organic solvents. *Biotechnology and Applied Biochemistry* **14,** 12-20.

Fawell, J.K. & Hunt, S. (1988). *Environmental toxicology: Organic pollutants.* Chapt. 19, pp 399-406. John Wiley & Sons, Chichester.

Fischer, U. (1991). Fundamentals of glucose sensors. *Diabetic Medicine* **8,** 309-321.

Forster, T. (1950a). Die pH-abhangigkeit der fluoreszenz von naphthalinderivaten. *Zeitschrift fur Elektrochemie* **54,** 531-535.

Forster, T. (1950b). Elektrolytische dissoziation angeregter molekule. *Zeitschrift fur Elektrochemie* **54,** 42-46.

Foster, D.W. (1989). Diabetes Mellitus. In: *The Metabolic basis of inherited disease,* pp 375-397. Eds. C. R. Scriver, A. L. Beaudet, W. S. Sly and D. Valle. McGraw-Hill, New York.

Foster, D.W. & McGarry, J.D. (1983). The metabolic derangements and treatment of diabetic ketoacidosis. *New Engl. J. Med.* **309,** 159-169.

Freeman, M.K. & Bachas, L.G. (1992). Fiber-optic biosensor with fluorescence detection based on immobilized alkaline phosphatase. *Biosensors & Bioelectronics* **7,** 49-55.

Frew, J.E. & Hill, H.A.O. (1987). Electrochemical biosensors. *Anal. Chem.* **59,** 933A-944A.

Furbee, J.W., Kuwana, T. & Kelly, R.S. (1994). Fractured carbon fiber-based biosensor for glucose. *Anal. Chem.* **66,** 1575-1577.

Furlinger, E. (1982). A Spectroscopic study on fluorescent pH indicators and their immobilisation on polymeric supports. PhD thesis, University of Graz, Austria.

Gabor, G. & Walt, D.R. (1991). Sensitivity enhancement of fluorescent pH indicators by inner filter effects. *Anal. Chem.* **63,** 793-796.

Galban, J., De Marcos, S. & Castillo, J.R. (1993). Fluorometric-enzymatic lactate determination based on enzyme cytochrome b_2 fluorescence. *Anal. Chem.* **65,** 3076-3080.

Gauillard, F., Richard-Forget, F. & Nicolas, J. (1993). New spectrophotometric assay for polyphenol oxidase activity. *Analytical Biochemistry* **215,** 59-65.

Gehrich, J.L., Lubbers, D.W., Opitz, N., Hansmann, D.R., Miller, W.W., Tusa, J.K. & Yafuso, M. (1986). Optical fluorescence and its application to an intravascular blood gas monitoring system. *IEEE Trans. BioMed. Eng.* **33,** 117-122.

Genovesi, L., Pedersen, H. & Sigel, G.H. (1988). The development of a generic hydrogen peroxide sensor with application to the detection of glucose. *SPIE, Chemical, Biochemical and Environmental Applications of Fibers* **990,** 22-27.

Gibson, Q.H., Swoboda, B.E.P. & Massey, V. (1964). Kinetics and mechanism of action of glucose oxidase. *Journal of Biological Chemistry* **239,** 3937-3934.

Glezer, V. & Lev, O. (1993). Sol-gel vanadium pentaoxide glucose biosensor. *J. Am. Chem. Soc.* **115,** 2533-2534.

Gomori, G. (1955). Preparation of buffers for use in enzymes studies. In: *Methods in Enzymology. Vol.I,* pp 138-146. Eds. S. P. C. &. N. O. Kaplan. Academic Press Inc., New York.

Gonzalez, E., Pariente, F., Lorenzo, E. & Hernandez, L. (1991). Amperometric sensor for hypoxanthine and xanthine based on the detection of uric acid. *Anal. Chim. Acta* **242,** 267-273.

Gopel, W., Jones, T.A., Kleitz, M., Lundstrom, I. & Seiyama, T. (1992). Chemical and biochemical sensors. Part II. In: *Sensors: A Comprehensive Survey.,* pp 2-41. Eds. W. Gopel, J. Hesse and J. N. Zemel. VCH Verlagsgesellschaft mbH, Weinheim.

Granner, D.K. & O'Brien, R.M. (1992). Molecular physiology and genetics of NIDDM. Importance of metabolic staging. *Diabetes Care* **15,** 369-395.

Gratzel, M. (1982). Artificial photosynthesis, light driven electron transfer processes in organized molecular assemblies and colloidal semiconductors. *Pure & Appl. Chem.* **54,** 2369-2382.

Green, J.H. (1976). *An introduction to Human Physiology.* pp 134-137. Fourth Edition. Oxford University Press, London.

Greenough, K.R., Skillen, A.W. & McNeil, C.J. (1994). Potential glucose sensor for perioperative blood glucose control in diabetes mellitus. *Biosensors & Bioelectronics* **9,** 23-28.

Guilbault, G.G. (1992). *Practical Fluorescence.* pp 1-37. Second Edition. Marcel Dekker, Inc., New York.

Gunasingham, H. & Tan, C.-H. (1992). Electrochemically modulated optrode for glucose. *Biosensors & Bioelectronics* **7,** 353-359.

Haemmerli, S.D., Suleiman, A.A. & Guilbault, G.G. (1990). Amperometric determination of hypoxanthine and inosine by use of enzyme sensor based on a Clark-type hydrogen peroxide or oxygen electrode. *Anal. Letters* **23,** 577.

Halfpenny, A.P. & Brown, P.R. (1985). Simultaneous HPLC assay of the activities of erythrocytic hypoxanthine-guanine phosphoribosyl transferase and purine nucleoside phosphorylase. *J. Chromat.* **349,** 275-282.

Hall, G., Best, D. & Turner, A.P.F. (1988). The determination of *p*-cresol in chloroform with an enzyme electrode used in the organic phase. *Analytica Chimica Acta* **213,** 113-117.

Harris, D.A. & Bashford, C.L. (1987). *Spectrophotometry & Spectrofluorimetry.* pp 1-27. IRL Press Ltd., Oxford.

Hartmann, P., Leiner, M.J.P. & Lippitsch, M.E. (1995). Luminescence quenching behavior of an oxygen sensor based on a Ru(II) complex dissolved in polystyrene. *Anal. Chem.* **67,** 88-93.

Heinz, F. & Reckel, S. (1983). Xanthine oxidase. Xanthine: oxygen oxidoreductase, EC 1.2.3.2. In: *Methods of Enzymatic Analysis. Volume III. Enzymes 1: Oxidoreductases, Transferases.*, pp 210-216. Eds. J. B. a. M. G. H. U. Bergmeyer. Verlag Chemie GmbH, Weinheim.

Hench, L.L. & West, J.K. (1990). The sol-gel process. *Chemical Reviews* **90,** 33-72.

Higgins, I.J. & Lowe, C.R. (1987). Introduction to the principles and applications of biosensors. *Phil. Trans. R. Soc. Lond. B* **316,** 3-11.

Hlavay, J., Haemmerli, S.D. & Guilbault, G.G. (1994). Fibre-optic biosensor for hypoxanthine and xanthine based on a chemiluminescence reaction. *Biosensors & Bioelectronics* **9,** 189-195.

Houssay, B.A., Lewis, J.T., Orias, O., Braun-Menendez, E., Hug, E., Foglia, V.F. & Leloir, L.F. (1955). *Human Physiology.* pp 466-469. Second Edition. Mc Graw-Hill Book Company Inc., New York.

Hulst, A.C. & Tramper, J. (1989). Immobilized plant cells: A literature survey. *Enzyme Microb. Technol.* **11,** 546-558.

Ishiji, T. & Kaneko, M. (1990). Luminescence characteristics of tris(2,2'-bipyridine)ruthenium(II) complex adsorbed in a Nafion film. *Kobunshi Ronbunshu* **47,** 869-873.

Ishiji, T., Kudo, K. & Kaneko, M. (1994). Microenvironmental studies of an $Ru(bpy)_3^{2+}$ luminescent probe incorporated into Nafion film and its application to an oxygen sensor. *Sensors and Actuators B* **22,** 205-210.

Ismail, K.Z. & Weber, S.G. (1991). Tris(2,2'-bipyridine)ruthenium(II) as a peroxide-producing replacement for enzymes as chemical labels. *Biosensors & Bioelectronics* **6,** 699-705.

Janata, J. (1987). Do optical sensors really measure pH? *Anal. Chem.* **59,** 1351-1356.

Janata, J. (1992). Chemical sensors. *Anal. Chem.* **64,** 196R-219R.

Janata, J., Josowicz, M. & Michael DeVaney, D. (1994). Chemical sensors. Review. *Anal. Chem.* **66,** 207R-228R.

John, P., McQuat, E.R. & Soutar, I. (1982). Fluorescence cell design and use to determine crude oil in water. *Analyst* **107,** 221-223.

Jordan, D.M., Walt, D.R. & Milanovich, F.P. (1987). Physiological pH fiber-optic chemical sensor based on energy transfer. *Anal. Chem.* **59,** 437-439.

Kaneko, M., Iwahata, S. & Asakura, T. (1992). Quenching of photoexcited 4,4'-dicarboxy-2,2'-bipyridinebis(2,2'-bipyridine) ruthenium(II) by oxygen in aqueous solution and in silk fibroin membrane. *Photochem. Photobiol.* **55,** 505-509.

Karube, I. & SangMok Chang, M.E. (1991). Microbial biosensors. In: *Biosensor Principles and Applications,* pp 267-301. Eds. L. J. Blum and P. R. Coulet. Marcel Dekker, Inc., New York.

Kauffmann, J.M. & Guilbault, G.G. (1991). Potentiometric enzyme electrodes. In: *Biosensor Principles and Applications,* pp 67-82. Eds. L. J. Blum and P. R. Coulet. Marcel Dekker, Inc., New York.

Kautsky, H. (1939). Quenching of luminescence by oxygen. *Transactions of the Faraday Society* **35,** 216-219.

Kautsky, H. & Hirsch, A. (1935). Detection of minutest amounts of oxygen via phosphorescence quenching. *Z. Anorg. Allg. Chem.* **222,** 126-131.

Keele, C.A. & Neil, E. (1975). *Samson Wright's Applied Physiology.* pp 184-209, 463-465. Twelfth Edition. Oxford University Press, London.

Kierstan, M.P.J. & Coughlan, M.P. (1991). Immobilization of proteins by noncovalent procedures: principles and applications. In: *Protein immobilization: fundamentals and applications.,* pp 34-37. Eds. R. F. Taylor. Marcel Dekker, Inc., New York.

Kim, J.M., Suzuki, M. & Schmid, R.D. (1989). A novel enzymatic assay method for hypoxanthine. In: *Biosensors Applications in Medicine, Environmental Protection and Process Control.,* pp 425-428. Eds. R. D. Schmid and F. Scheller. VCH, Braunschweig.

Kim, J.Y. & Lee, Y.H. (1988). Fast response glucose microprobe. *Biotechnology and Bioengineering* **31,** 755-758.

Kisaalita, W.S. (1992). Biosensor standards requirements. *Biosensors & Bioelectronics* **7,** 613-620.

Kito, M., Tawa, R., Takashima, S. & Hirose, S. (1990). Determination of purine nucleosides and their bases by HPLC using coimmobilized enzyme reactors. *J. Chromatogr. Biomed. Appl.* **93,** 91-99.

Kito, M., Tawa, R., Takeshima, S. & Hirose, S. (1989). Simultaneous assay of Hx, X and allopurinol by high-performance liquid chromatography and activation of immobilized xanthine oxidase as an enzyme reactor. *Chem. Pharm. Bull.* **37,** 2459-2462.

Klainer, S.M., Thomas, J.R. & Francis, J.C. (1993). Fiber-optic chemical sensors offer a realistic solution to environmental monitoring needs. *Sensors and Actuators B* **11,** 81-86.

Klimant, I., Belser, P. & Wolfbeis, O.S. (1994). Novel metel-organic ruthenium(II) diimin complexes for use as longwave excitable luminescent oxygen probe. *Talanta* **41,** 985-991.

Komives, C. & Schultz, J.S. (1992). Fiber-optic fluorometer signal enhancement and application to biosensor design. *Talanta* **39,** 429-441.

Kosa, N.B. (1991). Key issues in selecting plastic optical fibers used in novel medical sensors. *SPIE* **1592,** 114-121.

Kotte, H., Grundig, B., Vorlop, K.-D., Strehlitz, B. & Stottmeister, U. (1995). Methylphenazonium-modified enzyme sensor based on polymer thick films for subnanomolar detection of phenols. *Anal. Chem.* **67,** 65-70.

Kresse, G.-B. (1990). Enzymes in analysis and medicine. In: *Enzymes in Industry. Production and Applications.,* pp 151-162. Eds. W. Gerhartz. VCH Verlagsgesellschaft mbH., Weinheim.

Kricka, L.J., Ji, X., Nozaki, O. & Wilding, P. (1994). Imaging of chemiluminescent reactions in mesoscale silicon-glass microstructures. *J. Biolumin. Chemilumin.* **9,** 135-138.

Kruise, J. 1993. Perspectives of glucose sensing based on a charge-modulating competition reaction. PhD Thesis. Twente, Netherlands.

Kusai, K., Sekuzu, I., Hagihara, B., Okunuki, K., Yamauchi, S. & Nakai, M. (1960). Crystallisation of glucose oxidase from *Penicillium amagasakiense*. *Biochim. et Biophys. Acta* **40,** 555-557.

Lakowicz, J.R. & Szmacinski, H. (1993). Fluorescence lifetime-based sensing of pH, Ca^{2+}, K^{+}, and glucose. *Sensors and Actuators B* **11,** 133-143.

Lanouette, K.H. (1977). Treatment of phenolic wastes. *Chemical Engineering* **Oct 17,** 99-106.

Leary, N.O., Pembroke, A. & Duggan, P.F. (1992). Improving accuracy of glucose oxidase procedure for glucose determinations on discrete analyzers. *Clinical Chemistry* **38,** 298-302.

Lee, E.D., Werner, T.C. & Seitz, W.R. (1987a). Luminescence ratio indicators for oxygen. *Anal. Chem.* **59,** 279-283.

Lee, H.-B., Stokker, Y.D. & Chau, A.S.Y. (1987b). Analysis of phenols by chemical derivatization. V. Determination of pentachlorophenol and 19 other chlorinated phenols in sediments. *J. Assoc. Off. Anal. Chem.* **70,** 1003-1008.

Lee, W.-Y. & Nieman, T.A. (1995). Evaluation of use of tris(2,2'-bipyridyl)Ruthenium(III) as a chemiluminescent reagent for quantitation in flowing streams. *Anal. Chem.* **67,** 1789-1796.

Lee, W.W.-S., Wong, K.-Y. & Li, X.-M. (1993). Luminescent dicyanoplatinum(II) complexes as Sensors for the optical measurement of oxygen concentrations. *Anal. Chem.* **65,** 255-258.

Lee, Y.H. & Tsao, G.T. (1979). Dissolved oxygen electrodes. In: *Advances in biochemical engineering,* pp 35-86. Eds. A. F. T.K. Ghose and N. Blakebrough. Springer Verlag, Berlin.

Leiner, M.J.P. (1991). Luminescence chemical sensors for biomedical applications: scope and limitations. Review. *Analytica Chimica Acta* **255,** 209-222.

Leiner, M.J.P. & Hartmann, P. (1993). Theory and practice in optical pH sensing. *Sensors and Actuators B* **11,** 281-289.

Leiner, M.J.P. & Wolfbeis, O.S. (1991). Fiber optic pH sensors. In: *Fiber Optic Chemical Sensors and Biosensors. Volume I.,* pp 359-384. Eds. O. S. Wolfbeis. CRC Press Inc., Boca Raton, Florida.

Li, L. & Walt, D.R. (1995). Dual-analyte fiber-optic sensor for the simultaneous and continuous measurement of glucose and oxygen. *Anal. Chem.* **67,** 3746-3752.

Li, P.Y.F. & Narayanaswamy, R. (1989). Oxygen-sensitive optical fiber transducer. *Analyst* **114,** 1191-1195.

Lippitsch, M.E. & Draxler, S. (1993). Luminescence decay-time-based optical sensors: principles and problems. *Sensors and Actuators B* **11,** 97-101.

Lippitsch, M.E., Pusterhofer, J., Leiner, M.J.P. & Wolfbeis, O.S. (1988). Fibre-optic oxygen sensor with the fluorescence decay time as the information carrier. *Analytica Chimica Acta* **205,** 1-6.

Liu, Y., Hering, P. & Scully, M.O. (1992). An integrated optical sensor for measuring glucose concentration. *Applied Physics B* **54,** 18-23.

Liu, Y.S. & Ware, W.R. (1993). Photophysics of polycyclic aromatic hydrocarbons absorbed on silica gel surfaces. 1.Fluorescence lifetime distribution analysis: An "ill-conditioned" problem. *J. Phys. Chem.* **97,** 5980-5986.

Lubbers, D.W. (1993). Chemical *in vivo* monitoring by optical sensors in medicine. *Sensors and Actuators B* **11,** 253-262.

Lubbers, D.W. & Opitz, N. (1975). The pCO_2/pO_2 optode: A new probe for measurement of pCO_2 and pO_2 in gases or liquids. *Z. Naturforsch. C, Biosci.* **30c,** 532-533.

Lubbers, D.W. & Opitz, N. (1983). Optical fluorescence sensors for continuous measurement of chemical concentrations in biological systems. *Sensors and Actuators* **4,** 641-654.

Luong, J.H.T., Groom, C.A. & Male, K.B. (1991). The potential role of biosensors in the food and drink industries. *Biosensors & Bioelectronics* **6,** 547-554.

Luong, J.H.T., Male, K.B. & Nguyen, A.L. (1988). Development of a fish freshness sensor. *Am. Biotechnol. Lab.* **6,** 38.

Luong, J.H.T., Male, K.B. & Nguyen, A.L. (1989). Application of polarography for monitoring the fish postmorten metebolite transformation. *Enzyme Microbiol. Tech.* **11,** 277.

Lutty, G.A. (1978). The acute intravenous toxicity of biological stains, dyes, and other fluorescent substances. *Toxicology and Applied Pharmacology* **44,** 225-249.

MacCraith, B.D., Ruddy, V., Potter, C., McGilp, J.F. & O'Kelly, B. (1991). Fibre optic fluorescence sensors based on sol-gel entrapped dyes. *SPIE, Chemical and Medical Sensors* **1510,** 104-109.

Mansouri, S., Jones, C., Martin, R. & Heil, R. (1988). Absorbance-based affinity glucose sensor. *SPIE, Optical Fibers in Medicine III* **906,** 57-59.

Mascini, M. (1992). Biosensors for medical applications. *Sensors and Actuators B* **6,** 79-82.

Mascini, M., Fortunati, S., Moscone, D., Palleschi, G., Massi-Benedetti, M. & Fabietti, P. (1985). An L-lactate sensor with immobilized enzyme for use in *in vivo* studies with an endocrine artificial pancreas. *Clin. Chem.* **31,** 451-456.

Mascini, M., Moscone, D. & Pilloton, R. (1987). Pyruvate and lactate electrochemical sensors realized with immobilized enzymes for control in artificial pancreas. *Annali di Chimica (Rome), by Societa Chimica Italiana* **77,** 813-824.

Matthews, D.R., Burton, S.F., Bown, E., Chusney, G., Dornan, T. & Gale, E.A.M. (1991). Capillary and venous blood glucose measurements using a direct glucose-sensing meter. *Diabetic Medicine* **8,** 875-880.

Matthews, D.R., Holman, R.R., Bown, E., Steemson, J., Watson, A. & Hughes, S. (1987). Pen-sized digital 30-second blood glucose meter. *Lancet* **i,** 778-779.

Mattner, U. (1988). *Lactate in sports medicine.* pp 24-31. Boehringer Mannheim GmbH, Weinheim.

McCurley, M.F. (1994). An optical biosensor using a fluorescent, swelling sensing element. *Biosensors & Bioelectronics* **9,** 527-533.

McIlvaine, T.C. (1921). A buffer solution for colorimetric comparison. *J. Biol. Chem.* **49,** 183-186.

McMurray, H.N., Douglas, P., Busa, C. & Garley, M.S. (1994). Oxygen quenching of tris(2,2'-bipyridine) ruthenium(II) complexes in thin organic films. *J. Photochem. Photobiol. A: Chem.* **80,** 283-288.

Meadows, D. & Schultz, J.S. (1988). Fiber-optic biosensors based on fluorescence energy transfer. *Talanta* **35,** 145-150.

Meyerhoff, C., Bischof, F., Mennel, F.J., Sternberg, F., Bican, J. & Pfeiffer, E.F. (1993). On line continuous monitoring of blood lactate in men by a wearable device based upon an enzymatic amperometric lactate sensor. *Biosensors & Bioelectronics* **8,** 409-414.

Milanovich, F.P., Hirschfeld, T.B., Wang, F.T. & and Klainer, S.M. (1984). Clinical measurements using fiber optics and optrodes. *Proc. SPIE, Int. Soc. Opt. Eng.* **494,** 18-23.

Miller, W.W., Yafuso, M., Yan, C.F., Hui, H.K. & Arick, S. (1987). Performance of an *in-vivo*, continuous blood-gas monitor with disposable probe. *Clinical Chemistry* **33,** 1538-1542.

Moore, E.L. & De Paula, R.P. (1989). Optical fibers and integrated optics. In: *Sensors. A Comprehensive Survey. Fundamentals and General Aspects.*, pp 217-245. Eds. W. Gopel, J. Hesse and J. N. Zemel. VCH Publishers Inc., New York.

Moreno-Bondi, M.C., Orellana, G., Camara, C. & Wolfbeis, O.S. (1990a). New luminescent metal complex for pH transduction in optical fiber sensing. Application to a CO_2-sensitive device. *SPIE; Chemical, Biochemical, and Environmental Fiber Sensors II* **1368,** 157-164.

Moreno-Bondi, M.C., Wolfbeis, O.S., Leiner, M.J.P. & Schaffar, B.P.H. (1990b). Oxygen optrode for use in a fiber-optic glucose biosensor. *Anal. Chem.* **62,** 2377-2380.

Mosbach, K. (1976). Immobilized enzymes. In: *Methods in Enzymology.*, pp 11-332. Eds. S. P. Colowick and N. O. Kaplan. Academic Press, San Diego.

Mosbach, K. (1991). Thermal biosensors. *Biosensors & Bioelectronics* **6,** 179-182.
Mulchandani, A., Luong, J.H.T. & Male, K.B. (1989). Development and application of a biosensor for hypoxanthine in fish extract. *Anal. Chim. Acta* **221,** 215-222.
Nakamura, T. & Ogura, Y. (1962). Kinetics studies on the action of glucose oxidase. *J. Biochem.* **52,** 214-220.

Naley, A.M. (1983). Analysis of phenols in sea water by fluorometry: Direct analysis of the water phase. *Bull. Environ. Contam. Toxicol.* **31,** 494-500.

Narang, U., Prasad, P.N., Bright, F.V., Ramanathan, K., Kumar, N.D., Malhotra, B.D., Kamalasanan, M.N. & Chandra, S. (1994). Glucose biosensor based on a sol-gel-derived platform. *Anal. Chem.* **66,** 3139-3144.

Narayanaswamy, R. (1991). Current developments in optical biochemical sensors. *Biosensors & Bioelectronics* **6,** 467-475.

Narayanaswamy, R. (1993). Optical chemical sensors: transduction and signal processing. Tutorial review. *Analyst* **118,** 317-322.

Narayanaswamy, R., Edmonds, T.E., Ross, I.D., Jones, J.D.C., Jackson, D.A., Hilliard, L.A., Smith, A.M. & Dakin, J.P. (1985). Fibre optics for chemical sensing. *Analytical Proceedings* **22,** 204-217.

Navaratne, A., Lin, M.S. & Rechnitz, G.A. (1990). Eggplant-based bioamperometric sensor for the detection of catechol. *Analytica Chimica Acta* **237,** 107-113.

Nguyen, A.-L. & Luong, J.H.T. (1993). Development of mediated amperometric biosensors for hypoxanthine, glucose and lactate: a new format. *Biosensors & Bioelectronics* **8,** 421-431.

Nicholson, J.K., Foxall, P.J.D., Spraul, M., Farrant, R.D. & Lindon, J.C. (1995). 750 MHz ^{1}H and ^{1}H-^{13}C NMR spectroscopy of human blood plasma. *Anal. Chem.* **67,** 793-811.

Offenbacher, H., Wolfbeis, O.S. & Furlinger, E. (1986). Fluorescence optical sensors for continuous determination of near-neutral pH values. *Sensors and Actuators* **9,** 73-84.

Ogan, K. & Katz, E. (1981). Liquid chromatographic separation of alkylphenols with fluorescence and ultraviolet detection. *Anal. Chem.* **53,** 160-163.

Okazaki, T., Imasaka, T. & Ishibashi, N. (1988). Optical-fiber sensor based on the second- harmonic emission of a near-infrared semiconductor laser as light source. *Analytica Chimica Acta* **209,** 327-331.

Opitz, N., Graf, H.J. & Lubbers, D.W. (1988). Oxygen sensor for the temperature range 300 to 500 K based on fluorescence quenching of indicator-treated silicone rubber membranes. *Sensors and Actuators* **13,** 159-163.

Opitz, N. & Lubbers, D.W. (1984). Increased resolution power in PO_2 levels via sensitivity enhanced optical PO_2 sensors (PO_2 optodes) using fluorescence dyes. *Adv. Exp. Med. Biol.* **180,** 261-267.

Opitz, N. & Lubbers, D.W. (1987). Fluorescence-based optochemical sensors (optodes) and related biosensors using enzyme-catalyzed biochemical and antibody-linked immunological reactions. *GBF Monogr. Ser.* **10,** 207-216.

Opitz, N. & Lubbers, D.W. (1988). Electrochromic dyes, enzyme reactions and hormone-protein interactions in fluorescence optic sensor (optode) technology. *Talanta* **35,** 123-127.

Opitz, N., Merten, E. & Acker, H. (1994). Evidence for redistribution-associated intracellular pK shifts of the pH-sensitive Fluoroprobe carboxy-SNARF-1. *European Journal of Physiology, Pflugers Arch* **427,** 332-342.

Orellana, G., Moreno-Bondi, M.C., Segovia, E. & Marazuela, M.D. (1992). Fiber-optic sensing of carbon dioxide based on excited-state proton transfer to a luminescent ruthenium(II) complex. *Anal. Chem.* **64,** 2210-2215.

Ortega, F., Cuevas, J., Centenera, J. & Dominguez, E. (1992). Liquid chromatographic separation of phenolic drugs using catalytic detection: comparison of an enzyme reactor and enzyme electrode. *J. Pharm. Biomedical Analysis* **10,** 789-793.

Ortiz, P.I., Abu Nader, P.R. & Mottola, H.A. (1993). Glassy carbon electrodes coated with electropolymerized resole prepolymer mixtures: Amperometric response to phenols and application as chromatographic sensors. *Electroanalysis* **5,** 165-169.

Owen, V.M. (1996). Optical fluorescence biosensoring application and dersification - a case history. *Biosensors & Bioelectronics* **11,** v-viii.

Papkovsky, D.B. (1993). Luminescent porphyrins as probes for optical (bio)sensors. *Sensors and Actuators B* **11,** 293-300.

Papkovsky, D.B., Ghindilis, A.L. & Kurochkin, I.N. (1993a). Flow-cell fibre-optic enzyme sensor for phenols. *Analytical Letters* **26,** 1505-1518.

Papkovsky, D.B., Olah, J. & Kurochkin, I.N. (1993b). Fibre-optic lifetime-based enzyme biosensor. *Sensors and Actuators B* **11,** 525-530.

Papkovsky, D.B., Ponomarev, G.V., Chernov, S.F., Ovchinnikov, A.N. & Kurochkin, I.N. (1994). Luminescence lifetime-based sensor for relative air humidity. *Sensors and Actuators B* **22,** 57-61.

Parker, J.W. & Cox, M.E. (1986). Glucose/oxygen sensor. *SPIE, Optical Fibers in Medicine II* **713,** 113-120.

Parker, J.W., Laksin, O., Yu, C., Lau, M.-L., Klima, S., Fisher, R., Scott, I. & Atwater, B.W. (1993). Fiber-optic sensors for pH and carbon dioxide using a self-referencing dye. *Anal. Chem.* **65,** 2329-2334.

Pazur, J.H., Kleppe, K. & Ball, E.M. (1964). The oxidation of glucose and related compounds by glucose oxidase from Aspergillus niger. *Biochemistry* **3,** 578-583.

Peterson, J.I., Fitzgerald, R.V. & Buckhold, D.K. (1984). Fiber-optic probe for *in vivo* measurement of oxygen partial pressure. *Anal. Chem.* **56,** 62-67.

Peterson, J.I., Goldstein, S.R. & Fitzgerald, R.V. (1980). Fiber optic pH prode for physiological use. *Anal. Chem.* **52,** 864-869.

Peterson, J.I. & Stefansson, E. (1991). Origin, construction, and performance of an *in vivo* oxygen sensor. In: *Fiber Optic Chemical Sensors and Biosensors. Volume II.,* pp 259-266. Eds. O. S. Wolfbeis. CRC Press, Inc., Boca Raton, Florida.

Peterson, J.I. & Vurek, G.G. (1984). Fiber-optic sensors for biomedical applications. *Science Wash. DC* **224,** 123-127.

Pfeiffer, D., Setz, K., Schulmeister, T., Scheller, F.W., Luck, H.B. & Pfeiffer, D. (1992). Development and characterization of an enzyme-based lactate probe for undiluted media. *Biosensors & Bioelectronics* **7,** 661-671.

Pickup, J.C. & Rothwell, D. (1984). Technology and the diabetic patient. Review. *Med. Biol. Eng. Comput.* **22,** 384-400.

Pickup, J.C., Shaw, G.W. & Claremont, D.J. (1987). Implantable glucose sensors: choosing the appropriate sensing strategy. *Biosensors* **3,** 335-346.

Poitout, V., Moatti-Sirat, D., Reach, G., Zhang, Y., Wilson, G.S., Lemonnier, F. & Klein, J.C. (1993). A glucose monitoring system for on line estimation in man of blood glucose concentration using a miniaturized glucose sensor implanted in the subcutaneous tissue and a wearable control unit. *Diabetologia* **36,** 658-663.

Pollack, M., Pringsheim, P. & Terwoord, D. (1944). A method for determining small quantities of oxygen. *The Journal of Chemical Physics* **12,** 295-299.

Posch, H.E., Leiner, M.J.P. & Wolfbeis, O.S. (1989). Towards a gastric pH-sensor: an optrode for th pH 0-7 range. *Fresenius Z. Anal. Chem.* **334,** 162-165.

Preininger, C., Klimant, I. & Wolfbeis, O.S. (1994). Optical fiber sensor for biological oxygen demand. *Anal. Chem.* **66,** 1841-1846.

Pueyo, M.E., Darquy, S., Arbet-Engles, C., Poitout, V., Di Maria, S., Gangnerau, M.N. & Reach, G. (1995). Artificial pancreas and releated technology in diabetes and endocrinology. A method for obtaining monodispersed cells from isolated porcine islets of Langerhans. *The International Journal of Artificial Organs* **18,** 34-38.

Rabenstein, D.L., Millis, K.K. & Strauss, E.J. (1988). Proton NMR spectroscopy of human blood plasma. *Anal. Chem.* **60,** 1380A-1391A.

Racek, J. (1987). Lactate biosensor based on human erythrocytes. *Analytica Chimica Acta* **197,** 187-194.

Rajeshwar, K., Lezna, R.O. & de Tacconi, N.R. (1992). Light in an electrochemical tunnel? Report. *Anal. Chem.* **64,** 429A-441A.

Reach, G. (1994a). Artificial and bioartificial pancreas for the treatment of diabetes mellitus. *Diabete & Metabolisme* **20,** 183-193.

Reach, G. (1994b). Bioartificial pancreas. *Transpantation Proceedings* **26,** 397-398.

Reach, G. & Wilson, G.S. (1992). Can continuous glucose monitoring be used for the treatment of Diabetes? *Anal. Chem.* **64,** 381A-386A.

Realini, P.A. (1981). Determination of priority pollutant phenols in water by HPLC. *J. Chromatogr. Sci.* **19,** 124-129.

Rebrin, K., Fischer, U., Hahn von Dorsche, H., von Woetke, T., Abel, P. & Brunstein, E. (1992). Subcutaneous glucose monitoring by means of electrochemical sensors: fiction or reality? *J. Biomed. Eng.* **14,** 33-40.

Rehak, M., Snejdarkova, M. & Otto, M. (1994). Application of biotin-streptavidin technology in developing a xanthine biosensor based on a self-assembled phospholipid membrane. *Biosensors & Bioelectronics* **9,** 337-341.

Reisfeld, R. (1990). Spectroscopy and applications of molecules in glasses. *Journal of Non-Crystalline Solids* **121,** 254-266.

Rodriguez-Lopez, J.N., Escribano, J. & Garcia-Canovas, F. (1994). A continuous spectrophotometric method for the determination of monophenolase activity of tyrosinase using 3-methyl-2-benzothiazolinone hydrazone. *Analytical Biochemistry* **216,** 205-212.

Rogers, M.J. & Brandt, K.G. (1971). Interaction of D-glucal with *Aspergillus niger* glucose oxidase. *Biochemistry* **10,** 4624-4630.

Rohen, A., Krause, J. & Cammann, K. (1992). Fiberoptic biosensor for lactate with redox dyes as coenzyme. *GBF Monogr. Ser.* **17,** 91-94.

Rosenzweig, Z. & Kopelman, R. (1996). Analytical properties and sensor size effects of a micrometer-sized optical fiber glucose biosensor. *Anal. Chem.* **68,** 1408-1413.

Samoszuk, M., Ehrlich, D. & Ramzi, E. (1993). Preclinical safety studies of glucose oxidase. *The Journal of Pharmacology and Experimental Therapeutics.* **266,** 1643-1648.

Santiago, J.V. (1992). Clinical review 38. Intensive management of insulin dependent diabetes: Risks, benefits, and unanswered questions. *Journal of Clinical Endocrinology and Metabolism* **75,** 977-982.

Santiago, J.V. (1993a). Insulin therapy in the last decade. A pediatric perspective. *Diabetes Care* **16,** 143-154.

Santiago, J.V. (1993b). Perspectives in diabetes. Lessons from the diabetes control and complications trial. *Diabetes* **42,** 1549-1554.

Santiago, J.V., Clemens, A.H., Clarke, W.I. & Kipris, D.M. (1979). Closed-loop and open-loop devices for blood glucose control in normal and diabetic subjects. *Diabetes* **28,** 71-84.

Satoh, I., Inoue, K. & Arakawa, S. (1988). *Continuous determination of xanthine using enzyme sensor and thermistor probes.* Technical Digest of the 7th Sensor Symposium. Tokyo. 229-235

Saudan, P., Zakeeruddin, S.M., Malavallon, M.-A., Gratzel, M. & Fraser, D.M. (1994). Novel redox surfactants and their interactions with glucose oxidase of Aspergillus niger. *Biotechnology and Bioengineering* **44,** 407-418.

Schaffar, B.P.H. & Wolfbeis, O.S. (1989a). A calcium-selective optrode based on fluorimetric measurement of membrane potential. *Analytica Chimica Acta* **217,** 1-9.

Schaffar, B.P.H. & Wolfbeis, O.S. (1989b). A sodium-selective optrode. *Mikrochimica Acta [Wien]* **III,** 109-116.

Schaffar, B.P.H. & Wolfbeis, O.S. (1990). A fast responding fibre optic glucose biosensor based on oxygen optrode. *Biosensors & Bioelectronics* **5,** 137-148.

Schaffar, B.P.H. & Wolfbeis, O.S. (1991). Chemically mediated fiberoptic biosensors. In: *Biosensor Principles and Applications,* pp 163-194. Eds. L. J. Blum and P. R. Coulet. Marcel Dekker, Inc., New York.

Scharp, D.W., Lacy, P.E., Santiago, J.V., McCullough, C.S., Weide, L.G., Boyle, P.J., Falqui, L., Marchetti, P., Ricordi, C., Gingerich, R.L., Jaffe, A.S., Cryer, P.E., Hanto, D.W., Anderson, C.B. & Flye, M.W. (1991). Results of our first nine intraportal islet allografts in type 1, Insulin-Dependent Diabetic Patients. *Transplantation* **51,** 76-85.

Scheller, F. & Schubert, F. (1992). *Biosensors.* Volume 11, pp 50-65. Elsevier Science Publishers B.V., Amsterdam.

Schepartz, A.I. & Subers, H.H. (1964). Glucose oxidase of honey. *Biochim. et Biophys. Acta* **85,** 229-237.

Scheper, T. & Buckmann, A.F. (1990). Afiber optic biosensor based on fluorometric detection using confined macromolecular nicotinamide adenine dinucleotide derivatives. *Biosensors & Bioelectronics* **5,** 125-135.

Scheper, T., Muller, C., Anders, K.D., Eberhardt, F., Plotz, F., Schelp, C., Thordsen, O. & Schugerl, K. (1994). Optical sensors for biotechnological applications. *Biosensors & Bioelectronics* **9,** 73-83.

Scherer, G.W. (1988). Aging and drying of gels. *Journal of Non-Crystalline Solids* **100,** 77-92.

Schindler, J.G., Schindler, M.M., Herna, K., Pohl, M., Guntermann, H., Burk, B. & Reisinger, E. (1994). Langlebige β-D-glucose- und L-lactat-biosensoren fur kontinuierliche durchflußmessungen zur "fouling"-resistenten und selektivitatsoptimierten serum- und hamoanalytik. *Eur. J. Clin. Chem. Clin. Biochem.* **32,** 599-608.

Schmidt, H.L., Schuhmann, W., Scheller, F.W. & Schubert, F. (1992). Specific features of biosensors. In: *Chemical and Biochemical Sensors. Part II.,* pp 717-817. Eds. W. Gopel, T. A. Jones, M. Kleitz, I. Lundstrom and T. Seiyama. VCH Verlagsgesellschaft mbH, Weinheim.

Schulman, S.G., Chen, S., Bai, F., Leiner, M.J.P., Weis, L. & Wolfbeis, O.S. (1995). Dependence of the fluorescence of immobilized 1-hydroxypyrene-3,6,8-trisulfonate on solution pH: extension of the range of applicability of a pH fluorosensor. *Analytica Chimica Acta* **304,** 165-170.

Schulman, S.G., Townsend, R.W. & Zhang, Y. (1991). Operational pH in aqueous acetonitrile based upon the rate of a simple pH dependent reaction. *Analytica Chimica Acta* **255,** 329-334.

Schulman, S.G., Vogt, B.S. & Lovell, M.W. (1980). Kinetics and equilibria of proton-transfer reactions of weak bases in the lowest excited singlet state. *Chemical Physics Letters* **75,** 224-229.

Schultz, J.S., Mansouri, S. & Goldstein, I.J. (1982). Affinity sensor: A new technique for developing implantable sensors for glucose and other metabolites. *Diabetes Care* **5,** 245-253.

Scouten, W.H. (1987). A survey of enzyme coupling techniques. In: *Methods in Enzymology,* pp 30-65. Eds. K. Mosbach, S. P. Colowick and N. O. Kaplan. Academic Press, San Diego.

Seitz, W.R. (1984). Chemical sensors based on fiber optics. *Anal. Chem.* **56,** 16A-23A.

Seitz, W.R. (1988). Chemical sensors based on immobilized indicators and fiber optics. *CRC Critical Reviews in Analytical Chemistry.* **19,** 135-173.

Seitz, W.R. (1993). New directions in fiber optic chemical sensors: Sensors based on polymer swelling. *Journal of Molecular Structure* **292,** 105-114.

Senior, J.M. (1985). *Optical fiber communications. Principles and practice.* pp 12-57. Prentice Hall International(UK) Ltd, Hemel Hempstead, Hertfordshire.

Sethi, R.S. (1994). Transducer aspects of biosensors. *Biosensors & Bioelectronics* **9,** 243-264.

Shah, J.J. & Singh, H.B. (1988). Distribution of volatile organic chemicals in outdoor and indoor air. *Environmental Science Technology* **22,** 1381-1388.

Shoup, R.E. & Mayer, G.S. (1982). Determination of environmental phenols by liquid chromatography/electrochemistry. *Anal. Chem.* **54,** 1164-1169.

Sizer, I.W. (1948). The inactivation of invertase by tyrosinase. *Science* **108,** 335-336.

Skladal, P., Mascini, M., Salvadori, C. & Zannoni, G. (1993). Detection of bacterial contamination in sterile UHT milk using an L-lactate biosensor. *Enzyme Microb. Technol.* **15,** 508-512.

Skoog, D.A. & Leary, J.J. (1992). *Principles of instrumental analysis.* pp 125-136, 174-193. Fourth Edition. Saunders College Publishing (HBJ), Orlando.

Smith, J.L. & Krueger, R.C. (1962). Separation and purification of the phenolases of the common mushroom. *The Journal of Biological Chemistry* **237,** 1121-1128.

Smith, P.R., Tear, C.B., Barratt, N.R. & Thomason, H. (1992). Design considerations for a fibre-optic based polarimeter. *Optics & Laser Technology* **24,** 135-138.

Smith, S.D. (1995). *Optoelectronic devices.* pp 332-374. Prentice Hall International (UK) Ltd., London.

Steiner, D.F., Tager, H.S., Chan, S.J., Nanjo, K., Sanke, T. & Rubenstein, A.H. (1990). Lessons learned from molecular biology of insulin-gene mutations. *Diabetes Care* **13,** 600-609.

Sternberg, R., Bindra, D.S., Wilson, G.S. & Thevenot, D.R. (1988). Covalent enzyme coupling on cellulose acetate membranes for glucose sensor development. *Anal. Chem.* **60,** 2781-2786.

Stryer, L. (1995). *Biochemistry.* pp 577-579, 755-759 and 774-782. Fourth Edition. W. H. Freeman and Company, New York.

Suzuki, M., Suzuki, H., Karube, I. & Schmid, R.D. (1989). Disposable micro hypoxanthine sensors for freshness estimation. In: *Biosensors Applications in Medicine, Environmental Protection and Process Control.,* pp 107-111. Eds. R. D. Schmid and F. Scheller. VCH, Braunschweig.

Swoboda, B.E.P. & Massey, V. (1965). Purification and properties of the glucose oxidase from Aspergillus niger. *The Journal of Biological Chemistry* **240,** 2209-2215.

Symons, R.K. 1990. Analysis of environmental phenols. Ph.D. Thesis. La Trobe University, Victoria, Australia.

Szmacinski, H. & Lakowicz, J.R. (1993). Optical measurements of pH using fluorescence lifetimes and phase-modulation fluorometry. *Anal. Chem.* **65,** 1668-1674.

Takahashi, C., Kaneko, A., Komata, Y., Yokoyama, S. & Fujie, T. (1993). Studies of body fluids with optical fiber sensors. *Sensors and Actuators B* **13-14,** 756-757.

Tatsu, Y., Yamashita, K., Yamaguchi, M., Yamamura, S., Yamamoto, H. & Yoshikawa, S. (1992). Entrapment of glucose oxidase in silica gel by the sol-gel method and its application to glucose sensor. *Chemistry Letters* , 1615-1618.

Tattersall, R.B. (1985). Self-monitoring of blood glucose 1978-1984. In: *In The Diabetes Annual,* pp 162-177. Eds. K. G. M. M. Alberti and L. P. Krall. Elsevier, Amsterdam.

Tesarova, E. & Pacakova, V. (1983). Gas and high-performance liquid chromatography of phenols. *Chromatographia* **17,** 269-284.

Thompson, R.B. (1991). Fluorescence-based fiber-optic sensors. In: *Topics in Fluorescence Spectroscopy. Principles. Volume 2.,* pp 345-365. Eds. J. R. Lakowicz. Plenum Press, New York.

Thompson, R.B. & Lakowicz, J.R. (1993). Fiber optic pH sensor based on phase fluorescence lifetimes. *Anal. Chem.* **65,** 853-856.

Thompson, R.B. & Ligler, F.S. (1988). Recent developments in fiber optic biosensors. *SPIE, Microsensors and Catheter-Based Imaging Technology* **904,** 27-33.

Tieszen, K.L., Patrick, A.W., Smith, E., Williams, G. & Dornan, T.L. (1993). Accurate and precise blood glucose measurement in the hupoglycaemic range. *Diabetic Medicine* **10,** 560-563.

Tietze, E. & Baeyer, O. (1939). Die sulfosauren des pyrens und ihre abkommlinge. *Liebigs Ann. Chem.* **540,** 189-210.

Trettnak, W., Leiner, M.J.P. & Wolfbeis, O.S. (1988a). Fibre-optic glucose sensor with a pH optrode as the transducer. *Biosensors* **4,** 15-26.

Trettnak, W., Leiner, M.J.P. & Wolfbeis, O.S. (1988b). Optical sensors: Part 34. Fibre optic glucose biosensor with an oxygen optrode as the transducer. *Analyst* **113,** 1519-1523.

Trettnak, W. & Wolfbeis, O.S. (1989a). A fiber optic lactate biosensor with an oxygen optrode as the transducer. *Analytical Letters* **22,** 2191-2197.

Trettnak, W. & Wolfbeis, O.S. (1989b). Fully reversible fibre-optic glucose biosensor based on the intrinsic fluorescence of glucose oxidase. *Analytica Chimica Acta* **221,** 195-203.

Turner, A.P.F. (1992). *Advances in biosensors. A research annual.* Volume 2, pp xi-xii. JAI Press Ltd, London.

Turner, A.P.F. & Pickup, J.C. (1985). Diabetes mellitus: Biosensors for research and management. *Biosensors* **1,** 85-115.

Uchiyama, M. & Yamaguchi, M. (1977). Fluorometric determination of phenols in water. *Gunma Res. Cent. Environ. Sci.* **1977,** 872-874.

Uwira, J.W., Opitz, N. & Lubbers, D.W. (1984). Infuence of enzyme concentration and thickness of the enzyme layer on the calibration curve of the continuously measuring glucose optode. *Adv. Exp. Med. Biol.* **169,** 913-921.

Vieth, W.R. & Venkatasubramanian, K. (1976). Collagen-immobilized enzymes systems. In: *Immobilized enzymes,* pp 246-248. Eds. K. Mosbach. Academic Press, Inc., New York.

Volkl, K.-P., Grossmann, U., Opitz, N. & Lubbers, D.W. (1981). The use of O_2-optode for measuring substances as glucose by using oxidative enzymes for biological applications. *Adv. Physiol. Sci.* **25,** 99-100.

Wang, J. & Chen, Q. (1994). Lactate biosensors based on a lactate dehydrogenase/nicotinamide adenine dinucleotide biocomposite. *Electroanalysis* **6,** 850-854.

Wang, J. & Lin, M. (1988). Mixed plant tissue-carbon paste bioelectrode. *Anal. Chem.* **60,** 1545-1549.

Wang, J., Lu, F. & Lopez, D. (1994). Tyrosinase-based ruthenium dispersed carbon paste biosensor for phenols. *Biosensors & Bioelectronics* **9,** 9-15.

Wang, J., Naser, N., Angnes, L., Wu, H. & Chen, L. (1992). Metal-dispersed carbon paste electrodes. *Anal. Chem.* **64,** 1285-1289.

Wang, R., Narang, U., Prasad, P.N. & Bright, F.V. (1993). Affinity of antifluorescein antibodies encapsulated within a transparent sol-gel glass. *Anal. Chem.* **65,** 2671-2675.

Wasserman, K., Hansen, J.E., Sue, D.Y. & Whipp, B.J. (1987). *Principle of exercise testing and interpretation.* pp 14-21. Lea & Febiger, New York.

Watanabe, E., Ando, K., Karube, I., Matsuoka, H. & Suzuki, S. (1983). Determination of hypoxanthine in fish meat with an enzyme sensor. *J. Food Sci.* **48,** 496-500.

Watanabe, E., Endo, H., Hayashi, T. & Toyama, K. (1986). Simultaneous determination of hypoxanthine and inosine with an enzyme sensor. *Biosensors* **2,** 235-244.

Watanabe, E., Endo, H. & Toyama, K. (1988). Determination of inosine-5'-monophpsphate in the present of inosine and hypoxanthine with an enzyme sensor. *Appl. Microbiol. Biotechnol.* **29,** 341-345.

Watanabe, E., Toyama, K., Karube, I., Matsuoka, H. & Suzuki, S. (1984a). Determination of inosine-5'-monophosphate in fish tissue with an enzyme sensor. *J. Food Sci.* **49,** 114-116.

Watanabe, E., Toyama, K., Karube, I., Matsuoka, H. & Suzuki, S. (1984b). Multifuctional biosensor for the determination of fish meat freshness. *Annals New York Academy of Sciences (Enz.Eng.)* **434,** 529-532.

Webb, M.J. (1989). Practical considerations when using fiber optics with spectrometers. *Spectroscopy* **4,** 26-34.

Weibel, M.K. & Bright, H.J. (1971). The glucose oxidase mechanism: interpretation of the pH dependence. *Journal of Biological Chemistry* **246,** 2734-2744.

Weigl, B.H., Holobar, A., Trettnak, W., Klimant, I., Kraus, H., O'Leary, P. & Wolfbeis, O.S. (1994). Optical triple sensor for measuring pH, oxygen and carbon dioxide. *J. Biotechnol.* **32,** 127-138.

Weller, A. (1958). Protolytische reaktionen angeregter oxyverbindungen. *Zeitschrift fur Physikalische Chemie Neue Folge* **17,** 224-245.

Werner, T., Klimant, I. & Wolfbeis, O.S. (1995). Ammonia-sensitive polymer matrix employing immobilized indicator ion pairs. *Analyst* **120,** 1627-1631.

Wilson, G.S. & Thevenot, D.R. (1990). Unmediated amperometric enzyme electrodes. In: *Biosensors: A Practical Approach,* pp 1-7. Eds. A. E. G. Cass. Oxford University Press, New York.

Wilson, R. & Turner, A.P.F. (1991). Glucose oxidase: an ideal enzyme. *Biosensors & Bioelectronics* **7,** 165-185.

Wolfbeis, O.S. (1985). The fluorescence of organic natural products: Flavins coenzymes. In: *Molecular Luminescence Spectroscopy. Methods and applications: Part 1,* pp 180-184. Eds. S. G. Schulman. John Wiley & Sons Inc., New York.

Wolfbeis, O.S. (1988). Fiber optical fluorosensors in analytical and clinical chemistry. In: *Molecular Luminescence Spectroscopy. Methods and applications: Part 2.,* pp 129-281. Eds. S. G. Schulman. John Wiley & Sons Inc., New York.

Wolfbeis, O.S. (1989). The development of fiber optic chemical sensors by immobilization of fluorescent probes. *Applied Fluorescence Technology* **1,** 1-6.

Wolfbeis, O.S. (1991a). Achievements and new directions in analytical chemistry: Luminescence and optical sensors. *Analytical Proceedings* **28,** 357-358.

Wolfbeis, O.S. (1991b). *Fiber optic chemical sensors and biosensors. Volume I & II.* CRC Press, Inc., Boca Raton, Florida.

Wolfbeis, O.S. (1991c). Oxygen sensors. In: *Fiber Optic Chemical Sensors and Biosensors. Volume II.,* pp 19-53. Eds. O. S. Wolfbeis. CRC Press, Inc., Boca Raton, Florida.

Wolfbeis, O.S. (1992). Fiber optic biosensing based on molecular recognition. *Sensors and Actuators B* **7,** 752-757.

Wolfbeis, O.S., Furlinger, E., Kroneis, H. & Marsoner, H. (1983). Fluorometric analysis: 1.A study of fluorescent indicators for measuring near neutral ("physiological") pH-values. *Fresenius Z. Anal. Chem.* **314,** 119-124.

Wolfbeis, O.S., Leiner, M.J.P. & Posch, H.E. (1986). A new sensing material for optical oxygen measurement with the indicator embedded in an aqueous phase. *Microchimica Acta* **3,** 359-366.

Wolfbeis, O.S. & Offenbacher, H. (1986). Fluorescence sensor for monitoring ionic strength and physiological pH values. *Sensors and Actuators* **9,** 85-91.

Wolfbeis, O.S., Offenbacher, H., Kroneis, H. & Marsoner, H. (1984). A fast responding fluorescence sensor for oxygen. *Mikrochimica Acta (Wien)* **I,** 153-158.

Wolfbeis, O.S., Rodriguez, N.V. & Werner, T. (1992). LED-compatible fluorosensor for measurement of near-neutral pH values. *Mikrochim. Acta* **108,** 133-141.

Wolfbeis, O.S. & Sharma, A. (1988). Fibre-optic fluorosensor for sulphur dioxide. *Analytica Chimica Acta* **208,** 53-58.

Wolfbeis, O.S. & Trettnak, W. (1989). A new type of fiber optic biosensor based on the intrinsic fluorescence of immobilized flavoproteins. *SPIE* **1172,** 287-292.

Wolfbeis, O.S., Weis, L., Leiner, M.J.P. & Ziegler, W.E. (1988). Fiber optic fluorosensor for oxygen and carbon dioxide. *Anal. Chem.* **60,** 2028-2030.

Woodward, J. (1985). *Immobilised cells and enzymes. A practical approach.* pp 3-17. IRL Press Ltd., Oxford.

Wu, S., Ellerby, L.M., Cohan, J.S., Dunn, B., El-Sayed, M.A., Valentine, J.S. & Zink, J.I. (1993). Bacteriorhodops in encapsulated in transparent sol-gel glass: A new biomaterial. *Chemistry of Materials. American Chemical Society* **5,** 115-120.

Xie, X., Suleiman, A.A. & Guilbult, G.G. (1991). Determination of urea in serum by a fiber-optic fluorescence biosensor. *Talanta* **38,** 1197-1200.

Xu, W., McDonough III, R.C., Langsdorf, B., Demas, J.N. & DeGraff, B.A. (1994). Oxygen sensors based on luminescence quenching: Interactions of metal complexes with the polymer supports. *Anal. Chem.* **66,** 4133-4141.

Yamanaka, S.A., Nishida, F., Ellerby, L.M., Nishida, C.R., Dunn, B., Valentine, J.S. & Zink, J.I. (1992). Enzymatic activity of glucose oxidase encapsulated in transparent glass by the sol-gel method. *Chemistry of Materials. American Chemical Society* **4,** 495-497.

Yang, L. & Saavedra, S.S. (1995). Chemical sensing using sol-gel derived planar waveguides and indicator phases. *Anal. Chem.* **67,** 1307-1314.

Yoshioka, S., Ukeda, H., Matsumoto, K. & Osajima, Y. (1992). Simultaneous flow injection analysis of L-lactate L-malate in wine based on the use of enzyme reactors. *Electroanalysis* **4,** 545-548.

Zhou, X. & Arnold, M.A. (1995). Internal enzyme fiber-optic biosensors for hydrogen peroxide and glucose. *Analytica Chimica Acta* **304,** 147-156.

Zhujun, Z. & Seitz, W.R. (1984). A fluorescence sensor for quantifying pH in the range from 6.5 to 8.5. *Anal. Chim. Acta* **160,** 47-53.

Zubay, G. (1993). *Biochemistry.* pp 549-572, 660-665. Third Edition. WCB, Wm.C.Brown Publishers, Dubuque, Iowa.

Zusman, R., Rottman, C., Ottolenghi, M. & Avnir, D. (1990). Doped sol-gel glasses as chemical sensors. *Journal of Non-Crystalline Solids* **122,** 107-109.

APPENDIX A

ANALYSIS OF EXPERIMENTAL DATA

From the experimental analysis, it was found that during the oxidation of the specific analytes which were studied in the present thesis, the fluorescence intensity initially followed an almost linear relationship with time and then attained an asymptotically constant value when the reaction was completed, Figure A.1.

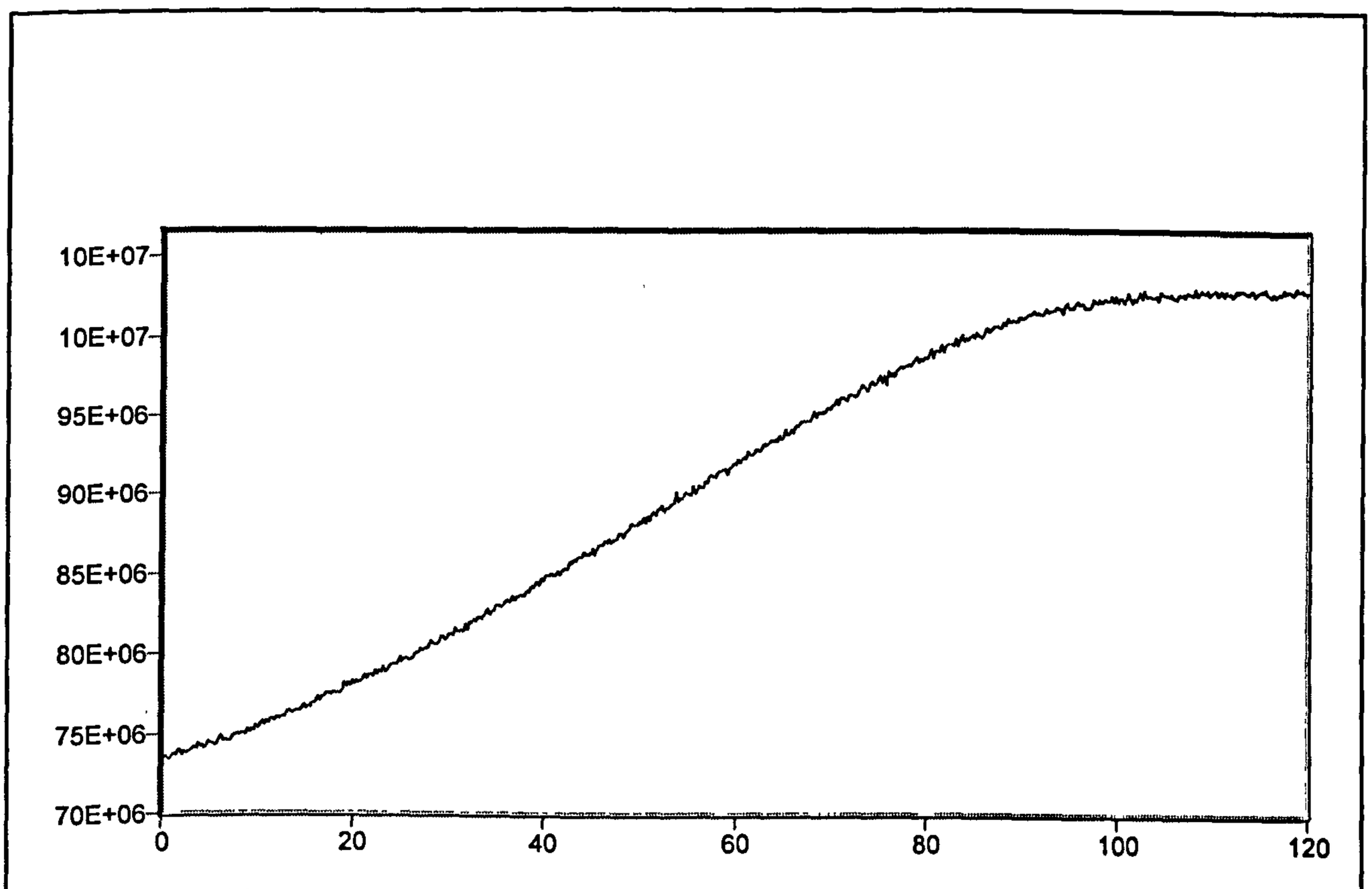

Figure A.1 Typical fluorescence intensity variation with time (this example refers to the data corresponding to Figure 3.12 for glucose concentration 6 mM).

The rate of change of the fluorescence intensity with time, during the initial phase of the reaction, was proportional to the analyte concentration which was present in the solution under investigation. A typical plot which explains the above observation is presented in Figure A.2 where the variations of the fluorescent intensity with time for different analyte concentrations, are depicted. The rate of change of fluorescence intensity with time, which is equal to the slope of the initial part of each curve, increased with analyte concentration.

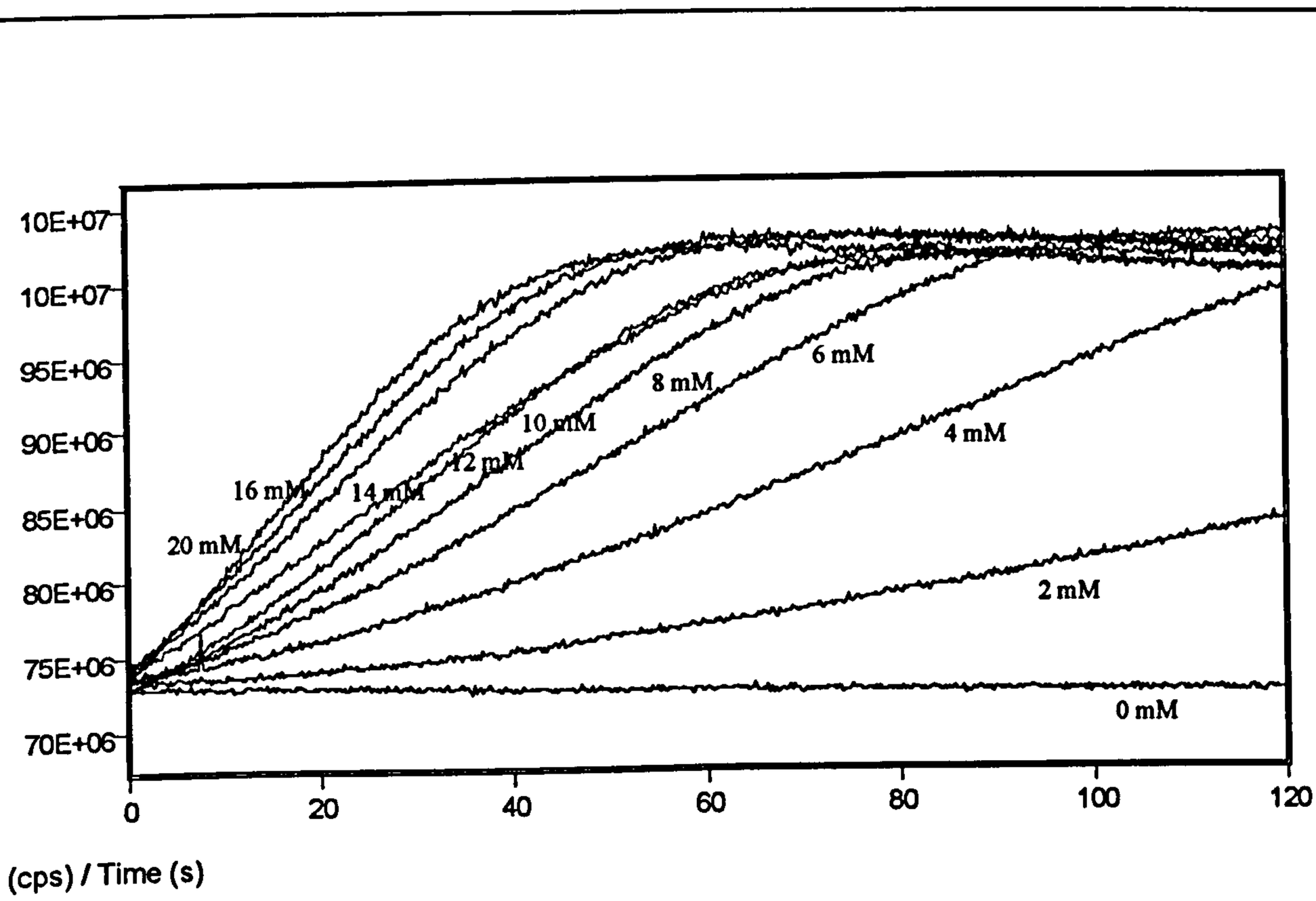

FIGURE A.2 Typical fluorescence intensity variation with time for different glucose concentrations (this example refers to the data corresponding to Figure 3.12).

The variation of the slope of the linear portion of these plots against the analyte concentration is illustrated in Figure A.3.

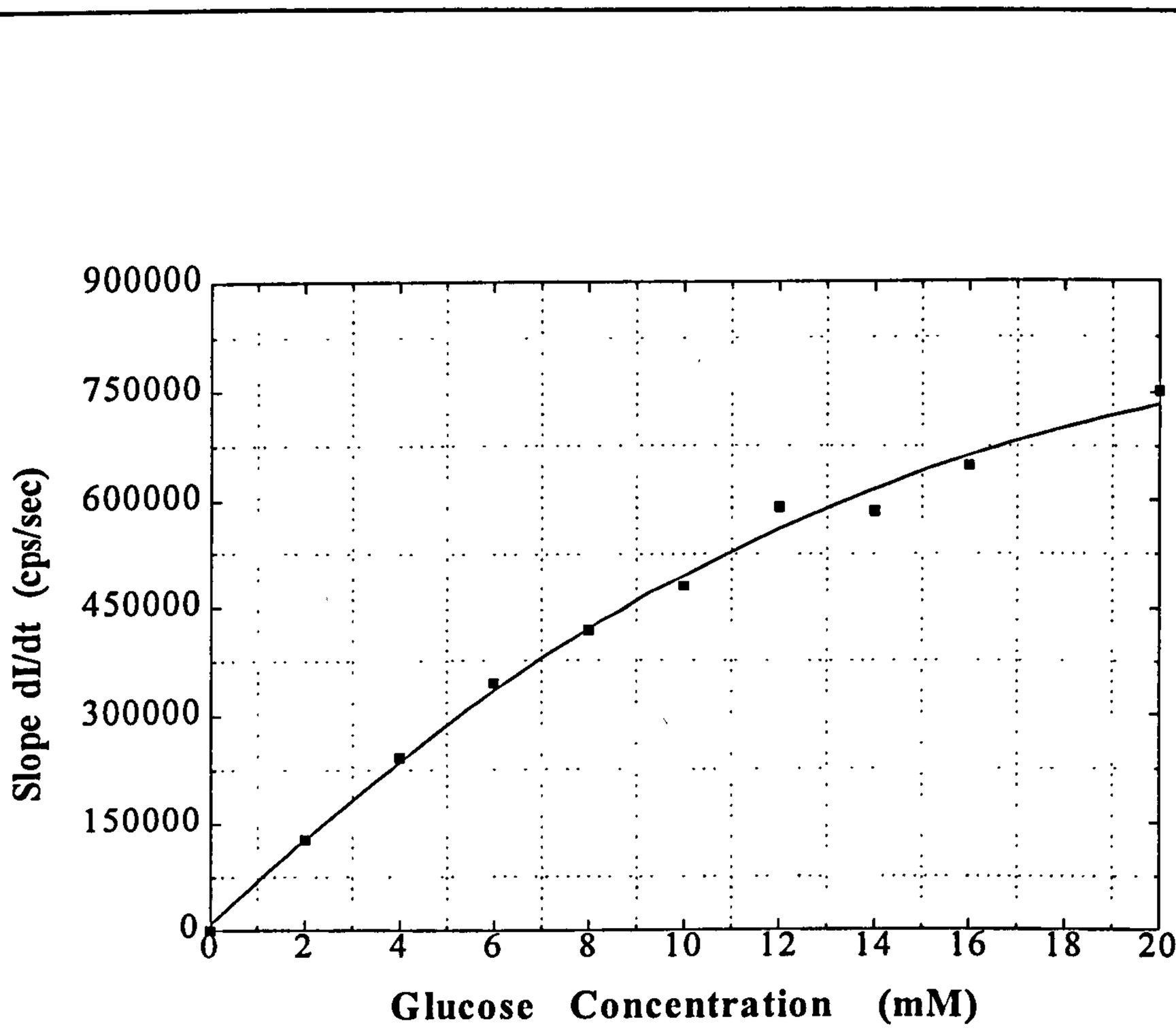

FIGURE A.3 Typical rate of change of fluorescence intensity variation against glucose concentration (this example refers to Figure 3.12).

The consistency of the results obtained allowed the rate of change of the fluorescence intensity (dI/dt) rather than the intensity itself to be utilised for the production of a calibration curve from which analyte concentration values could be obtained. An

analysis which indicates the repeatability of this approach has already been presented in Section 3.3.3 (Chapter 3).

The processing of the data including calculation of the initial slope was performed after the experiments had been completed using an appropriate software (Microcal Origin, Version 3.5). The total time used for the calculation of the initial slope was selected to represent the initial linear part of each curve and was different for different experiments. Typically, this time varied between 20 to 60 seconds for all the oxidation under investigation. As far as the error of the initial slope calculation concerns, the correlation coefficient of the linear regressions were in the range between 90% to 98% with an average value of 94%)

Data analysis when sol-gel-method was used for immobilisation

When the sol-gel immobilisation procedure was used in the oxidation of glucose was very slow and required a few hours to reach completion as compared to minutes in the solution experiments. As a consequence the variation of fluorescence intensity with time changed very slowly and noticeable differences could only be observed after a long period of time (e.g. half hour). For this reason, fluorescence intensity data have been obtained every half hour and for a duration of 30 seconds in 20±2 ^{0}C. During this period of 30 seconds the fluorescence intensity remained almost constant and an average value could be defined which is considered to be the fluorescence intensity measurement at the specific hour when the measurement was obtained.

Following the above procedure, a plot of variation of fluorescence intensity with time can be obtained, if the mean values are plotted against the time at which these measurements were taken. From the experimental work it was found that this variation could be approximated better with a second order parabola which has a decreasing slope and hence a negative second derivative, Figure A.4.

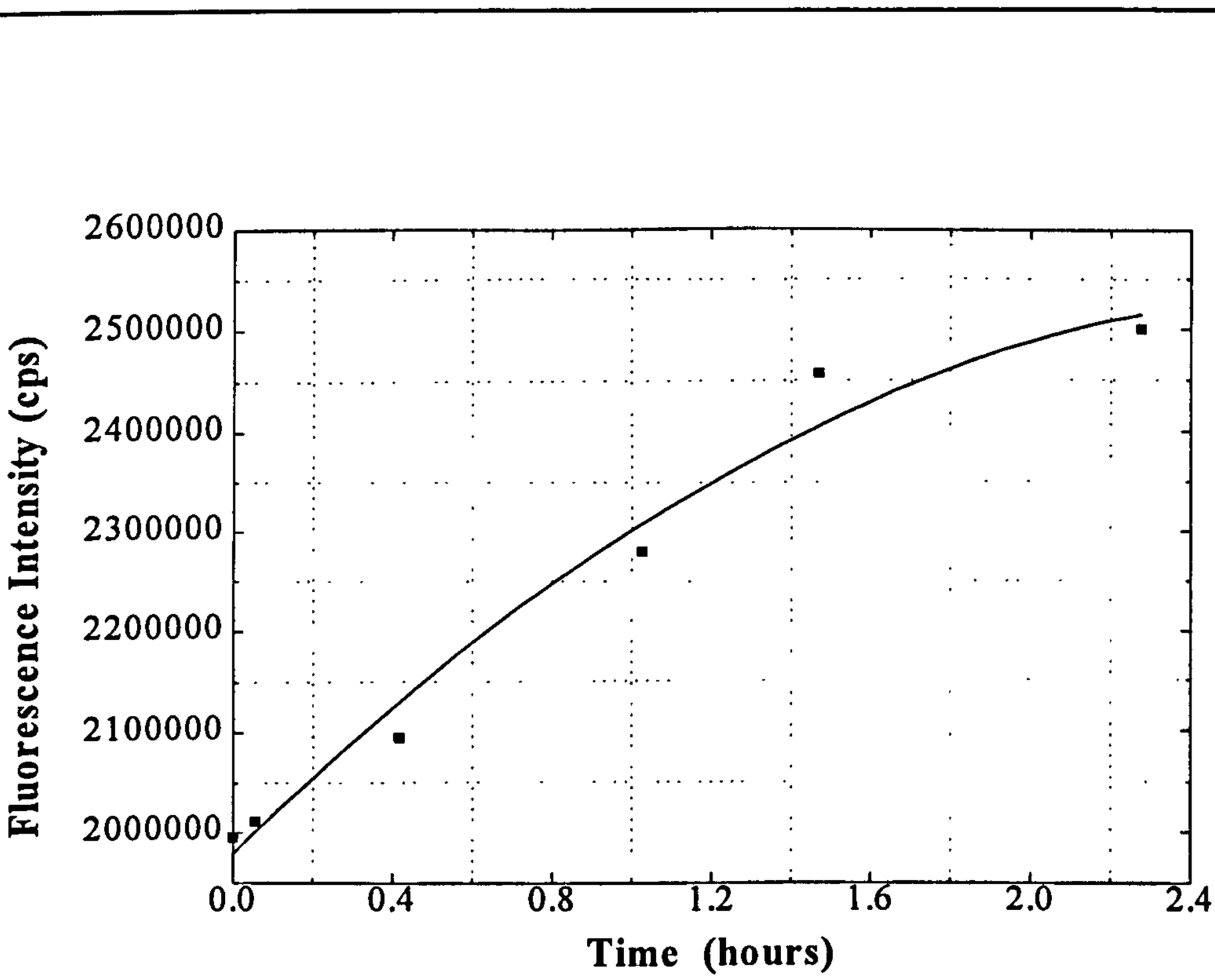

FIGURE A.4 Typical variation of fluorescence intensity variation against time when using the sol-gel immobilisation (this example refers to the data corresponding to Figure 7.3 for glucose concentration 30 mM).

The above analysis is valid for a specific glucose concentration. When different glucose concentrations were used, different curves were obtained which could be approximated by using parabolas. However, their slope, at Time = 0 hours, was proportional to the glucose concentration contained in the solution under investigation. A typical plot of this observation is depicted in Figure A.5.

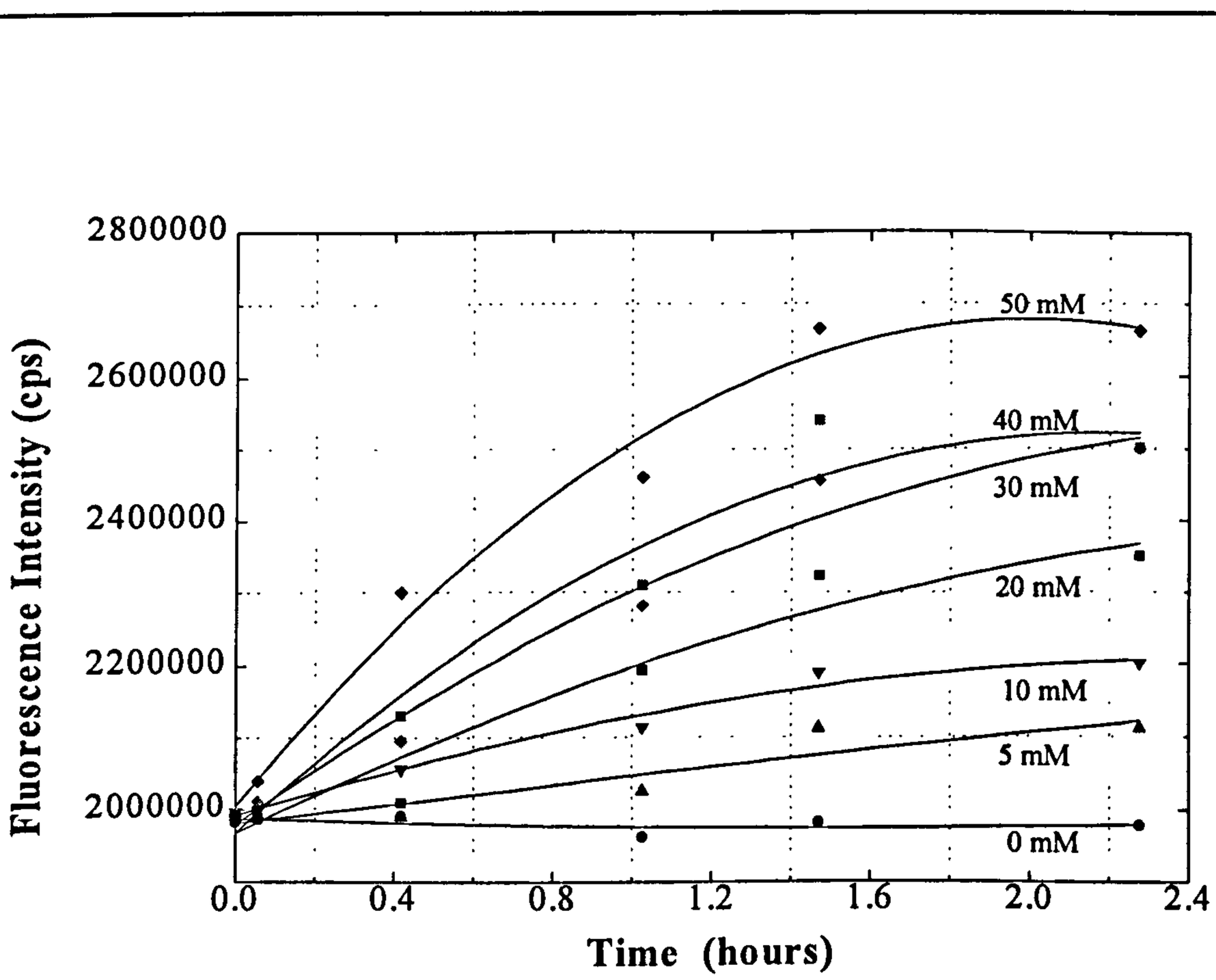

FIGURE A.5 Typical fluorescence intensity variation with time for different glucose concentrations when using sol-gel (this example refers to the data corresponding to Figure 7.3).

As described in the previous section, after considerable experimentation, it was decided that the initial slopes of the above curves, which express the rate of change of the fluorescent intensity with time, could be used as a reliable indication of the glucose concentration.

The calculation of the value of the slope for each of the second order parabolic curves, and the graphical representation of the variation of these slope values against glucose concentration is shown in Figure A.6 which is similar in shape to Figure A.3.

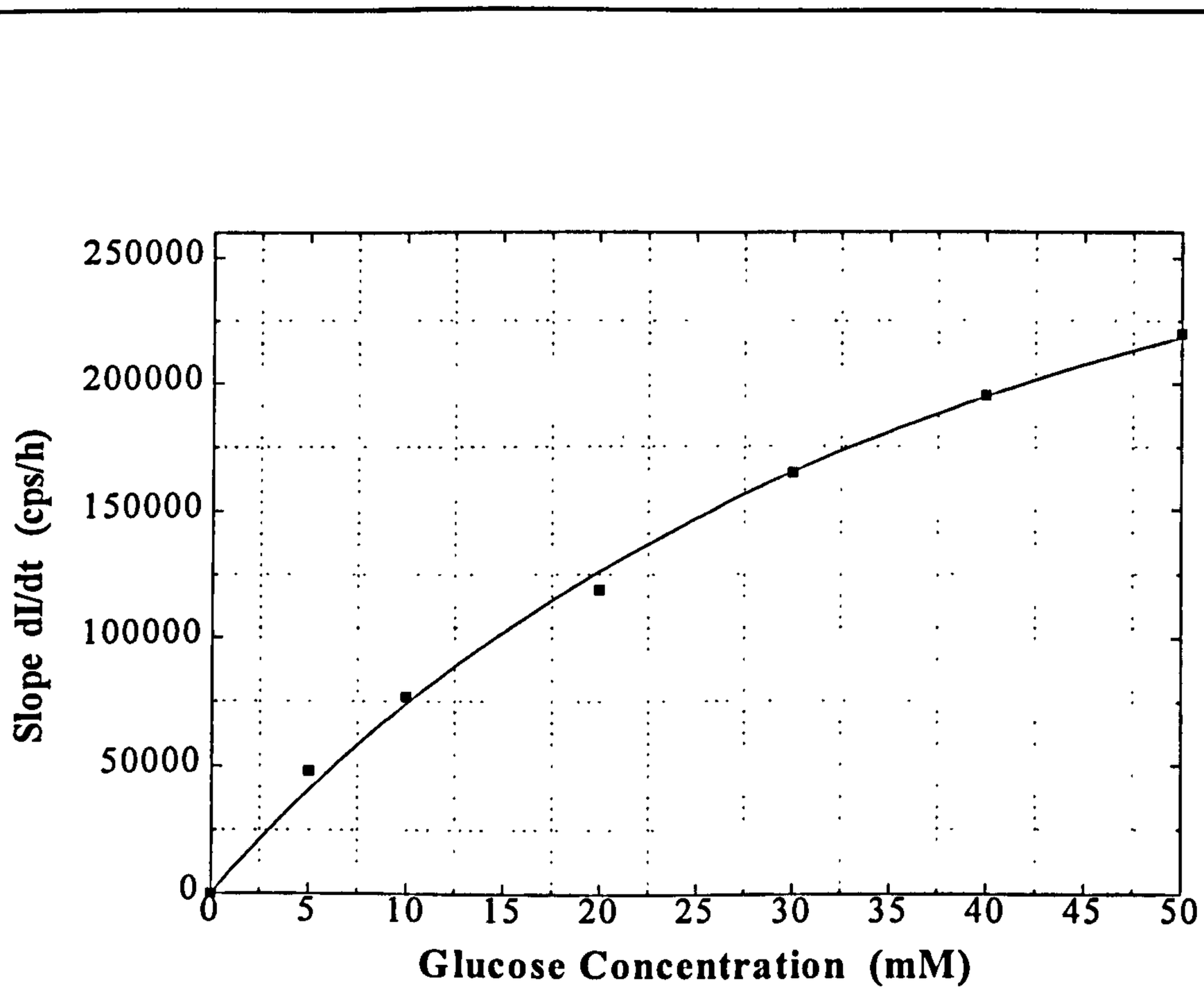

FIGURE A.6 Typical rate of change of fluorescence intensity variation against glucose concentration for sol-gel immobilisation (this example refers to the data corresponding to Figure 7.3).

A linear regression can be then performed in order to simulate this variation.

Each second order parabola depicted in Figure A.4, is described through the general equation form:

$$I = A_0 + A_1 \cdot t + A_2 \cdot t^2 \qquad \text{(a.1)}$$

The slope of the above equation is a function of the time t and given as follows:

$$\frac{dI}{dt} = A_1 + 2 \cdot A_2 \cdot t \qquad \text{(a.2)}$$

The coefficients A1 and A2 can be calculated using a linear regression analysis. In the present study, the graphics program Microcal Origin, Version 3.5 (1991-1994) by Microcal Software Inc. (One Roundhouse Plaza, Northampton, MA 01060 USA) which was used for the graphical representation of data, was also used to calculate these coefficients. For the figures presented in Chapter 7, the slope values were calculated at time t = 0. This means that the calculation of the slope of the curve was carried out at the start of the reaction being consistent with the analysis presented above for the experimental results from solutions.